UNIVERSITY OF LEEDS

Influence of hybrid fibre reinforcement on the flexural performance of concrete beams under static, sustained and cyclic loadings

Abdulrahman Mohammad I Abbadi

Submitted in accordance with the requirements for the degree of

Doctor of Philosophy

The University of Leeds

Faculty of Engineering
School of Civil Engineering

August, 2023

The candidate confirms that the work submitted is his own, except where work which has formed part of jointly authored publications has been included. The contribution of the candidate and the other authors to this work has been explicitly indicated below. The candidate confirms that appropriate credit has been given within the thesis where reference has been made to the work of others.

The following publication included the work described in chapter 4 and chapter 5 of this thesis:

Abbadi, A., Basheer, P. A. M., & Forth, J. P. (2021). The Effect of Hybrid Fibres on the static Load Performance of Concrete Beams. The international Conference on Advances in Construction Material and Structures (ICCMS 2021). 14–18 December 2021, Online Conference, India.

Abbadi, A., Basheer, P. A. M., & Forth, J. P. (2022). Effect of hybrid fibres on the static load performance of concrete beams. Materials Today: Proceedings.

Abbadi, A., Basheer, P. A. M., & Forth, J. P. (2022). The Effect of Hybrid Fibres on the Cyclic Load Performance of Concrete Beams. 41st Cement and Concrete Science Conference. 12–13 September 2022, Leeds, United Kingdom.

The candidate was in charge of the experimental research, data collecting and analysis. The co-author gave assistance at every stage of the work and in the creation of the manuscript.

Acknowledgments

I would like to take this opportunity to express my heartfelt gratitude to all who have assisted me in this effort and without whom it would not have been possible.

First and foremost, I want to express my gratitude to Allah for granting me patience, guidance, inspiration, strength, ability, knowledge, and grace throughout my career to undertake this research.

I would like to express my sincere gratitude and heartfelt appreciation to my supervisors, Prof Muhammed Basheer and Prof John Forth, for providing me with the opportunity to work under their supervision and for their continued support, wisdom, advice, inspiration and motivation throughout every stage of My PhD. I owe them a tremendous debt of gratitude for their invaluable assistance during my studies. They offered me guidance when they believed I needed it and were always eager to assist me in resolving any issues I faced.

Dr Amr Ebdelhady, my external supervisor, was extremely helpful during the numerical analysis phase of my work. His great assistance, precious suggestions, unending support, generous sharing of knowledge and insightful remarks were and continue to be greatly appreciated.

My heartfelt gratitude goes to my family, particularly my father, mother, brothers, and sisters, for their support, patience, encouragement, eternal love, spiritual support and loyal cooperation and for being a constant source of inspiration in helping me to successfully complete this degree. I cannot thank them enough for their unwavering support, especially for my parents' night-time prayers.

I am greatly indebted and grateful to my gorgeous wife who has contributed to my happiness and has become an integral part of my life. My wife has been by my side throughout my studies, supporting me in my efforts to attain this goal. Additionally, I would like to express my gratitude to my wonderful daughter, "**JULIA**", for her constant smile, which inspired me to pursue my dream. They have always been supportive of my ambitions and objectives.

I would like to convey my gratitude to the University of Leeds structural laboratory technical staff, Mr. Stephen Holmes, Mr. Robert Clarke, Mr. Marvin Wilman, Mr. Ghulam Khan, Mr Patrick Gregory and Mr. Ian Day for their assistance, advice and organisation during the preparation, manufacturing of test specimens,

casting, and testing of the beams. Mr Holmes and Mr Clarke deserve special thanks for their support and exceptionally precise work in preparing and managing test specimens. Also, I would like to express my heartfelt gratitude to my friends, especially Fahad Almutairi, for his continuous support and help. Additionally, I thank my friends Ahmed Al-Ali and Ali Al-Attas for their cooperation.

I would like to thank Bekaert for providing the steel fibres and Adfil for providing micro and macro polypropylene fibres used in this work.

Finally, I would like to extend my heartfelt appreciation to Jazan University for their collaboration and financial assistance throughout my research journey, which played a pivotal role in my successful completion of studies at the University of Leeds.

Dedication

This thesis is dedicated to the people that mean the most to me in this world;

To

The godfather of my life “Mohammad”

and my beloved mother “Shaqraa”

To

My dear brothers and sisters

To

My beloved wife and daughter “Abrar and Julia”

To

My co-workers and friends

who have always been and will continue to be, a source of joy, inspiration, and motivation for me

Abstract

Cracking of concrete members adversely affects both their structural behaviour and the durability. One of the ways to resist as well as reduce crack growth at different stages of loading is to introduce a variety of fibres randomly into the concrete mix at the time of manufacturing these structural members. Fibre-reinforced concrete (FRC) has been increasingly used in construction for several decades to reduce crack growth by incorporating one or two types of fibre in reinforced concrete elements under different types of load. Hybrid fibre system can, through their different lengths and constitution, help control the propagation of cracks in both the short and long term loadings and at both the micro and macro scales. Previous studies to reduce crack growth in reinforced concrete elements have been carried out by incorporating one or two types of fibre in concrete and under the static, cyclic / fatigue and sustained loadings. This study investigates the synergistic effects of hybrid fibre systems, combining micro and macro polypropylene fibres with steel fibres, to reduce both micro- and macro-cracking and hence enhance the performance of reinforced concrete (RC) beams subjected to static, repeated and sustained loadings.

The experimental programme involved casting and testing 41 short prismatic (100x100x500 mm) beams (0.5 m long) and twelve long (150x300x4200 mm) reinforced concrete beams (4.2 m long). The beams were split into two groups and each group was subjected to a different loading scenario (static and repeated for small prisms and static, repeated and sustained loadings for full-scale beams). Analysis of load-displacement curves, the width and spacing of cracks, crack distribution, and failure mode were used to evaluate the behaviour of the beams. Furthermore, this research utilised finite element analysis to verify the load deflection and cracking in experimental findings and obtain a deeper understanding of the flexural behaviour of the beams in terms of maximum load, deflection and cracking. FE models satisfactory match the experimental tests in terms of load-displacement curves under static and repeated loadings, hence they were acceptable to be utilised to conduct the parametric studies.

From the analysis of the experimental data, it has been found that the hybrid fibre system lowered the number of cracks, decreased the deflection, reduced the strain in the steel reinforcement bars and reduced the crack width. The beams, when taken to failure, also exhibited a more ductile failure under all loading conditions. The test results indicated that the addition of different types of fibre and different volume fractions resulted in higher compressive and splitting tensile concrete strengths. According to the test data obtained from this research, it was found that the hybrid fibre system comprising micro and macro polypropylene fibres along with steel fibres considerably improved the behaviour of concrete beams by enhancing their stiffness in the post cracking stage and, consequently, restricting the crack openings and deformations.

The inclusion of more than two different fibre types, especially the combination of steel, micro and macro polypropylene fibres, demonstrated a pronounced positive hybrid effect and suggest that the effect of hybrid fibres is very important to provide crack resistance at different scales/levels compared to the incorporation of a single fibre. In addition to what already established with the addition of steel or/and polypropylene fibre, this research has established the synergistic effect of the combination of steel, micro and macro polypropylene fibre and highlights that the inclusion of this combination in concrete results in superior performance and outweigh the using of single type of fibre even though the cost is higher.

This combination of fibres positively influence post-cracking behaviour, demonstrate a higher maximum load, maintain higher stiffness, and exhibit smaller reductions in stiffness compared to other fibre types. Additionally, the combination of steel, micro and macro polypropylene fibres in the hybrid system helps mitigate crack propagation, indicating a positive synergy effect and improved crack resistance, particularly under higher stress levels. These results represent a notable advancement compared to previous knowledge in the field. The outcome of this research indicated the need for further research on the effect of this combination on long-term sustained loads and lower stress cyclic loads.

The findings can be utilised to improve the design and evaluation of fibre-reinforced concrete structures subjected to static, repeated and sustained loadings.

Table of contents

List of Tables

List of Figures

Table of Notations

ACI	American concrete institute
ASTM	American society for testing and materials standard
EC2	Eurocode 2
FEA	Finite element analysis
FRC	Fibre-reinforced concrete
FWHM	Full Width at Half Maximum
HyFC-RP-1.5	Hybrid fibre with 1.5% subjected to repeated load
HyFC-ST-1.5	Hybrid fibre with 1.5% subjected to static load
HyFC-T	Hybrid fibre for calculating the loss of tension stiffening
HyFRC (1.5%)	Hybrid fibre-reinforced concrete contain 1.5% hybrid fibres (1% steel fibre, 0.1% micro polypropylene fibre and 0.4% macro polypropylene fibre)
HyFRC-ST-1.5	Hybrid fibre-reinforced concrete with 1.5% subjected to static load
HyFRC-RP-1.5	Hybrid fibre-reinforced concrete with 1.5% subjected to repeated load
HyFRC-SUS-1.5	Hybrid fibre-reinforced concrete with 1.5% subjected to sustained load
Macro PP (0.4%)	Macro polypropylene fibre contain 0.4% polypropylene fibre
MC2010	Model code 2010
Micro PP (0.1%)	Micro polypropylene fibre contain 0.1% polypropylene fibre
NC	Normal concrete
NC-RP-0	Normal concrete subjected to repeated load and without fibre
NC-ST-0	Normal concrete subjected to static load and without fibre
NC-T	Normal concrete for calculating the loss of tension stiffening
NRC	Normal reinforced concrete
NRC-RP-0	Normal reinforced concrete subjected to repeated load and without fibre

NRC-ST-0	Normal reinforced concrete subjected to static load and without fibre
NRC-SUS-0	Normal reinforced concrete subjected to sustained load and without fibre
0.1PPFC-ST-0.1	Micro polypropylene fibre with 0.1% subjected to static load
0.4PPFC-ST-0.4	Macro polypropylene fibre with 0.4% subjected to static load
RC	Reinforced concrete
RP	Repeated load
SFC-ST-1	Steel fibre with 1% subjected to static load
SFC-T	Steel fibre for calculating the loss of tension stiffening
SFRC (1%)	Steel fibre-reinforced concrete contain 1% steel fibre
SFRC-ST-1	Steel fibre-reinforced concrete with 1% subjected to static load
SFC-RP-1	Steel fibre concrete with 1% subjected to repeated load
ST	Static load
SUS	Sustained load

Chapter 1
Introduction

1.1 Research rationale

Reinforced concrete (RC) structures are subjected to cyclic loading during their service life; for instance, due to wind, vibration from machines, earthquakes, the traffic on highway structures and pedestrian footfall. Fatigue problems may arise when concrete structures such as bridges, airport pavements and highway pavements are subjected to repetitive loading during their service lives. The response of structures to dynamic loading conditions varies from their response under static loads. Due to the cyclic nature of loadings (fatigue/repeated) that structure members endure during actual usage, designers face the challenge of estimating fatigue life and its impact on the mechanical behaviour of the structures. Consequently, fatigue testing generally provides more reliable data compared to standard static loading tests in terms of predicting the operational lifespan of bridge structures. Estimating the fatigue life span is considered to be one of the most significant aspects in designing RC structures (Mohamadi et al., 2013). Cyclic loading initiates and propagates cracks in the material (Jiang et al., 2018). Cracking plays an essential role in compromising the structural performance and the durability of concrete structures.

Cracking is a visible indication of forces that exceed concrete's ability to resist either tension or compression. Concrete is a tension-weak construction material with a low strain capacity, hence is prone to cracking. The occurrence of cracks in concrete structures can be classified into two primary categories based on the underlying causes and the time of their appearance. These categories are known as structural cracks and non-structural cracks, as reported by Neville and Brooks (1985). Structural cracks emerge primarily due to tensile stresses within the concrete, resulting from applied loads or foundation movements. Generally, these cracks manifest after the concrete has undergone the hardening process. On the other hand, non-structural cracks can manifest both before and after the concrete has hardened. Cracks that appear before hardening often arise from settlement within the concrete mass, known as plastic settlement cracks, or from

the shrinkage of the surface, referred to as plastic shrinkage cracks. Conversely, cracks that develop after hardening can be attributed to various factors, including drying shrinkage and corrosion of reinforcement. Consequently, concrete is susceptible to cracking, in both the short-term, due to plastic shrinkage and the restraint of imposed strains and in the long-term, due to applied loading and degradation resulting from durability issues. To improve the cracking observed at the serviceability limit state and, hence, help control deflection and provide greater resistance to problems resulting from durability issues, traditional steel reinforced concrete can be strengthened with a variety of randomly distributed fibres in the concrete mix. When they are used in structural concrete, they will resist and reduce the crack growth at different stages of loading. Previous studies have indicated that the introduction of fibres in concrete can effectively prevent or control the formation, spreading, and merging of cracks when the material is under load (Guo et al., 2021). That is, the addition of fibres helps to minimise the risk of brittle failure and enhance the overall strength of the concrete (Guo et al., 2021). The control of cracking at the serviceability limit state is one of the main reasons for using fibre reinforced concrete (Tailhan et al., 2015).

Fibre reinforced concrete (FRC) offers numerous advantages over traditional RC, such as reducing the width and number of cracks, enhancing shear and flexural strengths, increasing ductility and reducing deflection (Kang et al., 2011). Further, the presence of discrete fibres enhances fracture toughness and fatigue resistance (Mobasher et al., 2015). FRC is commonly used to enhance the serviceability of concrete and improve its fatigue resistance (Juárez et al., 2007; Cucchiara et al., 2004; Hassanpour et al., 2012). Furthermore, considering that concrete is a composite material characterised by multiple phases and heterogeneous structure, introducing the appropriate fibre type into concrete holds the potential to enhance its performance at specific phases, including the plastic, hardening and curing phases as well as at different structural levels (Guo et al., 2021). The efficiency of these fibres within the matrix depends on their material composition, geometrical characteristics (such as cross-sectional shape, length, longitudinal profile and diameter) and the quantity incorporated. These factors significantly influence how effectively the fibres enhance the properties, such as tensile strength, dynamic parameters and toughness of the composite material (Pająk and Ponikiewski, 2017). It is

important to note that the effectiveness of a single type of fibre is limited to a specific range of cracks. In general, the utilisation of a single fibre can offer reinforcement at a specific scale or level, which refers to a particular size or dimension at the micro or macro levels, but it becomes challenging to provide crack resistance at other scales or levels, which the reinforcement properties of the single fibre might not extend well to other size ranges or dimensions (Ahmad et al., 2021). Micro fibres act as bridges, inhibiting the formation of micro-cracks, whereas longer fibres are more efficient at halting macro-cracks. However, by combining fibres of various lengths or types (known commonly as hybrid fibres), a synergistic effect can be achieved, leading to a significant improvement in tensile parameters (Pająk and Ponikiewski, 2017). Hence, the exploration of combining diverse fibre types to substantially enhance the overall concrete performance is a promising area for investigation (Guo et al., 2021).

Hybrid fibres are where more than one type of fibre is used. The use of hybrid fibres, which involves the combination of multiple fibre types, has gained considerable attention in the field of concrete reinforcement. The mix design for incorporating hybrid fibres primarily takes into account two aspects: first, considering the crack resistance mechanisms offered by different types of fibres; and second, aiming to achieve economic efficiency by determining the appropriate fibre volume ratio while considering the performance improvement (Wu et al., 2022). The ductility and strength of concrete are enhanced by the hybridisation of different types of fibres, while incorporating different types of fibres of varying lengths helps to control the propagation of micro and macro-cracks (Yang, 2011). Well-designed hybrid composites exhibit a positive interaction between the fibres, resulting in improved performances than the sum of individual fibre's performance (Abou El-Mal et al., 2015). This positive interaction between fibres plays an important role in enhancing the overall mechanical properties and durability of concrete. The combined effects of hybrid fibres result in improved properties through advantageous reinforcement mechanisms at various scales. Understanding the behaviour and characteristics of hybrid fibres is important for advancing the knowledge and application of hybrid fibre-reinforced concrete.

Previous studies to reduce crack growth in reinforced concrete elements have been carried out by incorporating one or two types of fibre in concrete and

under the static, cyclic/fatigue and sustained loadings. To the authors' best knowledge, none of the previous studies was carried out to determine the influence of hybrid fibre reinforcement containing steel fibres and both micro and macro polypropylene fibres on the flexural performance of concrete beams under static, sustained and repeated loadings. Incorporating hybrid steel and polypropylene fibres improves the flexural performance and provide the most suitable combination for hybrid fibres. The influence of combining micro and macro polypropylene fibres with steel fibres on the serviceability of concrete remains inadequately investigated and discussed. Concrete manufactured using different types of fibres may exhibit distinct cracking behaviours, which can have varying effects on the overall performance of the concrete. Therefore, this study intends to investigate experimentally how hybrid fibre systems (combination of micro and macro polypropylene fibres with steel fibres) can enhance the performance of RC beams subjected to both static, sustained and cyclic loadings by restricting the development of micro-cracks and macro-cracks. In addition, this study employed both finite element analysis to validate the experimental results and gain insights into the flexural performance of the beams. These analyses provide valuable information that can be utilised to predict the load-deflection behaviour of full-scale beams.

1.2 Aims and Objectives

This research aims to investigate the influence of hybrid fibre reinforcement on the flexural performance of concrete beams under static, sustained and cyclic loadings. The outcome of this research would provide a better understanding of the role of hybrid micro and macro polypropylene with steel fibres in preventing the detrimental effects of different types of load on cracking.

The following objectives are considered in order to achieve the aim of this project:

1. To concisely review previous studies and explain the rationale for this research.
2. To examine the influence of incorporating the hybrid fibre system on the strength characteristics of concrete, including the shrinkage and creep, by focusing on the following aspects:

- Mechanical properties.
- Flexural strength for the prisms.
- Repeated tests for the prisms.
- Time-dependent effects such as shrinkage, both compressive and tensile creep and loss of tension stiffening.

3. To assess how hybrid fibre reinforcement (micro and macro polypropylene fibres combined with macro steel fibres) can restrict the development of micro and macro cracks in full-scale RC elements subjected to static, repeated and sustained loadings.

3. To measure the width and spacing of cracks in full-scale RC flexural members with and without fibres and comparing them with code predictions.

4. To investigate the effect of hybrid fibres on cracking load, stiffness, toughness, peak load, deflection and crack width of small prisms and full-scale beams.

5. To conduct Finite Element Analysis (FEA) validation against the experimental findings.

6. After confirming the reliability of the FEA models, to carry out further FEA parametric investigations for further examination on predicting the flexural behaviour of full-scale beams.

1.3 Scope of the Research

Several experiments were conducted to study how a hybrid fibre system, consisting of steel fibre along with micro and macro polypropylene (PP) fibres, influenced the flexural behaviour of fibre-reinforced concrete (FRC) beams under different load conditions, including static, repeated, and sustained loads. The full-scale beams were reinforced with steel reinforcement bars, while the prisms were not reinforced with steel bars.

The research conducted in this PhD thesis involves a comprehensive investigation of the flexural behaviour of full-scale beams, particularly focusing on the effects of incorporating fibres into concrete. To validate these results, a numerical analysis was performed using the FEA with Abaqus software (Dassault Systemes, 2014). The simulation aims to replicate both static and repeated loadings in four-point bending conditions, comparing beams with and without fibres at different fibre volume fractions.

The anticipated results and conclusions drawn from this study could be valuable in the development of design guidelines, potentially leading to an increased utilisation of hybrid fibre concrete (HyFC) and hybrid fibre reinforced concrete (HyFRC) in diverse structural applications.

1.4 Thesis structure

To better comprehend this research topic and achieve the aims and objectives, this thesis is structured in the following chapters:

Chapter 1: Introduction

This chapter provides background information on the topic and a description of the research problem. The aim and the objectives are also presented.

Chapter 2: Literature review

The literature review summarises the research that has been done on investigating the effect of single and hybrid fibres on flexural behaviour and other properties under short-term and long-term. A summary of fibre types and their properties with different combination in reinforced concrete structures was given. It discusses the influence and performance of beams with normal concrete (NC), normal reinforced concrete (NRC), fibre concrete (FC), fibre-reinforced concrete (FRC), hybrid fibre concrete (HyFC) and hybrid fibre-reinforced concrete (HyFRC), under different types of loads. It discusses the effect of fibres on long-term behaviour such as shrinkage, creep and loss of tension stiffening. The chapter concludes with a summary of the previous studies and identifies some of the gaps found in the existing literature. Based on the review, it was recognised that there is a need to examine the influence of hybrid fibres on the development of micro-cracks and macro-cracks under different types of load.

Chapter 3: Experimental programme

The chapter describes the extensive experimental programme of this research. It describes the materials used and their properties, the design of test specimens, preparation, fabrication, casting technique and testing of the test specimens. It also includes the description of the instrumentation, measurements and setup of specimens.

Chapters 4: Experimental results – Part 1: small specimens (including the 0.5 m span of prismatic beams and the tension stiffening loss tests) and 5: Experimental results – Part 2: long beam (4.2 m span) under static, repeated and sustained loadings

The results and discussion chapters present the findings of the research. These chapters will discuss the test sample characteristics, provide an overview of the data obtained, and show the findings of the statistical analyses that were carried out. Further, the study outcomes are interpreted in this chapter in the context of the body of published studies. They explain the effect of hybrid fibre system on the crack pattern, flexural strength, stiffness, load-deflection curves, crack width, crack length and strains in steel bars and concrete surface strain. In addition, these chapters discuss the significance of results and provide suggestions for further investigations. The experimental findings and the analytical predictions derived from the existing code formula for long-term deflection and crack width are compared.

Chapter 6: Finite element analysis (FEA)

This chapter consists of FEA investigations. It presents the findings of the FEA investigations comparing to the experimental results. Also, the sensitivity of results of various parameters and parametric investigations were addressed and presented.

Chapter 7: Conclusions, limitations of the study and recommendations for future work

The key findings from the current investigations are presented in chapter 7 from the data presented in chapters 4 to 6, with the limitation of the study along with suggestions and recommendations for future research work that is worthy of further investigation.

Chapter 2

Literature Review

2.1 Introduction

In this Chapter, the context of fibre reinforced concrete and its behaviour in comparison with that of plain reinforced concrete is discussed. This is followed by a review of the behaviour of both types of concretes under static and dynamic loads, including their long-term effects. The review is then concluded by providing a fuller justification and scientific rationale for this project, by summarising the main findings from this review.

2.2 Fibre-reinforced concrete

As it is well known, normal concrete can display brittle behaviour and has low strain capacity, low tensile strength and is susceptible to the development and propagation of cracks. It is weak in tension and cracks often occur in both its plastic and hardened states (Nili and Afroughsabet, 2012). The aggregate-cement interface is usually the weakest part of the composite, affecting the properties of concrete according to Tulin et al. (2004) and Zheng et al. (2005) and it has low tensile stress and low tensile strain (Jebli et al., 2018). During loading, cracks normally develop at the interfacial transition zone (ITZ) as it is the weakest part of the hardened concrete, and this can affect the mechanical properties of the concrete (Afroughsabet et al., 2016). Researchers have sought ways to strengthen and address the brittle nature of concrete and make it more ductile (Nattaj and Nematzadeh, 2017). The use of reinforcing steel bars is the most common way to strengthen concrete in tension but randomly introducing small, discrete fibres into the concrete (known as fibre reinforced concrete) offers another way to strengthen the interface and alleviate cracks.

Fibre-reinforced concrete (FRC) has been extensively utilised in construction for several decades. It has been well-established that FRC can enhance the ductility and crack bridging behaviour of the concrete element (Branston et al., 2016; Khan and Abadel, 2013), as shown in Figure 2.1. FRC also reduces the crack formation and growth, both at the ITZ and in the bulk of the concrete, and can perform as shear reinforcement. FRC offers

numerous advantages compared to regular concretes, such as reducing the width and number of cracks, enhancing the shear and flexure strengths, increasing ductility and reducing deflection (Kang et al., 2011). Moreover, the presence of discrete fibres enhances fracture toughness and fatigue resistance (Mobasher et al., 2015). FRC is commonly used to enhance the serviceability of concrete and improve its fatigue resistance (Juárez et al., 2007; Cucchiara et al., 2004; Hassanpour et al., 2012). FRC can be used as repair material in seismic zones to rehabilitate existing structures (Okuyucu et al., 2011; Cucchiara et al., 2004). It is important to note that fibres in FRC control the propagation of cracks due to the bonding between the fibres and the surrounding concrete (Hassanpour et al., 2012). In plain concrete, the characteristics of the fracture process zone (FPZ) are influenced by the type of aggregate, with aggregate interlock being a significant factor. However, in the case of Fibre-Reinforced Concrete (FRC), the FPZ is impacted by mechanisms present in both plain concrete and the fibre-bridging zone, as illustrated in Figure 2.1(ii).

In the fictitious crack model, it is assumed that the material behaves linearly elastically before the onset of crack formation. Subsequently, once a crack initiates, the model assumes that stresses can still be transferred across the crack. This is why it's referred to as a "fictitious crack." The model incorporates crack-bridging stresses, which are determined based on the crack's width and its relationship with stress, as described in the stress-crack opening relationship. In FRC materials, the shape of the stress-crack opening relationship is intricate and heavily influenced by the quantity and variety of fibres employed. The main mechanism responsible for stress transfer across cracks in FRC is the pull-out of fibres, as noted by Li et al. (1993). Typically, fibres are capable of bearing a significant load even when cracks open wide, resulting in a notable difference in the initial shape of the stress-crack opening curve compared to its shape at wider crack openings (Olesen, 2001). As the crack extends from the base of the hinge, the stress distribution undergoes three clearly defined phases, as illustrated in Figure 2.1 (iii).

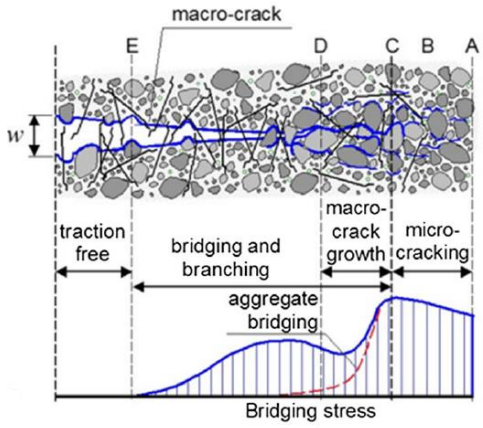

i) The effect of FRC on ductility and crack bridging behaviour (From Afroughsabet et al., 2016)

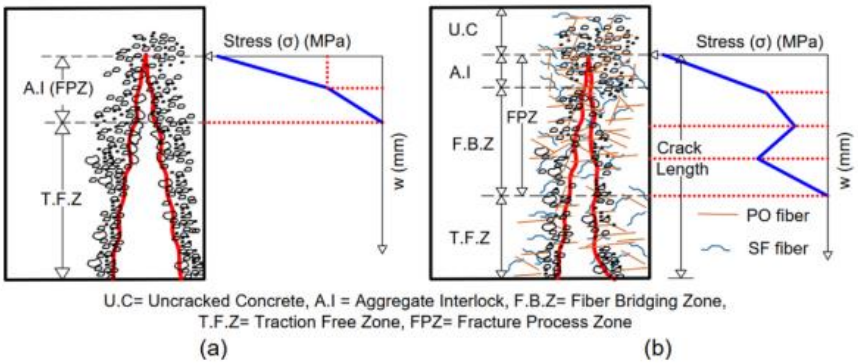

ii) Idealised stress-crack width behaviour of notched beams: (a) Plain concrete; (b) FRC (From Bhosale et al., 2020)

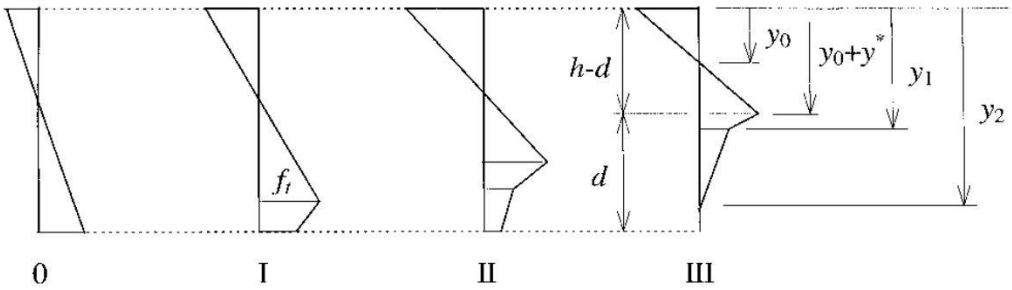

iii) Four phases of stress distribution within the elastic layer of the hinge: phase 0: the initial state of stresses before cracking occurs. Phases I–III: these represent the states of stresses that occur as the crack propagates during its growth (From Olesen, 2001)

Figure 2.1: The effect of fibre on the crack surface and the crack bridging

2.2.1 Fibre types and their properties

There are various types of fibres that can be utilised in concrete structures, including steel fibres, glass fibres, organic or mineral fibres, and synthetic fibres. Steel fibres and synthetic fibres are the most commonly used options for concrete reinforcement. Table 2.1 provides information on the physical characteristics of the different available fibre types.

2.2.1.1 Steel fibres

Low-carbon and high-strength steel wires are commonly used in the production of steel fibres. Steel fibres are available in various shapes, including straight, crimped, hooked, and wave-shaped. Due to their high strength, ductility, and ability to enhance post-cracking performance, steel fibres are widely used in concrete structures.

Table 2.1: Fibres properties

Fibres type	Specific gravity (g/cm^3)	Length (mm)	Diameter (mm)	Elastic modulus (GPa)	References
Polypropylene fibre	0.9-0.92	12-50	0.019-0.9	3.5-9.5	Multiple sources*
Monofilament	0.91	13.6	0.048	6.9	Li et al. (2018)
Dry basalt fibre	2.8	24	13-20 μm	89	Abbadi (2018)
Chopped basalt fibre	2.61	17-19	13 μm	78.2-94.1	Abbadi (2018)
Smooth steel fibre	7.9	30	0.3	200	Kim et al. (2011)
Corrugated steel fibre	7.9	45	0.75	200	Li et al. (2018)
Hooked-end steel fibre	7.85	50	0.8	200	Abbadi (2018)
Bundled steel fibre	7.85	31.84	0.49	200	Abbadi (2018)

* Fallah and Nematzadeh, (2016), Current study, Behfarnia and Behravan (2014), Sahoo et al. (2015)

2.2.1.2 Synthetic fibre

Synthetic fibres, which are derived from materials such as polypropylene, polyethylene, nylon, polyester, or acrylic, are manufactured in various forms such as monofilament, fibrillated, or bundled fibres. These fibres offer numerous advantages, including corrosion resistance, high tensile strength, and excellent resistance to cracking and impact. They are commonly used to control shrinkage cracking, enhance durability, and improve the behaviour of concrete after cracking. There is a paucity of experimental and analytical research focused on macro synthetic fibres when compared to steel fibres. Figure 2.2 illustrates micro and macro synthetic fibres including polypropylene fibres. These are typically non-corrosive, easy to apply, and exhibit resistance to alkali.

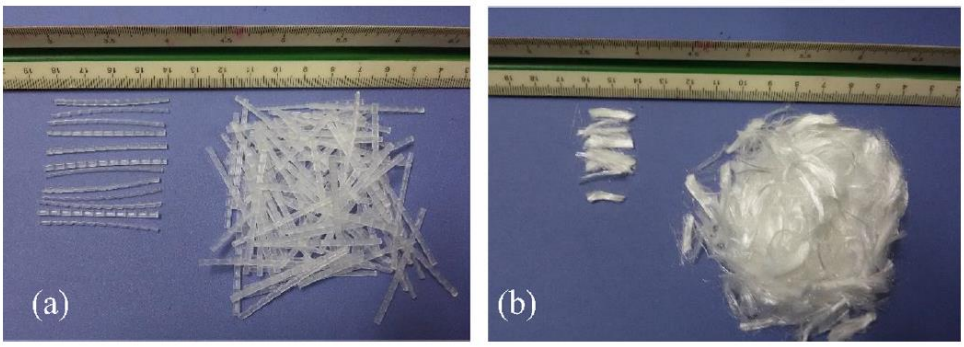

a) Macro polymeric b) Micro polypropylene fibres

Figure 2.2: Different types of fibres (From Fallah and Nematzadeh, 2016)

2.2.1.3 Hybrid fibres

The term ‘hybrid fibres’ refers to the utilisation of multiple type of fibres in concrete. The ductility and strength of concrete are enhanced by the hybridisation of different types of fibres, while incorporating different types of fibres of varying lengths helps to control the propagation of micro-cracks and macro-cracks (Yang, 2011). Well-designed hybrid composites exhibit a positive interaction between the fibres, resulting in improved performances than the sum of individual fibre’s performance. Studies have shown that the hybrid fibre reinforcement led to an increase in compressive strength ranging from 2%-13%, while splitting tensile strength increased by up to 14.8% compared to using a single type of fibre (Abou El-Mal et al., 2015).

Several combinations of fibres can result in "synergy," with the most widely recognised combinations being polypropylene and steel fibres. The reason for this could be attributed to any of the subsequent mechanisms (Banthia and Gupta, 2004). The first category involves incorporating fibres based on their constitutive response. In this category, one type of fibre is stronger and more rigid, enhancing the strength of the first crack and, the ultimate strength of the concrete by bridging micro-cracks. The other type of fibre is relatively flexible, contributing to greater toughness and strain capacity in the post-cracking zone by means of macro-crack bridging. The second category is based on the combination of fibre size, which is shown in Figure 2.3. Small types of fibre help to bridge, control and delay the formation of the first crack, thereby lead to an increase in tensile strength. On the other hand, the use of larger fibres is intended to control the formation and propagation of macro-cracks, thereby improving fracture toughness. The final category involves incorporating fibres based on their specific functions. One type of fibre is intended to enhance the properties of early age and/or fresh concrete, such as workability, production and shrinkage. The second type of fibre helps to improve the mechanical properties of hardened concrete.

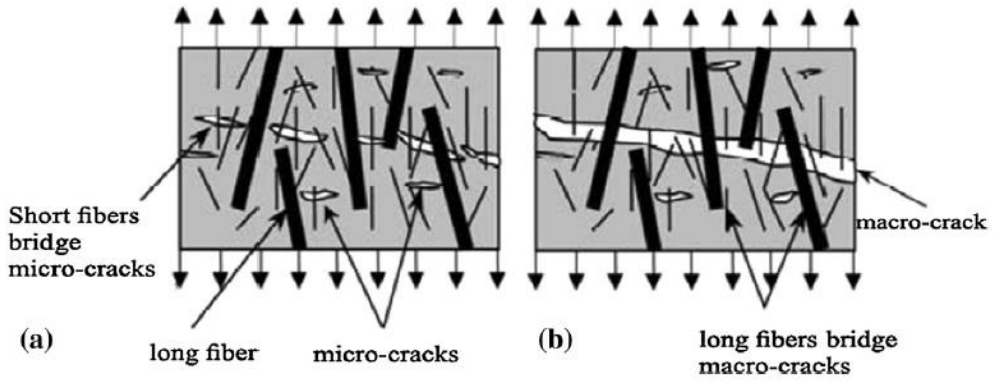

Figure 2.3: Illustrates the combination of fibres based on their size and corresponding functions (From Pakravan et al., 2017)

2.3 Influence of fibres on mechanical properties

This section focuses on evaluating the mechanical properties of normal concrete (NC), fibre-reinforced concrete (FRC) and hybrid fibre-reinforced concrete (HyFRC). The mechanical properties of concrete include compressive strength and tensile strength. Comparing the mechanical properties of NC and FRC is

crucial in assessing the impact of fibres on enhancing the overall strength and durability of concrete. Table 2.2 presents the comparative data of these properties for NC and FRC, providing insights into the effectiveness of fibres in improving the concrete performance.

The evaluation of mechanical properties in NC, FRC, and HyFRC has provided researchers with valuable insights into the influence of fibres on the behaviour of concrete (Afroughsabet et al., 2016). An example is presented in Figure 2.4. Through the analysis of these properties in NC, FRC, and HyFRC, a direct comparison can be made between fibre-reinforced concrete and normal concrete without fibres. This allows for the identification of any improvements or modifications that occur as a result of incorporating fibres into the concrete mix. Such comparisons aid in understanding the enhancements and changes brought about by the inclusion of fibres in concrete. The mechanical properties of hybrid fibre concretes have primarily focused on the combination of steel with micro or macro polypropylene fibres. However, the combination of micro and macro polypropylene with steel fibres has not been extensively studied and further investigation is needed to fully understand their characteristics.

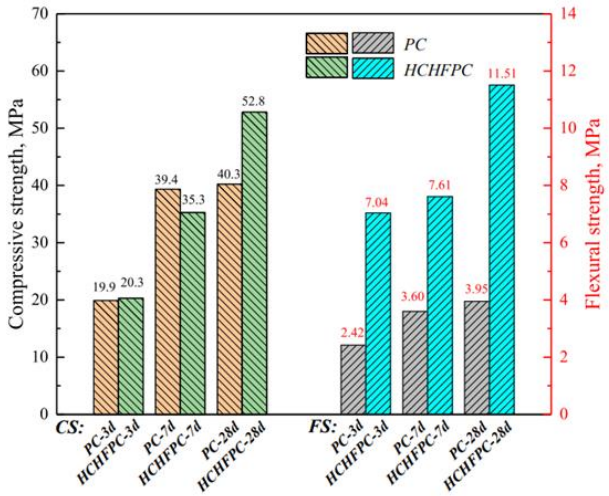

Figure 2.4: Effect of hybrid fibre on the compressive and flexural strength of plain concrete (PC) and high proportion of hybrid fibre-polymer (HCHFPC) (From Wu et al., 2022)

2.3.1 Performance of NC and FRC on mechanical properties

Based on the literature summarised in Table 2.2, previous research has primarily focused on investigating the effects of incorporating steel and polypropylene fibres on the mechanical characteristics of concrete. The findings presented in

Table 2.2 indicate that the addition of steel and polypropylene fibres to concrete mixes resulted in improvements in compressive strength, splitting tensile strength and modulus of elasticity. These results suggested that incorporating fibres led to enhancements in these mechanical properties, which was significant and highlighted the potential advantages of using fibre reinforcements in concrete structures. The increase in splitting tensile strength indicates improved resistance to cracking and enhanced durability, particularly in applications where tensile stresses are prominent. Additionally, the observed enhancement in the modulus of elasticity suggested that fibre reinforcements contributed to the stiffness and rigidity of concrete. Notably, according to the results in Table 2.2 the addition of steel fibres to concretes mixes exhibited the highest increase in the mechanical properties compared to the polypropylene fibre.

Table 2.2: Summary on influence of fibres on mechanical properties of NC and FRC

Authors	**Variables and fibres volume fraction**	**Effect of fibre on the property**
Behfarnia and Behravan (2014)	High performance polypropylene fibres (HPP) 0.8% Steel fibre 0.8%	- Effect of HPP fibre on compressive strength: 28-day strength increased by 3.3% compared to plain concretes. - Effect of steel fibre on compressive strength: 28-day strength increased by 16% and 13% compared to plain and HPP concretes, respectively. - Effect on splitting tensile strength: increased by 10% with the addition of each SF and polypropylene fibres. - Effect on modulus of elasticity: increased by 33.8% and 17.5% for SF and HPP fibres, respectively.
Yoo et al. (2013)	Four different volumes of steel fibres: 1%, 2%, 3% and 4%.	- Effect on the compressive strength, elastic modulus and load carrying capacity: increasing the fibre content led to an improvement by 12.1 % for compressive strength, recorded of 52.7 GPa elastic modulus and higher loading capacity when the fibre volume fraction up to 3% in fibre volume.
Yoo et al. (2014)	Compare the use of 2% steel fibre	- Effect on compressive strength: the fibre length rarely affected compressive strength.

	volume with four different fibre lengths (13mm, 16.3mm, 19.5mm and 30mm)	-The specimen with a fibre length of 16.3mm achieved the maximum compressive strength but it was only 0.9–3.6% higher than that of the other specimens.
Yoo et al. (2015)	Steel fibres with four different volumes (0%, 0.5%, 1.0% and 2.0%) for normal concrete (NC) and high strength concrete (HSC), with two fibre volumes (0% and 2%) for ultra-high strength concrete (UHSC)	- Effect on compressive strength: adding steel fibres somewhat reduced the compressive strength in the case of normal concrete (NC), which attributed to an increase in air content, formation of fibre balls…etc. - Adding steel fibres slightly increased the compressive strength in situations of high strength concrete (HSC) and ultra-high strength concrete (UHSC) ranges of 1.5% to 6.0%. - Effect on the elastic modulus: the fibre volume within the ranges of 1.5% to 6.0% was relatively small or negligible.
Singh et al. (2006)	Steel fibre of 1%, 1.5% and 2.0%	- Effect on compressive strength: the incorporation of 1.5% and 2.0% of steel fibres increased the compressive strength by 4.7% and 4.02%, respectively, compared to 1% of steel fibre.

2.3.2 Performance of HyFRC on mechanical properties

As summarised in Table 2.3, the majority of previous studies have focused on investigating the effects of incorporating hybrid steel-steel or hybrid steel-polypropylene fibres on the mechanical properties of concrete. According to Table 2.3, the addition of hybrid fibres (steel and polypropylene fibres) demonstrated the greatest increase in compressive strength compared to the addition of a single type of fibre. It can be anticipated that the addition of hybrid fibre showed an enhancement in the compressive and splitting tensile strength. However, none of the studies reviewed in the literature focused on the specific effect of a hybrid fibre system consisting of steel, micro polypropylene and macro polypropylene fibres and their role in enhancing the mechanical properties. Therefore, further research is needed to investigate the effect of a hybrid fibre system comprising the above combination on the mechanical properties of concrete.

Table 2.3: Summary on influence of fibres on mechanical properties of HyFRC

Authors	Variables and fibres volume fraction	Effect of fibre on the property
Fallah and Nematzadeh (2016)	Macro polymeric (MP) fibres ranged from 0.25% to 1.25%, whereas the amount of micro polypropylene fibres (PP) ranged from 0.1% to 0.5%. Different hybrid volumes of fibres (0.9MP and 0.1PP, 0.8MP and 0.2PP, 0.7MP and 0.3PP, 0.6MP and 0.4PP and 0.5MP and 0.5PP) were studied.	- Effect on compressive strength: Specimens cast with 0.9% MP and 0.1% PP fibres demonstrated the greatest increase with an average of 4.2% relative to the plain concrete. - PP exhibited greater compressive strength than MP fibres in high strength concrete by about 3.5%. - The maximum improvement with a single type of MP and PP fibres was achieved when using 0.25% macro and 0.1% micro fibres with an increase of 8.0% and 11.5%, respectively. - The most appropriate combination of hybrid fibres consisted of 0.9% macro and 0.1% micro fibres.
Li et al. (2018)	Steel-polypropylene hybrid FRC beams. The test parameters included three different steel fibres (straight, hooked-end and corrugated fibre) and monofilament polypropylene fibres	- Increasing the fibre volume of both types of fibre led to an increase in mechanical behaviour, such as splitting tensile strength and the compressive strength of the concrete. The addition of hooked end steel fibre with and without monofilament showed the highest increase in the flexural strength by 113% and 115%, respectively. The corrugated steel fibre with monofilament fibre showed the highest increase by about 94% compared to normal concrete. The increase in the compressive

		strength was approximately 18.26% for straight steel and monofilament fibre higher than normal concrete. - Effect on splitting tensile strength: corrugated steel fibres exhibited an increase of 7.78%, 19.02%, 28.24% and 54.47% for fibre volumes from 0.5-2.0%. - The hybridisation of straight steel and polypropylene fibres offered the most suitable combination for hybrid fibres.
Sahoo et al. (2015)	Incorporating steel and polypropylene fibres. Two different volumes of steel fibres and polypropylene fibres (0.5% and 1.0%) as well as three different volumes of hybrid fibres: 0.5% and 0.5%, 1.0% and 0.5%, and 1.0% and 1.0% for steel and polypropylene fibres, respectively.	- Effect on compressive strength: the inclusion of fibres had little effect. The CFRC3 (1% steel fibre and 1% polypropylene fibre) cubes offered the greatest compressive strength, thereby indicating a modest improvement of 7.5% relative to plain concrete. - Effect on splitting tensile strength: the addition of 1% steel fibre produced an increase of approximately 70%, whereas the incorporation of 1% of both steel and polypropylene fibres resulted in an increase of approximately 100%.
Soutsos et al. (2012)	Hybrid steel-polypropylene fibres. Three different fibre dosages (30kg/m^3, 40kg/m^3 and 50kg/m^3) and two different dosages (4.6kg/m^3 and 5.3kg/m^3) for steel and polypropylene fibres were employed, respectively.	- Effect on compressive strength: incorporating steel fibres into the concrete resulted in an increase of approximately 4 and 5 *N/mm²* for fibre dosage rates of 30 *kg/m³* and 50 *kg/m³* respectively. However, the increase in compressive strength was lower for synthetic fibres, with an increase of approximately 2-3 *N/mm²* for dosage rates ranging from 4.5-5.3 *kg/m³*.

2.4 Influence of fibres on flexural properties

This section examines the effect of fibres on the flexural properties of concrete. Previous research has demonstrated that the inclusion of fibres in concrete leads to improvements in flexural strength, toughness, and ductility, all of which are critical factors in structural applications. These enhancements in flexural properties contribute to the overall performance and reliability of concrete structures. As in the case of mechanical properties, the discussion in this section has two parts, viz. comparison of FRC with NC and then critically reviewing the benefits of hybrid fibres with FRCs.

2.4.1 Performance of NC and FRC beams on flexural properties

As summarised in Table 2.4, the incorporation of various types of fibre has been reported to have shown a significant increase in flexural strength and toughness of concrete. The type, length and volume fraction of fibres affected the rate at which the flexural strength increased, as can be seen in Figure 2.5. Beams reinforced with hooked-end steel fibres exhibited higher maximum loads compared to those with straight fibres, with this dependency increasing as the volume content increased (Pająk and Ponikiewski, 2013). The increase in flexural strength and deflection at the peak of a concrete structure was caused by superb fibre bridging at the crack surfaces which led to a greater load carrying capacity. Additionally, an increase in fibre length up to 19.5mm led to an increase in peak flexural load. However, a fibre length of 30mm resulted in a reduction in the peak load (Yoo et al., 2014).

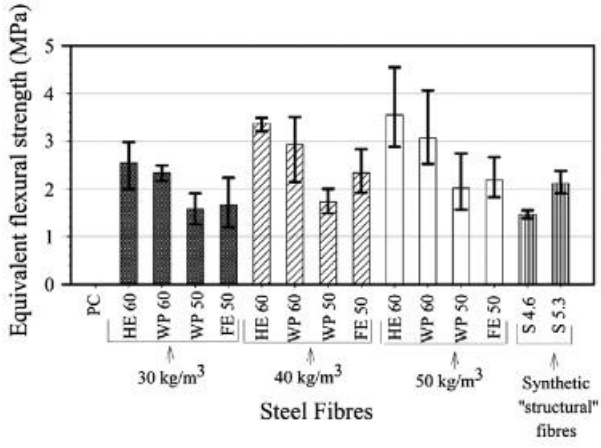

Figure 2.5: Flexural strength for all different types of fibre (From Soutsos et al., 2012). Load–deflection curves can be generated from which the

equivalent flexural strength, Re,3 value (the average load applied as the 45 cm span beam deflects to 3 mm expressed as a ratio of the load to first crack), can be estimated

Regarding the first crack load, there are conflicting conclusions in the literature, as can be seen in Table 2.4. Some studies reported that the addition of steel or synthetic fibres into concrete increased the first crack load, with improvements of up to 17.4% and 33.7% respectively compared to plain concrete. However, in many cases, beams exhibited a similar load at the formation of the first visible crack in the tension zone (Meza and Siddique, 2019). Yoo et al. (2013) found that the volume content of steel fibre had no effect on the initial stiffness. The results of the flexural tests also indicated insignificant improvements in peak load and first crack load (Hamoush et al., 2010). This change in behaviour at higher fibre volume is important to consider for the optimal fibre dosage and to avoid potential negative effects. The increase in the volume fraction of fibre of hooked-end and straight fibres resulted in an increase in the maximum load (Pająk and Ponikiewski, 2013). The incorporation of fibres led to an increase in the flexural strength (Yoo et al., 2015; Singh et al., 2006; Oh, 1992).

Oh (1992) reported that the inclusion of steel fibres significantly increased ductility and ultimate resistance. Hamoush et al. (2010) stated that the contribution of microfibres was more noticeable in the post-cracking response, showing an increase in post-cracking ductility. Additionally, Meda et al. (2012) found that the addition of 30 kg/m^3 of steel fibres increased ductility by approximately 73.1%. On the other hand, as reported by Meda et al. (2012), the addition of higher amount of steel fibre had no effect on the ductility

In summary, the inclusion of fibres showed an enhancement in the peak load ductility and toughness of concrete beams. However, further research is needed to address some of the conflicting conclusions regarding the effects of fibre addition on parameters such as cracking load, peak load and ductility to provide more comprehensive insights.

Table 2.4: Summary on influence of fibres on flexural properties of NRC and FRC

Authors	Variables, fibres volume fraction and dimension of beams (mm)	Effect of fibre on the property
Behfarnia and Behravan (2014)	High performance polypropylene fibres (HPP) 0.8% Steel fibre 0.8% Dimension of the specimens: 100x100x350	- Effect of fibres on the mode of failure: the addition of either steel or synthetic fibres led to more ductile failure where the fibres prevented the sudden failure, while plain concrete showed a brittle failure. - Effect on the first crack load: the addition of steel fibre resulted in an increase of up to 17.4%, while synthetic fibre resulted in an increase of up to 33.7% compared to the plain concrete. - Effect on the flexural strength: the incorporation of synthetic fibre outperformed concrete with steel in terms of flexural strength as the flexural strength ratio of HFRC samples to SFRC samples (HFRC/SFRC) for all fibre volume percentages exceeded 0.86. - Effect on toughness: significantly larger area under the toughness diagram can be observed for specimens with synthetic fibre with a value of 22.6 compared to specimens with steel fibre with a value of 11.6 once the first crack occurred.
Yoo et al. (2013)	Four different volumes of steel fibres: 1%, 2%, 3% and 4%. Dimension of the specimens: 100x100x500	- Effect on the initial stiffness: the steel fibre volume content had no effect. - Effect on the maximum load: an increase in steel fibre content had a significant impact with no rapid load drop after failure, which showed an increase of 27%, 42% and 47% for 2% (V2), 3% (V3) and 4% (V4), respectively, compared to 1% (V1) of steel fibre.

Yoo et al. (2014)	Comparing the four different fibre lengths for steel fibre content of 2% (13mm, 16.3mm, 19.5mm and 30mm). Dimension of the specimens: 100x100x400	- Effect on the initial stiffness: the length of fibre had minimal effect. - Effect on the peak flexural load: as the effective bonding area between the fibre and matrix at fracture surfaces increased, the peak flexural load increased following an increase in fibre length up to 19.5mm. Conversely, the specimen with a fibre length of 30mm exhibited a reduction in peak load because it was challenging to equally distribute the fibre in the matrix and there were fewer fibres at the crack planes.
Yoo et al. (2015)	Steel fibres with four different volumes (0%, 0.5%, 1.0% and 2.0%) for normal concrete (NC) and high strength concrete (HSC), with two fibre volumes (0% and 2%) for ultra-high strength concrete (UHSC). Dimension of the specimens: 100x100x400	- Effect on the flexural strength: The inclusion of fibres resulted in higher flexural strength compared to the reference beams without fibres for high strength concrete (HSC). Specifically, at fibre percentages of 0.5%, 1.0%, and 2.0%, the flexural strength increased by 8%, 13%, and 29% respectively.
Meda et al. (2012)	Two different dosage of steel fibre (30kg/m^3 and 60kg/m^3) Dimension of the specimens: 200x300x4000	- Effect of fibre on the mode of failure: the addition of fibres shifted the failure mode from a sudden fracture in concrete to more ductile failures, likely due to reinforcement rupture rather than concrete crushing.

		- Effect on the ductility: the addition of 30kg/$m^3$of steel fibres increased ductility by approximately 73.1% when compared to plain concrete, whereas the addition of 60kg/m^3 steel fibres had an insignificant effect on ductility when compared to the lower fibre volume (30kg/m^3), but showed a higher ductility compared to plain concrete by approximately 21.2%.
Pająk and Ponikiewski (2013)	The use of different types of steel fibres (straight and hooked end) with three different volumes (0.5%, 1.0% and 1.5%). Dimension of the specimens: 150x150x500	- Effect on the flexural behaviour: the type of steel fibres significantly affected the flexural behaviour of the tested beams. Hooked-end steel fibres achieved a higher flexural strength than the straight fibres and plain concrete; these increases were 5%, 76% and 117% and 55%, 150% and 239% for 0.5%, 1.0%, and 1.5%, respectively, when compared to straight fibres and plain concrete - Effect on the maximum load: the increase in the percentage of fibre volume of both straight and hooked-end steel fibres increased the maximum load. These increases were 35%, 53% and 94% for straight steel fibre with volume fraction of 0.5, 1.0 and 1.5, respectively. - Hooked-end steel fibres achieved a higher maximum load than the straight fibres and plain concrete; these increases were 13%, 46% and 57% and 53%, 123% and 205% for 0.5%, 1.0%, and 1.5%, respectively, when compared to straight fibres and plain concrete.
Kim et al. (2013)	PVA fibre was used as the reinforcement. Dimension of the specimens: 300x500x3400	- Effect on the mode of failure: all specimens exhibited a typical failure of under reinforced beams. The failure occurred by the yielding of the tensile reinforcement followed by the crack propagated upwards towards the upper part of the beams.
Meza and Siddique (2019)	The test consisted of comparing virgin fibres with	- Effect on the mode of failure: plain concrete failed almost after the formation of the first visible crack in the tension zone.

	recycled plastic fibres with 2kg/m^3, 6kg/m^3, and 10kg/m^3 Dimension of the specimens: 150x150x500	- The incorporation of both types of fibres prevented concrete beams from breaking into two pieces during failure and continued to carry the load until the concrete beam could no longer carry any additional load. - Effect on the first visible crack: most of the beams exhibited a similar load at the formation of the first visible crack in the tension zone. - Effect on the flexural toughness: the incorporation of the fibres generally enhanced the flexural toughness index value ranged from 20 to 80 based on the fibre volume fraction.
Hamoush et al. (2010)	Micro Polyvinyl Alcohol (PVA) and micro PVA fibre with steel bars. Dimension of the specimens: 102x102x356 133x140x1830	- Effect on the mode of failure: the specimens with micro fibre reinforcement showed signs of ductile failure and carried load until complete failure occurred, while the plain concrete suffered a brittle failure. - Effect of fibre on the ductility: the contribution of micro fibres was more noticeable in the post-cracking response, as witnessed by an increase in post cracking ductility which was associated with the pull-out of fibre's bridging effect at failure, whereas the pre-cracking behaviour was not significantly changed. - Effect on the peak load and the first cracking strength: the addition of fibre also demonstrated that the peak load and first cracking strength had insignificant improvements.
Oh (1992)	Steel fibres ranged from 0 to 2%. Dimension of the specimens: 120x180x2000	- Effect of fibre on the ductility: the inclusion of steel fibres significantly increased the ductility and ultimate resistance. - Effect on the flexural strength and peak load: the incorporation of steel fibres significantly increased the flexural strength by 60% when the fibre content was increased to 2% and the peak load increased up to 50% when compared to the reference beams without fibres.

Singh et al. (2006)	1.0%, 1.5% and 2.0% volumes of steel fibres	- Effect on the static flexural strength: the static flexural strength of SFRC significantly increased relative to that of plain concrete by 39%, 58% and 67% for 1.0%, 1.5% and 2.0% volumes of fibres added to concrete, respectively.
Meng et al. (2018)	A cementitious composite made of PVA for static and fatigue flexural loading. Dimension of the specimens: 100x100x350	- Effect on the mode of failure: the polyvinyl alcohol engineered cementitious composite (PVA-ECC) beams had a superior ductile failure mechanism in addition to having greater flexural strength, which is 1.9 times higher and ductility, while normal concrete beams, a brittle failure mode was observed in which a single crack formed rapidly and with a sharp reduction in the flexural stress at peak from 5 MPa to zero.
Chenkui and Guofan (1995)	Steel fibre ranged from 0% to 2% with three different lengths of fibre (25mm, 35mm and 45mm). Dimension of the specimens: 150x150x550	- Effect on the flexural strength and toughness: incorporating steel fibres improved ultimate flexural strength and flexural toughness of every set of specimens. The increase in the flexural strength was approximately 3%, 8% 16% and 18.5% for volume fraction of 0.5, 1, 1.5 and 2, respectively, compared to normal concrete. The flexure toughness, as indicated by the flexural index, varied between 5 and 9 for different volume fraction of steel fibres.

Vasanelli et al. (2014)	Different types of fibres: steel (ST) and polyester (POL) fibres with volumes of 0.6% and 0.9%, respectively. Dimension of the specimens: 250x250x3000	- Effect on the mode of failure: all of the tested beams failed by concrete crushing after yielding of steel bars in tension. - Effect on the first cracking load: only for ST beams compared to control specimen (TQ) beam was there a slight increase in the first cracking load (almost 14%) and steel yielding load (almost 8%). - Effect on the stiffness: the increase in stiffness caused by fibres was quite noticeable after cracking (at step 1, equal to 26%) and after steel bars yielded (at step 5, equal to 14%). In fact, compared to plain concrete, the post-cracking residual strength of FRC increased tension stiffening. This effect was most significant immediately after cracking when the stress contribution of plain concrete was significantly reduced, and after steel bar yielding when the abrupt increase in steel deformability was mitigated by the presence of fibres.

2.4.2 Performance of HyFRC beams on flexural properties

As summarised in Table 2.5, previous studies consistently demonstrated that the hybridisation techniques lead to improvements in the flexural properties. The literature provides significant evidence of the positive effects of hybridisation of steel and polypropylene fibres (Li et al., 2018; Yap et al., 2014; Guo et al., 2021). Incorporating fibres of different types and lengths resulted in significant enhancement in flexural strength and toughness, as can be seen in Figure 2.6 and Figure 2.7. This finding emphasised the importance of selecting and combining fibres to achieve the desired mechanical properties.

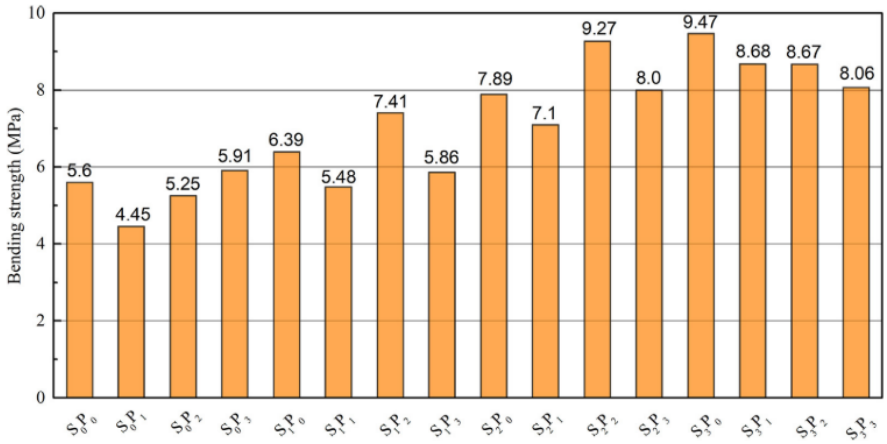

Figure 2.6: Bending strength hybrid steel-polypropylene fibres (From Guo et al., 2021): where is S_0, S_1, S_2, S_3: Steel fibre volume fraction of 0%, 2.0%, 2.5%, and 3.0%, respectively. P_0, P_1, P_2, P_3: Polypropylene fibre volume fraction of 0%, 0.12%, 0.17%, and 0.22%, respectively

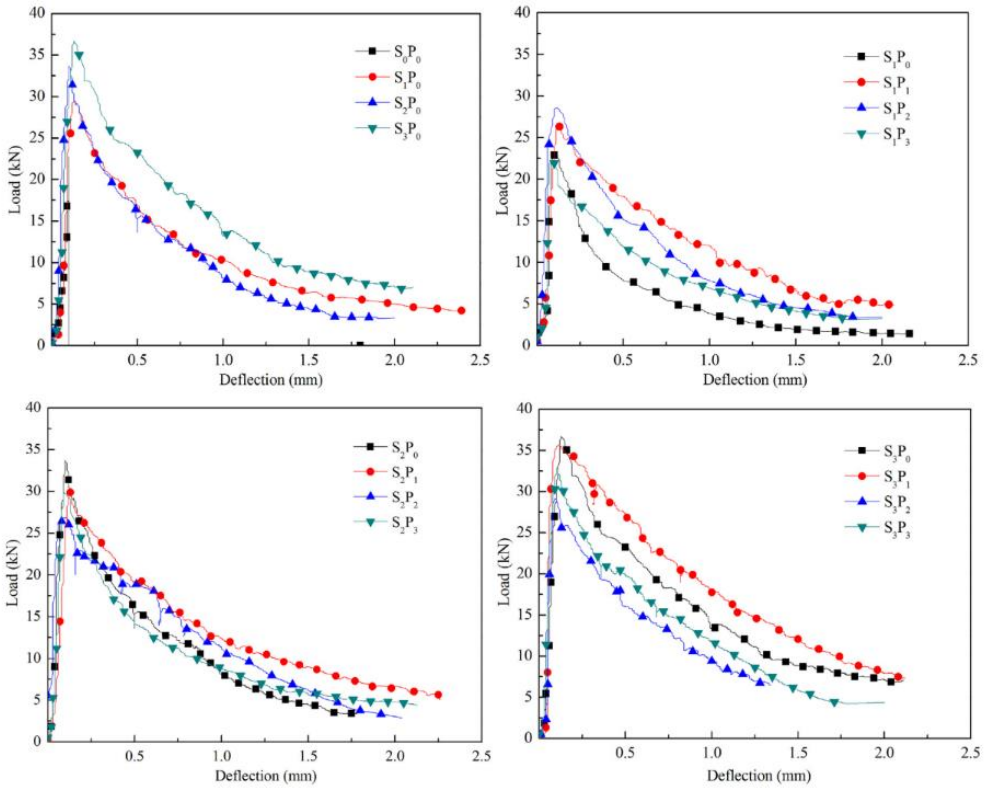

Figure 2.7: Load-deflection curves for the effect of combining hybrid steel-polypropylene fibres (From Guo et al., 2021). S_0, S_1, S_2, S_3: Steel fibre volume fraction of 0%, 2.0%, 2.5%, and 3.0%, respectively. P_0, P_1, P_2, P_3: Polypropylene fibre volume fraction of 0%, 0.12%, 0.17%, and 0.22%, respectively

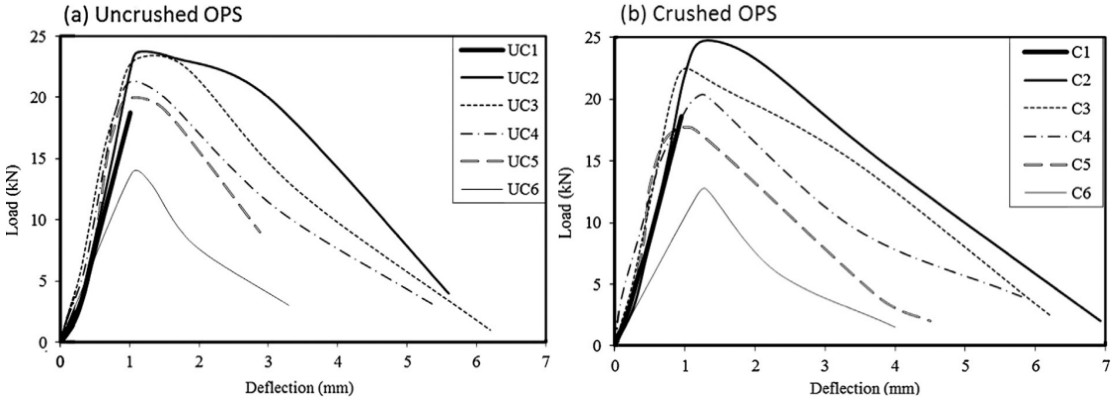

Figure 2.8: Load-deflection curve of specimens with steel and polypropylene fibres (From Yap et al., 2014). Uncrushed aggregate (UC1) and crushed aggregate (C1): Steel fibre volume fraction of 1.0% and polypropylene fibre volume fraction of 0.0%. UC2 and C2: Steel fibre volume fraction of 0.9% and polypropylene fibre volume fraction of 0.1%. UC3 and C3: Steel fibre volume fraction of 0.75% and polypropylene fibre volume fraction of 0.25%. UC4 and C4: Steel fibre volume fraction of 0.6% and polypropylene fibre volume fraction of 0.4%. UC5 and C5: Steel fibre volume fraction of 0.0% and polypropylene fibre volume fraction of 1.0%

The combination of steel and polypropylene fibres has been identified as the optimal choice for hybrid fibres (Li et al., 2018). This particular combination exhibited superior performance in terms of flexural strength, peak load, and post-crack toughness, as can be seen in Figure 2.8 and Figure 2.9. These results suggested that the hybridisation of steel and polypropylene fibres enhanced the durability and load-carrying capacity. Furthermore, the incorporation of fibres with different types and geometries has been found to change the mode of failure from brittle to more ductile. This change indicated an improvement in the material's ability to undergo deformation and absorb energy before failure occurred. This finding was particularly significant as it suggested that the hybridisation of fibres enhanced the structural behaviour and the consistency of the composite material. Hence, the benefit of combining micro and macro polypropylene fibres to steel fibres was not studied together and further research is needed.

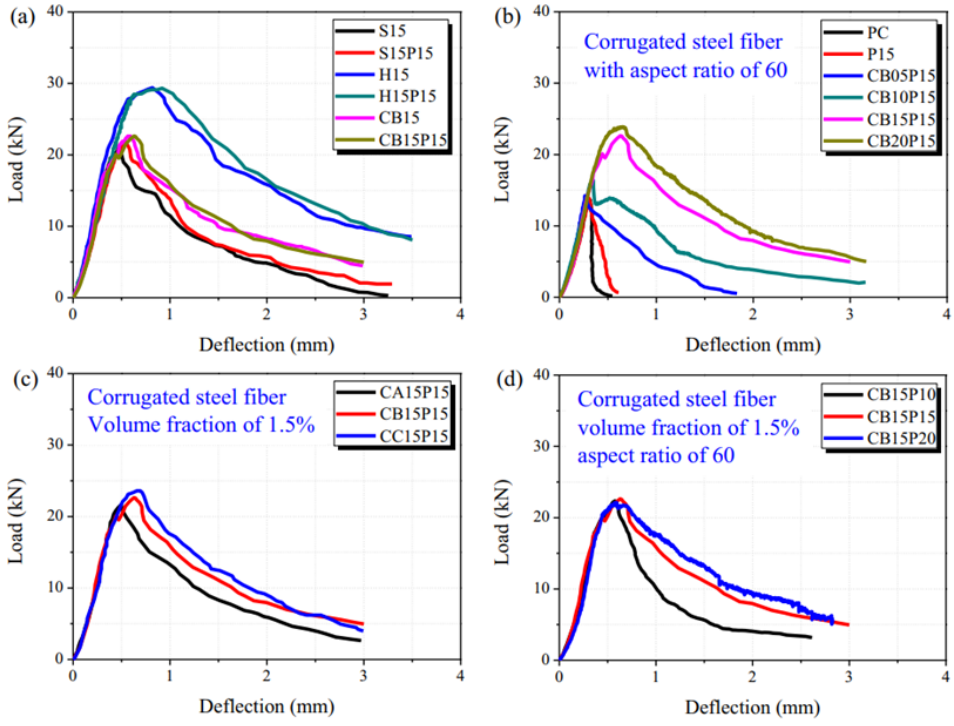

Figure 2.9: Load-deflection curves of different combination of steel-polypropylene hybrid fibre (From Li et al., 2018). PC for plain concrete without fibre, P15 for polypropylene fibre volume fraction of 0.15%, P20 for polypropylene fibre volume fraction of 0.2%, S15 for straight steel fibre volume fraction of 1.5%, H15 for hooked-end steel fibre volume fraction of 1.5, CB05 for corrugated steel fibre volume fraction of 0.5%, CB10 for corrugated steel fibre volume fraction of 1.0%, CB15 for corrugated steel fibre volume fraction of 1.5%, CA15 for corrugated steel fibre volume fraction of 1.5% and CC15 for corrugated steel fibre volume fraction of 1.5%

Table 2.5: Summary on influence of fibres on flexural properties of HyFRC

Authors	Variables, fibres volume fraction and dimension of beams (mm)	Effect of fibre on the property
Fallah and Nematzadeh (2016)	Macro polymeric (MP) fibres ranged from 0.25% to 1.25%, whereas the amount of micro polypropylene fibres (PP) ranged from 0.1% to 0.5%. Different hybrid volumes of fibres	- Effect on the flexural strength: specimens cast with 0.5% macro and 0.5% micro fibres exhibited that the flexural strength was reduced by 8.23%. - Specimens cast with 0.9% MP and 0.1% micro polypropylene fibres demonstrated the greatest increase in flexural strength with an average of 18.04% relative to the plain concrete.
Kim et al. (2011)	Different types for hybrid fibres of macro and micro steel fibres. The volume fractions of fibre varied from 0.0%, 0.5%, 1.0%, and 1.5%.	- Effect on the flexural strength: beams which were cast with macro fibres recorded significantly greater flexural performance in terms of energy absorption and deflection than those cast only with micro fibres. These increases in deflection were 45.4-75.9% higher when the volume fraction of macro fibre was 1% and micro fibre (SS) was 1% compared to a volume fraction of 2% for micro fibre. Additionally, the toughness was higher by approximately 48.7-67.9%. - Beams cast with HB (hooked-end) steel fibres demonstrated superior performance in terms of flexural strength compared to other fibre types. The increase in volume fraction of fibres from 0% to 1.5% resulted in an improvement in flexural strength, with HB fibres showing the highest increase at 94%. Long smooth fibres (LS) had an increase

		of 78%, twisted fibres (T) had an increase of 67%, and HA (hooked-end) fibres had the lowest increase at 28%. - Effect on the toughness: beams cast with hybrid fibres of LS-SS, HA-SS, HB-SS and T-SS offered greater toughness by 65%, 49%, 67% and 55%, respectively, relative to only micro fibres (SS) with 2%.
Caggiano et al. (2012)	Steel fibre with volumes of 0.5% and 1.0% with five different percentages and two different lengths. Dimension of the specimens: 150x150x600	- Effect on the first crack strength: fibre combination had a minimal effect on first-crack strength when the volume fraction of fibre is 0.5% for both short and long fibres. On the other hand, the increase of fibre content to 1.0% showed a slightly more regular trend, which means that the presence of higher volume fraction of fibres started to have a noticeable strength. - Effect on the post-cracking toughness: fibres significantly increase the SFRC's post-crack toughness at volumes both 0.5% and 1.0%, which indicated the ability of a material to resist further crack propagation and absorbed energy after the initiation of cracks. - It was observed from the test results that the specimens containing 1.0% steel short fibres exhibited a significant hardening behaviour in the flexural post-cracking regime, which indicated the effect of short fibres with higher content on the peak and post peak strength but specimens with 0.5% fibre often displayed a softening behaviour.
Li et al. (2018)	Steel-polypropylene hybrid FRC beams.	- Effect on the flexural behaviour and peak load: the hybridisation of steel-polypropylene improved the residual

	The test parameters included three different steel fibres (straight, hooked-end and corrugated fibre) and monofilament polypropylene fibres. Dimension of the specimens: 100x100x400	strength, led to more ductile behaviour and fibres, showed positive effect on the mode of failure from brittle to ductile failure. The addition of hooked-end steel fibres to beams exhibited the highest flexural loads, compressive, tensile strength toughness and deflection due to their higher bond strength. - Specimens with only hooked-end steel fibres offered the greatest peak load by approximately 29 kN followed by the hybridisation of hooked-end and polypropylene fibres with almost the same load. Specimens with hooked-end steel fibres and polypropylene fibres (volume fraction of 1.5% and 0.15%, respectively) exhibited the highest residual strength of 28.561 kN, which was accredited to the bond strength between fibres and the matrix.
Yap et al. (2014)	Different fibre combinations (hybrid steel-polypropylene fibres). Dimension of the specimens: 100x100x500	- Effect on the post-cracking failure: none of the control concrete specimens exhibited post crack-failure strength, but the specimens with fibres exhibited greater flexural toughness. The concrete composition (fibres) can significantly enhance the post-failure strength of concrete after the first crack. - It was observed that 1% polypropylene PP fibres diminish the tensile strength, flexural deflection and ductility. - Beams cast with 1% steel fibre achieved the greatest increase in flexural toughness, which was between 40% and 70% greater than the control mixes for crushed and uncrushed oil palm shell (OPS) concrete. - Effect on the flexural strength: the incorporation of hybrid fibres (0.9% steel

		and 0.1% polypropylene fibres) improved the flexural strength by up to 34% and enhanced post-cracking toughness.
Guo et al. (2021)	Combining hybrid steel-polypropylene fibres. The test parameters included three different volumes of steel fibres (2.0%, 2.5% and 3.0%) and three different volumes of polypropylene fibres (0.12%, 0.17% and 0.22%). Dimension of the specimens: 100x100x400	- Effect on the mode of failure: based on the load-deflection curve for plain concrete, brittle fractures occurred when the load approached the failure limit, with elastic deformation being the dominating stage. - Effect on the fracture toughness: the fracture toughness of the concrete significantly increased as the volume of steel fibres was increased, owing to their high tensile strength and elastic modulus. However, when the volume of steel fibres was increased from 2% to 3%, the addition of steel fibres had no effect in terms of toughness. - The incorporation of hybrid steel-polypropylene fibres had the greatest toughening effect, particularly when the volume of steel fibres was 2%, 2.5% and 3.0% with 0.12% of polypropylene fibres. - Effect on the bending strength: increasing the amount of steel fibre gradually enhanced the bending strength by 14%, 41% and 69% for volume fraction of 2, 2.5 and 3, respectively. However, the addition of polypropylene fibre initially decreased the bending strength at volume fraction of 0.12 and 0.17, but higher levels of polypropylene (0.22) increased the bending strength by approximately 5.5%. The addition of 3% steel fibre produced the greatest increase in bending strength followed by the hybrid 2% of steel fibre and 0.17% polypropylene fibre.

Pajak and Ponikiewski (2017)	Two different types of steel fibres (straight and corrugated), two different lengths (6mm and 35 mm) and different volumes of steel fibres varied from 1% to 3%. Dimension of the specimens: 100x100x400	- Effect on the mode of failure: all of the specimens exhibited the typical failure pattern with a single crack. - Effect on the flexural strength: the flexural characteristics of hybrid fibre of self-compacting concrete (HFR-SCC) were improved by incorporating long corrugated fibres to a greater extent than by incorporating short fibres by approximately 35.56% when compared to normal concrete. In terms of flexural behaviour, the straight fibres with 0.5% when mixed with corrugated 1.5% improved the peak load by approximately 35.49% for (0.5 straight and 1.5 corrugated fibres). Similarly, the incorporation of same fibre content improved the flexural strength by 35.56% and improved the post-peak parameters. The toughness was improved with the addition of 1% straight and 1% corrugated fibres by about 35.48 Nm. Further increase in the toughness was obtained by mixing a hybrid combination of 1.5% straight and 1.5% corrugated fibres, resulted in an improvement of approximately 36.95 Nm.
Sahoo et al. (2015)	Steel and polypropylene fibres with two different volumes (0.5% and 1.0%), different volumes of hybrid fibres: 0.5% and 0.5%, 1.0% and 0.5%, and 1.0% and 1.0% for steel and	- Effect on the flexural strength: it was established that the flexural tensile strength for the SFRC1 (0.5% of steel fibre) and CFRC1 (0.5% of steel fibre and 0.5% of polypropylene fibre) specimens were almost identical for the load displacement curve, which showed a displacement of 20 mm at a load of 100 kN, indicating that the contribution of polypropylene fibres to the flexural tensile strength was insignificant in

	polypropylene fibres, respectively. Dimension of the specimens: 150x200x2000	comparison to that of the steel fibres. As expected, the initial flexural stiffness of each specimen was almost identical, which is equal to 12 kn/mm. - The incorporation of two different volumes of steel fibres to the test beams increased the ultimate resistance (approximately 6%) higher than that of the RC specimens, whereas the incorporation of 1% polypropylene fibre to the test beams produced a reduction in peak load of approximately 7% when compared to the reference specimens.
Soutsos et al. (2012)	Hybrid steel-polypropylene fibres with four different types of steel fibres and one type of polypropylene fibre were used for the FRC specimens. Three different steel fibre dosages (30kg/m^3, 40kg/m^3 and 50kg/m^3) and two polypropylene fibres dosages (4.6kg/m^3 and 5.3kg/m^3) for steel and polypropylene fibres were employed. Dimension of the specimens: 150x150x550	- Effect on the flexural strength: the hooked-end type achieved the highest flexural strength of 2.6 MPa, 3.4 MPa and 3.6 MPa for 30kg/m^3, 40kg/m^3 and 50kg/m^3. - Effect on the post-crack behaviour and flexural toughness: the length of the fibres also had an impact on the post-crack behaviour, with the 60mm length outperforming the 50mm length. It was established that the addition of hooked-end steel fibres significantly increased the flexural toughness of concrete with a value of 80 J. The lowest flexural toughness value attained with a steel fibre dosage of 30kg/m^3 was almost exactly matched by the synthetic fibres at the dosage of 4.6kg/m^3 by approximately of 36 J A similar pattern was observed when the dosage was increased to 5.3kg/m^3, which had a flexural toughness of 48 J, which was close to the low end values attained with 50 kg/m^3 of steel fibres.
Suthiwarapirak et al. (2004)	Two different volumes of 2.1%	- Effect on the flexural strength: it was demonstrated from the test results that

	and 1.5% for polyvinyl (PVA) and polyethylene (PE), respectively, mixed with 1% steel fibre. Dimension of the specimens: 100x100x400	both PVA-ECC and PE-ECC had higher ultimate flexural strengths by 29.23% and 47.33% than FRC, respectively.
Zhu et al. (2022)	Three different fibre volumes of each hybrid type (1.5% and 0.5%, 1.25% and 0.75%, and 1.0% and 1.0%, for polyethylene and steel fibre, respectively) with a total of 2% hybrid fibre were used.	- Effect on the flexural strength and ductility: using more PE fibre often led to greater ductility and lower flexural strength, whereas using more steel fibre enhanced the flexural strength but reduced the ductility of the beams. These increases in the flexural strength were 46.98 MPa, 49.29 MPa and 53.50 MPa for(1.5%PE+0.5%ST), (1.25%PE+0.75% ST) and (1.0%PE+1.0%ST). It is apparent from the test results that the ECC-A (1.5%PE+0.5%ST) offered the best ductility (nearly twice as much as ECC-C) in terms of the biggest deformation at peak load, whereas ECC-C (1%PE+1%ST) demonstrated the highest flexural strength (approximately 13% more than ECC-A) but the lowest ductility.
Wu et al. (2022)	Hybrid fibre-polymer (HCHFPC), namely steel ultrashort-fine (USHSF) and hooked-end steel fibre (HESF) and polypropylene fibres (PF). Three different fibre volumes of	- Effect on the flexural strength: HCHFPC consistently had a greater flexural strength than PC approximately by 190%, 111% and 191% for 3-day, 7-day and 28-day, respectively. The authors reported that HCHFPC formed a phenomenon of coupling through the bonding between the hybrid fibres and concrete, indicating that HCHFPC did not break immediately

	USHSF, HESF and PF (4.0%, 1.92% and 0.27%, respectively) were used.	following cracking and continued to provide a limited amount of flexural bearing function under the bonding effect of fibres.

2.5 Influence of fibres on fatigue

In various concrete structures such as airport runways, railway bridges, road pavements and offshore structures, fatigue is a prevalent phenomenon (Bhowmik and Ray, 2018). Fatigue failure in reinforced concrete (RC) structures occurs as a result of damage to the material components (concrete or steel) and the bond between them (Yuan et al., 2018). Therefore, the design of RC structures is with fatigue-resistant is intended to address these capacity limitations. Fatigue is considered the most critical factor in controlling the design of RC structures that experience repeated loading (Yuan et al., 2018). Researchers have observed that the fatigue resistance of each specimen can vary due to inherent flaws, resulting in variations in fatigue life under the same fatigue load. This indicates that the ability of a specimen to withstand fatigue depends on its individual characteristics and quality.

2.5.1 Performance of NC and FRC beams on fatigue

The findings summarised in Table 2.6 demonstrated that the incorporation of steel fibres in concrete beams extended their fatigue life, as reported by Parvez and Foster (2014). The study showed a significant improvement in fatigue life for concrete beams with fibre volumes of 0.4% and 0.8% and an aspect ratio of 80, while beams with an aspect ratio of 65 showed no improvement in fatigue life. This discrepancy was attributed to the influence of aspect ratio on fatigue performance, suggesting that the aspect ratio played a crucial role in determining the effectiveness of steel fibres in enhancing fatigue resistance. Similar results reported by Singh et al. (2006) demonstrated that increasing fibre content from 0% to at least 1.0% led to significant improvements in fatigue performance, as shown in Figure 2.10.

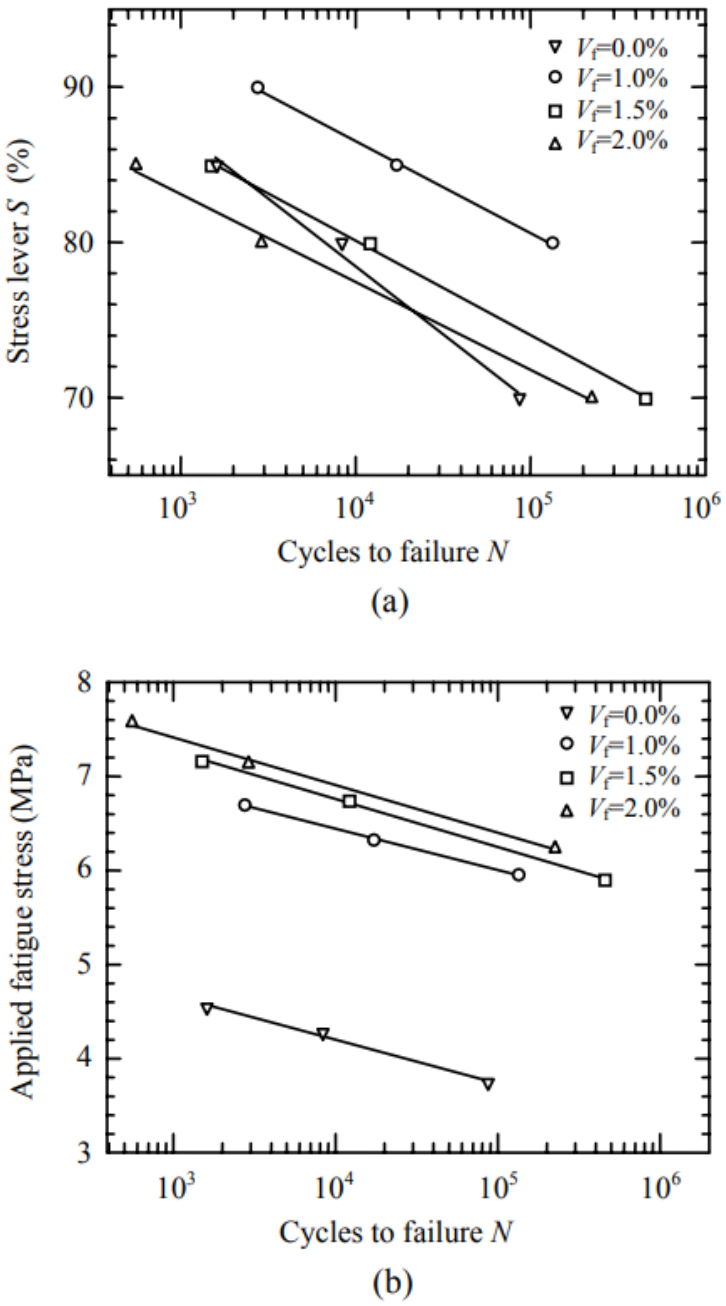

Figure 2.10: Effect of steel fibre with different stress levels and applied fatigue stress represented with number of cycles (From Singh et al., 2006)

However, their results also indicated a decline in performance when higher fibre volumes were added, suggesting the existence of an optimal fibre content for enhanced fatigue resistance. Banjara and Ramanjaneyulu (2018) observed a decrease in fatigue life when using a fibre volume of 2% compared to specimens with 1% steel fibre volume, attributing the decline to fibre-fibre interaction or congestion that hindered the reinforcing effect. In addition to steel fibres, the incorporation of polypropylene fibres in concrete was found to increase fatigue

life, as indicated by the studies of Mohamadi et al. (2013) and Meng et al. (2018), as demonstrated in Figure 2.11. Different fatigue stress levels indicated a different number of cycles and the reduction in stress levels led to a higher number of cycles, as depicted in Figure 2.12 (Gao et al., 2021). Meng et al. (2018) and Gao et al. (2021) stated that the stress ranges influenced how mid-span deflection and crack width evolve. With a reduction in stress range, the maximum deflection and crack width that can be maintained before the ultimate failure stage declined, as shown in Figure 2.13 and 0% fibre volume fraction (BF0-6): specimens with 0% fibre volume fraction and a stress level of 0.6, 0.5% fibre volume fraction (BF0.5-6): specimens with 0.5% fibre volume fraction and a stress level of 0.6, 1.0% fibre volume fraction (BF1.0-6): specimens with 1.0% fibre volume fraction and a stress level of 0.6 and 1.5% fibre volume fraction (BF1.5-6): specimens with 1.5% fibre volume fraction and a stress level of 0.6.

Figure 2.14. The incorporation of fibres resulted in a reduction in the mid-span deflection and crack width and with an increase in the fibre volume fractions led to a higher reduction, as can be seen in 0% fibre volume fraction (BF0-6): specimens with 0% fibre volume fraction and a stress level of 0.6, 0.5% fibre volume fraction (BF0.5-6): specimens with 0.5% fibre volume fraction and a stress level of 0.6, 1.0% fibre volume fraction (BF1.0-6): specimens with 1.0% fibre volume fraction and a stress level of 0.6 and 1.5% fibre volume fraction (BF1.5-6): specimens with 1.5% fibre volume fraction and a stress level of 0.6.

Figure 2.14 and Figure 2.15.

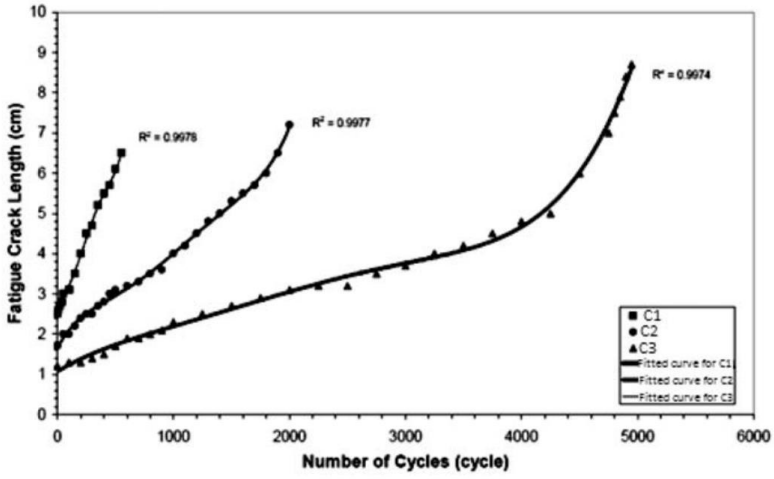

a) For plain concrete (C)

C1: Applied load of 0.7 times the bending strength of plain concrete, C2: Applied load of 0.8 times the bending strength of plain concrete and C3: Applied load of 0.9 times the bending strength of plain concrete

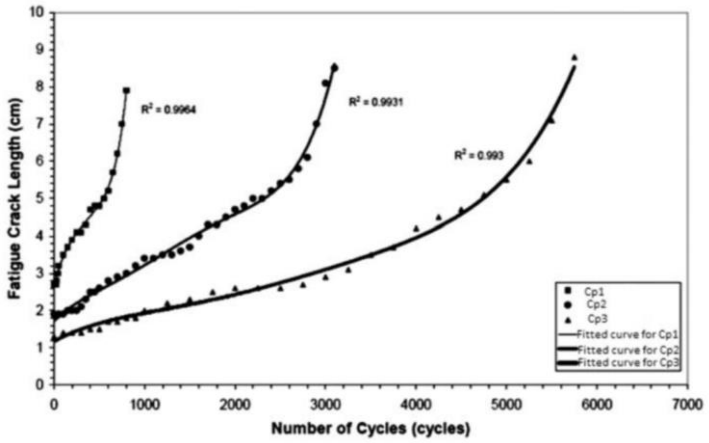

b) For polypropylene fibre reinforced concrete (C_p)

C_{p1}: Applied load of 0.7 times the bending strength of plain concrete, C_{p2}: applied load of 0.8 times the bending strength of plain concrete and C_{p3}: Applied load of 0.9 times the bending strength of plain concrete

Figure 2.11: Fatigue crack growth of plain and polypropylene fibre-reinforced concrete with three different stress levels (From Mohamadi et al., 2013)

These findings collectively emphasised the potential of steel fibres in improving fatigue life and flexural fatigue strength of concrete. It is important to consider the optimal fibre dosage to avoid potential negative effects on fatigue resistance, as clustering and reduced stress transfer between fibres can hinder the reinforcing effect. Further research is needed to determine the optimal fibre content and aspect ratio for different applications and loading conditions to maximise the fatigue performance of concrete structures.

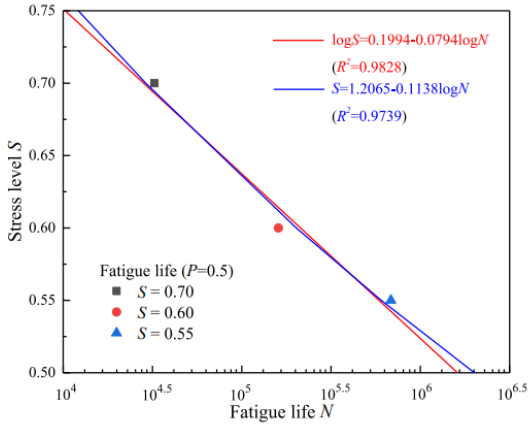

Figure 2.12: Different stress level with fitting the S-N relation with a 50% reliability (From Wu et al., 2022). Stress level of 0.7 as a percentage of the maximum static strength, stress level of 0.6 as a percentage of the maximum static strength and stress level of 0.55 as a percentage of the maximum static strength

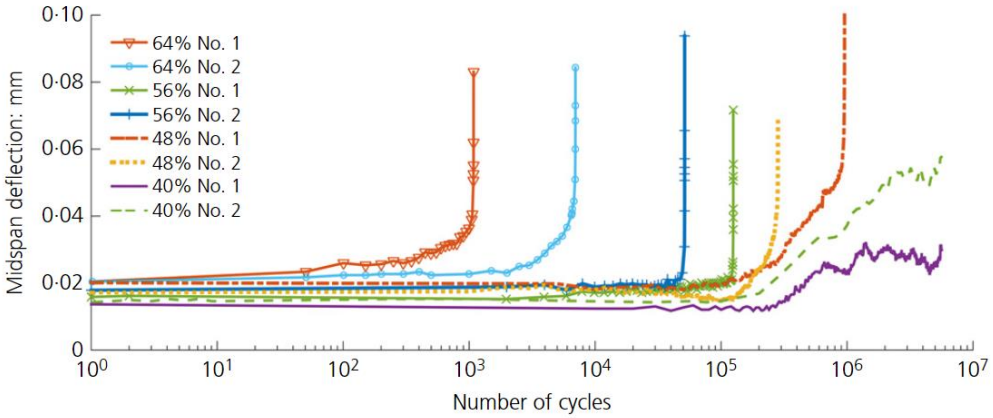

a) The development of mid-span deflection of normal concrete beams vs fatigue life

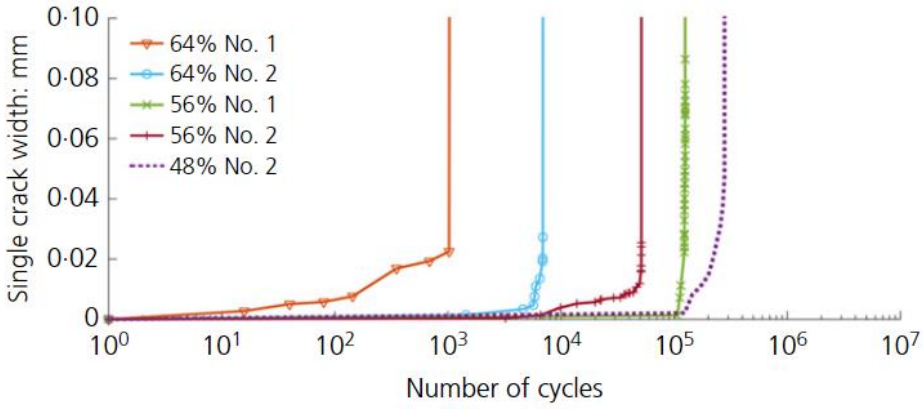

b) The development of crack width of normal concrete beams vs fatigue life

64% max static strength: stress level of 0.64 as a percentage of flexural strength of corresponding materials, 56% max static strength: stress level of 0.56 as a

percentage of flexural strength of corresponding materials, 48% max static strength: stress level of 0.48 as a percentage of flexural strength of corresponding materials, 40% max static strength: stress level of 0.40 as a percentage of flexural strength of corresponding materials and 32% max static strength: stress level of 0.32 as a percentage of flexural strength of corresponding materials

Figure 2.13: The development of mid-span deflection and crack width for all beams vs fatigue life (From Meng et al., 2018)

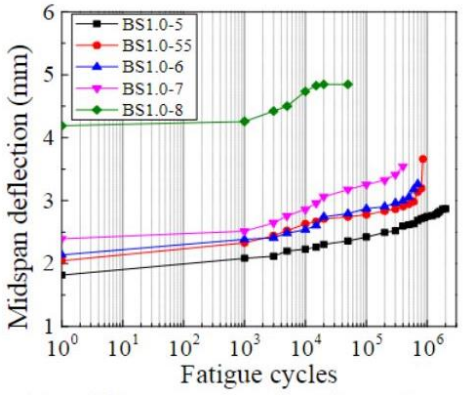

a) Different stress levels series

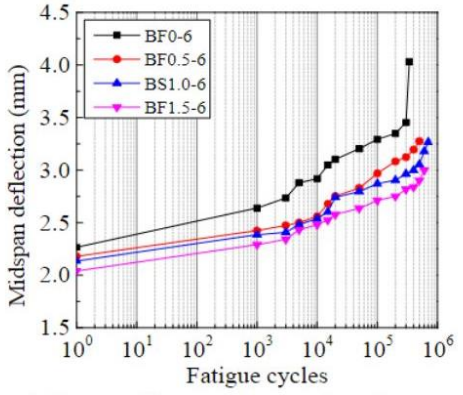

b) Different fibre volume fraction series

i) Effect of stress levels and fibre volume fraction on deflection

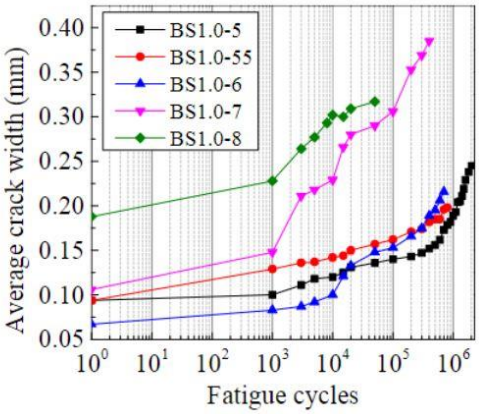

c) Different stress levels series

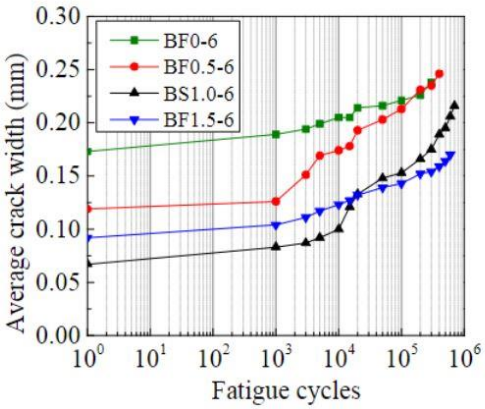

d) Different fibre volume fraction series

ii) Effect of stress levels and fibre volume fraction on crack width

For specimens with different stress levels with 1% of steel fibre in Figure 2.14(a), stress level of 0.5 as a percentage of the maximum static strength (BS1.0-5), stress level of 0.55 as a percentage of the maximum static strength (BS1.0-55), stress level of 0.6 as a percentage of the maximum static strength (BS1.0-6), stress level of 0.7 as a percentage of the maximum static strength (BS1.0-7) and stress level of 0.8 as a percentage of the maximum static strength (BS1.0-8).

For specimens with the same stress levels of 0.6 with different volume fraction of steel fibre in Figure 2.14(b), 0% fibre volume fraction (BF0-6): specimens with 0% fibre volume fraction and a stress level of 0.6, 0.5% fibre volume fraction (BF0.5-6): specimens with 0.5% fibre volume fraction and a stress level of 0.6, 1.0% fibre volume fraction (BF1.0-6): specimens with 1.0% fibre volume fraction and a

stress level of 0.6 and 1.5% fibre volume fraction (BF1.5-6): specimens with 1.5% fibre volume fraction and a stress level of 0.6.

Figure 2.14: Mid-span deflection and crack widths with the number of fatigue cycles (From Gao et al., 2021)

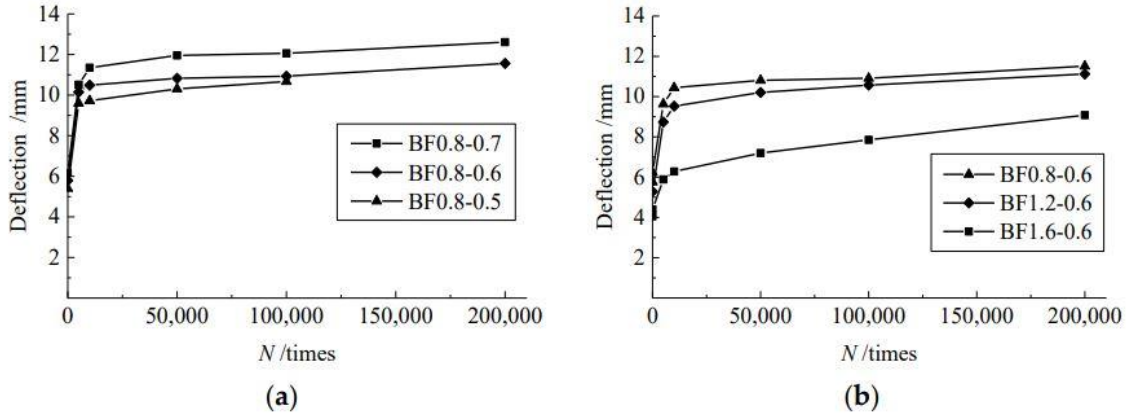

i) Various depth

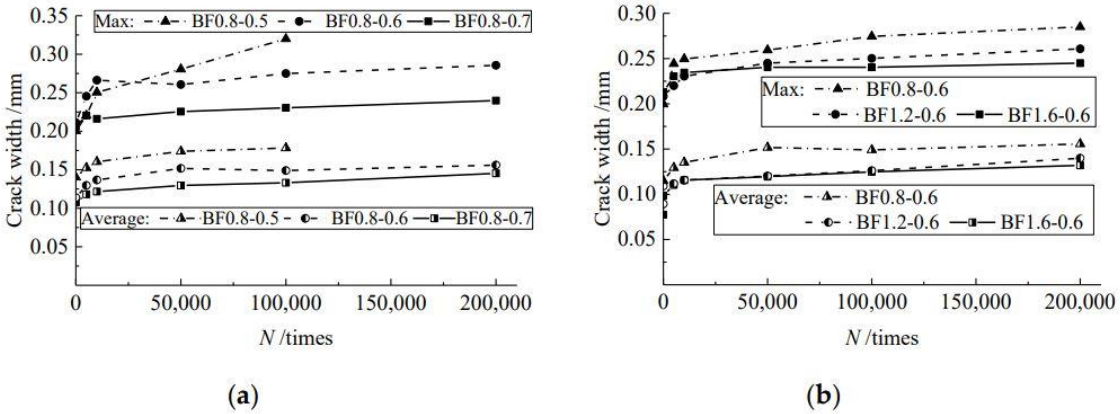

ii) Volume fractions of fibres

For specimens with different stress levels with 0.8% of steel fibre in Figure 2.15(a), stress level of 0.5 as a percentage of the maximum static strength (BF0.8-0.5), stress level of 0.6 as a percentage of the maximum static strength (BF0.8-0.6) and stress level of 0.7 as a percentage of the maximum static strength (BF0.8-0.7).

For specimens with the same stress levels of 0.6 with different volume fraction of steel fibre in Figure 2.14(b), specimens with 0.8% fibre volume fraction and a stress level of 0.6 (BF0.8-0.6), specimens with 1.2% fibre volume fraction and a stress level of 0.6 (BF1.2-0.6) and specimens with 1.6% fibre volume fraction and a stress level of 0.6 (BF1.6-0.6).

Figure 2.15: Mid-span deflection and crack width with number of cycles (From Qu et al., 2019)

Table 2.6: Summary on the influence of fibres on fatigue

Authors	Variables, fibres volume fraction and dimension of specimens (mm)	Effect of fibre on the property
Parvez and Foster (2014)	Steel fibre with variable fibre volumes of 0%, 0.4% and 0.8% with different load levels of 20-74% and 20-70%. Dimension of the specimens: Series one: 100x200x1200 and series two: 180x300x3000	- Effect on fatigue: the addition of steel fibres prolongs the fatigue life of concrete beams. Beams of series one exhibited an increase in fatigue life by an average of 39% and 40% with 0.4% and 0.8% fibre, respectively. Meanwhile, beams of series two with 0.4% and 0.8% fibre and an aspect ratio of 80 at a stress level of 0.7 exhibited an increase in fatigue life of approximately 47% and 182%, respectively. However, beams in series one with an aspect ratio of 65 and fibre volume of 0.4% and 0.8% exhibited no improvement in fatigue life, which this can be explained by the influence of aspect ratio on fatigue performance. Additionally, there existed an optimal fibre dosage for achieving this effect.
Singh et al. (2006)	Steel fibres with three different volumes of 1.0%, 1.5% and 2.0% and two different fibre lengths of 25mm and 50mm. Dimension of the specimens: 100x100x500	- Effect on fatigue: the performance under fatigue significantly improved when the fibre content was increased from 0% to at least 1.0%. However, the performance started to decline as more fibres were added beyond that point. For instance, the corresponding two million cycle fatigue strengths for fibre contents of 0%, 1.0%, 1.5%, and 2.0% were found to be 58.30%, 72.10%, 65.40%, and 62.00%, respectively. When comparing applied stress expressed as a percentage of the equivalent static flexural stress of SFRC, it was apparent that SFRC containing 1.0% fibre content performed the best, followed by SFRC containing 1.5% and 2.0% fibre content.

Banjara and Ramanjaneyulu (2018)	Steel fibre with three different fibre volumes (0.5%, 1.0% and 2.0%) with different load levels of (20-65%, 20-75%, and 20-85% of ultimate load) with a frequency of 5Hz. Dimension of specimens: 100x100x500	- The addition of 0.5%, 1% and 2.0% of steel fibres increased fatigue life by approximately 80%, 303% and 217% in comparison to plain concrete when the load range was 20-85% of ultimate load. Similarly, the addition of 0.5%, 1% and 2.0% of steel fibres increased fatigue life by approximately 74%, 553% and 251% in comparison to plain concrete when the load range was 20-75% of ultimate load. Also, the addition of 0.5%, 1% and 2.0% of steel fibres increased fatigue life by approximately 50%, 180% and 110% in comparison to plain concrete when the load range was 20-65% of ultimate load.
Meng et al. (2018)	PVA-ECC with different stress ranges between 64% and 32% of the equivalent static flexural strength of the material. Two different frequencies were used (4Hz and 8Hz) for higher and lower stress ranges.	- Effect on fatigue: the flexural stress range maintained by the PVA-ECC for specimens tested under high-stress low-cycle fatigue was more than double that of normal concrete. At 10^5 cycles, the stress ranges of normal concrete and PVA-ECC were 2.7 MPa and 5.3 MPa, respectively. For the same stress range of 3 MPa, normal concrete failed after a few thousand cycles whereas PVA-ECC resisted 5.6 million cycles. On the other hand, the flexural stress range for low stress high-cycles fatigue was more than 1.5 times higher for PVA-ECC compared to normal concrete.
Gao et al. (2021)	Steel fibre With various volumes of (0%, 0.5%, 1.0%, and 1.5%). Different stress levels based on the maximum static strength were tested (0.5%, 0.55%,	- Effect of stress on fatigue: increased stress levels resulted in a shorter fatigue life. Stress levels of 0.5, 0.55, 0.6, 0.7 and 0.8 showed a fatigue life of 200 $x10^4$, 85 $x10^4$, 80 $x10^4$, 40 $x10^4$ and $10x10^4$, respectively, when the fibre volume fraction was 1%. - Effect of fibre on fatigue: the incorporation of various fibre volumes (0.5%, 1.0% and 1.5%) improved the fatigue life of the beams by 38%, 106% and 61%, respectively in comparison to non-FRC beams. Comparing the fatigue life of the beam cast with 1.5%

	0.6%, 0.7%, and 0.8%), while the minimum stress level was set at 0.1% for all beams. Dimension of the specimens: 120x120x1200	of fibre to the beam cast with 1.0% of fibre, the beam with 1.5% fibre had a shorter fatigue life.
Qu et al. (2019)	Steel fibre volume fraction varied from 0.8% to 1.6%.	- Effect of fibre on fatigue behaviour: the incorporation of 1.6% fibre caused the mode of failure for the beams to change to a ductile failure, thereby prolonging their fatigue life. The growth of total strain with the number of cycles of all of the tested beams was found to have three distinct stages.
Chenkui and Guofan (1995)	A sine waveform with a frequency of 5-20Hz was used to load the sample.	- Effect of fibre on fatigue behaviour: by increasing steel fibre content, fatigue life was prolonged for the same stress ratio. For example, at a stress ratio of 0.8, the specimen's fatigue life was approximately 60 times longer due to the inclusion of 1.5% steel fibres compared to without steel fibre. Similarly, the addition of 0.5 and 1.0% of steel fibres showed an increase in the fatigue life by up to 33% and 67%, respectively.
Mohamadi et al. (2013)	Polypropylene fibres with three different levels (0.7, 0.8 and 0.9 of the maximum bending strength), while the minimum applied load was 2kN with a frequency of 1Hz.	- The incorporation of polypropylene fibres in concrete increased the fatigue life (number of cycles) loading from 554, 2,013, 4,971 to 822, 3,142 and 5,817 for loading levels of 0.7, 0.8 and 0.9, respectively

2.5.2 Performance of HyFRC beams on fatigue

The study conducted by Zhu et al. (2022) found that engineered cementitious composite (ECC) with a higher volume of polyethylene (PE) fibre showed superior performance in applications where high stress levels and low-cycle fatigue were expected. On the other hand, steel fibres exhibited better fatigue resistance at lower stress levels. Additionally, PE fibres showed higher fatigue resistance in terms of interfacial bond at high stress levels compared to low stress levels. It was demonstrated that the use of hybrid fibres (steel and polyethylene fibres) might produce some synergistic effects that led to lower mid-span deflection and the mid-span deflection decreased with a decrease in the stress ranges as reported by Zhu et al. (2022) and can be seen in Figure 2.16. These findings in Table 2.7 highlighted the influence of fibre type and stress levels on the fatigue behaviour of fibre-reinforced materials. Wu et al. (2022) demonstrated that a high proportion of hybrid fibre-polymer (HCHFPC) exhibited greater fatigue resistance compared to other materials under the same fatigue load. This suggested that the combination of multiple fibres in concrete significantly improved flexural fatigue performance. The study also indicated that incorporating various sizes of fibres into polymer composite concrete and increasing their content greatly enhanced the flexural fatigue performance. This finding emphasised the importance of fibre size and content to achieve improved fatigue durability in concrete structures.

Future research should focus on understanding further the synergic effect between fibres and the concrete matrix to optimise the fatigue performance of fibre-reinforced concrete structures. Understanding the interplay between stress levels, fibre types, and composite compositions will provide valuable insights for optimising the fatigue resistance of fibre-reinforced materials. Therefore, exploring the combined use of steel and polypropylene fibres and their potential synergistic effects on fatigue performance would be beneficial. Additionally, studying the long-term behaviour of fibre-reinforced concrete under cyclic loading will contribute to more comprehensive knowledge for practical applications. This research can help assess the performance of fibre-reinforced materials over extended periods, providing valuable information for practical applications.

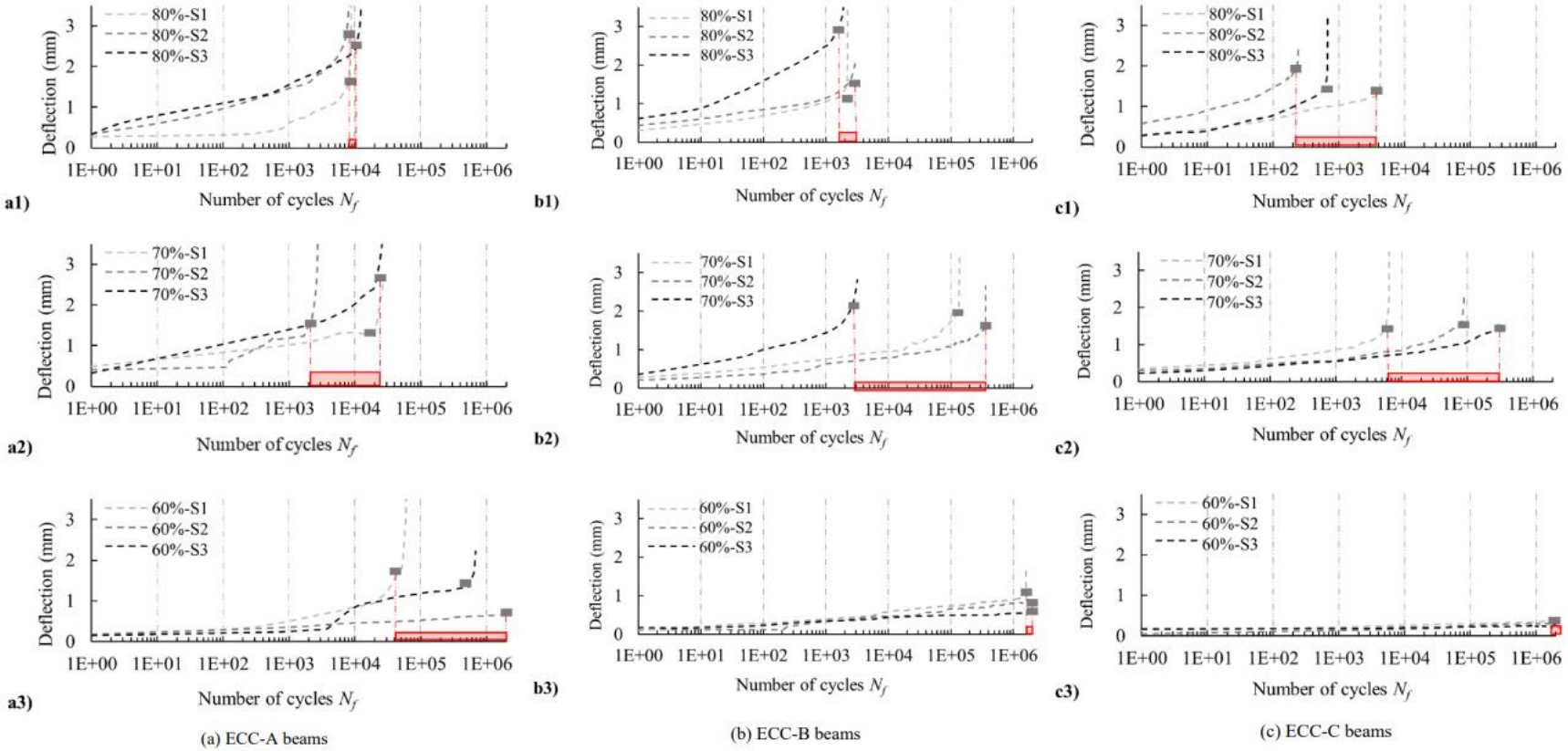

Figure 2.16: Deflection-cycle curves of tested beams under various stress levels: a) ECC-A (1.5% PE + 0.5% ST), b) ECC-B (1.25% PE + 0.75% ST), and c) ECC-C (1% PE + 1% ST) (From Zhu et al., 2022), stress level of 60%, 70% and 80% as a percentage of the maximum static strength

Table 2.7: Summary on the influence of hybrid fibres on fatigue

Authors	Variables, fibres volume fraction and dimension of specimens (mm)	Effect of fibre on the property
Suthiwarapirak et al. (2004)	Two different volumes of 2.1% and 1.5% for PVA and PE, respectively, mixed with 1% steel fibre for different stress levels of (90%, 85%, 75%, 65% and 50%) and the ratio between the minimum and maximum flexural stress was 0.2 for all specimens with a frequency of 8Hz. Dimension of the specimens: 100x100x400	- Effect on fatigue life: a longer fatigue life was observed in ECCs at higher levels of fatigue stress (0.75 to 1.0) varied from 100% to 900% higher when compared to FRC. On the other hand, at lower fatigue stress levels (0.5 to 0.7), their fatigue life often equalled or became shorter than that of FRC.
Zhu et al. (2022)	Steel and polyethylene fibres with three different fibre volumes for each hybrid type (1.5% and 0.5%, 1.25% and 0.75%, and 1.0% and 1.0%, for polyethylene and steel fibre, respectively) for three different stress levels (48%, 56% and 64%) with an applied frequency of 4Hz. Dimension of the specimens: 100x100x350	- Effect on fatigue: all ECC-C (1%PE+1%ST) beams withstood two million fatigue cycles for the tests with a stress range of 48%. ECC-A (1.5%PE+0.5%ST) and ECC-B (1.25%PE+0.75%ST) specimens, one and two beams, respectively, continued to function after two million cycles. The anticipated fatigue life for a stress range ratio of 64% is in the following order: ECC-A (1170) > ECC-B (1200) > ECC-C (590). - Effect of stress range on fatigue: When lowering fatigue stress ranges, the order of fatigue life among the three hybrid ECCs changed. In fact, ECC-A beams achieved better fatigue performance under the low cycle scenarios (i.e., high maximum stress level/range) but a marginally worse fatigue performance under the

		high cycle scenarios (i.e., low maximum stress level/range). - Effect of fibre on fatigue: ECC-A with more PE fibre offered a superior option for applications involving constructions that were subject to a high maximum stress level/range and low-cycle fatigue with a fatigue life of 1170. Steel fibres ECC-C (1%PE+1%ST) offered superior fatigue resistance at lower stress levels with a fatigue life of $3.77x10^{6,}$ which was 20.45% and 308% higher than ECC-B (1.25%PE+0.75%ST) and ECC-A (1.5%PE+0.5%ST), respectively, whereas PE fibres generally exhibited higher fatigue resistance in terms of interfacial bond at high stress levels than at low stress levels.
Wu et al. (2022)	hybrid fibre-polymer (HCHFPC), namely steel ultra-short-fine (USHSF) and hooked-end steel fibre (HESF) and polypropylene fibres (PF) with three different fibre volumes of USHSF, HESF and PF (4.0%, 1.92% and 0.27%, respectively) were used. Four different stress levels were applied (0.70%, 0.60%, 0.55% and 0.50%) with an applied frequency of 10Hz. Dimension of the specimens: 100x100x400	-Effect of stress on fatigue: different fatigue stress levels resulted in varying numbers of cycles, with lower stress levels leading to a higher number of cycles. For instance, stress levels of 0.7, 0.6 and 0.55 exhibited fatigue life of 32441, 160467 and 684570, respectively. However, when the stress level was reduced to 0.5, specimens exhibited a fatigue life of more than $2x10^{6}$. -Effect of fibre on fatigue: test results revealed that there was almost no visible fracture as the USFST glided out of the cracked concrete. In contrast, some of the HESFs broke, illustrating their dual function as

		both a macro-fibre and a micro-scale fibre crack prevention mechanism. These results highlighted the significant role played by the connection between the fibre and the concrete in enhancing the flexural capacity of HCHFPC. Based on the test results, it was established that increasing the fibre volume of a single type of steel fibre had a less pronounced influence on flexural fatigue durability compared to the addition of multiple fibres to the concrete, which significantly improved flexural fatigue performance. The data indicated that incorporating various sizes of fibres into polymer composite concrete through mixing and increasing their content could greatly enhance the flexural fatigue performance of the concrete.

2.6 Influence of fibres on deflection

The influence of fibres on deflection in concrete structures is a topic of significant interest in the field of construction materials. Understanding the impact of fibre addition on deflection can provide valuable insights for designing more durable and resilient concrete structures.

2.6.1 Performance of NC and FRC beams on deflection

As summarised in Table 2.8 the studies reported in various publications present different findings about the effect of incorporating fibre on the deflection of the concrete beams. Yoo et al. (2013) and Yoo et al. (2015) revealed that the increase in steel fibre content led to an increase in deflection at peak load for small prisms. Notably, the peak load values varied significantly among the specimens in both studies, even though none of the specimens had any main reinforcement. Similarly, Hamoush et al. (2010) found that the deflections of the micro fibre-reinforced beams were greater than those of plain concrete beams, with mid-span approximately three times larger. Pająk and Ponikiewski (2013) found that the specimens cast with hooked-end steel fibres exhibited a larger deflection at the maximum stress than plain concrete without fibres. Meza and Siddique (2019) reported that the presence of virgin polypropylene fibre and recycled plastic fibres increased the deflection bearing capacity of concrete. The studies by Qu et al. (2019) and Meda et al. (2012) presented contrasting findings regarding the effect of fibre reinforcement on mid-span deflection for long beams that had tensile reinforcement. These findings highlighted the potential of fibre-reinforced concrete in enhancing the service life and controlling deformation. Overall, these studies suggested that the effect of fibre content on deflection behaviour can vary depending on factors such as fibre type, shape, and volume.

Table 2.8: Summary on influence of fibres on deflection of NRC and FRC beams

Authors	Effect of fibre on the property
Yoo et al. (2013)	- An increase in steel fibre content showed an increase in deflection at peak load by 22%,50% and 78% for 2%(V2), 3%(V3) and 4%(V4), respectively, compared to 1%(V1) of steel fibre.

Yoo et al. (2014)	- Changing fibre lengths had no discernible effect on the deflection and first crack strength, whereas specimens with concrete placed in the centre exhibited slightly higher deflection and first crack strength. - The incorporation of fibres of 30mm in length exhibited deterioration in terms of strength and deflection and had a large deviation in results.
Yoo et al. (2015)	- The increment of fibre content from 0.5% to 1.0% for normal concrete (NC) and from 1.0% to 2.0% for high strength concrete (HSC) revealed a higher deflection at peak than that of the reference beams without fibres. Similarly, the incorporation of 2% steel fibres for ultra-high strength concrete (UHSC) achieved a higher deflection of almost 3 times at peak than that of the reference beams. - Regardless of the fibre content and deflection point, NC offered greater toughness than HSC.
Meda et al. (2012)	- A clear correlation was noted between the behaviour of beams at service load and the fibre content which emphasises the significance of FRC in terms of enhancing service life, such as controlling the deformation of specimens with 60kg/m^3 by approximately a 17% reduction compared to plain concrete.
Pająk and Ponikiewski (2013)	- The plain concrete showed an almost linear response until the formation of the first visible crack, with a quick reduction in load observed with an increase in deflection in the post-peak response. - Effect of type of fibre on deflection: regardless of the volume of straight steel fibres, the load-deflection curves of the pre-peak portion showed nonlinearity with a well-defined initial first peak. Specimens with 1.0% fibre volume of straight steel fibre had a deflection of 0.06mm, while specimens with 1.5% fibre volume had a maximum deflection of 0.11mm. In contrast, specimens cast with hooked-end steel fibres exhibited a larger deflection at the maximum stress than plain concrete without fibres. Specimens with 1.0% fibre volume of hooked-end steel fibre had the highest measured deflection of 0.92mm, while specimens with 1.5% fibre volume had a maximum deflection of 0.64mm. For hooked-end steel fibres, a deflection-hardening response was observed, while a deflection-softening flexural response was observed for straight steel fibres.

Meza and Siddique (2019)	- Plain concrete failed almost after the formation of the first visible crack in the tension zone. - On the other hand, the presence of virgin polypropylene fibre and recycled plastic fibres increased the deflection bearing capacity of concrete.
Hamoush et al. (2010)	- As anticipated, the deflections of the micro fibre-reinforced beams were greater than those of plain concrete beams. - Deflections at mid-span were approximately three times greater than in plain concrete beams.
Kim et al. (2011)	- Beams which were cast with macro fibres recorded significantly greater flexural performance in terms of energy absorption and deflection than those cast only with micro fibres. - Beams cast with macro and micro fibres with 1% volume showed higher deflection values of 45.4-75.9% than those with only micro fibres with a volume equal to 2%.
Meng et al. (2018)	- The mid-span deflection exhibited gradual and steady growth until a rapid increase occurred in the final failure stage. - Effect of stress ratio on deflection: it was established that the stress ranges had an influence on the evolution of mid-span deflection and crack width. As the stress range decreased, the maximum deflection that could be sustained before reaching the ultimate failure stage decreased and was found to be lower than the average deflection at the flexural strength determined from static flexural testing (1.47mm). - Effect of fibre on deflection: the PVA-ECC beams' average mid-span deflection at flexural strength was 1.47mm, which is 35 times greater than the mid-span deflection at flexural strength of normal concrete beams (0.042mm).
Gao et al. (2021)	- The mid-span deflection of 1.5% of fibre had lower value when compared to 1.0% fibre in the early stage of the fatigue process.
Chenkui and Guofan (1995)	- The mid-span deflection curves were classified into three stages because they were comparable to one another. Both the first stage and the last stage were short, taking up only approximately 5% of the total loading cycles.
Sahoo et al. (2015)	- The displacement ductility of the concrete was increased by 40% and 80%, respectively, when adding 0.5% and 1% steel fibres whereas the displacement ductility response of only polypropylene fibre increased 120% when compared to the RC

	specimen, thereby indicating that polypropylene fibres were more effective in terms of enhancing ductility than steel fibres.
Vasanelli et al. (2014)	- The incorporation of FRC led to a reduction in the mid-span deflection when compared to the reference beams.
Higgins et al. (2013)	- The test results reported that the repeated load exhibited a greater deflection and strain than the sustained load. In addition, extra deformations arose between 0-10 days caused by repeated load, whereas the deformation rate appeared to be similar after that period which related to initial load and material properties. Higher loading amplitude produced greater deflections and strains when compared to its counterparts. Section stiffness was affected by the repeated load in the initial age of loading (0-10 days) which might be attributable to material stiffness. The effect of loading frequency was small when compared to the effect of loading amplitude. The test results suggested the importance of the influence of previous load stages and regimes in addition to the current loading condition. It becomes apparent that for the case where $\beta = 1$, the Eurocode provides an accurate prediction of the curvature exhibited by beams subjected to sustained loads. The noteworthy observation here is that beams S-a and S-b, which were tested under static test conform closely to the predictive curve outlined by the Eurocode when $\beta = 1$, rather than when $\beta = 0.5$. This observation raises inquiries into the accurate characterization of long-term and short-term loading as well as the tension stiffening behaviour of beams, particularly when subjected to high load levels. The study emphasises the significance of accounting for not just the present loading circumstances but also the impact of previous load stages and regimes. It has been demonstrated that the distribution coefficient, denoted as 'ζ' and calculated using Expression 7.19 in EC2, solely factors in the current loading conditions.
Daud et al. (2015 & 2018)	The additional deformations took place in the 10-20 days that caused by repeated load after the load application, which is more likely to rely on the material properties and reinforcement. The deformation of repeated load seems to be different than that of sustained load, so relevant coefficients (regime and previous load) should be included to reflect its effect for the long

	term in Eurocode 2. 10% of the overall deflection was caused by the loss of stiffening only which might be attributed to creep and shrinkage. It is evident that both EC2 and Midas FEA provide conservative estimates of mid-span deflection at 90 days. However, EC2 also tends to overestimate deflection up to 50 days, which could be attributed to the curvature resulting from shrinkage. This discrepancy arises because shrinkage strain is initially overestimated in the first 40 days and underestimated towards the end of the testing period. In contrast, Midas FEA assumes concrete behaves elastically, leading to shrinkage curvature originating solely from the un-cracked section, with shrinkage uniformly distributed across the cross-section.
Sryh (2017)	The finding showed that when 50 and 100% of RAC were introduced, the RAC's maximum mid-span defection increased by roughly 8 and 15%, respectively. All the specimens generally displayed a consistent increase in deflection over time. The finding showed that the rate of long-term deflection increased significantly more quickly over the first 20 days of loading. Approximately 65% of the long-term deflections happened during this time. Additionally, the finding showed that increasing the replacement ratio of RAC led to considerable increases in long-term deflection. As a result of replacing 50 and 100% of the aggregate the long-term deflection increased by 20 and 38%, respectively. Evaluating the Eurocode 2 method's predictive accuracy revealed that it did not adequately account for the influence of steel fibres on improving long-term tension stiffening behaviour and enhancing the stiffness of cracked sections in its calculation procedures. An interpolation analysis determined values of 0.65 for concrete with 0.5% steel fibres and 0.8 for 1.0% steel fibre content in tension stiffening for β factor. However, it's crucial to remember that solely assessing steel fibres' impact on tension stiffening doesn't provide a complete understanding of their role in long-term flexural performance of reinforced concrete beams.

*The experimental variables were defined in previous sections.

2.6.2 Performance of HyFRC beams on deflection

As summarised in Table 2.9, Kim et al. (2011) observed that beams cast with a combination of macro and micro fibres exhibited higher deflection values at peak load, which is different in each specimens compared to those with only micro fibres even if the fibre volume fraction was higher than the hybrid fibre. Similarly, Kim et al. (2011) reported that HB hooked-end steel fibres performed better in terms of deflection with 1.5% micro fibres. The addition of hybrid fibres had an effect on the deflection of the specimens, as can be seen in Figure 2.7 and Figure 2.9 from Section 2.4.2. According to Sahoo et al. (2015) the normal concrete specimens, specimens cast with steel fibres, specimens with polypropylene fibres and specimens with hybrid steel-polypropylene fibres exhibited nearly linear curves up to a mid-span deflection of 10mm. Furthermore, the deflection at failure was higher for specimens with the addition of fibres, as can be seen in Figure 2.17.

Further research is, however, needed to explore the combined effects of hybrid fibres with different fibre types, configurations, and volumes on deflection behaviour. It would be valuable to examine the mechanisms behind the observed variations in deflection response, including the contribution of using hybrid fibre with different lengths and aspect ratios. Understanding these factors will provide valuable insights for optimising the use of fibre-reinforced concrete in designing structures with improved deflection control and durability.

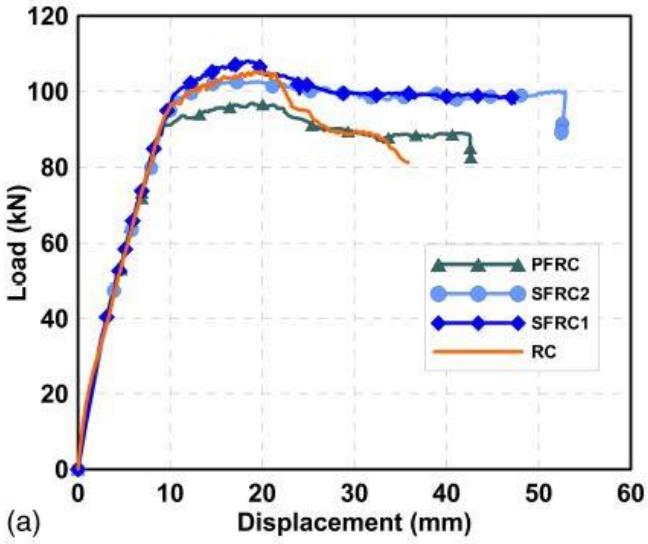

a) Single fibre, Normal concrete (RC), Specimens with 0.5% steel fibre (SFRC1), Specimens with 1.0% steel fibre (SFRC2) and Specimens with 1.0% polypropylene fibre (PFRC)

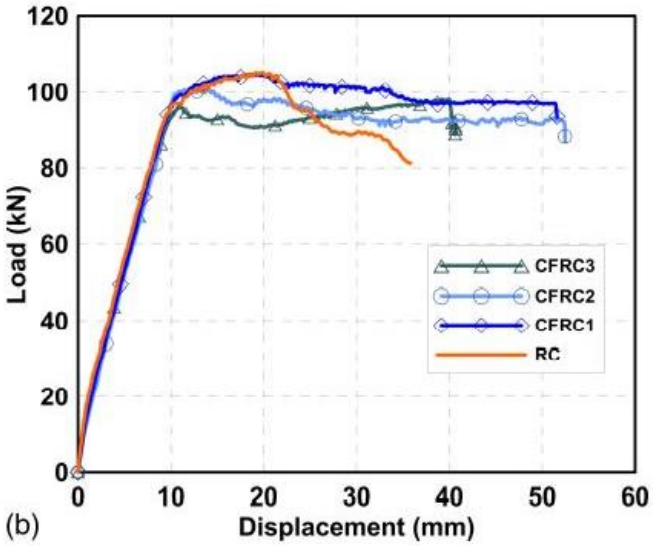

b) Mixed fibres, Normal concrete (RC), specimens with 0.5% of steel fibre and 0.5% of polypropylene fibre (CFRC1), specimens with 1.0% of steel fibre and 0.5% of polypropylene fibre (CFRC2) and specimens with 1.0% of steel fibre and 1.0% of polypropylene fibre (CFRC3)

Figure 2.17: Load-displacement behaviour of specimens (From Sahoo et al., 2015)

Table 2.9: Summary on influence of fibres on deflection of HyFRC beams

Authors	Effect of fibre on the property
Kim et al. (2011)	- Effect of fibre on deflection: beams which were cast with macro fibres recorded significantly greater flexural performance in terms of energy absorption and deflection than those cast only with micro fibres. - HB hooked-end steel fibres performed better in terms of deflection with 1.5% micro fibres, followed by twisted, long smooth and hooked-end steel fibres (HA) with 1.5mm, 1.274mm, 1.836mm and 1.593mm, respectively.
Yap et al. (2014)	- Control beams without fibre recorded a deflection of 1mm during the formation of the first visible crack. - Effect of fibre on deflection: the addition of steel fibres increased the deflection of the oil palm shell steel FRC (OPSFRC) mixes, except the beams cast with 1%

	PP. Adding more steel fibres caused a higher first crack deflection and led to greater flexural strength.
Sahoo et al. (2015)	- The CFRC1 specimen, consisting of 0.5% steel and 0.5% polypropylene fibres, exhibited the same level of displacement ductility as the SFRC2 specimen, which contained 1% volume of steel fibres. Both specimens displayed an 80% higher displacement ductility compared to RC specimens.
Pajak and Ponikiewski (2017)	- The incorporation of a hybrid composition consisting of 1.5% short straight fibre and 1.0% long corrugated fibres resulted in the highest deflection, with a value of 0.162mm, On the other hand, the incorporation of a hybrid composition consisting of 0.5% short straight fibre and 1.0% long corrugated fibres showed a lower deflection value of 0.035mm.
Suthiwarapirak et al. (2004)	- Effect of fibre on deflection: the results clearly revealed that both types of PVA-ECC and PE-ECC had substantially greater deformation capability than steel FRC. The ECC specimens exhibited a deflection at ultimate strength which varied between 1mm and 2mm, whereas it was approximately 0.05mm for steel FRC. - Effect of stress level on deflection: at higher levels of fatigue stress, ECCs showed that displacement evolved up to approximately 1-2mm before failure, whereas steel FRC exhibited a deflection of less than 0.1mm before failure. It was revealed that the level of fatigue stress affected how the mid-span deflection evolved as the higher level showed higher deflection. Specifically, the mid-span deflection experienced an increase of over two times under high fatigue stress levels (S = 0.8-0.9) compared to the deflection observed under low stress levels (S = 0.5-0.6).
Zhu et al. (2022)	Static test results reported that ECC-A (1.5% PE + 0.5% ST) offered a larger average deflection of 63% relative to ECC-B (1.25% PE + 0.75% ST) but 5% less strength. The deflection-cycle curve initially developed slowly for each of the three types of ECCs before abruptly increasing close to the point at which the beam failed under fatigue loading.

*The experimental variables were defined in previous sections.

2.7 Influence of fibres on crack pattern and crack width

The influence of fibres on crack pattern and crack width in concrete structures is a critical aspect of understanding the behaviour and performance of fibre-reinforced concrete. This section highlights the significance of studying the effect of fibres on crack pattern and crack width to improve the durability and structural integrity of fibre-reinforced concretes.

2.7.1 Performance of NC and FRC beams on crack pattern and crack width

The findings of the literature reported in Table 2.10 indicate that the addition of fibres effectively reduced the crack width of concrete beams and exhibited the ability to bridge cracks, effectively slowing down the process of crack propagation under different types of load. While some of the literature reported that the aspect ratio of fibre had a lower influence on the initial crack width, on the other hand, Tan et al. (1995) indicated that the inclusion of steel fibres had no discernible effect on major crack spacing and using steel fibres significantly reduced the maximum crack widths in reinforced concrete beams for short and long-term and the crack width tend to stabilise after 140 days, as can be seen in Figure 2.18. Similarly, the average crack width for specimens cast with steel and polypropylene fibres was lower than normal concrete and the crack width of the FRC beams (Steel (ST) and polyester (POL)) appeared to have stabilised after 10 months of loading, as shown in Figure 2.19 (Vasanelli et al., 2014). Gao et al. (2021) reported that the SFRC beam had a much larger number of cracks than the beam without fibre. Mohamadi et al. (2013) indicated that the addition of polypropylene fibres had no influence in terms of reducing the crack width. It was apparent that the mean crack spacing reduced as the fibre content increased (Tiberti et al., 2014; Gao et al., 2021). However, it was evident that the average crack spacing increased when the fibre volume reached 1.5% (Gao et al., 2021). It is important to take into account the change in behaviour that occurs with increasing fibre volume, as it helps determine the ideal fibre dosage to prevent any potential adverse effects.

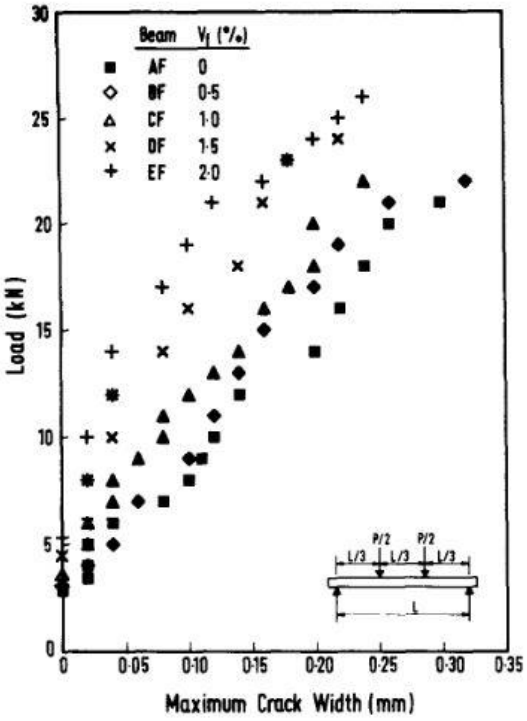

a) Load-crack width curve for short-term load, specimens without fibre (AF), specimens with 0.5% volume fraction of steel fibre (BF), specimens with 1.0% volume fraction of steel fibre (CF), specimens with 1.5% volume fraction of steel fibre (DF) and specimens with 2.0% volume fraction of steel fibre (EF)

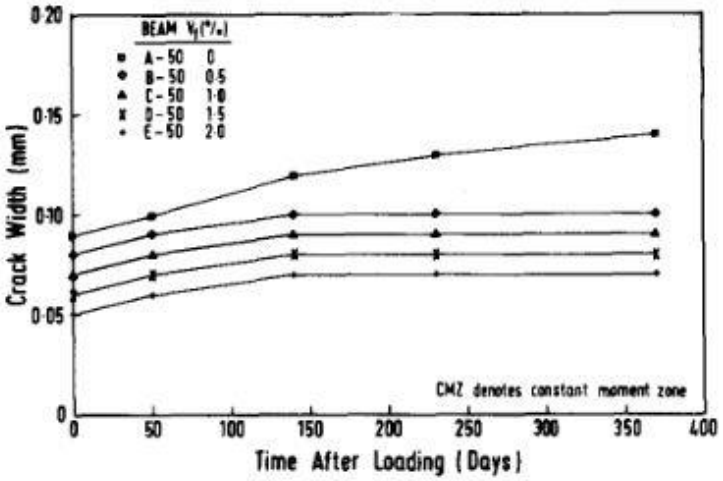

b) Crack width over time for specimens subjected to 0.5 times the design ultimate load (50%), specimens without fibre (A), specimens with 0.5% volume fraction of steel fibre (B), specimens with 1.0% volume fraction of steel fibre (C), specimens with 1.5% volume fraction of steel fibre (D) and specimens with 2.0% volume fraction of steel fibre (E)

Figure 2.18: Crack width for short-term and long-term (From Tan et al., 1995)

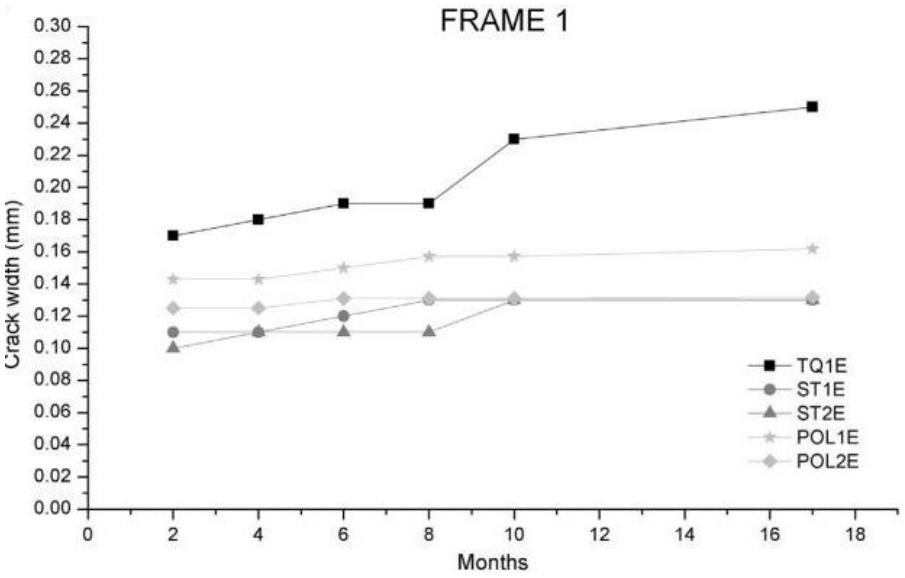

Figure 2.19: Typical crack width over time (From Vasanelli et al., 2014), specimens without fibre reinforcement (TQ1E), Specimens with 0.6% volume fraction of steel fibre (ST1E and ST2E) and specimens with 0.9% volume fraction of polyester fibre (POL1E and POL2E)

Table 2.10: Summary of literature on influence of fibres on cracks of NRC and FRC beams

Authors	Effect of fibre on the property
Meda et al. (2012)	- Effect of fibre on crack: the cracks tended to be smaller and narrower as the fibre content increased, but they became more diffused and included some shear-inclined cracks for a higher reinforcement ratio. The addition of 30kg/m^3 and 60kg/m^3 increased the number of cracks by 8.33% and 12.5%, respectively.
Pająk and Ponikiewski (2013)	- The crack mouth opening displacement of beams with 1.5% straight steel fibres of 5 mm at a deflection of 2 mm whereas the specimens cast with hooked-end steel fibres, 0.5% and 1.0% straight steel fibres caused about 5 mm at deflection of 3 mm.
Meza and Siddique (2019)	- Recycled plastic fibres offered crack arresting and bridging properties comparable to virgin polypropylene fibres.
Uygunoglu (2008)	- Effect of fibre on crack: the increment of the fibre volume led to a significant reduction in the width of the first crack. They showed a crack width of 1.3 mm and 1.1 mm for low carbon and hooked-end steel fibres, respectively, when the

	fibre content was 2%. Also, the low carbon and hooked-end steel fibres showed values of 0.3 mm and 0.32 mm for the first crack, respectively, when the fibre content was 0.8%. The initial crack width was less affected by aspect ratio and concrete age when the fibre volume was increased from 0.2% to 0.8%.
Vandwalle (2000)	- Effect of fibre on crack spacing: it was observed that the crack spacing was reduced by the steel fibres incorporated in the concrete. The addition of 45 kg/m^3 showed a reduction of 10.94% in crack spacing for the lower aspect ratio whereas the addition of 45 kg/m^3 showed an increase of 10% in the crack spacing when compared to the addition of 30 kg/m^3. It was apparent that the crack spacing decreased as the aspect ratio of the steel fibre increased at higher bending moments. These reductions were about 28.61% and 11.84% for 30 kg/m^3 and 45 kg/m^3, respectively. - Effect of fibre on crack width: a significant approximately 37% reduction in crack width caused by fibre incorporation. Incorporating steel fibres with a higher aspect ratio led to a significant reduction in crack width which was apparent at higher bending forces.
Oh (1992)	- Effect of fibre on crack width: the crack widths for the concrete beam without steel fibres were approximately 0.22 mm, whereas the crack widths for the concrete beam with 2% steel fibres were 0.12 mm when the steel stress was 200MPa. This indicated that the steel fibres serve as crack arresters and were very helpful in limiting the spread of cracks. - Effect of fibre on crack spacing and pattern: as the amount of steel fibres in the beam increased, the crack spacing at a given steel stress decreased. At each load step, the reinforced concrete beam with 2% fibre exhibited significantly reduced cracking. The addition of 1% and 2% steel fibres showed a reduction in the number of cracks at a load of 20 kN by 23.08% and 38.46%, respectively when compared to the beams without fibres.
Guo et al. (2021)	- Effect of fibre on crack: a few micro-cracks developed during the failure process closed to the main crack when polypropylene fibre was added, which reduced the

	accumulation of stress at the tip of the main crack. According to their different geometric shapes and properties, steel and polypropylene fibres played a role in the formation of cracks at various stages.
Parvez and Foster (2014)	- Effect of fibre on crack: plain concrete beams tended to have evenly distributed cracks along their length. Meanwhile, beams cast with steel fibres exhibited smaller crack widths and lower deflection than those of the control beams with an average reduction in crack width of 38% and 46% for the volume fraction of 0.4% and 0.8%, respectively, for series two with higher dimensions.
Singh et al. (2006)	- Effect of fibre on crack: almost all of the SFRC specimens that failed under fatigue loading had a single crack that started in the middle-third of the specimen. The specimen completely failed as a result of the crack spreading and widening with an increase in the number of cycles. When the first obvious crack started at higher stress levels, failure occurred almost immediately. However, the fibre concrete specimens withstood a substantial amount of load cycles even after the onset of the first visible crack at lower stress levels. This shows that the fibres employed in this experiment improved bond qualities and crack bridging features as a result of their deformed shape.
Banjara and Ramanjaneyulu (2018)	- Effect of fibre and stress ratio on crack: when the cracks were initiated, they propagated as the number of cycles increased. When comparing fatigue with a load range of 0.2Pu-0.85Pu to a load range of 0.2Pu-0.65Pu, it was observed that the crack propagation was slower in the load range of 0.2Pu-0.65Pu with a value of 0.1 mm at the initiation of cracks compared to 0.2 mm for load range of 0.2Pu-0.85Pu. Furthermore, with a load range of 0.2Pu-0.65Pu, the fatigue-induced crack propagation required a longer duration. Sudden failure occurred once the crack initiated under a higher load range, whereas this phenomenon was absent under the lower load range. Fibres exhibited the ability to bridge cracks, effectively slowing down the process of crack propagation.

Tan et al. (1995)	- Effect of fibre on crack: a combination of sustained beam curvature and increased ductility led to the cracks. - Effect of fibre on crack height: the initial cracks had lower heights in beams with higher steel fibre content. This resulted from the action of the fibres which prevented cracks from spreading up the depth of the beams. - Effect of fibre on crack spacing: the inclusion of steel fibres had no discernible impact on major crack spacing. The smaller crack width was typically correlated with higher fibre content. This occurred as a result of the steel fibres bridging fissures, thereby helping to reduce the stress in the tensile steel reinforcement. - Effect of fibre on crack width: in the case of reinforced SFC beams, the crack widths were often smaller at any point after loading and the higher the fibre content, the smaller the crack width over the long-term. The addition of steel fibres to the test beams appeared to stabilise the crack width after 140 days under load, whereas the cracks in normal reinforced concrete beams seemed to increase after 370 days under load. Consequently, it was deduced that the fibres helped to prevent the widening of cracks in beams under sustained loading.
Meng et al. (2018)	- Effect of fibre on crack width: the development of crack width was found to be dependent on the stress range and the reduction in stress level led to a reduction in the micro-cracks. The crack widths corresponding to stress levels of 64%, 56%, 48%, 40%, and 32% were approximately 3 mm, 2.8 mm, 1 mm, 1 mm, and 0.9 mm, respectively.
Gao et al. (2021)	- Effect of fibre on crack: the SFRC beam had a much larger number of cracks than the beam without FRC. - The effect of fibre on crack spacing was observed, showing that the average crack spacing decreased when the fibre volume reached 1.5%. Specifically, the average crack spacing was approximately 70 mm for a fibre volume of 1.5%, whereas it was 81 mm for normal concrete. In contrast, the crack spacing decreased from 0.5% to 1.0% fibre volume, with a value of 50 mm. Comparing a beam with 1.0% fibre to a beam with 1.5% fibre, the average crack spacing increased by 32.6% in the latter case. This increase

	was primarily attributed to the development of weak spots in the beam due to the overlapping of fibres. - Effect of fibre on crack width: the average crack widths decreased as the fibre percentage increased from 0% to 1.0%. Specifically, the average crack widths were 0.24 mm and 0.21 mm for the 0% and 1.0% fibre volume fractions, respectively. However, it is important to note that during the early fatigue phase, the average crack widths of the beam with 1.5% fibre volume were found to be greater than those of the beam with 1.0% fibre volume. Nevertheless, at failure, the beam with 1.5% fibre volume exhibited a lower crack width value of 0.18 mm compared to 0.21 mm for the beam with 1.0% fibre volume. -Effect of stress levels on crack width: increasing the stress levels increased the crack width under loading, but the crack width at failure differed. Stress levels of 0.5, 0.55, 0.6, 0.7, and 0.8 exhibited crack widths of 0.25 mm, 0.19 mm, 0.23 mm, 0.38 mm, and 0.31 mm, respectively
Mohamadi et al. (2013)	- Effect of stress ratio on crack: the change in fatigue crack growth rate was dependent on the number of cycles at lower cyclic stress. However, the crack growth rate decreased after the initial stages, whereas in the last stage, the rate of crack growth increased. Increasing the stress level increased the crack width of plain and polypropylene FRC. - Effect of fibre on crack width: the addition of polypropylene fibres had no influence in terms of reducing the crack width, which showed an increase in crack width relative to plain concrete of 21.5%, 18% and 1% for stress levels of 0.7, 0.8 and 0.9.
Vasanelli et al. (2014)	- Effect of fibre on crack width: it is important to note that the FRC beams had smaller crack widths than the reference beams and that this effect increased over time. The average crack width was found to have increased by 8% in the TQ1-E (reference) beams and by 13% in the TQ2-E (reference) beams between the tenth and seventeenth month of exposure, whereas no significant increase in crack width was found in the FRC beams. Therefore, it appeared that the presence of fibres helped to prevent the development of long-term cracks. In fact, there was no considerable

	difference between the final values of the average crack widths of the POL and ST beams.

*The experimental variables were defined in previous sections.

2.7.2 Performance of HyFRC beams on crack pattern and crack width

Most of the previous research focused on the hybridisation of steel-polypropylene and steel-steel fibres taking into account their different geometric shapes and properties, which played a role in the formation of cracks at various stages, as reported in Table 2.11. The incorporation of hybrid steel and polypropylene fibre improved crack performance and provided the most suitable combination for hybrid fibres. However, there is a lack of research focusing on the flexural performance of micro and macro hybridisation of polypropylene fibres combined with steel fibre. The majority of the research published in the literature focused on the effect of normal concrete, one type of fibre and two different shapes or lengths of steel fibres with polypropylene fibres. However, concrete made from different mixes and types of fibres may exhibit distinct cracking behaviours which could have a different effect on the performance of the concrete. From the above analysis, the influence of microcracks is also very important and can cause serious durability concerns, thus, it is necessary to carry out more research on crack width.

Table 2.11: Summary of literature on influence of fibres on cracks of HyFRC beams

Authors	Effect of fibre on the property
Caggiano et al. (2012)	- Effect of fibre on crack: the presence of short fibres improved the peak and post-peak strength for small crack widths. Conversely, specimens reinforced with only long steel fibres (SFRC) (L100-10) exhibited an instantaneous post-peak softening behaviour in the first crack range. Eventually, the findings showed that the S75-10 mixes was the composite that performed best overall.
Suthiwarapirak et al. (2004)	- Effect of stress ratio on crack: the ECC specimens exhibited multiple cracks, whereas the steel FRC specimens exhibited one major crack initiated and propagated with the increase in static loading. For instance, PVA-ECC, PE-ECC

	and steel FRC exhibited a crack mouth opening displacement of approximately 1.25 mm, 1.5 mm and 0.1 mm, respectively. The level of fatigue stress had a considerable impact on the number of cracks that appeared. When the specimens were subjected to high levels of fatigue stress, the number of cracks increased, whereas FRC only had one crack at all stress levels. At a stress level of 0.9, higher number of cracks were formed, which were 8 and 15 for PVA-ECC and PE-ECC, respectively. Whereas at a stress level of 0.6, smaller number of cracks were observed, which were approximately 3 and 7 for PVA-ECC and PE-ECC.
Zhu et al. (2022)	- Effect of fatigue on crack: the average number of cracks at failure for static loading were 33, 27 and 18 for ECC-A (1.5% PE + 0.5% ST), ECC-B (1.25% PE + 0.75% ST) and ECC-C (1.0% PE + 1.0% ST), respectively. The number of cracks exhibited a decrease as the stress range decreased. For ECC-A, with stress ranges of 64%, 56%, and 48%, the average number of cracks were 23, 20, and 17, respectively. Similarly, for ECC-B, with stress ranges of 64%, 56%, and 48%, the average number of cracks were 19, 19, and 16, respectively. In the case of ECC-C, with stress ranges of 64%, 56%, and 48%, the average number of cracks were 16, 13, and 9, respectively. - Effect of stress ratio on crack width: the crack width increased as the maximum stress level increased. The major crack width was effectively managed and kept within the specified limits of 0.3 mm (under normal exposure conditions) and even 0.2 mm (under aggressive exposure conditions) at the inflection points for a maximum load level of 60%. The widths of the minor cracks were effectively constrained, remaining within the limits of 0.2 mm and even 0.1 mm until the specimen reached failure.

*The experimental variables were defined in previous sections.

2.8 Effect of fibres on tension stiffening, creep and shrinkage

Studying the effect of fibres on tension stiffening, creep, and shrinkage is important to understanding how the inclusion of fibres affects the mechanical and

time-dependent properties of concrete. Therefore, tension stiffening and both creep and shrinkage are described first and then the effect of fibres on these properties is discussed.

2.8.1 Tension stiffening

Tension stiffening is an effective mechanism in concrete which resists the tensile forces generated during bending. It occurs between the primary crack regions as a result of the bond action of reinforcement. Although the tensile strength of concrete is approximately one-tenth of its compressive strength, it still makes a significant contribution to the beam's flexural behaviour (Scott and Beeby, 2012). The deformation properties of the beam elements of cracked reinforced concrete (RC) are highly dependent on the influence of tension stiffening, which is due to the intact concrete between the cracks in the tension zone being capable of maintaining certain tensile stress levels and contributing to flexural stiffness (Pui-Lam et al., 2019).

2.8.2 Creep and shrinkage

Creep and shrinkage in concrete have a significant effect on structural behaviour under service loads. Creep and shrinkage are considered to lead to the time-dependent deformation of concrete. Creep and shrinkage are primarily associated with the hydrated cement paste, but they can also be influenced by other factors within the concrete matrix, such as, temperature, relative humidity and the age of concrete. While the cement paste plays a significant role in creep and shrinkage, other components such as aggregates, admixtures, and the overall mix design can also affect these properties (ACI Committee 209, 1997). In concrete, the combined effects of creep and shrinkage, which are rheological phenomena, can diminish the contribution of stress stiffening compared to reinforced concrete. Creep and shrinkage introduce additional deformations and changes in dimensions over time, which can counteract the stress stiffening effect. These rheological effects can reduce the overall stiffness of the concrete and affect its resistance to deformation under applied loads.

Creep can be defined as the slow deformation of a material that occurs under a sustained load over time (ACI Committee 209, 1997). Creep in concrete primarily occurs in the hardened concrete and is related to the slow growth of

micro-cracks and the movement of moisture (ACI Committee 209, 1997). The gradual development and propagation of micro-cracks in the cement paste contribute to the time-dependent deformation observed in creep. These micro-cracks occur due to stress concentrations and the inherent material properties of the cement paste. As the load is sustained over time, these micro-cracks continue to grow, leading to creep deformation.

Creep is obtained by subtracting the sum of the initial instantaneous (usually called elastic) strain from the maximum measured strain in a loaded sample due to sustained stress, shrinkage and eventual thermal strain in an equal load-free specimen that is subject to the same background of relative humidity and temperature conditions (ACI Committee 209, 1997). In addition, the creep definition combines basic creep and drying creep. Basic creep occurs under conditions where there is no transfer of moisture to or from the environment. “Drying creep is the additional creep caused by drying” (ACI Committee 209, 1997). Creep potentially enhances reinforced concrete members' long-term deflection through two mechanisms (Forth, 2015). First, the grouping of compressive and tensile creep, regardless of shrinkage, changes the slope of the strain profile, thereby increasing the curvature over time. Second, the tension stiffening capacity of the composite section influences the deflection of a beam or slab. Creep caused by traffic loads is likely to be a major cause of higher deflection or even cracking in concrete bridges (Qian, 2019). Whaley and Neville (1973) found that the creep strain due to cyclic load was approximately 1.2 to 2.3 times higher than that due to static load and the cyclic load had a significant effect on creep.

Shrinkage can occur in both the plastic (fresh) and hardened state of concrete, but the focus here is on the volume reduction that takes place after the concrete has hardened. Shrinkage is defined as the reduction of concrete volume over time after the hardening of concrete when it is exposed to drying conditions (Barr and El-Baden, 2003; Sryh, 2017). The reduction is an indicator of changes in moisture content of concrete and physio-chemical changes that occur without external force due to behaviours outside the concrete (ACI Committee 209, 1997). Shrinkage strain represents the relative contraction or shortening of the concrete material as it undergoes drying. This strain is calculated by dividing the change in length or dimension of the concrete by the original length or dimension.

The resulting value is a dimensionless quantity that represents the magnitude of the shrinkage (ACI Committee 209, 1997).

2.8.3 Influence of fibres on tension stiffening

In the analysis of flexural behaviour in reinforced concrete structures, it is conventionally assumed that concrete primarily bears compressive loads while tensile loads are solely carried by the steel reinforcement. However, it is important to recognise that concrete does have the ability to withstand tensile loads, despite its tensile strength being approximately one-tenth of its compressive strength (Scott and Beeby, 2012).

Moreover, the incorporation of 60kg/m^3 and 30kg/m^3 fibres in the concrete mixes resulted in a 20% and 10% decrease in tension stiffening, respectively, indicating that fibre-reinforced concrete (SFRC) significantly affects the performance of tension ties under serviceability limit state (SLS) conditions for the three bonded specimens under 4-point loading scheme to determine tension stiffening effect (Meda et al., 2012). SFRC affected the performance of tension-ties during serviceability limit state (SLS) conditions by diminishing crack width and leading to crack patterns characterised by narrower and closely spaced cracks (Tiberti et al., 2014).

2.8.4 Influence of fibres on creep and shrinkage

As reported in Table 2.12, Tan et al. (1994) stated that creep and the measured deflection of steel FRC beams were lower when compared to plain concrete and the effect of incorporating steel fibres was pronounced in terms of controlling time dependant deflections. Meanwhile, Mangat and Azari (1985) claimed that the addition of steel fibres had only a minor effect on concrete creep. Chern and Young (1989); Afroughsabet and Teng (2020) indicated that the addition of steel fibres reduced creep strain. In contrast, Blyszko (2017); Saje et al. (2013) concluded that the presence of 0.5% short steel fibres resulted in 8% greater creep than the normal concrete. Furthermore, Balaguru and Ramakrishnan (1988) reported that the addition of steel fibres exhibited a higher creep strain when compared to normal concrete, as can be seen in Figure 2.20(a).The time-dependent properties of hybrid fibre concretes' performance have not been

extensively studied and require further investigation to fully understand their characteristics.

As summarised in Table 2.12, Tan et al. (1994) stated that shrinkage and the measured deflection of steel FRC beams were lower when compared to plain concrete and the effect of incorporating steel fibres was pronounced in terms of controlling time dependant deflections. Mangat and Azari (1984 and 1988) claimed that the addition of deformed fibres to concrete resulted in a reduction in concrete shrinkage of up to 40%. Kovler and Bentur (1997); Saje et al. (2013) found that the addition of discrete fibre reinforcement to concrete did not have a noticeable effect on shrinkage. However, other studies by Chern and Young (1989); Barr and El-baden (2003); Afroughsabet and Teng (2020) reported a significant effect on shrinkage when reinforcement fibres were added. Furthermore, Balaguru and Ramakrishnan (1988) stated that the addition of steel fibres had an effect on shrinkage when compared to normal concrete, as can be seen in Figure 2.20(b). Kiviste et al. (2011) reported that the incorporation of steel and polypropylene fibres resulted in a lower shrinkage compared to normal concrete.

The conflicting measurements of creep and shrinkage obtained by researchers have hindered them from drawing broad conclusions on the effect of the addition of fibres, as summarised in Table 2.12. It is possible that these studies did not consider all the factors that influence long-term behaviour. Based on previous studies, it can be concluded that the shape and volume fraction of fibre affected the creep and shrinkage behaviour of concrete mixes.

Additionally, hybridisation of steel fibres with PVA fibres significantly reduced drying shrinkage, as they were commonly used to mitigate shrinkage cracking. Most previous studies focused on the effect of steel fibres on creep, shrinkage and loss of tension stiffening. Future research should aim to conduct comprehensive studies that consider all influencing factors to draw conclusive results regarding the effect of fibre addition on creep and shrinkage. Further investigations are needed to explore the effect of different combinations of fibre and hybridisation of steel and polypropylene fibres on the creep and shrinkage behaviour of concrete mixes, particularly in managing shrinkage cracking.

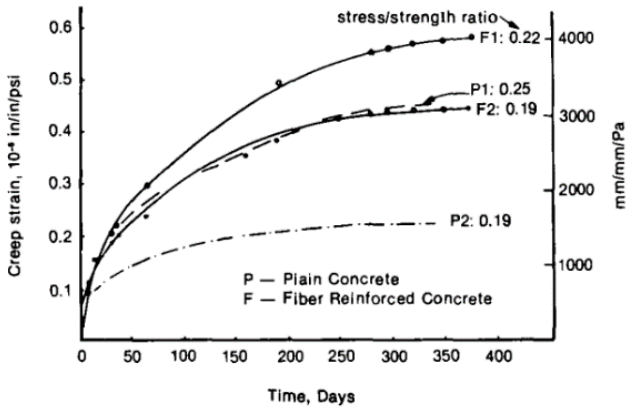

a) Effect of fibre on creep strain with different water/cement ratio (for normal concrete P1=0.38 and P2=0.28) and (for fibre reinforced concrete F1=0.4 and F2=0.3)

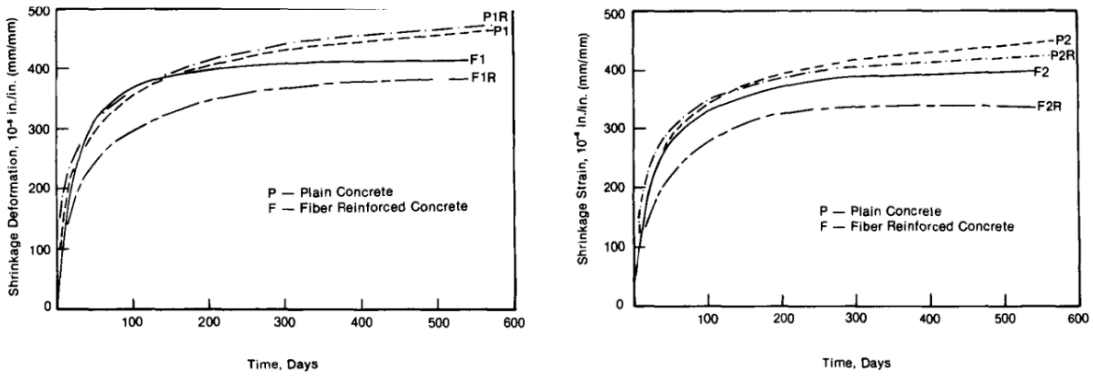

b) Effect of fibre on shrinkage strain for different mixes and different temperature (for normal concrete P1=20.5°C, P1R=21.6°C, P2=21.1°C and P2R =22.2°C) and (for fibre reinforced concrete F1=20°C, F1R=22.2°C, F2=20°C and F2R=21.1°C)

Figure 2.20: Effect of steel fibres on creep and shrinkage (From Balaguru and Ramakrishnan, 1988)

Table 2.12: Summary on influence of fibres on tension stiffening, creep and shrinkage of NRC and FRC beams

Authors	Variables, fibres volume fraction and dimension of specimens (mm)	Effect of fibre on the property
Meda et al. (2012)	Two different dosage of steel fibre (30kg/m^3 and 60kg/m^3)	- Effect on tension stiffening: for the serviceability limit state (SLS), the addition of FRC improved the structural performance of all specimens by giving better post-cracking stiffness and enhanced tension stiffening. The addition of fibres with 60kg/m^3 and 30kg/m^3 reduced the tension stiffening by 20% and 10%, respectively.
Saje et al. (2013)	Steel fibre with a volume ranging from 0% to 2% with short and long (L=16mm and 30mm)	- Effect of fibre on shrinkage: the overall shrinkage of such composites was typically 15% less than that of the corresponding plain concrete without fibres. The shrinkage of the composite with 2% short steel fibres was approximately 63-65% less during the initial time and final measurement times than that of the equivalent plain concrete, whereas the drying shrinkage of longer steel fibres ranged from 44% to 68% less than that of the comparable plain concrete at all fibre dosages. - Effect of fibre on creep: the addition of 0.5% short steel fibres increased the creep value by approximately 8% relative to plain concrete. Conversely, the addition of 0.5% of long steel fibres produced the lowest creep value over all timeframes and for all fibre dosages, which was approximately 12% less than that of plain concrete. The incorporation of 1.0%, 1.5% and 2.0% of long steel fibres produced a higher creep value than that of the plain concrete; up to 11% greater at 127 days until the end of measurement.

Afroughsabet and Teng (2020)	Single (HE) and double hooked-end (DHE) steel fibres and PVA fibres were used. Various volumes of fibres (0%, 0.6% and 1.2%) for hybrid fibre-reinforced concrete (HPHyFRC).	- Effect of fibre on creep: the HPHyFRC results showed that the replacement of DHE with HE steel fibres resulted in a minor increase in the creep of specimens. Depending on the volume percentage and hybridisation of the fibres, the particular creep of FRC was reduced by 5-21%. The addition of 0.6% and 1.2% DHE resulted in a reduction in the creep by 42% to 49% and 43% to 51%, respectively. - Effect of fibre on shrinkage: the drying shrinkage was significantly reduced when steel fibres were hybridised with PVA fibres. The addition of 0.6% and 1.2% fibre volume led to a reduction in shrinkage strain of approximately smaller than that of the equivalent plain concrete without fibres. These reductions for the addition of 0.6% were 3%-34% and 2%-20% at 56 and 448 days, respectively. Similarly, the reductions with the addition of 1.2% were 6%-30% and 9%-22% at 56 and 448 days, respectively.
Błyszko (2017)	Steel and polypropylene fibres with two levels of applied load: 40% and 80%	- Effect of fibre on creep: FRC exhibited a significant increase in compressive creep relative to normal concrete. It was found that the creep coefficient of normal concrete was 91% and 25% lower than that of FRC at 24 and 672 hours, respectively, under 40% load. However, normal concrete had a negligibly greater creep coefficient than FRC at 96 and 168 hours. At 24 hours, the creep coefficient of FRC concrete with an applied load of 85% was 52% higher than that of normal concrete, but at 96 hours, it was 36% lower. The creep of FRC in hardened concrete (28 days) at a 40% load was found to be greater than that of normal concrete.
Kiviste et al. (2011)	Volumes of 0.32% and 0.51% for the steel fibres and volumes of 0.44% and	- Effect of fibre on shrinkage: the least amount of shrinkage was observed in concrete reinforced with steel fibres (0.51%) and synthetic fibres (0.77%). In comparison to the shrinkage of plain concrete, specimens with a fibre content of 0.32% did not practically

	0.77% for polypropylene fibres	exhibit changes in shrinkage (the difference was 1.3% at 60 days). However, at the same age, the shrinkage of specimens with a 0.51% fibre content was 13.8% lower. The test results clearly showed that at 60 days, the shrinkage of specimens with a fibre content of 0.77% was 7.8% smaller than the shrinkage of plain concrete. However, specimens with a lower volume of 0.44% fibre exhibited approximately 11% greater shrinkage than the plain concrete specimens.
Chern and Young (1989)	Steel fibres with volumes ranging from 0% to 2%.	- Effect of fibre on shrinkage: it was observed that as more fibres were added, the shrinkage decreased. Additionally, the effect of steel fibres became more pronounced in restricting the shrinkage and creep of concrete with longer loading time. Furthermore, the shape of the SFRC shrinkage curve was found to be comparable to that of plain concrete. - Effect of fibre on creep: the findings showed that the creep of concrete was significantly reduced by steel fibre reinforcement, and the creep decreased over time as the volume of fibres increased. Additionally, the test results indicated that the reduction in creep value was greater when the fibre volume was increased from 0% to 1% compared to when it was increased from 1% to 2%.
Barr and El-baden (2003)	Three different fibre volumes of 1%, 2% and 3% with five different concrete strengths ranging from 40MPa to 120MPa were employed	- Effect of fibre on shrinkage: the ability of the fibres to minimise shrinkage was particularly pronounced during the early drying stages (4-6 weeks). The fundamental benefit of fibre reinforcing was that it prevented early shrinkage strains from developing and a 1% fibre concentration was found to be adequate to achieve this. However, after approximately three months, the benefit of fibres in reducing shrinkage was only around a 20% reduction.

		In the case of high-strength concrete (HSC), it was established that almost 80% of the 3-month shrinkage values occurred within the first month of drying.
Balaguru and Ramakrishnan (1988)	Hooked-end fibres. The applied stress was approximately 0.22 and 0.19 of stress strength ratios for mixes 1 (F1, PI) and mixes 2 (F2, P2), respectively.	- Effect of fibre on shrinkage: FRC exhibited less shrinkage when compared to conventional concrete. After a period of approximately 150 days, the differences became more noticeable, which was approximately 100 microstrain less. For FRC, the rate of growth reduced in the early stage. Shrinkage of FRC seemed to stabilise after 500 days, whereas for conventional concrete, it continued for as long as 600 days. - Effect of fibre on creep: as would be expected, increasing the stress-to-strength ratio led to an increase in creep strain. The creep strain of FRC was consistently greater than that of plain concrete at 375 days with a value of 0.46 and 0.59 in./in./psi compared to a value of 0.47 and 0.23 for plain concrete. For combinations that featured a higher cement concentration and a lower water-cement ratio, the difference was more noticeable.
Bissonnette et al. (2007)	0.5% and 1.0% of crimped steel fibres and 0.5% of hooked-end steel fibres were tested	- Effect of fibre on shrinkage: the outcomes further demonstrated that the behaviour of drying shrinkage was not considerably influenced by fibres, it showed approximately 4% reduction. - Effect of fibre on creep: the overall creep of FRC was slightly greater than the reference concrete in the experiments that started at 7 days. However, the creep rate of the fibre-reinforced mixes reduced rather quickly to almost zero 14 days after loading in comparison to those that were started at 28 days, where it was substantially lower. - Effect of the shape of fibre on creep: it was shown that using hooked fibres at a dosage of 40 kg/m^3 increased the total creep by approximately 30-35%. Conversely, using crimped fibres at the same dosage resulted in a reduction of 30-35%.

		- Effect of the fibre volume fraction on creep: moreover, creep significantly increased following an increase in the dosage of crimped fibres from 40kg/m^3 to 80kg/m^3.
Tiberti et al. (2014)	Micro and macro steel fibre with volume fraction of 0% to 3.0% and different lengths	In RC specimens, the elastic stiffness remained comparatively high before the first crack appeared, at which point the tension stiffening behaviour started and the total stiffness rapidly decreased. - Effect of fibre on shrinkage: the incorporation of different combination of micro and macro fibres with volume fraction (length/diameter) of 0.5% (30/0.38), 1.0% (30/0.38), 1.5% (30/0.38), 1.5% (30/0.55) and 1.5% (50/1.05) resulted in an increase in the shrinkage by approximately 71.3%, 128.4%, 146.9%, 126.2% and 34.6%, respectively. - Effect of fibre on the main crack spacing of tension stiffening specimens: the mean crack spacing reduced significantly when HSC was used instead of NSC. This trend was sufficiently demonstrated for both RC and SFRC specimens: with increased strength in non-fibrous parts, a decline of approximately 40% was observed and a reduction of up to 50% in SFRC specimens. By reducing crack width and producing crack patterns with narrower and closer-spaced cracks, SFRC has an impact on the behaviour of tension ties at SLS.

2.9 Summary of research gaps and justification of current research

- The incorporation of hybrid straight steel and polypropylene fibres has been shown to improve flexural performance and provide a suitable combination for hybrid fibres. However, there is a lack of research focusing on the flexural performance of micro and macro hybridisation of polypropylene fibres under fatigue load.
- It should be noted that using a single type of fibre for concrete reinforcement may only have a slight effect on the desired qualities, such as, mechanical properties, stiffness and flexural strength. Most previous studies focused on hybrid combinations of various steel fibres and a single type of polypropylene fibre under static load conditions.
- The majority of research published in the literature examined the effect of normal concrete, one type of fibre and two different shapes or lengths of steel fibres with polypropylene fibres. However, concrete made from different mixes and types of fibres may exhibit distinct cracking behaviours, which could have a different effect on the performance of the concrete.
- The hybridisation of micro and macro polypropylene fibres with steel fibres under fatigue load is rare, emphasising the need to study the potential of these hybrid fibre systems in limiting micro-cracks and macro-cracks.
- Further research is needed to establish a reliable understanding of the performance of hybrid fibre systems (combining micro and macro polypropylene fibres with steel fibres) under fatigue load for concrete beams.

Overall, the use of fibres in concrete has shown promising potential for enhancing its mechanical properties, durability, and resistance to cracking and deformation. However, further investigations are necessary to advance our understanding and enable the effective and optimised use of fibre-reinforced concrete in practical applications.

The following points identify some of the gaps found in the existing literature:

- Limited research on the performance of small and full-scale beams with hybrid fibres under fatigue load.
- Lack of comprehensive knowledge on the long-term behaviour of hybrid fibre systems (HyFRC).
- Insufficient information on the influence of hybrid fibre reinforcement on the flexural performance of concrete beams under static, sustained and cyclic loadings.

In conclusion, incorporating steel and polypropylene fibres can enhance the performance of concrete, as demonstrated in various studies. However, further research is needed to explore different fibre combinations, mixes and their effects on cracking behaviour to optimise the use of fibre-reinforced concrete. The objectives likely aim to investigate the effects of hybridising steel and polypropylene fibres, particularly in relation to flexural strength, load-bearing capacity, toughness, and failure behaviour. By addressing these research gaps, this study has the potential to contribute valuable insights and advancements in the development of hybrid fibre-reinforced materials.

Chapter 3

Experimental Programme

3.1 Layout of the Experimental Programme

This chapter provides details of the experimental programme, material properties, concrete mixes, test specimen preparation and procedures, and the test setup used in this research.

In order to achieve the aims and objectives set out in Chapter 1, the work was accomplished in different phases. The notations for the experimental programme are shown in Figure 3.1(a). Also, different phases are shown in Figure 3.1(b) and described in this chapter. Also, the experimental variables and tests are summarised in Table 3.1.

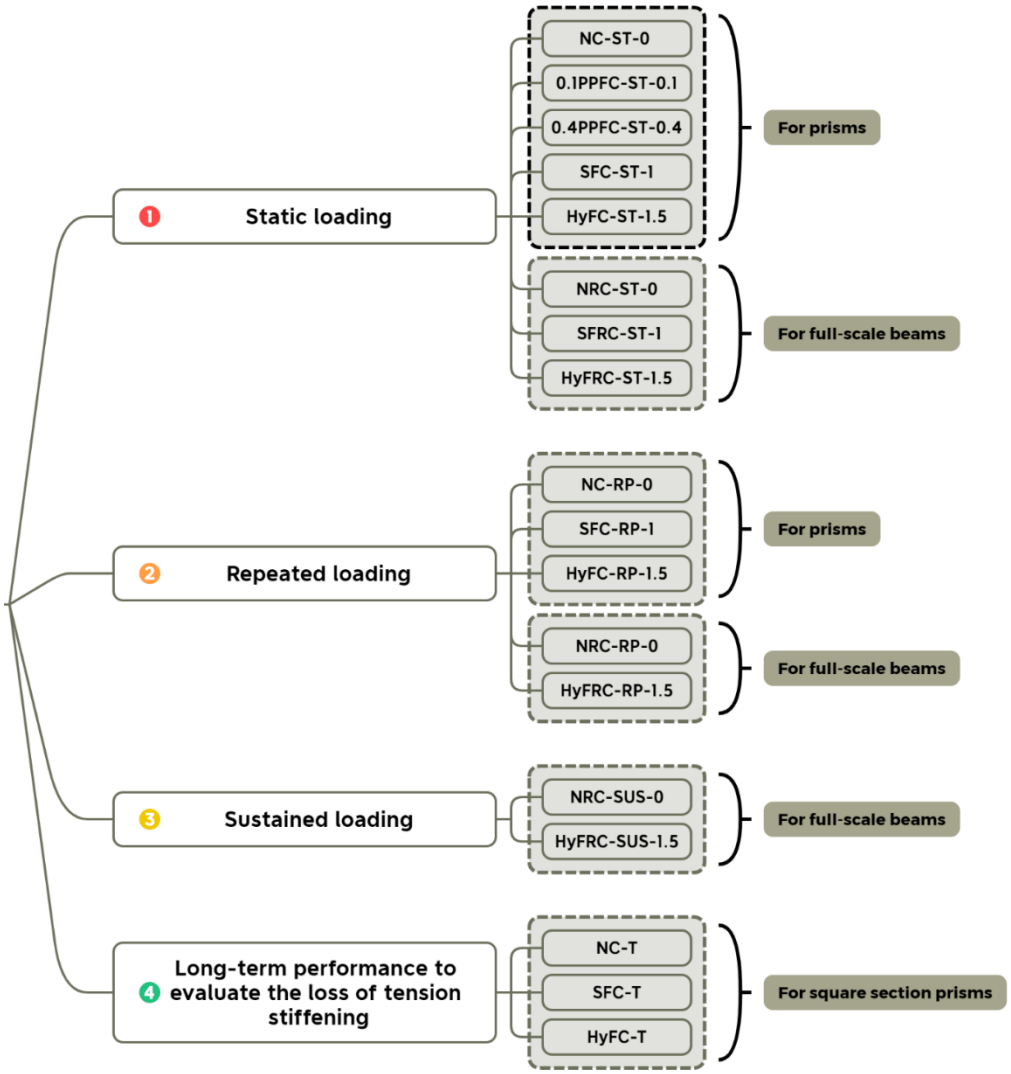

a) Notations for the experimental variables

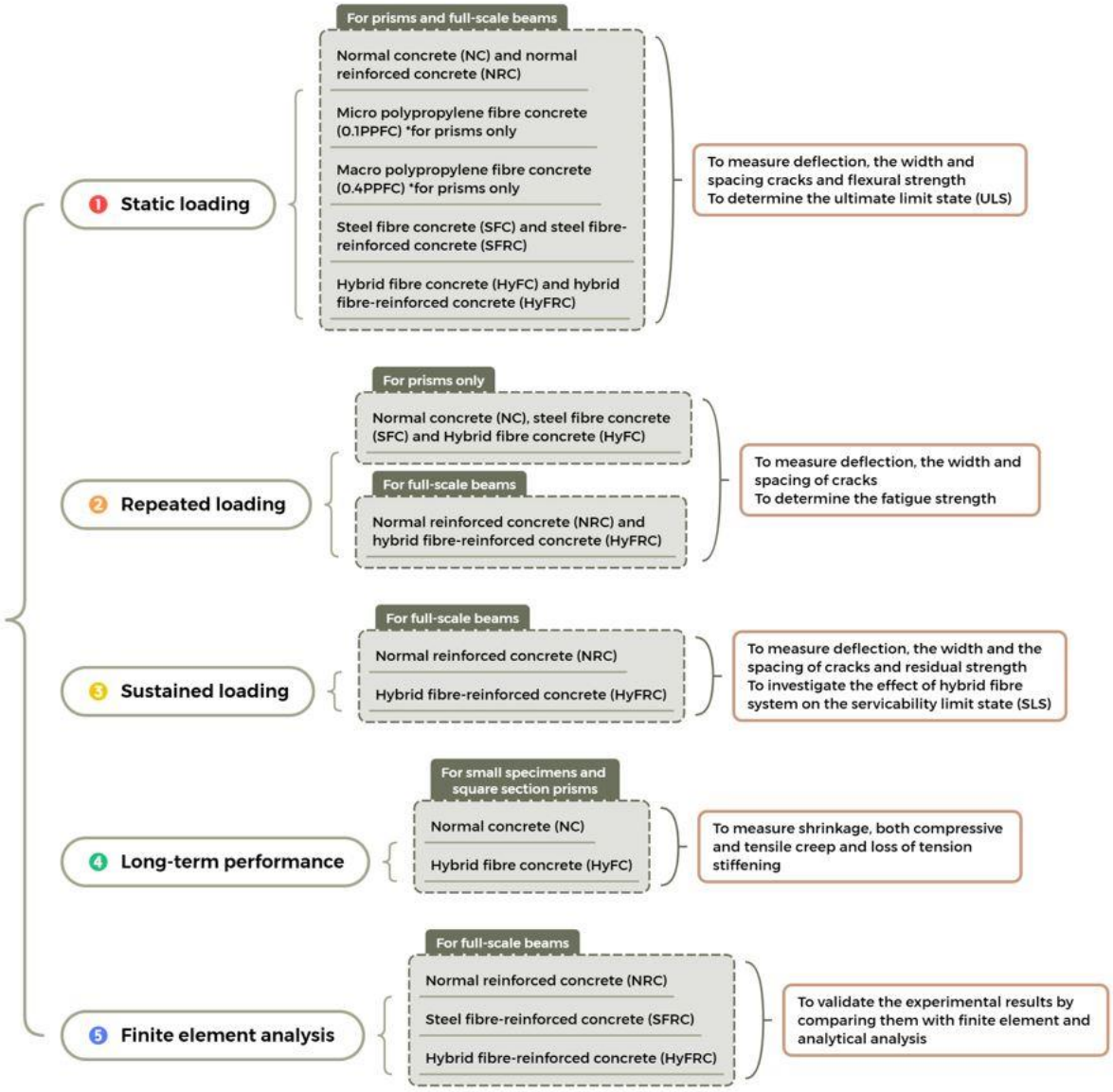

b) Summary of the test programme

Figure 3.1 Layout of the test programme

A series of experiments was performed to investigate the effect of a hybrid fibre system (which comprised steel fibre and both micro and macro polypropylene (PP) fibres) on the flexural behaviour of fibre-reinforced concrete (FRC) beams under static, repeated and sustained load types. The full-scale beams were reinforced with steel reinforcement bars whereas there were no steel reinforcement bars for the prisms.

Table 3.1: Summary of the experimental programme

No.	Beam labels	No. and size of bottom bars	No. and size of top bars	Volume fraction of fibre	Fibre type	Size of specimens (mm)	No. of specimens*
1	NC-ST-0	-	-	0	-	100x100x500	3
	NC-RP-0						10
2	0.1PPFC-ST-0.1	-	-	0.1%	Micro PP fibre	100x100x500	3
3	0.4PPFC-ST-0.4	-	-	0.4%	Macro PP fibre	100x100x500	3
4	SFC-ST-1	-	-	1%	steel	100x100x500	3
	SFC-RP-1						6
5	HyFC-ST-1.5	-	-	1.5%	0.1% micro, 0.4% macro PP and 1% steel	100x100x500	3
	HyFC -RP-1.5						10
6	NRC-ST-0	3 -16ϕ	2 –10ϕ	0	-	150x300x4200	2
	NRC-RP-0						2
	NRC-SUS-0						1
7	SFRC-ST-1	3 –16ϕ	2 –10ϕ	1%	steel	150x300x4200	2
8	HyFRC-ST-1.5	3 –16ϕ	2 –10ϕ	1.5%	0.1% micro, 0.4% macro PP, and 1% steel	150x300x4200	2
	HyFRC -RP-1.5						2
	HyFRC-SUS-1.5						1

*The number of specimens in the experimental programme was reduced due to time constraints in the lab for conducting the long-term tests and because of restrictions that were imposed due to the Covid-19 pandemic, so the number of specimens for short prismatic beams was higher than the full-scale beams.

The main parameters investigated were loading type and fibre type and volume. The loading type comprised static (ST), repeated (RP) and sustained (SUS) loads and the types of fibre were steel, micro and macro polypropylene fibres, hybrid fibre system, which is a combination of steel and polypropylene fibres and micro and macro polypropylene fibre. The fibre volume fractions were 0% of fibres for reference concrete specimens, 0.1% and 0.4% for micro and macro polypropylene fibre, 1% and 1.5% for steel and 1% steel, 0.1% micro, and 0.4% macro polypropylene for hybrid. Crack propagation, crack width and deflection were monitored. Five different types of concrete viz. Normal concrete (NC), micro polypropylene fibre concrete (0.1% 0.1PPFC), macro polypropylene fibre concrete (0.4% 0.4PPFC), steel fibre concrete (1% SFC), hybrid fibre concrete (1.5% HyFC), were tested for the compressive strength, splitting tensile strength, stress-strain relationship and flexural strength of small prisms. Also, only three of these (NC-RP, SFC-RP and HyFC-RP) were tested for repeated tests, while three (NC-T, SFC-T and HyFC-T) were tested to evaluate the loss of tension stiffening. Furthermore, only two mixes that were NC and HyFC were investigated for their long-term behaviour, such as shrinkage, and both compressive and tensile creeps. Full-scale beams (4.2 m long) manufactured

with normally reinforced concrete (NRC-ST) as a reference, steel fibre-reinforced concrete (SFRC-ST) and hybrid fibre-reinforced concrete (HyFRC-ST) were manufactured and tested under static load. Only two of these were tested for repeated (NRC-RP and HyFRC-RP) and sustained (NRC-SUS and HyFRC-SUS) loadings.

3.2 Scope of the work

As reported in Table 3.1, the experimental programme consisted of forty-one short prismatic (100x100x500 mm) beam tests (0.5 m long) and twelve long (150x300x4200 mm) beam tests (4.2 m long). They were produced to study five concrete mixes for prisms, viz. normal concrete (NC), micro polypropylene fibre concrete, macro polypropylene fibre concrete, steel fibre concrete (SFC) and hybrid fibre concrete (HyFC). Also, three different types of concrete were used to manufacture full-scale beams: normally reinforced concrete (NRC) with steel reinforcement bars, steel fibre-reinforced concrete (SFRC) with steel reinforcement bars, and hybrid steel and polypropylene fibres (HyFRC) reinforced with steel reinforcement bars, respectively. The fibre volume fraction is included in the beam labels shown in (i.e., 0% – no fibres - for the reference concrete specimens, 1 to represent the amount of steel fibres and 1.5% for the hybrid fibre system (which is 1% steel, 0.1% micro, and 0.4% macro polypropylene fibres). Three types of loading were used; static - short term (ST) to failure, static - long-term sustained (SUS)) and repeated (RP) loading.

3.3 Material

This section describes the physical, mechanical, and chemical properties of the materials used in this research. Where appropriate, reference is made to all corresponding standards and manufacturer specifications.

3.3.1 Cement

Portland cement (high strength cement 52.5N) (CEM I) was used for all concrete mixes. CEM1 is appropriate for multiple purposes and conforms to the requirements of BS EN 197-1.

3.3.2 Fine aggregate (FA)

The type of fine aggregate used in this research was natural sand with a maximum particle size of 5 mm. The sieve analysis of the natural sand is shown in Table 3.2. Figure 3.2 shows the grading curve for the natural sand and the standard limit requirements according to BS 882 (1992).

Table 3.2: Sieve size and percent passing of natural sand

Sieve size (mm)	10	5	2.36	1.18	600µm	300µm	150µm
Passing (%)	100	96.93	88.57	84.18	77.55	25.72	5.78
Specification limits	100	89-100	60-100	30-100	15-100	5-70	0-15

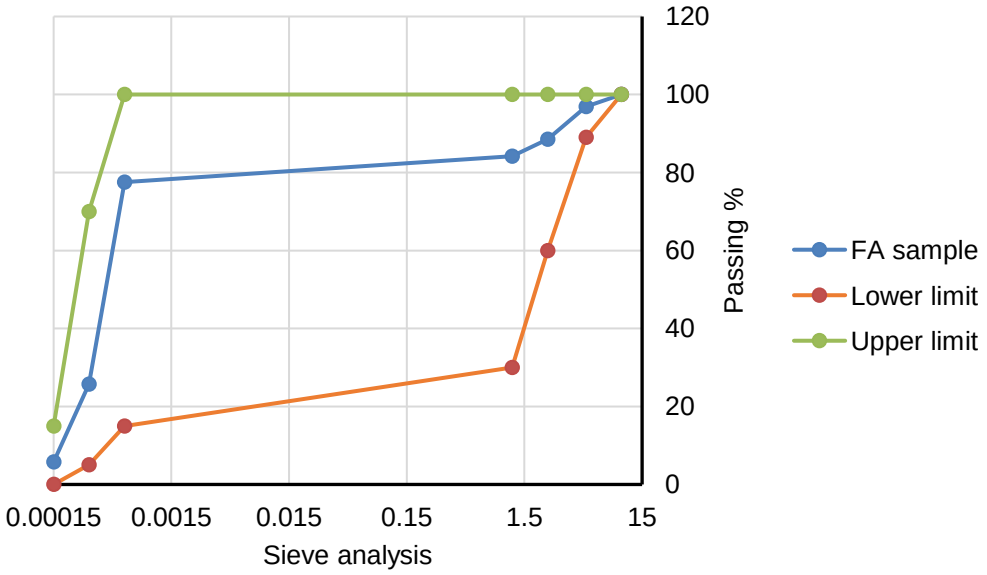

Figure 3.2: Grading curve for natural sand

3.3.3 Coarse aggregate (CA)

The coarse aggregate used in this research was natural coarse quartzite gravel aggregate with a maximum size of 20 mm. The sieve size, passing percent and specification limits according to BS 882 (1992) are shown in Table 3.3. Figure 3.3 shows the grading curve for the natural coarse aggregate and the standard limit requirements according to BS 882 (1992).

Table 3.3: Sieve size and percent passing of coarse aggregates

Sieve size (mm)	37.5	20	14	10	5	2.36
Passing (%)	100	99.57	22.70	3.41	0.97	0.54
Specification limits	100	85-100	0-70	0-25	0-5	-

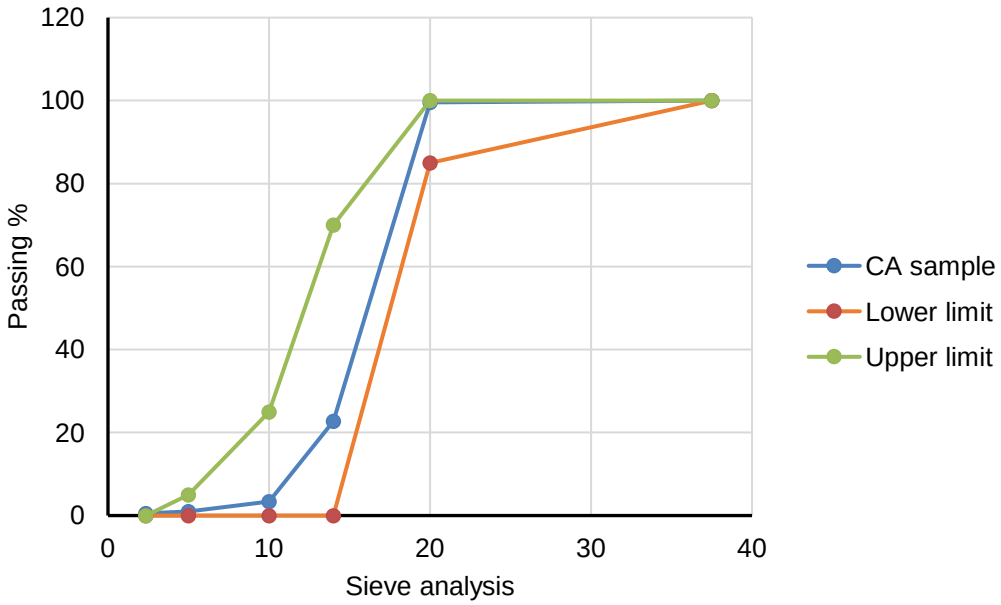

Figure 3.3: Grading curve for coarse aggregate

3.3.4 Mixing water

Tap water, free of impurities and organic/inorganic substances in accordance with BS EN 1008 (2002) was used.

3.3.5 Admixture

The superplasticizer used in this research was Sika ® Visco Crete 25 MP, which is a high range water reducing admixture that complies with the requirements of BS EN 934-2 (2009). Sika ® Visco Crete 25 MP is based on modified polycarboxylate polymers. It was used to ensure that the concrete is workable. The dosage of the superplasticizer depended on the amount of added fibres, as shown in Table 3.5.

3.3.6 Reinforcement bars

In all full-scale (4.2 m) long beam specimens, three deformed steel bars of diameter ⌀ = 16 mm were used as a bottom tensile longitudinal reinforcement. Two steel bars of ⌀ = 10 mm placed in the compression zone acted as hangar bars for the shear links. For the shear links, deformed bars of ⌀ = 8 mm were spaced at 150 mm along the length of the beam, only in the shear zones; there were no shear links in the constant moment zone between the applied loads and the distance was 1500 mm, as shown in Figure 3.4.

Figure 3.4: Reinforcement cage

3.3.7 Fibres

As reported in Chapter 2, fibres have been commonly used in concrete over the last few decades. In this study, two types of fibres, namely, micro and macro polypropylene and steel fibres, have been used due to their reported positive contribution to reducing the number of cracks and crack widths. Fibrin (micro) and Durus (macro) polypropylene fibres were obtained from Adfil, the hooked end steel fibre (Dramix 3D) was obtained from Bekaert; these are shown in Figure 3.5(a), Figure 3.5(b) and Figure 3.5(c), respectively. The polymer fibres were classified in terms of diameter according to EN-14889. Macro fibres are those with a diameter more than 0.3 mm, whereas micro fibres are those with a diameter less than 0.3 mm. The properties of micro (Fibrin) and macro (Durus) polypropylene fibres and steel fibres, as reported by the manufacturers, are summarised in Table 3.4.

Table 3.4: Properties of fibres

Fibre type	Specific gravity (kg/m^3)	Length (mm)	Diameter	Aspect ratio
Fibrin (micro 1960/650)	910	18	50 µ	-
Durus (macro S500)	922	48	0.7	69
Steel (Dramix 3D 65/35BG)	7850	60	0.9	65

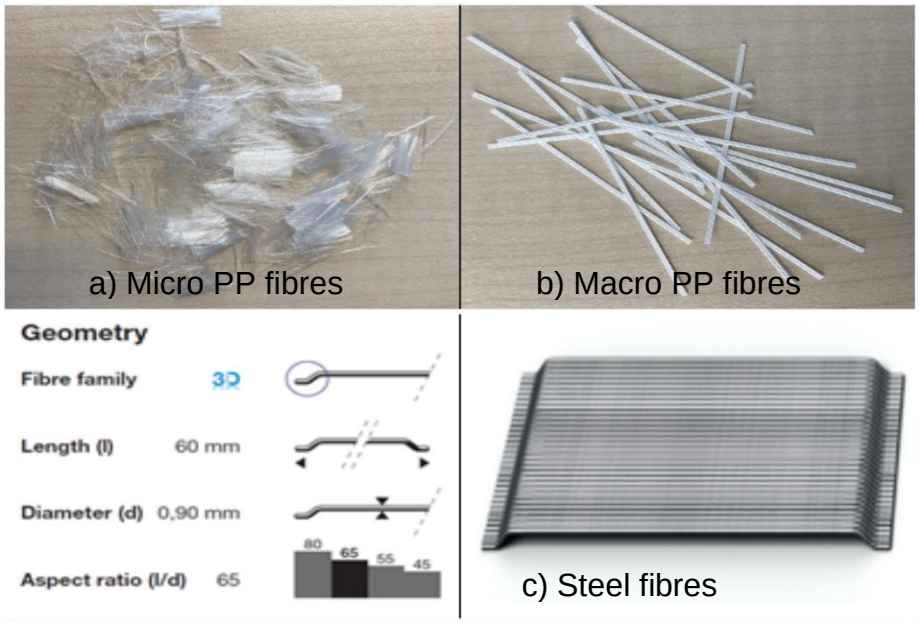

Figure 3.5: Different fibres type

3.4 Concrete mix

The mixes were formulated based on previous studies and trial mixes conducted to determine the appropriate mix proportions, achieve the desired workability, and attain the target compressive strength. The normal concrete mix was designed to achieve an S3 slump class, which was 100 mm. The target compressive strength was 40 MPa. The way the correct proportion for the mix design was discovered through trial and error until reaching the required workability and compressive strength of the concrete in order to ensure the consistency of the mix design. After that, the proportions of the different concrete mixes were as reported in Table 3.5. All mixes had a water-cement ratio (w/c) of 0.42.

Table 3.5: Mix proportions

	Quantity (kg/m^3)				Quantity (L/m^3)		Fibres
Mix type	Cement	Water	Fine aggregate	Coarse aggregate	Super-plasticizer	Volume fraction (%)	Fibre type
NC and NRC	422	177	754	1024	-	-	-
0.1 PPFC	422	177	754	1024	0.1	0.1%	0.1% micro polypropylene (PP)
0.4 PPFC	422	177	754	1024	0.4	0.4%	0.4% macro PP
SFC and SFRC	422	177	754	1024	1	1%	Steel
HyFC and HyFRC	422	177	754	1024	1.5	1.5%	0.1% micro-PP, 0.4% macro-PP, and 1% steel

3.5 Test specimens

Details of the test specimens used to determine the properties of the hardened concrete for each type of concrete mix are summarised in Table 3.6. All beams, i.e., the prisms (100x100x500) and the full-scale long beams (150x300x4200 mm), were manufactured in the casting shop at the University of Leeds. Additional specimens were cast and tested for each mix. Cylinders (150x300 mm) were used to determine compressive and splitting tensile strength. Also, cubes (100x100x100 mm) were used to determine the compressive strength. Small prisms (75x75x200 mm) were used to measure shrinkage and compressive creep, whereas bobbins (75x365 mm) were used to measure the tensile creep. Additionally, two square section prisms (120×120×1200 mm) were cast and tested to determine the loss of tension stiffening for NC-T, SFC-T and HyFC-T mix.

3.6 Preparation of specimens

All beams were cast in steel formwork and the internal walls of the formwork had been covered with release oil in order to make it easier to remove the beams from the formwork. For all the full-scale beams, the reinforcement cages were placed inside the formwork and positioned on small pieces of concrete (packers) to maintain a clear concrete cover of 25 mm along the span. All beams had a rectangular cross-section of 150x300 mm. This type of beam is called a Wide-Shallow Beam (WSB). According to Conforti et al. (2013), a WSB is characterised by a depth, in general, lower than 350 mm and a cross-section having the width (b) over the effective depth (d) ratio equal to or greater than 2 (i.e. $b/d \geq 2$). Furthermore, this type of beam will produce a higher deflection than normal beams (by about 10%), which is important in this research as one of the aims is to study the deflection of beams.

Table 3.6: Testing for hardened concrete properties

Test type	Type of the mould	Specimen dimensions (mm)	No. of specimens	Curing time (days)
Splitting tensile strength	Cylinders	150x300	3	28
Modulus of elasticity	Cylinders	150x300	3	
Compressive strength	Cylinders and cubes	150x300 and 100x100x100	6	
Shrinkage	Prisms	75x75x200	4	
Compressive creep	Prisms	75x75x200	4	
Tensile creep and Direct tensile strength	Bobbins	75x365	4	
Tension stiffening	Prisms	120x120x1200	2	

3.6.1 Mixing Procedure

The concrete mixes were manufactured in accordance with British Standard 1881-125: 2013. A drum mixer was used to mix the concrete. The concrete specimens were cast in the casting shop at a temperature of 20 (±5) ºC and a relative humidity of 50%. All the materials were weighed prior to adding them to the mixer; an extra 15% by weight was included to account for losses. The drum mixer was wetted to make the mixer slightly wet and avoid the loss of the mixing water. The materials were placed in the drum mixer in the following order: 1) fine and coarse aggregates were added and then mixed dry for 15 to 30 seconds; 2) the mixer was stopped, then the cement was added and mixed for 30 seconds with the aggregate to ensure homogeneity of the mix; 3) superplasticizer was added to the water if required as per the mix design and then it was added to the mix while the mixer was still running; the material components, including the water (and superplasticizer) were mixed for a further two minutes. For the fibre

concrete mixes, there was an additional step. After finishing Step 3; 4) the fibres were added while the mixer was still running; the mixer was kept running for a further two minutes to ensure the uniform distribution of all fibres.

3.6.2 Manufacturing of test specimens

After placing the concrete in the mould, the concrete was compacted to reduce the trapped air. Compaction was carried out using a shaking table for the cubes, cylinders, bobbins and small prismatic beams, and by a hand-held mechanical vibrator for the long (4.2 m) beams. Segregation of the concrete through over-compaction was avoided by carefully observing the concrete during the application of vibration. After compaction, the exposed surface of the concrete was floated off using a trowel. Floating was performed to ensure that any load is applied to a flat surface (see Figure 3.6).

Figure 3.6: Specimens during and after casting

3.6.3 Curing procedure

The concrete specimens were cured in accordance with BS EN12390-2 (2009). After the specimens were cast, they were covered with wet burlap to keep the specimens moist and to prevent loss of moisture from the exposed surface of the specimens. The small concrete specimens were kept in their moulds for at least 24 hours. After 24 hours, all small concrete specimens were removed from their moulds and stored next to the full-scale beams under wet burlap and polythene sheets. Curing of the long (4.2 m) beams was slightly different; these beams were initially kept in their moulds for curing, being covered with wet hessian and

polythene sheet, and then demoulded after four days. After that, all small specimens and full-scale beams were moved to a controlled environmental fog room for 25(±1) days where the temperature was 20 (± 2) ºC and the relative humidity was ≥ of 95% (see Figure 3.7).

Figure 3.7: Curing condition for specimens

3.7 Testing of fresh concrete

3.7.1 Workability

The test used to determine the workability of fresh concrete was the slump test. The slump test was carried out according to BS EN 12350-2 (2009). Three to five slump tests were used for each concrete mix. A metal cone mould with a height of 300 (± 2) mm was used to perform the slump test; the diameter of the base was 200 (± 2) mm and the diameter of the top was 100 (± 2) mm. The cone was filled in three layers and each layer was compacted by tamping the concrete with 25 strokes using a straight steel rod with a length of 600 (± 5) mm and a diameter of 16 (± 1) mm. After tamping of the third layer was complete, the excess concrete

was struck from the top of the cone using the tamping rod. Any excess concrete surrounding the base of the cone mould was removed and then the cone was cautiously removed in a vertical direction. The slump test was carried out within 150 seconds of the end of the mixing. The slump was obtained using a ruler which measured the height difference between the highest point of the concrete and the top of the cone mould, as shown in Figure 3.8.

Figure 3.8: Slump test

3.8 Testing of hardened concrete

As already reported in Table 3.6, three cylinders (150x300 mm), three cubes (100x100x100 mm), four small prisms (75x75x200 mm), two bobbins (75x365 mm), two prisms (120x120x1200 mm) and three prisms (100x100x500 mm) were cast and tested to obtain splitting tensile strength, modulus of elasticity, compressive strength, shrinkage and compressive creep, tensile creep, tension stiffening and flexural strength for each mix.

3.8.1 Compression test on cylinders and cubes

This test was performed according to BS EN 12390-3 (2009). The test was performed on cubes (100×100×100 mm) and cylinders (150×300 mm) to determine the compressive strength, as shown in Figure 3.9(a) and Figure 3.9(b), respectively. The top and bottom surfaces were prepared to be smooth, ensuring flat surfaces for applying the load. Three cylinders and three cubes were used to

determine the 28-day compressive strength for each concrete mix. The load was increased at a constant rate (3 kN/sec) and failure loads were determined. The following equation (3-1) was used to calculate the compressive strength from the failure loads:

$$f_c = \frac{P}{A} \qquad \text{Eq. 3-1}$$

Where

f_c: is the compressive strength (MPa), P is the maximum load at failure (N), A is the area of concrete specimen (mm^2).

a) Cubes b) Cylinders

Figure 3.9: Compression Test

3.8.2 Indirect tension test on cylinders

This test was carried out according to BS EN 12390-6 (2009). This test was performed on cylinders, which were 150 mm in diameter and 300 mm in length, to determine the splitting tensile strength, as shown in Figure 3.10. For each mix, three cylinders were tested at the age of 28 days. The specimen was initially placed in a specific rig that ensured the sample was precisely located in the

machine's centre. The load was applied after the samples were placed in the testing equipment. The load was increased at a constant rate (0.2 kN/s) and failure loads were determined. The splitting tensile strength was calculated using the expression below (3-2) from the failure loads:

$$f_{ct} = \frac{2P}{\pi LD} \quad \text{Eq.3-2}$$

Where

f_{sp}: is the splitting tensile strength (MPa), P is the maximum load at failure (N), L is the cylinder length, and D is the cylinder diameter

Figure 3.10: Splitting tensile strength test

3.8.3 Modulus of elasticity

This test was carried out in accordance with BS EN 12390-13 (2009). Three-cylinders were tested to determine the static modulus of elasticity at the age of 28 days. The top and bottom surfaces were prepared to be smooth, ensuring flat surfaces for applying the load. The two-side surfaces of the specimens were ground using an electrically powered grinder and sandpaper to produce a flat surface on which the Electrical Resistance Strain (ERS) gauges could be installed. The ERS gauges were placed on the side surfaces of the concrete with glue to monitor the strains in the concrete, as shown in Figure 3.11. Strains in

some gauges were not recorded due to gauge malfunctions after the cracking of the specimen, so only some of them will be plotted and reported in Chapter 4 (Figure 4.1). Also, strain readings after cracking of specimens were not recorded. The deformations under the applied compressive load were measured using the ERS gauges and recorded. The secant modulus refers to a material's stiffness, and it specifically measures the stress-to-strain ratio as the material undergoes increasing levels of stress. The secant modulus is a measure of material stiffness in the inelastic region of the stress-strain curve and can be expressed as a percentage of the Young's modulus. It provides an average measure of stiffness between the two selected points on the stress-strain curve. The secant modulus is calculated by dividing the change in Young's modulus by the change in strain between the two points. The load was increased at a constant rate (3 kN/s) and failure loads were determined. The following equation (3-3) calculates the static modulus of elasticity from the failure loads:

$$E_c = \frac{\sigma_2 - \sigma_1}{\epsilon_2 - 50 \times 10^{-6}} \qquad \text{Eq.3-3}$$

Where

E_c is the static modulus of elasticity, σ_2 is the stress corresponding to 40% of the ultimate load, σ_1 is the stress corresponding to a strain of 50×10^6 , and ϵ_2 is the longitudinal strain at σ_2.

Figure 3.11: Test set up for measuring modulus of elasticity

3.8.4 Shrinkage test

Four small prisms (75×75×200 mm) were tested to determine the free shrinkage for each type of concrete mix according to BS ISO 1920-8:2009. All specimens were cast and then cured for 28 days in the same environment of the full-scale beams (150×300×4200 mm) and creep tests, as mentioned in 3.6.3. Two Demountable Mechanical (Demec) gauge points were placed at a spacing of 150 mm on each side of the specimen (but not on the floated surface), as shown in Figure 3.12. The shrinkage was measured and recorded at the same time as it was recorded on the full-scale beams; all measurements were taken from specimens stored in an environment where the temperature was 20 (± 2) ºC and relative humidity was 45% (± 5)%. The shrinkage for each concrete mix was calculated as the average value of the shrinkage measured from the four prisms.

Figure 3.12: Shrinkage test specimen

3.8.5 Compressive creep test

Four small prisms (75×75×200 mm) were tested to determine the compressive creep for each concrete mix according to BS ISO 1920-9 (2009). All specimens were cured for 28 days and then tested in the same environment (a temperature of 20 ± 2 ºC and a relative humidity of 55% ± 5%) as the full-scale beams (150×300×4200 mm), as mentioned in 3.6.3. Two Demec gauge points were placed on two of the four sides of the specimens prior to testing. Two creep rigs were used for the determination of the creep. Each rig held two prisms and one steel dynamometer/load cell, as shown in Figure 3.13(a). A constant stress of 10 MPa was applied to the other two specimens (a stress equal to 23-25% of the 28-

day compressive strength). Before applying the load, the load cells were calibrated and was connected to the data logger, as shown in Figure 3.13(b). Prior to applying the load, the strain reading was taken and was used as a reference for calculating the strain for each of the subsequent readings. The initial elastic strain reading was recorded after the application of the initial load. After that, strain values were monitored and recorded at different times to test the specimens under repeated loads. The total strain obtained from the creep rigs was used to calculate the compressive creep. The compressive creep was calculated by subtracting the drying shrinkage of unloaded specimens and the elastic strain of loaded specimens from the total strain obtained from the loaded specimens. The creep coefficient is defined as the relationship between the immediate elastic strain and creep. The stress-strength ratio is eliminated in terms of the creep coefficient.

a) Test rigs

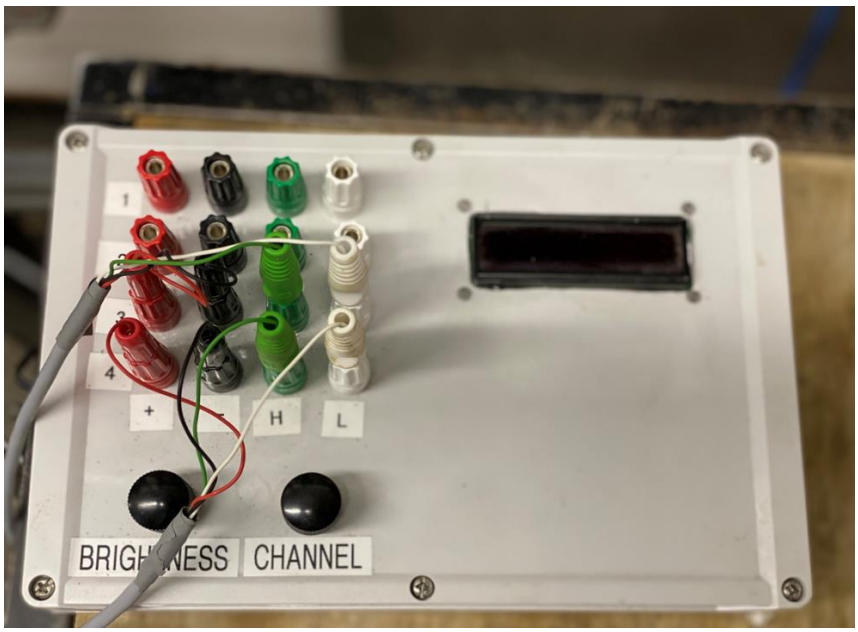

b) Data logger

Figure 3.13: Compressive creep test

3.8.6 Tensile creep test

As previously detailed in Sections 3.8.4 and 3.8.5, a similar procedure was followed for measuring the tensile creep. Two bobbin specimens (75×365 mm) were tested to determine the tensile creep for each mix according to BS ISO 1920-9 (2009). Similarly to shrinkage and compressive creep, all specimens were cured for 28 days, as mentioned in section 3.6.3. Two sets of two Demec points gauges were installed on the circumference of the bobbins, 180° apart, prior to testing. The tensile creep rig is shown in Figure 3.14. The load cells were calibrated before applying the load. The applied stress to the specimens being measured for tensile creep was equal to 1 MPa. The strain reading was taken and was used as a reference for calculating the strain for each of the subsequent readings prior to applying the load. The initial elastic strain values were measured using the Demec gauge and recorded after the load was applied. Then, the tensile creep was calculated and recorded at the same time as testing the full-scale beams over time. The total strain obtained from the creep rigs was used to calculate the tensile creep. The tensile creep was calculated by adding the strain of the shrinkage specimens and then subtracting the initial elastic strain of the loaded specimens from the total strain obtained from the loaded specimens.

Figure 3.14: Tensile creep test set up

3.8.7 Long-term tension stiffening tests

Two square section prisms (120×120×1200 mm) were tested to determine the loss of tension stiffening for each type of mix viz. normal concrete (NC-T), steel fibre-reinforced concrete (SFC-T) and hybrid fibre-reinforced concrete (HyFC-T) in accordance to BS ISO 1920-9 (2009). One of the prisms was subjected to a sustained load to determine the loss of tension stiffening (see Figure 3.15(a)), while the second one was unloaded and utilised to quantify the shrinkage of the concrete specimens (see Figure 3.15(b)). The second specimen was stored next to the loaded specimen to quantify the shrinkage of the concrete specimens in order to determine the loss of tension stiffening. A central bar of diameter Ø = 16 mm was used for all the tension stiffening tests. Seven Demec gauge points were installed on both sides, positioned every 150 mm on the side of the specimens, before testing to measure the surface strain. Three ERS gauges were installed in each specimen at 300 mm alongside the steel bars to monitor the strains in the steel bars after the concrete cracked at different places. The specimens were placed in the special rig, which was used for testing the specimens. This rig was created and built exclusively for this test, and it was based on Scott and Beeby's test setup (2005), as demonstrated in Figure 3.15(a). A hydraulic jack was used to apply a direct tensile load to the steel bar and kept at a constant value of 45KN for a period of 35 days. This load caused a 200 MPa stress in the bar, which was identical to the tensile stress induced in the steel reinforcement in the full-scale

beams tests. Prior to applying the load, the strain readings in both specimens were recorded and were used as a reference for calculating the strain for each of the subsequent readings. To reach the required load, the applied load was completed in ten minutes. The initial elastic strain values were measured and recorded immediately after loading. After that, the surface strain was monitored and measured by using a hand-held mechanical strain gauge, which was used to take regular readings over time. ERS gauges were connected to the data logger to record the strains in the steel bars. Additionally, the applied load was connected to the data logger and monitored over time by using the load cell, as shown in Figure 3.15(c). The strain in the steel reinforcement bars and on the concrete surfaces were then measured and recorded over the course of 35 days.

a) Loaded specimen

b) Unloaded specimen

c) Data logger

Figure 3.15: Tension stiffening test

3.9 Flexural strength test setup for prismatic (0.5 m) beams

In line with BS EN 12390-5 (2009), prismatic beams (100×100×500 mm) were used to determine the flexural strength of each mix under static and repeated loads. Prisms were tested to failure at the age of 28 days. All beams were simply supported and subjected to a four-point bending load. A hydraulic jack was used

to apply the load at two locations spaced 100 mm apart, as shown in Figure 3.16. All specimens had a clear span of 300 mm. The applied load was increased steadily at the rate of 0.1 kN/s until failure. The test programme was designed and conducted to investigate the effect of the hybrid fibre system (the fibres include steel fibre and micro and macro polypropylene fibres) on the performance of different loading types (static and repeated) of fibre concrete (FC) beams with no steel reinforcement bars. Three prismatic beams (0.5 m) were tested to failure load; the aims of these tests were to determine the ultimate flexure strength and obtain the level of loading required for the repeated tests. They were produced to study five concrete mixes, viz. Normal concrete (NC), micro polypropylene fibre concrete (0.1% PPFC), macro polypropylene fibre concrete (0.4% PPFC), steel fibre concrete (1% SFC) and hybrid fibre concrete (1.5% HyFC). Six prismatic (0.5 m) beams (minimum of three prismatic beams for each different stress level) were tested under repeated load to determine the fatigue strength for each beam manufactured with each concrete mix. Different stress ranges for maximum and minimum flexural stress were used to plot the relationship between stress and fatigue life (Δσ–N). Thus, the applied frequency for the prismatic beams was 2 Hz. Three of these concretes (NC, SFC and HyFC) were studied also for their performance under repeated loading. The following expression (3-4) was used to calculate the ultimate flexure strength (F_{cf}):

$$F_{cf} = \frac{F \times I}{d_1 \times {d_2}^2} \qquad \text{Eq.3-4}$$

F_{cf} is the flexural strength (MPa), F is the maximum load (N).

Figure 3.16: Details of the flexural strength tests using the short prismatic beams

3.9.1 Instrumentation and measurements

3.9.1.1 Mid span deflection (LVDT)

All central beam deflections were measured using a linear variable displacement transducer (LVDT) located at the mid-span of the beam, as shown in Figure 3.16.

3.9.1.2 Crack pattern inspection

The monitoring of the crack growth helped with the investigation of the influence of fibres on the development of the cracks. The crack width of the prismatic (0.5 m) beams was recorded by installing another LVDT at the mid-span between the point loads, and the distance between the applied loads was 100 mm, as can be seen in Figure 3.17; the load was recorded at the same time the crack width was recorded.

Figure 3.17: Location of the crack width measurement

3.10 Flexural strength test for the full-scale beams (4.2m)

As detailed in Figure 3.18, twelve full-scale beams (150x300x4200 mm) were tested at an age of 28 days. Six full-scale beams were tested statically to determine flexural strength. Four full-scale beams were tested under a repeated load and two beams were tested under a sustained load.

All beams were simply supported and subjected to a four-point bending load, as shown in Figure 3.18. A hydraulic jack was used to apply the load at two locations spaced 1500 mm apart. Chemical metal was used to 'bed' the loading and support plates to ensure the beams were level and the load acted vertically at the start of the test. The clear span between supports was 4000 mm.

Two long beams (4.2 m) were tested to failure load for each beam manufactured with a concrete mix; one of the aims of these tests was to obtain the level of loading required for the repeated tests. Two long (4.2 m) beams (one beam for each different stress level) were tested under repeated load to determine the fatigue strength for each beam manufactured with a concrete mix (i.e., NRC and HyFRC). Different stress ranges for maximum and minimum flexural stress were used to plot the relationship between stress and fatigue life (Δσ–N). Thus, the applied loading frequency was 1 Hz for full-scale beams. In addition, one long beam incorporating the hybrid fibre systems (i.e. HyFRC), and one long beam as

a reference beam (i.e. NRC) were subjected to a sustained load. The applied force was equal to 50 % of the ultimate flexural strength (this applied load produced a tensile stress of 200 MPa in the steel reinforcement bars) which is the stress generally associated with stabilised crack pattern for these types of beams loaded in flexure.

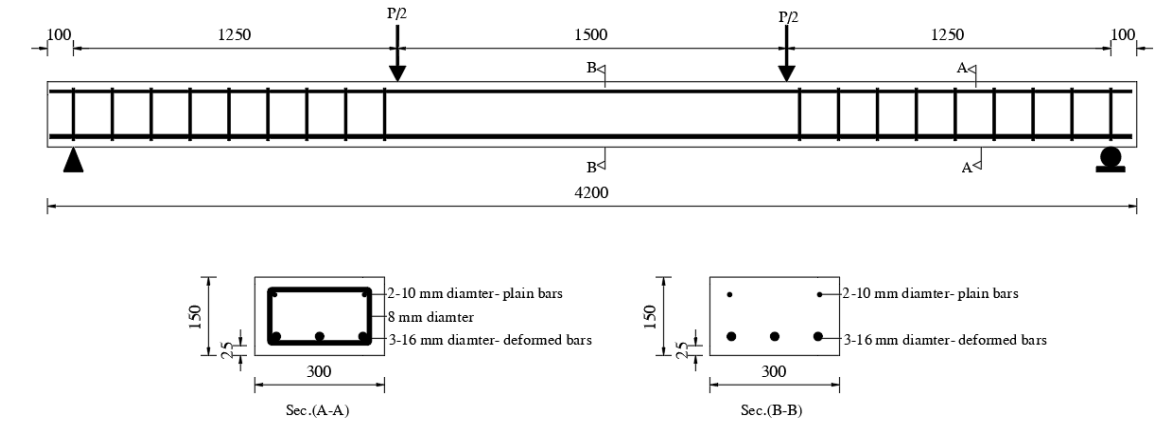

Figure 3.18: Details of the beam specimens

3.10.1 Instrumentation, measurements, and setup

3.10.1.1 Steel and concrete surface strain measurement

Each of the three main steel tensile reinforcement bars used in the beams was fitted with a five-millimetre-long ERS at their mid-span. Before the ERS gauges could be fitted, the steel surface of the bars had to be ground smooth using an electrically powered grinder and sandpaper. The bars were then cleaned with acetone before the gauges were attached to the bars using the cyanoacrylate adhesive. Electrical wires were soldered to the ends of the strain gauges and connected to electrical terminals on the steel bar. The sensors were then checked and covered with a protective coating of chemical metal (Figure 3.19).

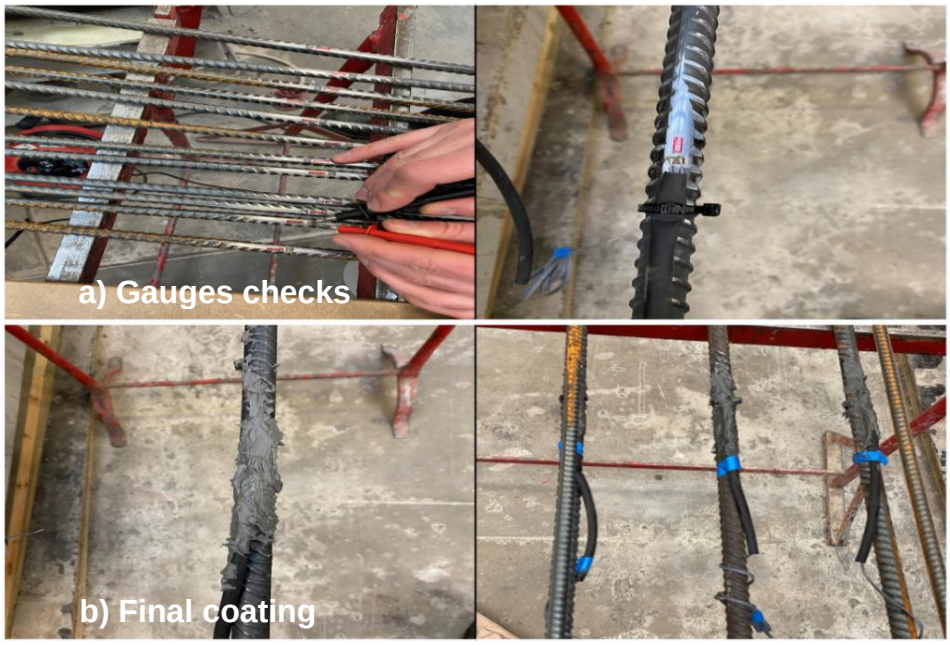

Figure 3.19: Installation of strain gauges on bars

Two 60mm long ERS gauges were mounted on the other side of the beam in line with the position of the top and bottom reinforcement, as shown in Figure 3.20(a). All ERS gauges were connected automatically to a data logger to track the strains on the steel bars during testing, as shown in Figure 3.20(a). Before testing, four rows of Demec gauge points were installed on one side of the long (4.2 m) beam specimens within the constant moment zone (the Demec points were spaced at 150 mm) to monitor the change in neutral axis depth and the curvature. These Demec gauge points were divided into ten zones along the span of the beam in the constant moment zone, which were called A, B, C, D, E, E', D', C', B' and A'. Also, they were divided into four rows along the height of the beams, which were called 1, 2, 3 and 4, as illustrated in Figure 3.20(b). Two rows of Demec gauge points were placed along the line of the top (hanger/compression) and bottom (tension) reinforcement of the beam to compare the strain in the concrete and steel reinforcement bars. The positions of the Demec points are shown in Figure 3.20(b). The surface strains of the concrete were measured using a hand-held 150mm mechanical strain gauge. The steel and concrete strains were measured at each loading step

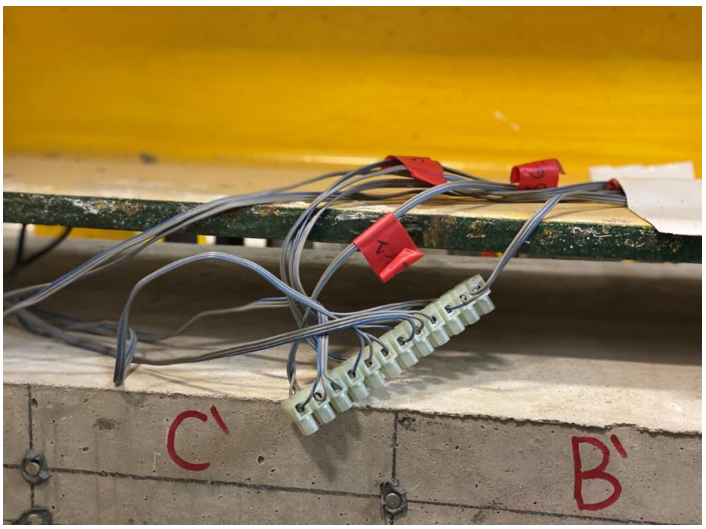

a) Strain gauge on concrete surface and its connection to the data logger

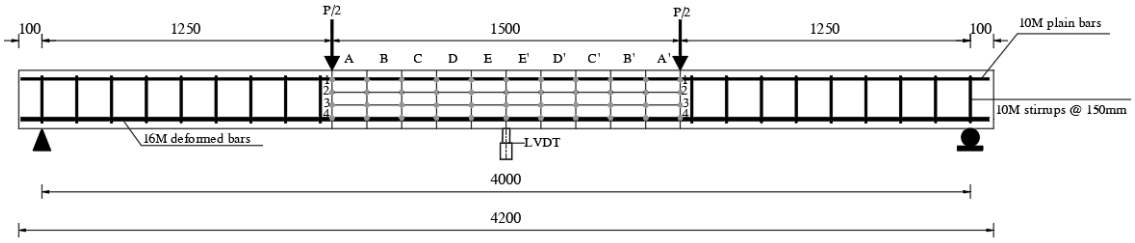

b) Demec gauge points installation in the moment zone

Figure 3.20: Schematic drawing for full-scale beams test set up with dimension, reinforcement, instrumentation and measurements

3.10.1.2 Mid span deflection (LVDT)

All central beam deflections were measured using LVDT located at the mid-span of the beam, as illustrated in Figure 3.20. Another LVDT was attached to the hydraulic jack similar to the prismatic beams, as shown in Figure 3.16.

3.10.1.3 Crack pattern inspection

The crack pattern on the surface of the concrete was observed during testing and highlighted using a marker, as shown in Figure 3.21(a). The monitoring of the crack growth helped with the investigation of the influence of fibres on the development of the cracks. The crack width of the long (4.2 m) beams was recorded using a digitronic caliper (or graduated magnifier), as shown in Figure 3.21(b); the load was recorded at the same time the crack width was recorded.

a) Visual examination of the crack pattern

b) Crack width measurement

Figure 3.21: Crack monitoring

3.11 Fatigue load limits for prismatic (0.5 m) and the full-scale beams

The fatigue load limits were determined for each beam manufactured with each concrete mix. As calculated by the static tests previously, beams were subjected to repeated load from 20% to 80% of the ultimate load capacity of each beam

type. The mean load of all specimens was kept at 50% of the ultimate loads, while the maximum level of loads were 70% and 80% of the ultimate loads, and the minimum level of loads were 30% and 20% of the ultimate loads. The minimum and maximum level of repeated loading were calculated by multiplying the average static tests by the required level of loading. These levels were chosen based on common cyclical studies on concrete specimens, as reported in the literature (Nagabhushanam et al., 1989; Johnston and Zemp, 1991; Cachim et al., 2002; Banjara and Ramanjaneyulu, 2018; Mohammadi and Kaushik, 2005; Ramakrishnan et al., 1989; Schäfer et al., 2019). Different stress ranges for maximum and minimum applied stress were used to plot the relationship between stress and fatigue life (Δσ–N), as reported by Banjara and Ramanjaneyulu, (2018) and Meng et al., (2019). The fatigue life of concrete beams refers to the number of cycles or duration of repeated loading that the beams can withstand before failure occurs.

According to Ramakrishnan et al. (1989), the maximum limit for specimens under loading that can be applied to all practical applications of concrete structures is two million cycles. For example, the concrete overlays for highway or bridge decks are predicted to resist millions of cycles through their service life of repetitive axle loads from passing traffic (Nagabhushanam et al., 1989). According to BS EN 1990:2002 +A1 (2005), the design working life category of monumental building structures, bridges, and other civil engineering structures is category no.4, which is about 100 years. So, an upper limit of $2x10^6$ cycles was selected to make the testing less time-consuming. Thus, the test was terminated when the samples either suffered failure or reached an upper bound of $2x10^6$ cycles.

3.12 Summary

In this chapter, the experimental details have been given, with both details of materials used, test specimens cast and tests carried out described. Electronic data loggers were used to monitor and record the displacements and strains. The final test data were calculated by using the Excel spreadsheet and other relevant software. All the data were evaluated and used to compare with the experimental results from previous studies and existing code specifications. Also, software

such as Abaqus was used to compare and evaluate the accuracy and suitability of the experimental results with analytical modelling.

With regard to the influence of the addition of fibres on the performance of FRC beams, each of the following aspects are discussed separately in comparison with normal concrete and different parameters in the following chapters:

- Mechanical properties of concrete (compressive strength, splitting tensile strength, modulus of elasticity, compressive and tensile creep, shrinkage and loss of tension stiffening)
- Flexural strength and deflection of normal RC and FRC on (0.5 m) prismatic beams and long (4.2 m) beams under different types of loads.
- The crack widths in reinforced concrete flexural members with and without fibres were measured experimentally and compared with code predictions.

However, the researcher cannot control limitations, which could influence the research work. The experimental programme was reduced due to time constraints in the lab for conducting the long-term tests and because of restrictions that were imposed due to the Covid-19 pandemic. The practical limitations include the number of specimens and parameters studied (i.e. fibres volume fractions, different stress levels and different loading frequencies). However, the modelling part of the work is expected to compensate for this reduction in experimental data.

Chapter 4 Experimental results – Part 1: small specimens

4.1 Introduction

As described in the previous chapter, the experimental work comprised comparison of fibre concretes with normal concrete as reference. Five different mixes, viz. Normal concrete (NC), micro polypropylene fibre concrete (0.1% 0.1PPFC) and macro polypropylene fibre concrete (0.4% 0.4PPFC), steel fibre concrete (1% SFC) and hybrid fibre concrete (1.5% HyFC), were tested for determining the compressive strength, splitting tensile strength, and flexural strength. Three of these concretes (NC, SFC and HyFC) were studied also for their short term stress-strain behaviour, performance under repeated loading and loss of tension stiffening. Furthermore, two mixes, i.e., NC and HyFC were monitored for the long-term behaviour. The reason for not testing all the five types of concretes in all these three strands of investigation is because restrictions were imposed on lab utilisation for each research project following the Covid-19 related closure of the labs in 2020 and 2021. As a result, a compromise was made also on the number of specimens tested for each type of mix in the experimental programme. However, the hybrid fibre system was included in all strands of the investigation because most of the previous research reported in the literature focused on the effect of the addition of single and two types of fibre. The following aspects were given emphasis in the experimental programme reported in this chapter:

(i) The effect of the addition of fibres on the mechanical properties, such as compressive strength, splitting tensile strength and modulus of elasticity;

(ii) The performance of the prismatic beams (0.5 m span) in the short-term and long-term when subjected to the four-point flexural tests, followed by creep and shrinkage deformations and long-term loss of tension stiffening of the different concrete mixes;

(iii) The failure modes, load-deflection behaviour and flexure strength;

(iv) Effectiveness of hybrid fibre reinforcement (micro and macro polypropylene fibres combined with macro steel fibres) for restricting the development of

micro and macro cracks in RC elements subjected to static, repeated and sustained loads.

Each of these aspects shall be discussed separately in terms of the influence of the added fibres by comparing the performance of fibre specimens with that of the reference.

4.2 Fresh concrete properties

Table 4.1 shows the slump recorded for the different mixes used in this investigation. The normal concrete mix was designed to achieve an S3 slump class (80-170mm slump), and its slump was 100mm. As expected, the introduction of fibres reduced the measured slump, which agrees with the findings in the literature that fibres tend to reduce the concrete workability (Li et al., 2018; Yin et al., 2015; Sadrinejad et al., 2018). The addition of 0.1% micro polypropylene fibres showed the lowest reduction in the slump result, with a value of 80 mm (20% lower than the reference concrete mix without fibre), which was followed by 1% of steel fibre mix with a value of 75 mm (25% lower). However, the addition of 0.4% macro polypropylene fibres showed the highest reduction in the slump, with a value of 55 mm (45% lower) compared to the concrete mix without fibres. Concrete mixes containing steel fibres recorded a slump of 75mm, whilst the hybrid steel-polypropylene fibre mixes produced a slump of 50mm, both less than that of the reference. The high coefficient of variation (COV) reported in Table 4.1 for the results of hybrid fibres affected the slump test results, which indicated a higher degree of variability in either the mixing procedure or the characteristics of the fibres themselves and the uneven distribution of the fibres. As hybrid fibres are made of different types of fibres with different properties, the uniform dispersion of them is a challenge, which might have been the reason for the high variability of the slump values. These slump test results show that sufficient workability (slump class S2 (30-110mm)) may be maintained even with high fibre content by adjusting the amount of superplasticizer (SP) used in the mixes for different types and volume of fibres, as reported in Table 4.1.

Concretes containing polypropylene fibres are known to reduce the workability and increase both bleeding and segregation, which are attributed to the fibres' shape and low deformability (Ramakrishnan et al., 1987; Yin et al., 2015). This decrease in slump in this experimental programme could be attributed to the large surface area and quantity of fibres, which can absorb more cement

paste, resulting in an increase in viscosity and a reduction in slump (Mehta and Monteiro, 2014; Chen and Liu, 2005).

Table 4.1: Descriptions of mixes and slump test results

Concrete mix	**NC**	**0.1% 0.1PPFC**	**0.4% 0.4PPFC**	**1% SFC**	**1.5% HyFC**
Fibre type	No fibres	0.1% micro polypropylene	0.4% macro polypropylene	1% steel	1% steel, 0.1% micro and 0.4% macro polypropylene
Super-plasticiser content (L/m^3)	-	0.1	0.4	1	1.5
Average slump result (mm)	100	80	55	75	50
Reduction percentage compared to reference, NC (%)	0	20	45	25	50
COV (%)	5	0	0	3.3	50

4.3 Mechanical properties

The 28-day compressive strength, splitting tensile strength and modulus of elasticity of the concretes are summarised in Table 4.2.

4.3.1 Compressive strength

The cube and cylinder compressive strengths (BS EN 12390-3, 2009) reported in Table 4.2 indicate that the addition of different types of fibres and at different volume fractions can result in higher compressive strength. The inclusion of hybrid fibres in the HyFC mix showed a notable benefit on the compressive strength compared to the other fibre concrete mixes. Both the cube and cylinder compressive strengths were the highest with the inclusion of 1.5% hybrid steel-polypropylene fibres (i.e., HyFC); these strengths were about 13.01% and 7.65%, respectively, higher compared to the reference specimens without fibres. It was also noted that the incorporation of 0.1% micro polypropylene fibres (0.1PPFC) showed an increase in the compressive strength of cubes by 6.62% when compared to the reference specimens, whereas it had little effect on the cylinder compressive strength. As can be seen in Table 4.2, the addition of 0.4% macro

polypropylene fibres (0.4PPFC) showed an improvement in the compressive strength of cubes and cylinders by 8.54% and 2.25%, respectively.

Comparing SFC with NC, the average compressive strength of SFC for cubes (58.15 MPa) was higher than that of NC (52.72 MPa) by approximately 10.3%. Whereas the average compressive strength of SFC for cylinders was higher than that of NC by 7.33%. Also, the average compressive strength of SFC for cubes was higher than that of 0.1PPFC and 0.4PPFC by approximately 3.45% and 1.62, respectively. Similarly, the average compressive strength of SFC for cylinder was higher than that of 0.1PPFC and 0.4PPFC by approximately 7.46% and 4.97, respectively. This suggested that the incorporation of fibres in SFC contributed to an enhancement in compressive strength.

Similarly, comparing HyFC with NC, the average compressive strength of HyFC for cubes (59.58 MPa) was higher than that of NC (52.72 MPa) by approximately 13.01%. It is also higher than the average compressive strength for cubes by 6% and 4.12% compared to 0.1PPFC and 0.4PPFC, respectively. This indicated that the inclusion of fibres in HyFC led to an improvement in compressive strength compared to the normal concrete. When comparing SFC with HyFC, it can be observed that HyFC exhibited a slightly higher average compressive strength for cubes (59.58 MPa) compared to SFC (58.15 MPa) by approximately 2.46%. Similarly, the average compressive strength for cylinders was higher than NC, 0.1PPFC, 0.4PPFC and SFC by approximately 7.65%, 7.79%, 5.29% and 0.30%, respectively. This suggested that the hybrid fibres used in HyFC might have provided additional benefits in terms of compressive strength compared to the steel fibres used in SFC. The hybrid fibres, which are a combination of different types of fibres (such as steel, micro and macro polypropylene), offer synergistic effects that contribute to the enhancement of compressive strength. This benefit highlighted the effectiveness of using a combination of fibres in achieving higher compressive strength properties in concrete structures, particularly in applications where higher strength is desired or required.

Table 4.2: Experimental results for normal and fibre concretes (hardened concrete at 28 day)

Concrete mix identification	Cube compressive strength (MPa) and Coefficient of variation (%)	Cylinder compressive strength (MPa) and Coefficient of variation (%)	Splitting tensile strength (MPa) and Coefficient of variation (%)	Modulus of elasticity (MPa)*
NC and NRC	52.72 (0.85)	40.51 (6.06)	3.25 (9.34)	30,172
Micro 0.1 PPFC	56.21 (5.11)	40.46 (1.82)	3.16 (8.96)	31,241
Macro 0.4 PPFC	57.22 (6.78)	41.42 (5.63)	3.38 (6.33)	31,444
SFC and SFRC	58.15 (1.68)	43.48 (5.36)	5.03 (0.39)	31,069
HyFC and HyFRC	59.58 (4.51)	43.61 (3.53)	5.86 (6.14)	31,916

* Due to the malfunction of strain gauges in some test specimens, it was not possible to calculate the coefficient of variation for Modulus of Elasticity.

4.3.2 Splitting tensile strength

The splitting tensile strength (BS EN 12390-6, 2009) of cylinders at the age of 28 days, with and without fibres, are also presented in Table 4.2. As reported in Table 4.2, based on the test results, it was evident that the inclusion of 0.1% micro polypropylene (PP) fibres in the mix resulted in a reduction in the splitting tensile strength compared to the reference concrete, indicating that this dosage may be insufficient to significantly enhance the splitting tensile strength. However, when the dosage was increased to 0.4% macro PP, there was a noticeable improvement of approximately 4% compared to the reference concrete. The addition of 0.1%, 0.2%, and 0.3% polypropylene fibres in the study by Fallah and Nematzadeh (2017) showed higher improvements in the splitting tensile strength of approximately 9.06%, 12.81%, and 10.77% respectively, compared to the improvement of 4% observed with 0.4% macro PP fibres in the current study.

The addition of 1% of steel fibres only produced an increase in the splitting tensile concrete strength of approximately 54.77%, 59.18% and 48.82% compared to NC, 0.1PPFC and 0.4PPFC, respectively. As reported in Table 2.3, Li et al. (2018) and Sahoo et al. (2015) found that the addition of fibre resulted in an increase in the splitting tensile strength of up to 54% and 70%, respectively.

As observed in the case of the compressive strength, the incorporation of hybrid steel-polypropylene fibres (i.e., HyFC) produced the greatest increase in splitting tensile strength; approximately 80.31%, 85.44%, 73.37% and 16.50%

greater than the reference specimens, 0.1PPFC, 0.4PPFC and SFC, respectively. This improvement was notably higher compared to the increase achieved with the addition of 1% steel fibres, indicating that the hybrid fibres concrete specimens exhibited a 16.5% higher improvement in splitting tensile strength compared to steel fibres concrete specimens.

According to Afroughsabet et al. (2016), the incorporation of hybrid steel-polypropylene fibres increased the splitting tensile strength between 23% and 52%; the extent of increase depended on the fibre replacement percentage and the testing age. This enhancement was attributed to the fibres' bridging activity across cracks with a range of fibres to help resist the different scales of cracking at the interfaces between aggregate and the cement matrix. So, the incorporation of polypropylene fibres generally prevented micro cracks whereas the steel fibres mainly inhibited the spread of large cracks. Subsequently, the stress is transferred to the bridging fibres after the first crack forms, delaying the growth of cracks and thereby increasing the splitting tensile strength (Smarzewski, 2018). The test findings of the current study showed that the splitting tensile strength of the hybrid fibre concrete is greater than that of the single fibre concrete. In conclusion, based on the test results, it is evident that the addition of more than two types of fibres demonstrated a clear and beneficial hybrid effect.

4.3.3 Modulus of elasticity

Strains recorded up to first cracking of test specimens (for which the strain gauge functioned during the test) are plotted against their corresponding stress in Figure 4.1. These plots were used to calculate the modulus of elasticity and secant modulus, as discussed in Section 3.8.3. The secant modulus was calculated based on Figure 4.1. The normal concrete showed a value of 26,250 MPa, whereas the addition of different fibres resulted in an increase in the secant modulus. The incorporation of macro polypropylene fibres had a slight effect on the secant modulus, increasing it by approximately 1.4%. Conversely, the inclusion of micro polypropylene fibres had a greater impact, raising the secant modulus by approximately 6.1% compared to normal concrete. However, the addition of steel fibres increased the secant modulus by approximately 3.8%, while the inclusion of hybrid fibres had an even higher effect of approximately 6.4% compared to the normal concrete. Notably, the addition of hybrid fibres exhibited the most significant increase in the secant modulus. In Figure 4.1, the

ascending part of the curve was significantly affected by the addition of either steel or hybrid fibres to concrete, with the peak compressive stress increasing with increasing fibre volume fraction.

According to test results, the incorporation of micro and macro polypropylene fibres increased the modulus of elasticity by about 3.54% and 4.22%, respectively, compared to NC. The addition of steel fibres produced an increase in the modulus of elasticity by about 2.97% compared to NC. The addition of hybrid fibres produced an increase in the modulus of elasticity by about 5.78%, 2.16%, 1.51% and 2.73% compared to NC, 0.1PPFC, 0.4PPFC and SFC, respectively, as reported in Table 4.2. The presence of micro and macro polypropylene fibres in concrete can enhance the bond between the fibres and the surrounding matrix, resulting in a more efficient load transfer and increased resistance to deformation. This improved load distribution and stress transfer mechanism can lead to higher values of the modulus of elasticity, reflecting the enhanced rigidity of the concrete. The increase in the modulus of elasticity with the addition of macro polypropylene fibres might be due to their crimped shape and long length when compared to the micro polypropylene fibre. The PP fibres may reduce the micro-cracking produced during initial stages of loading, resulting in fewer internal micro-cracks and fewer cracks to propagate and form macro-cracks. However, the polypropylene fibres had no effect after the cracking of specimens, because their effect was primarily to reduce micro-cracking. Similar results were reported by Fallah and Nematzadeh (2017) who stated that the addition of 0.5% and 0.1% of macro and micro polypropylene fibres showed an increase in the modulus of elasticity by about 2.9% and 9.7%, respectively. In the study by Yoo et al. (2015), as reported in Table 2.2, the addition of fibres exhibited a minor effect on the modulus of elasticity, ranging from 1.5% to 6%. This increase in the modulus of elasticity might be attributed to the higher beneficial hybrid effect of fibres with different mechanical properties. From these results, it can be seen that the hybrid fibre mix is more beneficial to improve the modulus elasticity when compared to any single fibre mix.

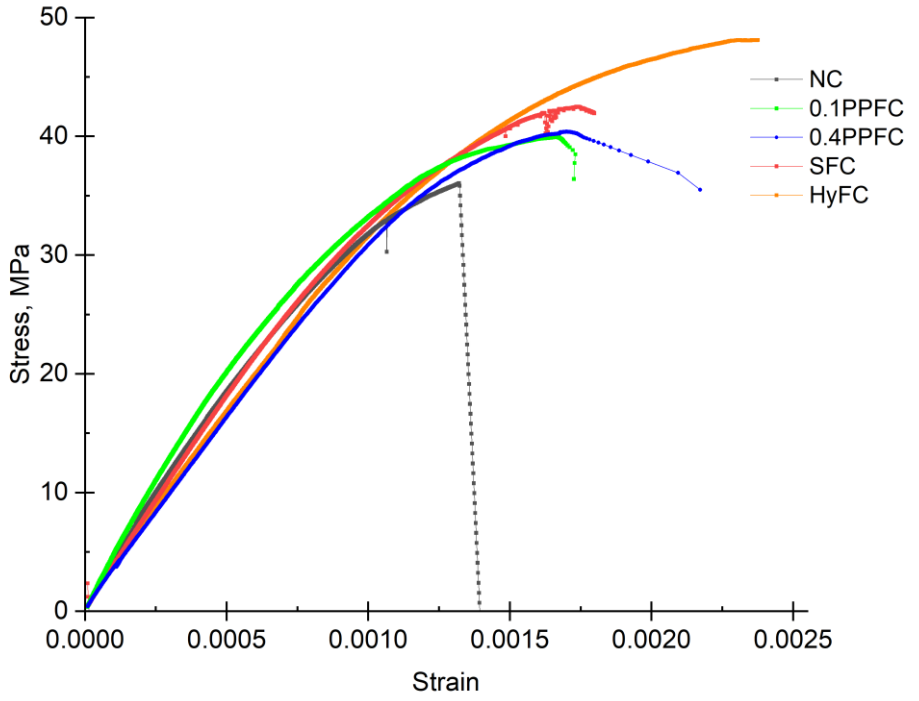

Figure 4.1: Stress-strain curves for normal and fibre concrete specimens

4.4 Flexural strength for the prismatic beams (0.5 m)

4.4.1 Mode of failure and crack pattern under static load

The failure patterns of the short prismatic beams are presented in Figure 4.2. It can be seen in Figure 4.2(a) that in all normal concrete prismatic beams, the specimens exhibited a brittle flexural failure. The normal concrete beams' brittle failure began with a small crack that spread at each increment of loading up to the maximum load. The addition of all types of fibres changed the failure of the beams from rapid and brittle to ductile, as shown in Figure 4.2(b-e).

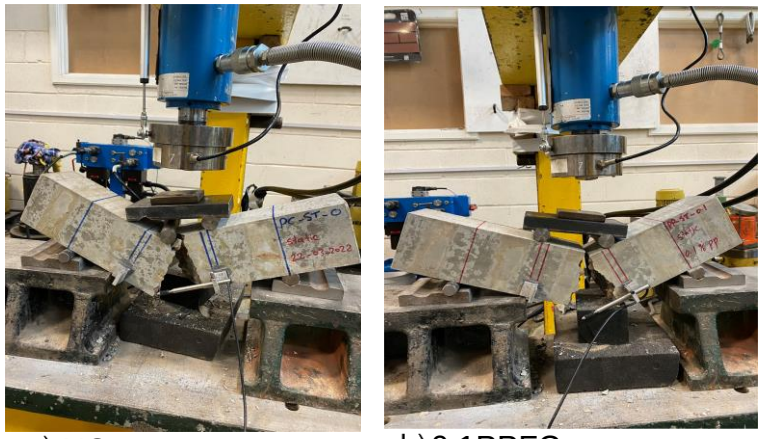

a) NC b) 0.1PPFC

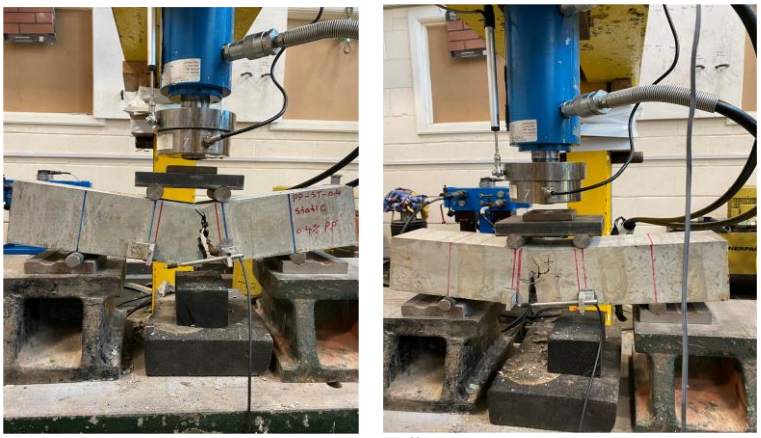

c) 0.4PPFC d) SFC

e) HyFC

Figure 4.2: Crack pattern and mode of failure for normal and fibre concrete beams

The failure of the normal concrete beams occurred with a slight load drop after the peak load was reached, with no sign of post-peak resistance of the beams. Beams cast with micro 0.1PPFC showed almost the same brittle failure as the reference beams without fibres. This similarity in failure behaviour was possibly because the amount of fibres was small. On the other hand, beams cast with macro 0.4PPFC exhibited a more ductile failure. This increased ductility can

be attributed to the ability of the fibres to resist cracking under load, especially at lower load levels during the service stage (Hamoush et al., 2010; Yap et al., 2014). The impact of macro PP fibres on enhancing the ductility of the beams is more pronounced compared to micro PP fibres.

For beams cast with steel and hybrid fibres, cracks formed and developed vertically towards the upper portion of the beam at a higher load. These beams showed higher resistance to cracking and continued to carry the load, which gave some indication that failure was imminent. The role of fibres is to bridge and restrict the propagation of cracks (Hassanpour et al., 2012; Guo et al., 2021; Afroughsabet et al., 2016; Li et al., 2018). Polypropylene fibres primarily prevent micro cracks from forming (Afroughsabet and Ozbakkaloglu, 2015) and Guo et al., 2021), while steel fibres greatly slow down the development of macro cracks when loads are applied on the concrete structure (Guo et al., 2021). The amount and type of fibres in the concrete had a positive impact on the failure of the beams. The inclusion of fibres in the concrete altered the failure mechanism, making it more ductile and improving the overall structural performance of the beams.

During the test, one major flexural crack occurred randomly at the bottom of the beams in the constant bending moment area, which is located between the load points, and propagated upwards on the sides of the beams in no particular pattern. In the failure section of the specimen, the volume of fibres within the section could be considered to be lower compared to other sections of the beam. The lower volume of fibre was attributed to an uneven distribution during the casting or mixing process, the fibres may not have been evenly dispersed throughout the entire section, resulting in variations in fibre concentration within different sections of the beam. This is because the critical crack, which is the main crack responsible for the failure, tends to propagate through areas where the fibre distribution is comparatively lower. The path of least resistance refers to the path that the crack finds easier to propagate through, which may coincide with regions of lower fibre concentrations. Therefore, the failure section may have a lower fibre volume fraction compared to the overall average due to the influence of the crack propagation path. A visual examination was undertaken at each increment of loading to trace the progression of cracks on the side of the beams. Crack developed upward towards the compressed concrete zone and the crack

width expanded until the failure of the tested beams occurred. The primary crack's fibre bridging effect was no longer able to sustain the applied load for the FC beams. As a result, the primary crack's width rapidly expanded in the last stage until the failure of the beams occurred. The incorporation of fibres in the concrete beams resulted in a significant reduction in crack propagation compared to the normal concrete beams without fibres. Normal concrete beams split apart after reaching the peak load, whereas the beams that were manufactured with the incorporation of different types of fibres were not totally damaged and continued to carry the load until the peak load achieved, which caused the failure of beams, as shown in Figure 4.2(a-e). A similar observation was reported by Meza and Siddique (2019) and Yap et al. (2014) who stated that the addition of plastic fibres inhibits the broken failure of concrete beams.

4.4.2 Load-deflection curve

Table 4.3 summarises the test results of the static flexural tests for various mixes (see Table 3.5 for details of the mixes) used in this study. For each mix, three beams were tested and the average values for each mix were used to plot the load-deflection curve for each short beam, in Figure 4.3. For clarity, the data for each type of mix are plotted separately in this figure. The utilisation of average load-deflection curves enhances the clarity and accuracy of the description, enabling a more robust and precise analysis of the beam behaviour.

The load-deflection curve of specimens is found to have two distinct stages, pre-cracking and post-cracking. Most of the beams showed a nonlinear behaviour from the start of the test up to the formation of the first visible crack. All beams responded linearly after the formation of the first visible crack until the peak load. As mentioned in the previous section, the initiation of the crack will occur at the weakest point and that crack will propagate through the more vulnerable areas. These weaker areas are not uniform, which leads to different resistances and, therefore, will show nonlinear behaviour. Yoo et al. (2015) claimed that the nonlinear behaviour decreased with an increase in the compressive strength in the pre-peak part of the load-deflection graph. After the first visible crack occurs, the energy required to propagate the crack is a lot less and will flow a lot easier through the rest of the section so that it will show more linear behaviour, as can be seen in Figure 4.3. Li et al. (2018) stated that the load increased gradually after the formation of the first visible crack up to the peak. It

can be seen in Figure 4.3 that the incorporation of fibres had a minor effect on the pre-cracking behaviour of the beams and through most of the serviceability phase. This finding is in agreement with some of the other published work (Yoo et al., 2014). The load–deflection curve for normal concrete (NC) shows that the elastic deformation stage is dominant, with brittle fracture occurring when the load reaches the failure limit. This is also in agreement with some of the other published work, for instance by Guo et al. (2021).

The salient results from Figure 4.3 are summarised in Table 4.3, which shows that adding fibres to specimens increased the cracking load in all three specimens for each mix. On average, the cracking load was increased by 17% and 29% for micro 0.1PPFC and macro 0.4PPFC, respectively, higher than the reference beams (NC). The addition of steel fibres (SFC) resulted in an even greater increase in the cracking load by 75%, 50% and 35% higher than NC, 0.1PPFC, 0.4PPFC, respectively. Whereas the addition of hybrid fibres to the beams (HyFC) significantly increased the cracking load by approximately 142%, 107%, 87% and 38% higher than NC, 0.1PPFC, 0.4PPFC and SFC, respectively.

The peak load also increased with the addition of fibres. For 0.1PPFC and 0.4PPFC, there was an increase in the peak load by 8% and 20% higher than NC, respectively. Additionally, SFC showed a higher increase in the peak load by 74%, 61% and 45% higher than NC, 0.1PPFC and 0.4PPFC, respectively. HyFC also showed a significant increase in the peak load by 147%, 129%, 106% and 42% when compared to NC 0.1PPFC, 0.4PPFC and SFC, respectively. The results for a single type of fibre agree with previous work by Yoo et al. (2013), Yoo et al. (2014), Caggiano et al. (2012) and Yap et al. (2014). However, the addition of hybrid fibre has not been found in the literature. In this research, the hybrid fibres resulted in superior performance compared to the addition of a single type of fibre.

Yoo et al. (2014) stated that the increase of peak load due to the addition of fibres is only applicable for fibres up to 19.5 mm because it is challenging to distribute fibres longer than 30 mm in the matrix uniformly. As fibres longer than 19.5mm were used in this study (Table 3.4), it can be concluded that the findings by Yoo et al. (2014) are not applicable to the fibre concretes in this study.

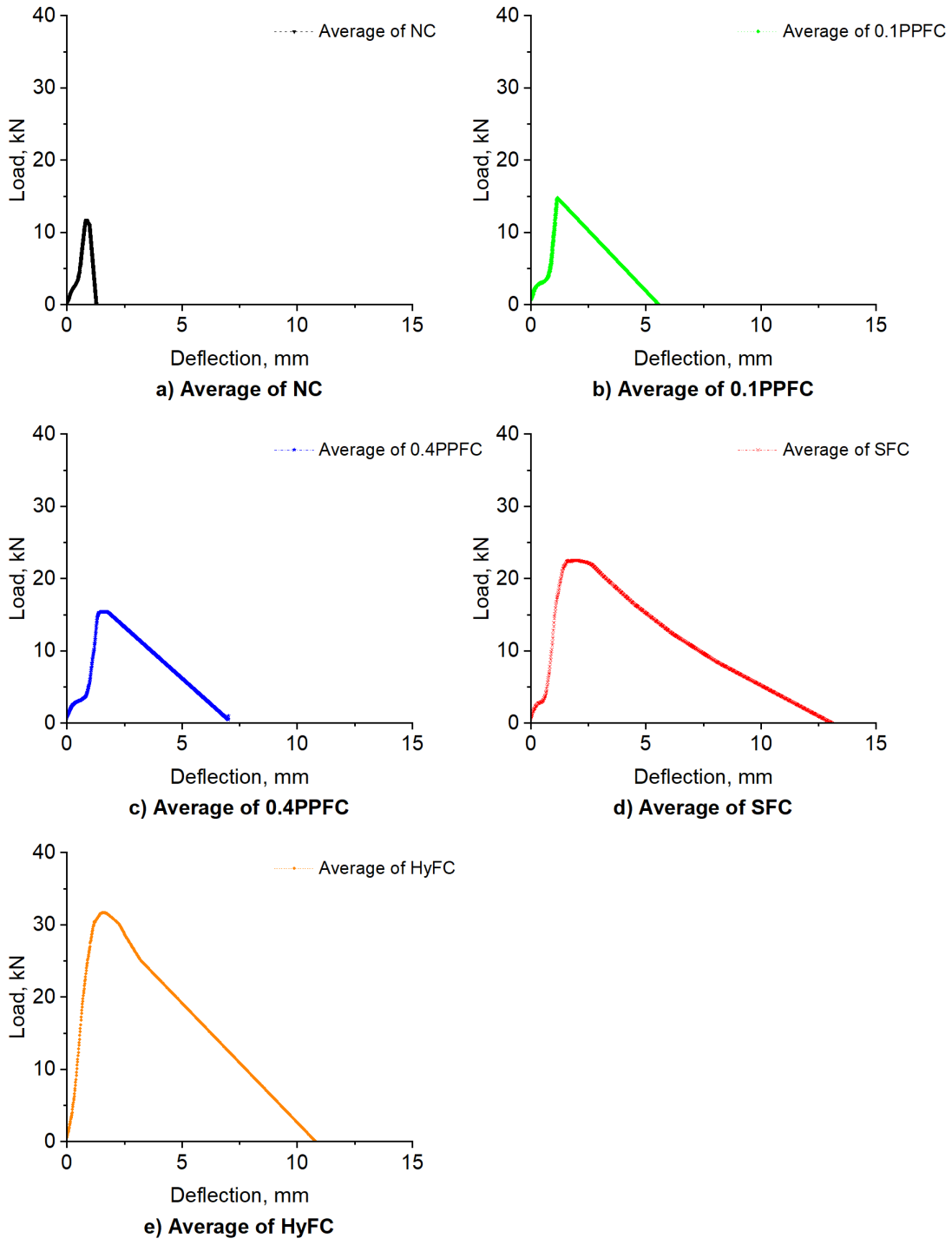

Figure 4.3: Average load-deflection curve for test beams

Table 4.3: Test results for normal and fibre concrete beams under static load

Type of beam	Load at the formation of first visible crack		Deflection at the formation of first visible crack		Failure load	
	In kN	Percentage* (%)	In mm	Percentage** (%)	In kN	Percentage*** (%)
NC-ST-0	12	-	0.83	-	13.56	-
0.1PPFC-ST-0.1	14	17%	1.12	35%	14.63	8%
0.4PPFC-ST-0.4	15.5	29%	1.32	59%	16.25	20%
SFC-ST-1	21	75%	1.32	59%	23.61	74%
HyFC-ST-1.5	29	142%	1.1	33%	33.46	147%

*Increase in load at first crack compared to NC, **Increase in deflection at first crack compared to NC and ***Increase in failure load compared to NC.

The comparison of first crack and peak loads in Table 4.3 reveals that beams reinforced with steel and hybrid fibres have a similar effect on the ultimate load and the first crack load, on the other hand, the addition of micro and macro polypropylene fibres has a minimal effect on the first crack load than the ultimate load. Based on this information, it seems that the inclusion of hybrid fibre in this study is a novel contribution that has not been previously documented in the literature. This finding highlights the potential superiority of hybrid fibres compared to using a single type of fibre, providing valuable insights to the field.

As can be seen in Figure 4.3, normal concrete specimens exhibited a lower slope compared to other beams when the deflection scale up to 15mm at different load as the peak load was different for all specimens. The addition of fibres to the beams resulted in larger deflections compared to the reference concrete without fibres. Table 4.3 and Figure 4.3 demonstrate that the incorporation of fibres in the beams increased the deflection at the formation of the first visible crack. For 0.1PPFC and 0.4PPFC, there was an increase in deflection by 35%, 59%, respectively, compared to the reference specimen without fibres. Furthermore, the addition of steel fibre to beams (SFC) showed a higher increase in the deflection at the formation of the first visible cack by 59% and 18% higher than NC and 0.1PPFC, respectively. However, SFC showed the same value of 0.4PPFC. In contrast, the addition of hybrid fibre to beams (HyFC) resulted in an increase in the deflection by 33% compared to NC. However, the deflection showed a reduction by 1.79% 16.67% and 17% when compared to 0.1PPFC, 0.4PPFC and SFC, respectively.

Table 4.4 provides a summary of the deflection values for the beams. The addition of micro 0.1PPFC, macro 0.4PPFC and SFC resulted in approximately 47%, 67% and 25% higher mid-span deflection at a load of 5 kN, respectively, as reported in Table 4.4. The rate of increase in mid-span deflection decreased with higher loads, but remained higher than that of normal concrete. This can be attributed to the effect of micro and macro polypropylene fibres at smaller loads. Beams cast with hybrid steel-polypropylene fibres exhibited a more noticeable reduction in mid-span deflection compared to other specimens at lower loads. The reductions were approximately 51% and 42% at loads of 5 kN, and 10 kN, respectively, compared to the reference concrete beam without fibres, as summarised in Table 4.4. These reductions in mid-span deflection can be attributed to the initial behaviour of the beams, a stiffer system and less variation in the different materials, which can be related to the positive interaction of the hybrid fibre system. The PP fibres may reduce or stiffen the micro cracking produced during hydration, resulting in fewer internal micro cracks (stiffer) and fewer cracks propagating to macro cracks.

Similarly, the incorporation of fibres to the beams showed an increase in the deflection just before reaching the failure load by 31%, 67%, 85% and 90% for micro 0.1PPFC, macro 0.4PPFC, SFC and HyFC, respectively, when compared to the reference beam. Significantly, the peak load values varied among all the specimens. The addition of steel and hybrid fibres produced almost two times greater deflection at the peak load than the normal concrete. Yoo et al. (2015) and Hamoush et al. (2010) reported that the addition of fibres resulted in a deflection that is almost three times higher than that of the reference beams; this increase is attributed to the bridging action of the fibres at the fracture interfaces.

Table 4.4: Deflection of the beams at different applied loads

Type of beam	Applied load (kN)								
	5		10		15		20	Peak	
	Deflection (mm)	%*	Deflection (mm)	%*	Deflection (mm)	%*	Deflection (mm)	Deflection (mm)	%*
NC-ST-0	0.57	-	0.76	-	1.69	-	-	0.87	-
0.1PPFC-ST-0.1	0.84	47 %	1.01	33%	-	-	-	1.14	31 %
0.4PPFC-ST-0.4	0.95	67 %	1.17	54%	1.37	(-19%)	-	1.45	67 %
SFC-ST-1	0.71	25 %	0.91	20%	1.05	(-38%)	1.32	1.61	85 %
HyFC-ST-1.5	0.28	-51 %	0.44	-42%	0.59	(-65%)	0.72	1.65	90 %

*Difference in deflection at different stages of load compared to reference beams

The increased post-cracking ductility resulting from the contribution of the added fibres is most apparent in the behaviour of the specimens after the peak load, as can be seen in Figure 4.3. Unlike normal concrete specimens, which typically demonstrate a lower post-cracking behaviour and fail directly, the addition of fibres enhances the post-cracking response. This increased ductility can be observed in the specimens' ability to sustain deformation and resist further crack propagation, leading to a more gradual and controlled failure mode. Different types of fibres were included in the beams, resulting in a significant improvement in the cracking load, failure load and flexural strength. The flexural load was increased with no rapid load drop or sudden crack width increase after failure, which is seen in Figure 4.3 and Table 4.3 because of the different fibre volume fractions used.

The addition of fibres to the beams resulted in an increase in the maximum applied load, as can be seen in Figure 4.4. The inclusion of micro polypropylene fibres had a minimal effect on the post-cracking behaviour up to the peak load, compared to normal concrete without fibres. Both micro and macro polypropylene fibres exhibited similar behaviour, despite the higher percentage of macro polypropylene fibres in the latter case. However, the presence of steel, hybrid fibres and macro polypropylene fibres had a greater influence on the post-cracking behaviour in Figure 4.4. Soutsos et al. (2012) stated that the post cracking behaviour was affected with the addition of fibres and both their shapes and lengths play an important role. It is important to note that the addition of hybrid

fibres affected post-cracking behaviour and demonstrated a higher maximum load. This differentiates the current results from previous research in the field.

Table 4.5: Results of area under the curve for the normal and fibre concrete beams

Type of beam	Area under the curve (N/mm^2)	Full Width at Half Maximum (FWHM)
NC-ST-0	3.09	0.51
0.1PPFC-ST-0.1	36.57	2.43
0.4PPFC-ST-0.4	54.75	3.41
SFC-ST-1	139.20	5.75
HyFC-ST-1.5	167.29	5.41

Flexural toughness under static stress is defined by the American Concrete Institute (ACI 544, 1998) as the area under the load-deflection curve. It is, in other words, the total energy seen prior to separation. Normal concrete showed a lower toughness after reaching the peak load, with area of 3.09mm^2 with FWHM (Full Width at Half Maximum, which refers to the width of a peak or curve at half of its maximum height) of 0.51, as can be clarified in Table 4.5. However, the incorporation of steel fibres, hybrid fibres and macro polypropylene fibres showed a higher level of toughness, as can be seen in Figure 4.4 with different stages of the deflection. Also, the addition of micro and macro polypropylene showed a higher ductility with an area of 36.57N/mm^2 and 54.75N/mm^2, respectively. Moreover, the incorporation of both steel and hybrid fibres showed the highest ductility, with area of 139.20N/mm^2 and 167.29N/mm^2 respectively. That is, the addition of hybrid fibres exhibited higher toughness compared with the addition of steel fibres by approximately 20.18%. This finding highlights the superior performance and enhanced mechanical properties achieved through the synergistic effect of using hybrid fibres compared to using steel fibres alone. The incorporation of fibres to the concrete mix affects the post-ultimate-load behaviour of the prism specimens when subjected to static load by softening the descending part of the load-deflection curve and preventing rapid and sudden failure with an increase in the ductility.

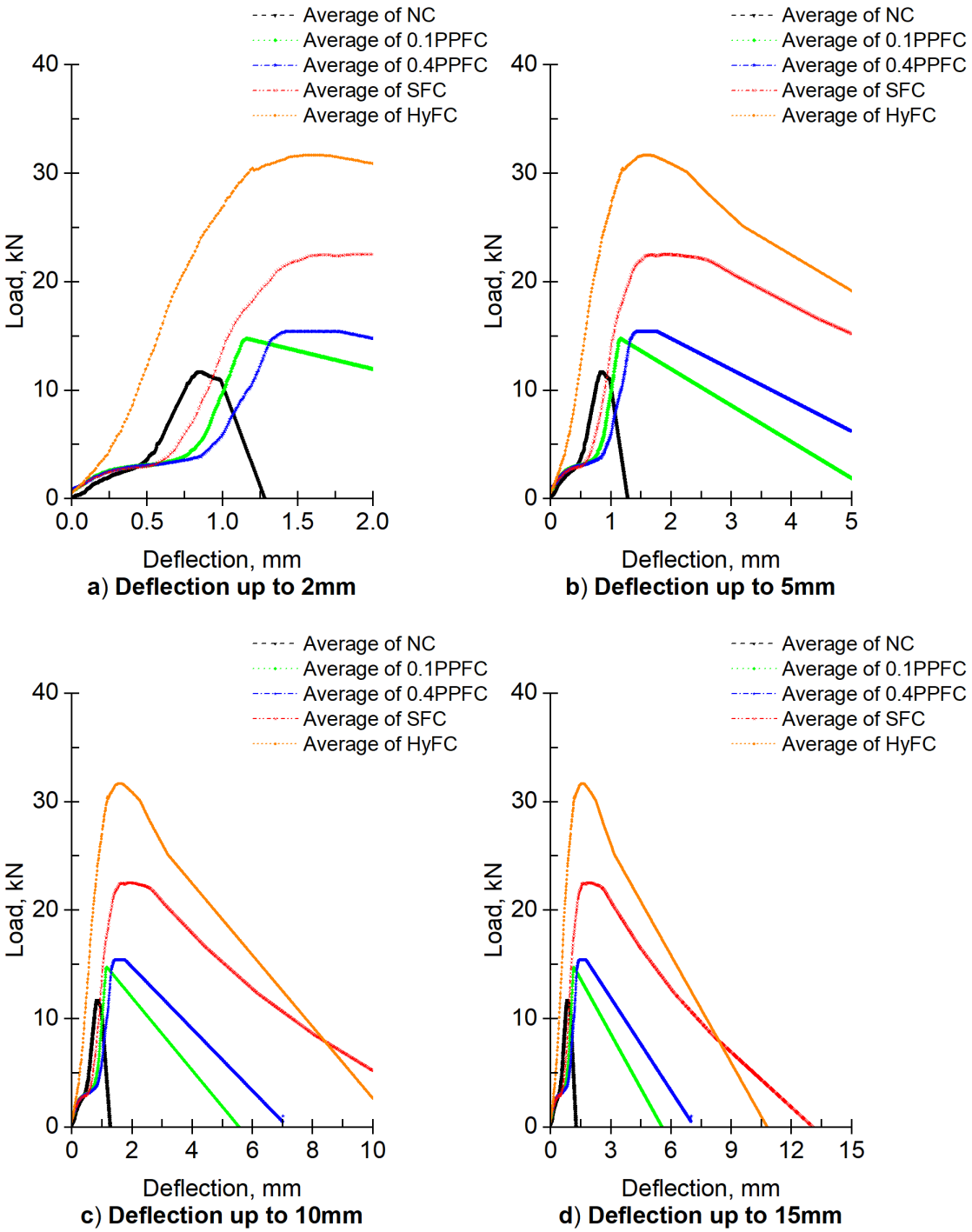

Figure 4.4: Different stages of the load-deflection curve for test beams

4.4.3 Flexural strength and stiffness

Table 4.6 and Figure 4.5 show the flexural strength and stiffness results for the normal and fibre concrete beams according to BS EN 12390-5 (2009). The flexural strength was calculated as previously mentioned in Section 3.9. According to the test results, the contribution of fibre can be highlighted in the flexural strength results. As the test results report in Table 4.6 show, the addition of micro and macro polypropylene fibres only produced an increase in the flexural strength of approximately 8% and 20%, respectively, compared to NC. The addition of reinforcing fibres such as steel fibres resulted in a higher increase in the flexural strength by about 74%, 61% and 45% compared to NC without any fibres, 0.1PPFC and 0.4PPFC, respectively. Similarly, the addition of reinforcing fibres, such as hybrid fibres, led to a significant increase in the flexural strength by about 147%, 129%, 106% and 42% compared to the reference specimen without any fibres (NC), 0.1PPFC, 0.4PPFC and SFC, respectively.

Table 4.6: Flexural strength results and stiffness for the normal and fibre concrete beams

Type of beam	Flexural strength			Stiffness		
	In MPa	Percentage* (%)	Coefficient of variation (%)	In kN/mm	Percentage** (%)	Coefficient of variation (%)
NC-ST-0	4.07	-	10.6	15.81	-	18.6
0.1PPFC-ST-0.1	4.39	8%	9.9	12.97	(-18%)	8.1
0.4PPFC-ST-0.4	4.88	20%	6.7	10.95	(-31%)	10.5
SFC-ST-1	7.08	74%	30.9	13.14	(-17%)	2.74
HyFC-ST-1.5	10.04	147%	9.0	22.68	43%	25.4

*Increase in the flexural load compared to NC and **Stiffness percentage compared to NC

All specimens revealed a significant loss of stiffness at peak load except hybrid fibre beams, as well as a large increase in point load deflections. The performance of hybrid fibres in the test beams demonstrated their superior effect by maintaining a higher stiffness and exhibiting a significantly smaller reduction in stiffness compared to other fibre types. However, the test results revealed that

the incorporation of SFC and HyFC fibres into test beams showed an increase in stiffness of approximately 10% and 59%, respectively, compared to the reference beams at the formation of first visible crack. Beams cast with micro and macro polypropylene fibres had similar stiffness results, both of which showed a reduction in stiffness of approximately 14% and 19%, respectively. At the peak load, the specimens showed a significant loss in their stiffness accompanied by a considerable increase in deflections. At the peak load, the addition of hybrid fibres resulted in a remarkable 43%, 75%, 107% and 73% increase in stiffness compared to NC, 0.1PPFC, 0.4PPFC and SFC, respectively, highlighting their enhanced performance and ability to mitigate stiffness loss.

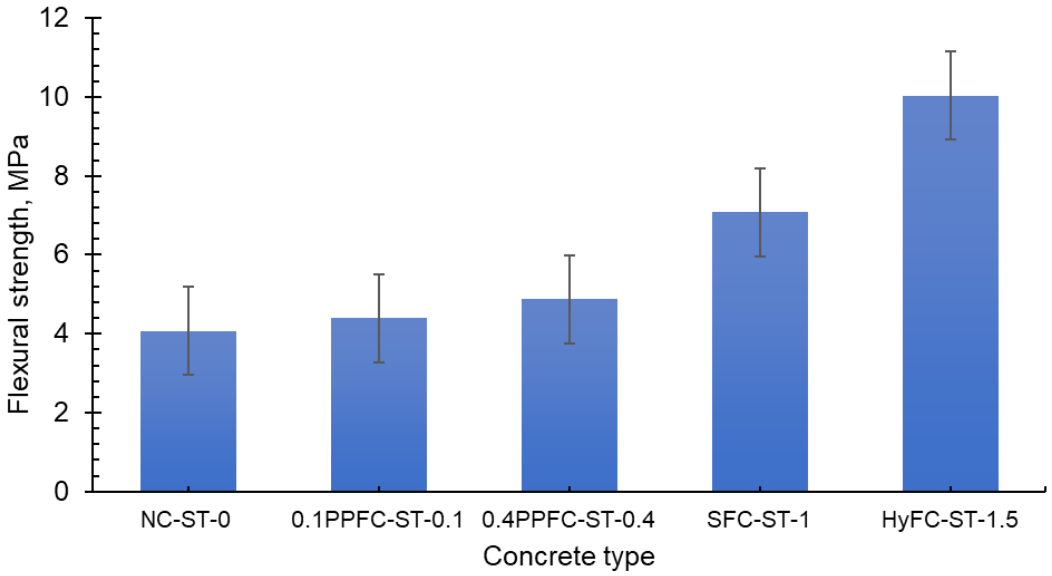

Figure 4.5: Flexural strength results

4.4.4 Crack width

From the test results, the load-crack curves were drawn, as can be seen in Figure 4.6(a-e) and Figure 4.7(a-e). The crack width values were recorded at the bottom face of the beams. An early crack was noticed near the mid-span of the beams at different loads depending on the compressive and tensile strength of concrete used in the beams. At this stage, the main cracks propagated rapidly upward through the beam as the displacement of the beam increased due to the loading. When the vertical cracks reached the top of the beam, the specimens lost their load carrying capacity. According to test results, specimens with hybrid fibres exhibited the most significant reduction in crack width compared to specimens with single type of fibres. Normal concrete specimens recorded the highest crack

width after failure as the specimens were broken into two pieces, so the crack width just before the failure was recorded. Beams with 0.1% micro polypropylene fibres demonstrated similar behaviour to that of the normal concrete beams. After the maximum load was reached, crack widths larger than 1.50 mm were observed, and shortly after, the beam failed.

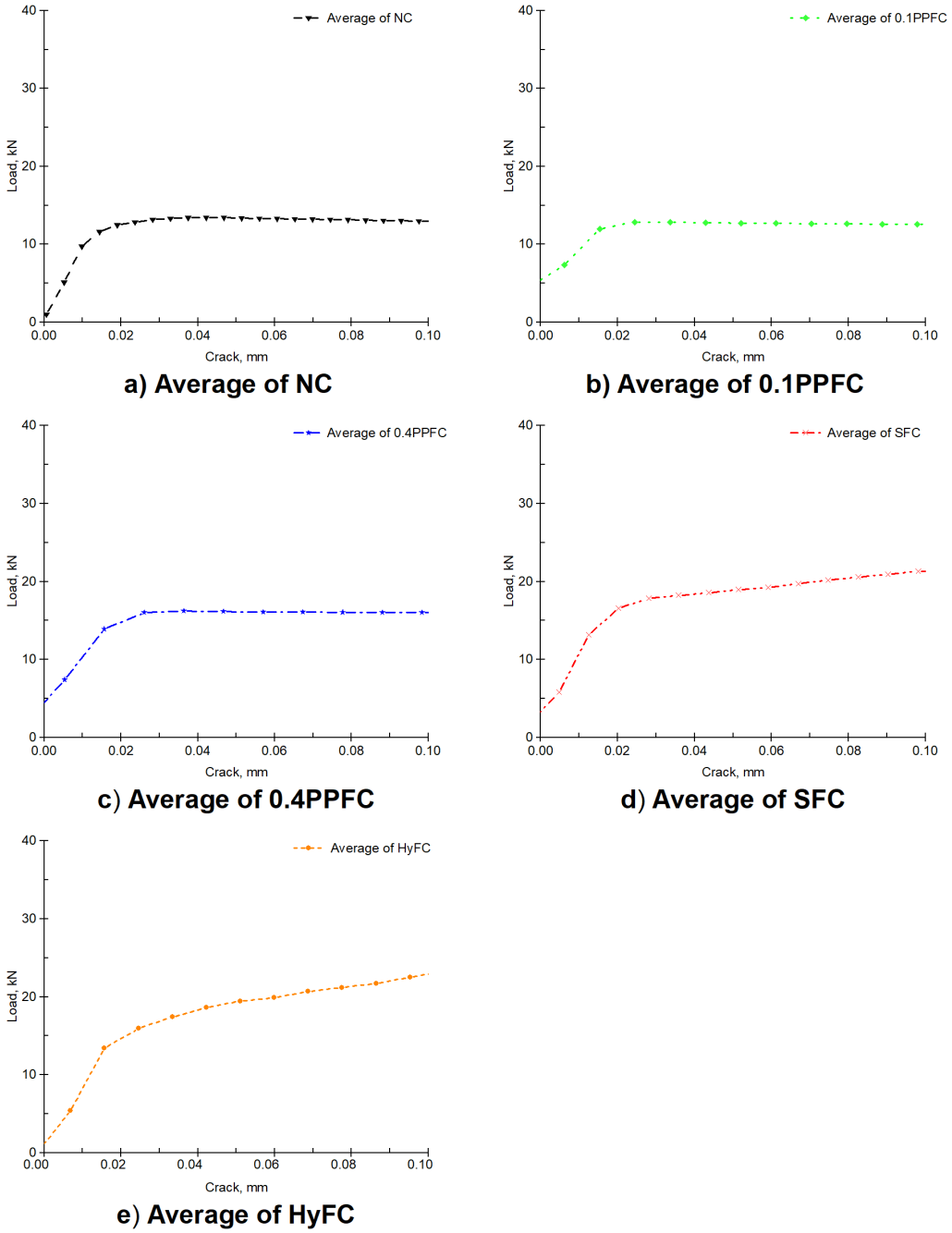

Figure 4.6: Average load-crack width curves for the beams (This shows the crack width only at a scale of 0.1 mm to see the development of crack at earlier stages, while Figure 4.7 shows the load-crack width curves for different prismatic beams with different scales and the individual plots are shown in Appendix)

As reported in Table 4.7, most of the fibre concrete beams displayed smaller cracks compared to the reference beam. The addition of different types of fibre resulted in a decrease in the crack width. Beams cast with micro and macro polypropylene fibres presented a more pronounced reduction in crack width and exhibited the finest cracks compared to other specimens at the service stage (in the early stage of loading) by about 20% and 40% respectively when the loading was 30%, whereas they showed a reduction in the crack width when the loading was 40% by about 50% and 33.3%, respectively; this decrease is mainly credited to crack-bridging by fibres (Gao et al., 2021; Zainul et al., 2021). The crack width of the beams based on the applied load is summarised in Figure 4.8. Based on the findings in Table 4.8 and Figure 4.7(a-d), hybrid fibres exhibited the most significant reduction in crack width, surpassing specimens with only steel fibres by reducing crack width by approximately 20% at a load of 10 kN and 12% at a load of 15 kN. Macro polypropylene fibres showed a reduction in the crack width by about 20% and 48% when the load was at 10 kN and 15 kN, respectively, as summarised in Table 4.8. Beams cast with steel and hybrid steel-polypropylene fibres showed a more pronounced reduction in crack width and exhibited the finest cracks compared to other specimens when the load was at 10 kN by about 20% and 40% respectively, as demonstrated in Table 4.8. They showed a reduction in the crack width when the loading was at 15 kN by about 51% and 64%, respectively. It was noticed that most of the beams had finer cracks than the reference beam, with those cast with hybrid fibres demonstrating the finest cracks compared to other specimens at higher loads, as can be demonstrated in Figure 4.7(a) and Figure 4.7(b) with a smaller scale. Steel fibres had an effect in crack bridging after the formation of the first visible cracks, as can be seen in Figure 4.7(a). A similar observation was made by Guo et al. (2021), who stated that due to its abundance and strong flexibility, polypropylene fibres primarily avoid micro cracks, but steel fibres greatly slow the development of macro cracks after they initiated as a result of the steel fibre material's high elastic modulus and other properties such as the shape and bonding.

Table 4.7: Crack width of the beams (based on the percent of the ultimate load)

Type of beam	Percentage of the ultimate load (%)					
	30%	40%	50%	60%	70%	80%
	Crack width in (mm)					
NC-ST-0	0.005	0.006	0.006	0.007	0.009	0.015
0.1PPFC-ST-0.1	0.004	0.003	0.006	0.006	0.008	0.010
0.4PPFC-ST-0.4	0.003	0.004	0.006	0.008	0.009	0.013
SFC-ST-1	0.004	0.007	0.010	0.015	0.021	0.050
HyFC-ST-1.5	0.018	0.028	0.038	0.044	0.065	0.129

Table 4.8: Crack width of the beams (based on the applied load)

Type of beam	Applied load								
	5 kN	Percentage*	10 kN	Percentage *	15 kN	Percentage *	20 kN	25 kN	30 kN
	Crack width in (mm)								
NC-ST-0	0.002	-	0.010	-	0.033	-	-	-	-
0.1PPFC-ST-0.1	0.003	50%	0.009	(-10%)	0.010	(-70%)	-	-	-
0.4PPFC-ST-0.4	0.002	0	0.008	(-20%)	0.017	(-48%)	-	-	-
SFC-ST-1	0.004	100%	0.008	(-20%)	0.016	(-52%)	0.065	0.071	0.176
HyFC-ST-1.5	0.004	100%	0.006	(-40%)	0.012	(-64%)	0.021	0.056	0.239

* Percentage is in relation to NC

According to Figure 4.7(a-d), hybrid fibres had the most influence on reducing the crack widths followed by the steel and macro polypropylene fibres. The crack bridging was similar between normal concrete beams and that cast with micro-fibres, demonstrating that the addition of micro fibres did not have much benefit. Macro polypropylene fibres demonstrated enhanced crack bridging capabilities in the failed beams when compared to both normal concrete and those cast with micro-fibres. More specifically, the crack measurements showed that macro polypropylene fibres indicated an intermediate behaviour between the hybrid fibres and micro polypropylene fibres. Additionally, the performance of steel fibres showed higher resistance to crack width when compared to the inclusion of macro polypropylene fibre. Based on publications by Yoo et al. (2003 and 2015), it has been reported that the incorporation of fibres, specifically a

single type of fibre, provides a bridging effect that enhances the load-bearing capacity of concrete, even after the initial crack has developed.

The incorporation of steel and hybrid fibres led to the highest reduction in crack width after failure and the crack width remained constant until the total failure occurred. Beams containing steel fibres and hybrid fibres exhibited smaller cracks, at the same load levels, when compared to the reference NC beams. It was noticed that beams cast with hybrid fibres exhibited the finest cracks than beams cast with steel fibres. Guo et al. (2021) and Yap et al. (2014) stated that the addition of different fibre geometries plays a role in resisting the development of cracks at different stages for beams cast with two different types of fibres. The resulting mechanism of crack control leads to a delay in failure. The addition of multiple types of fibres might have helped to mitigate crack openings and reduce their widths significantly in the case of hybrid fibres in this research.

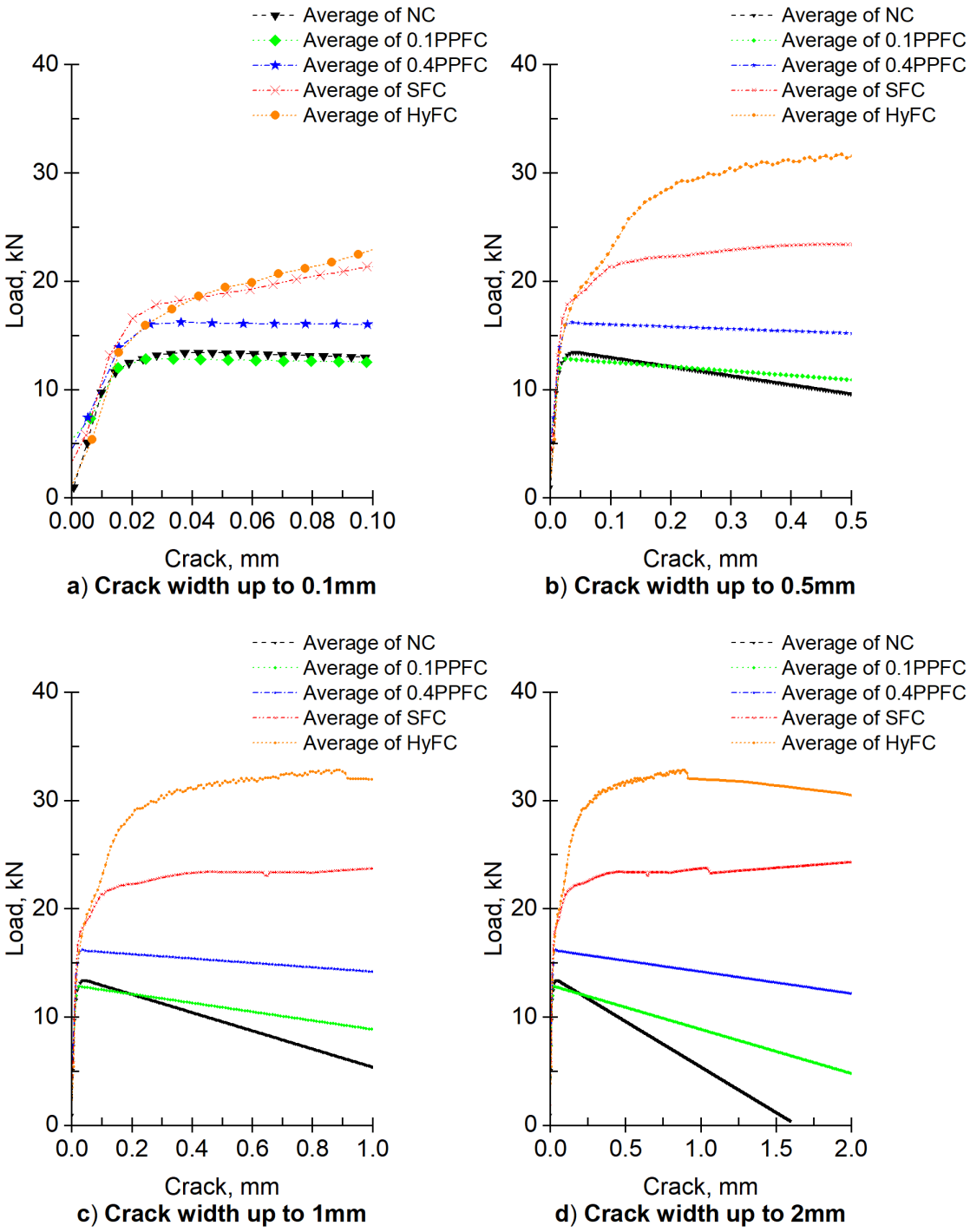

Figure 4.7: Load-crack width curves for different prismatic beams

4.5 Repeated test on prisms of 0.5 m length

4.5.1 S-N Curves

S-N curves are utilised in fatigue analysis for estimating the fatigue lifespan of a material subjected to cyclic loading. The letter "S" denotes the applied stress level relative to the maximum flexural strength, whereas "N" signifies the number of cycles leading to failure. Fatigue strength is a crucial factor in the design of concrete structures including pavements, bridges and offshore structures because they are typically subjected to millions of cycles of repetitive fatigue load throughout their service life. As fatigue testing is a time-consuming and expensive process, which requires a large number of samples to be tested, an upper limit of two million cycles was imposed in the current study. The fatigue load limits were determined for each beam manufactured with each type of concrete mix. A common measure of fatigue strength is the fraction of static strength that can be sustained repeatedly over a specified number of cycles.

The rate of loading has an effect on the fatigue load performance (Medeiros et al., 2014), the chosen frequency of 2 Hz for the prismatic beams represents an average frequency associated with pedestrian use. This means that the frequency selected is an approximation of the typical frequency at which pedestrians generate dynamic loads when walking on a pedestrian bridge or structure. Different stress ranges for the maximum and minimum applied stress were used to plot the relationship between applied stress, $\Delta\sigma$ and fatigue life, N. The maximum stress level represents the peak value of the cyclic load, while the minimum stress level corresponds to the lowest value reached during each loading cycle.

Table 4.9, Table 4.10 and Table 4.11 demonstrate that there is a significant scatter in the number of cycles before failure of the beams for each load level. The relationship between the maximum applied stresses to the maximum flexural strength (S_{max}/F_s) with fatigue life for three different types of concrete is illustrated in Figure 4.8(a-b), which is called S-N curves. Figure 4.8(a) shows the maximum applied stresses to the maximum flexural strength (S_{max}/F_s) against the number of cycles in log scale of NC, SFC and HyFC beams, which refers to the logarithm of the number of cycles to failure, as using a logarithmic scale allows for a more linear representation of the data, making it easier to

analyse and compare different types of concrete. Figure 4.8(b) shows the result of NC, SFC and HyFC beams with number of cycles, which refers to the actual number of cycles endured by the specimen until failure. As shown in Figure 4.8(a) Figure 4.8(b), the addition of fibres always resulted in higher fatigue life compared to NC beams. This observation suggests that the fibres have the potential to prevent cracking and enhance the crack resistance at different scales. The addition of steel fibres to the beams led to an increase in fatigue strength when compared to NC beams. The addition of fibres to the test beams resulted in an improvement in fatigue life, particularly when hybrid fibres were incorporated, showcasing a significant enhancement compared to the SFC beams. The addition of hybrid fibres demonstrated a higher resistance to fatigue strength than single type of fibre. The results reported in Table 4.9, Table 4.10 and Table 4.11 and Figure 4.8 indicate that the test data with different load levels exhibit a significant scatter. Bajaj et al. (2012) and Goel et al. (2012) stated that the addition of fibres led to even more variability or scatter in fatigue life when compared to normal concrete. However, Bawa and Singh (2020) reported that the addition of 100% polypropylene fibres led to a reduction in the variability of fatigue life.

Table 4.9: Test results for normal concrete (NC) beams

Concrete mix	**Load level**	**Number of cycles****	**Deflection (mm)**	**Crack width (mm)**
NC	80-20%*	64	1.38	0.027
NC	80-20%*	120	0.75	0.043
NC	80-20%*	18240	1.3	0.37
NC	80-20%*	33120	1.48	0.065
NC	80-20%*	33480	5.21	3.172
Mean	-	-	2.02	0.73
S.D	-	-	1.80	1.37
COV%	-	-	129.41	186.83
NC	70-30%*	36	4.31	3.158
NC	70-30%*	396	0.67	0.657
NC	70-30%*	88680	0.23	0.003
NC	70-30%*	117360	0.61	0.028
NC	70-30%*	130560	0.17	0.007
Mean	-	-	1.20	0.77
S.D	-	-	1.75	1.36
COV%	-	-	146.39	176.94
Mean***			**1.61**	**0.75**

* The load levels are expressed as a percentage of the maximum static load. ** It shows how many cycles the specimens sustained until failure. *** Average of both NC specimens

Table 4.10: Test results for steel fibres (SFC) beams

Concrete mix	Load level	Number of cycles**	Deflection (mm)	Crack width (mm)
SFC	80-20%*	2160	1.54	0.947
SFC	80-20%*	2219	1.34	0.254
SFC	80-20%*	17047	3.17	3.746
SFC	80-20%*	199164	1.33	0.38
Mean	-	-	1.85	1.33
S.D	-	-	0.89	1.64
COV%	-	-	48.16	122.96
SFC	70-30%*	57000	3.91	3.918
SFC	70-30%*	331880	1.33	0.38
Mean	-	-	2.62	2.15
S.D	-	-	1.82	2.50
COV%	-	-	69.63	116.41
Mean***			**2.23**	**1.74**

* The load levels are expressed as a percentage of the maximum static load. ** It shows how many cycles the specimens sustained until failure. *** Average of both SFC specimens

Table 4.11: Test results for hybrid steel-polypropylene fibres (HyFC) beams

Concrete mix	Load level	Number of cycles**	Deflection (mm)	Crack width (mm)
HyFC	80-20%*	246	2.58	2.258
HyFC***	80-20%*	336	-	-
HyFC	80-20%*	506	1.89	2.341
HyFC	80-20%*	1320	3.97	5.525
HyFC	80-20%*	23280	0.41	0.019
HyFC	80-20%*	30480	1.06	0.582
HyFC	80-20%*	47230	0.4	0.020
HyFC	80-20%*	56400	0.93	0.444
HyFC***	80-20%*	86447	-	-
HyFC***	80-20%*	140000	-	-
HyFC	80-20%*	157800	1.16	0.177
HyFC	80-20%*	174240	0.43	0.04
Mean	-	-	1.43	1.27
S.D	-	-	1.20	1.84
COV%	-	-	84.27	145.55
HyFC	70-30%*	40	1.43	0.243
HyFC	70-30%*	1111	3.15	1.844
HyFC	70-30%*	1200	2.82	2.546
HyFC	70-30%*	215176	5.28	0.083
HyFC	70-30%*	310680	1.57	0.386
Mean	-	-	2.85	1.02
S.D	-	-	1.55	1.11
COV%	-	-	54.50	108.37
Mean***			**2.14**	**1.14**

* The load levels are expressed as a percentage of the maximum static load. ** It shows how many cycles the specimens sustained until failure. *** Data for these specimens is unavailable due to unforeseen technical issues during testing, therefore, only the number of cycles is reported. **** Mean for all HyFC specimens.

The (Smax/Fs) values for fibre-reinforced concrete are lower because the applied stress is divided by the value of the maximum flexural strength for fibre concrete to calculate the ratio of (Smax/Fs). Fibre-reinforced concrete typically has a higher maximum flexural strength (Fs) compared to conventional (normal) concrete. This is often a result of the reinforcing fibres, which improve the tensile strength and toughness of the concrete matrix. The maximum flexural strength (Fs) for fibre-reinforced concrete is higher than that of normal concrete, dividing the applied stress (Smax) by this higher value results in a lower Smax/Fs ratio.

In this case, the lower Smax/Fs ratio for fibre-reinforced concrete indicates that it can withstand higher applied stresses compared to its maximum flexural strength, which suggests improved load-carrying capacity and potentially greater resilience to flexural loads. This ratio can be a useful metric for assessing the performance of different concrete types in structural applications, particularly when evaluating their resistance to flexural stress.

The incorporation of steel fibres resulted in an increase in the number of cycles when compared to normal concrete. The addition of steel fibres enhances the fatigue behaviour of concrete because they improve the concrete's fatigue life when compared to NC. Another study reported that increasing the fibre volume fraction of steel fibre from 0% to 1% brought about a significant increase in performance in terms of flexural fatigue (Singh et al., 2006). Bawa and Singh (2020) found that the incorporation of 25% of polypropylene fibres and 75% steel fibres offered the best performance under fatigue load which is attributed to the synergy between steel and polypropylene fibres. Similarly, Paskova and Meyer (1997) established that the presence of steel and polypropylene fibres increased fatigue life with fibre content of 1%, but it was found that the presence of 0.75% resulted in a significant reduction in fatigue life.

While the incorporation of hybrid fibres resulted in an increase in the number of cycles when compared to SFC, the addition of hybrid fibres enhances the fatigue behaviour of concrete because they improve the concrete's fatigue life compared to SFC. The increase in fatigue life is attributed to the combination of the reduction in the crack width and shorter length of the crack due to the fibre bridging effect. The benefit of the hybrid fibres to test beams led to an improvement in the number of cycles and fatigue life with different stress levels

indicating the positive interaction of the hybrid fibre system under repeated loadings.

The S-N curve indicated that when reducing the stress level, the number of cycles that caused the failure of the specimens continued to increase. This might be attributed to a process known as fatigue crack propagation, in which small cracks in the material gradually grow over time as a result of cyclic loading. Test results indicated that adding steel fibres to test beams enhanced the capacity of concrete to sustain fatigue loads compared to NC. Also, test results indicated that adding hybrid steel-polypropylene fibres to test beams enhanced the capacity of concrete to sustain fatigue loads compared to SFC. By adding different combination of fibres to the concrete mix, the test beams can exhibit improved resistance to fatigue loads, meaning they are more capable of withstanding repeated loading cycles without experiencing significant degradation or failure.

Test result of S-N curve indicated how the fatigue cycle affects the degradation of concrete beams with different types of concrete, even if the stress levels are high, the number of cycles indicated the resistance of the test beams when subjected to different stress levels. The addition of hybrid steel-polypropylene fibres to concrete mixes has been observed to have beneficial effects. The combination of these fibres offers a synergistic effect, providing advantages that go beyond what each fibre type can achieve individually. This hybrid effect contributes to the improved performance and durability of structures. The S-N curve in Figure 4.8 reveals a linear relationship, indicating that the different types of concrete have constant amplitude fatigue behaviour, where the ratio of cycles to failure to applied stress level is proportional. Also, the S-N curve can be used to predict the number of cycles under different load levels with the available equations.

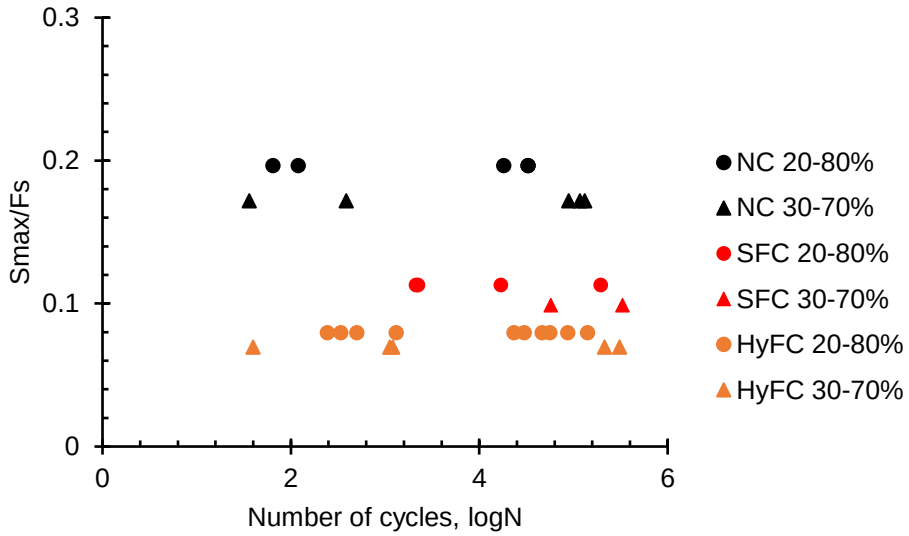

a) The relationship between (S_{max}/F_s) and the logarithm of the number of cycles to failure

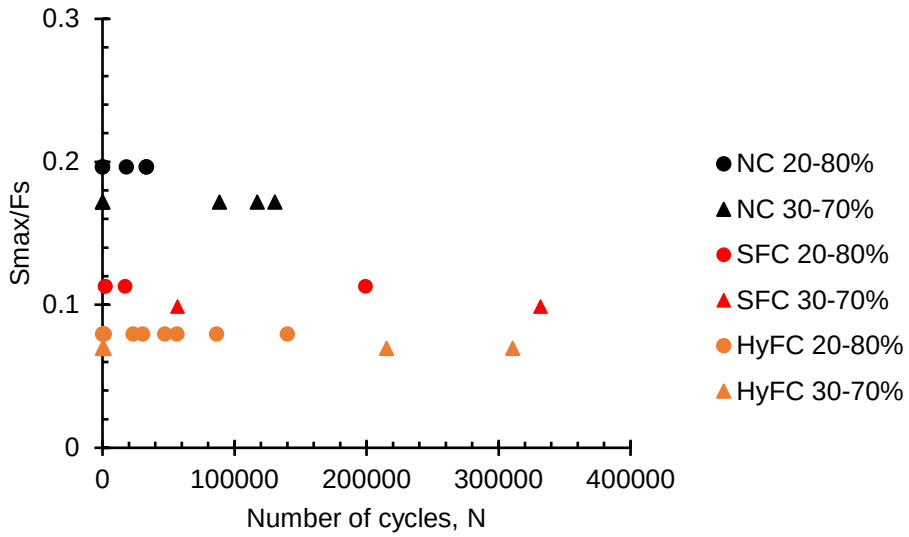

b) The relationship between (S_{max}/F_s) and the number of cycles to failure

Figure 4.8: S-N curve for all the beams

4.5.2 Mode of failure

The cracking pattern observed in all beams under different load types, as shown in Figure 4.9, is similar. The development of crack propagation under cyclic loads follows a similar pattern to that observed in static loading. In the case of normal concrete (NC) prisms, it was expected that they would exhibit a brittle flexural failure, as depicted in Figure 4.9. This finding aligns with previous literature, including the work of Goel and Singh (2014). The brittle failure of NC beams initiated as a small crack, which gradually increased in size with each cycle until

ultimate failure occurred. As the number of loading cycles (N) increased, cracks gradually developed in a manner comparable to static loading conditions. These cracks progressed upwards towards the compressed concrete zone, and the crack width expanded until the beams eventually failed after accumulating damage with an increasing number of cycles. This observation is consistent with the findings reported by Bawa and Singh (2020).

In contrast, beams incorporating various types of fibres were not completely destroyed and continued to carry the load even with an increasing number of cycles until failure. This is in contrast to NC beams, which typically failed abruptly after a specific number of cycles with the initiation of a crack. Similar results were reported by Goel and Singh (2014) for single type of fibre. The incorporation of steel fibre in the concrete resulted in improved performance compared to the NC specimens. Steel fibre concrete exhibited enhanced crack resistance and a more ductile failure mode, indicating its superior mechanical behaviour compared to NC beams without fibres. With the addition of different types of fibres, the failure mechanism of the prisms changed from sudden and brittle concrete failure to a more ductile failure mode.

In almost all cases of NC, steel fibre concrete (SFC) and hybrid fibre concrete (HyFC) specimens that failed under fatigue loading, a single major crack originated in the centre of the specimen between the point loads. When the first obvious crack initiated at higher stress levels, failure occurred almost immediately. The incorporation of hybrid fibres potentially influenced the failure mode, as it may depend on the bond between the fibres and the concrete. The inclusion of hybrid fibres led to a more ductile failure mode, providing resistance to crack propagation and giving some indications of an impending failure, which is preferable to sudden and brittle failure. The addition of hybrid fibres in the concrete mix outperformed the steel fibre specimens in terms of crack control and resistance to crack propagation. The hybrid fibre concrete (HyFC) exhibited superior ductility and enhanced performance compared to the steel fibre concrete (SFC) specimens.

a) NC

b) SFC

c) HyFC

Figure 4.9: Crack pattern and mode of failure for normal and fibre concrete beams

4.5.3 Deflection-cycles curves under different load levels

Table 4.9 Table 4.10 and Table 4.11 summarise the test results. Figure 4.10 and Figure 4.11 illustrate the development of the mid-span deflection of the NC, SFC and HyFC beams versus the number of cycles. Figure 4.10 corresponds to the load levels of 20-80% and Figure 4.11 corresponds to the load levels of 30-70% of the maximum static load where the deflections are reported when the load level was 50%. Selecting a load level of 50% for taking a measurement allows for a comparison between different types of beams (NC, SFC, HyFC) at the same relative load level, as can be seen in Figure 4.10(a). This facilitates a fair and direct comparison of their respective deflection characteristics, aiding in evaluating the effectiveness of fibre inclusion in improving beam performance.

The number of cycles is represented by a log scale plot. Figure 4.10 and Figure 4.11 only display a typical outcome for the mid-span deflection for each load range with number of cycles. Outlier results were omitted from the representation of the test results. The results for the NC, SFC and HyFC beams are presented and compared in this section.

The deflection curve of the specimens has three distinct stages. The addition of steel fibres to test beams resulted in improved performance compared to the NC specimens. Similarly, the addition of hybrid fibres to test beams led to improved performance compared to the SFC specimens, as shown in Figure 4.10 and Figure 4.11. All beams exhibited a rapid increase in mid-span deflection during the loading process and most of the deflection occurred in the early stages. Germano et al. (2016) and Chenkui and Guofan (1995) reported that the mid-span deflection showed three different stages and the mid-span deflection increased in the loading process. Due to stiffness degradation, the mid-span deflection of the beam gradually increased as the number of cycles increased in the early stages. The observed decrease in stiffness and/or increase in deflection of the concrete beams can be attributed to the fact that the beams were subjected to higher loads than they were designed to withstand, which can lead to the initiation and propagation of cracks in concrete beams. As cracks form and grow, they reduce the beams' stiffness and increase their deflection. This excessive loading caused the beams to exceed their capacity, resulting in the formation of cracks. As a result of these cracks, the stiffness of the beams decreased, leading to greater deflections. It is evident that the mid-span deflection increased gradually and steadily in the second stage. As can be observed, the mid-span deflection of NC beams rapidly increased in the last stage before the complete failure of the beams. Similarly, the mid-span deflection of SFC beams showed a gradual increase in the second stage before a rapid increase in the last stage. The mid-span deflection of HyFC beams under different load levels exhibited a more gradual and steady increase with a reduction in the maximum deflection compared to the rapid increase observed in the NC and SFC beams, indicating the superior crack resistance and enhanced stiffness retention of HyFC when the load levels were 20-80% of the maximum static test.

The NC, SFC and HyFC graphs are distinctly different, as can be seen in Figure 4.10 and Figure 4.11, respectively. Additionally, Figure 4.10 demonstrates that

mid-span deflection increased when the maximum load level was increased for NC beams. When the beams are subjected to a load level of 20-80% of the maximum static test, NC is prone to cracking under repeated load and has a relatively low tensile strength. Consequently, when subjected to repeated loads, cracks in the concrete expanded and propagated, resulting in increased mid-span deflection. The SFC beams exhibited a reduction of approximately 29.4% in mid-span deflection compared to the NC beams at load levels ranging from 20% to 80%. However, by further incorporating hybrid fibres into the test beams, an additional reduction of approximately 22.7% was achieved compared to the SFC beams. In contrast, SFC and HyFC with higher tensile strength, achieved through the incorporation of fibres, improved crack control and reduced deflection when subjected to higher repeated loads. Incorporating hybrid fibres into test beams, there was an observed increase in resistance to cracks and a subsequent reduction in deflection. The fibres in HyFC contributed to enhanced tensile strength, effectively distributing the load more evenly throughout the concrete and reducing the formation and propagation of cracks, highlighted the superior performance of HyFC in comparison to NC and SFC. Furthermore, when comparing NC and HyFC, HyFC demonstrated improved crack control and reduced deflection, primarily due to the incorporation of hybrid fibres.

On the other hand, the mid-span deflection of NC showed a reduction in the mid-span deflection when the load level was decreased whereas the addition of fibres did not have any effect on the reduction of the stress level. The mid-span deflection of SFC for load levels of 30-70% of the maximum static test showed an increase compared to NC whereas the mid-span deflection of HyFC exhibited an increase when compared to SFC. It is worth noting that there were specific load levels (30-70% as a percentage of the maximum static test) where the incorporation of steel fibres and hybrid fibres resulted in an increase in mid-span deflection compared to the NC beams, similar to the static test results. The exact figures were approximately 118.3% and 137.5% increase, respectively. This suggests that the effects of steel and hybrid fibres on the deflection behaviour of the beams varied depending on the applied load levels. It was also observed that the load ranges have an impact on the development of mid-span deflection because they affect the initiation and the growth of fatigue crack.

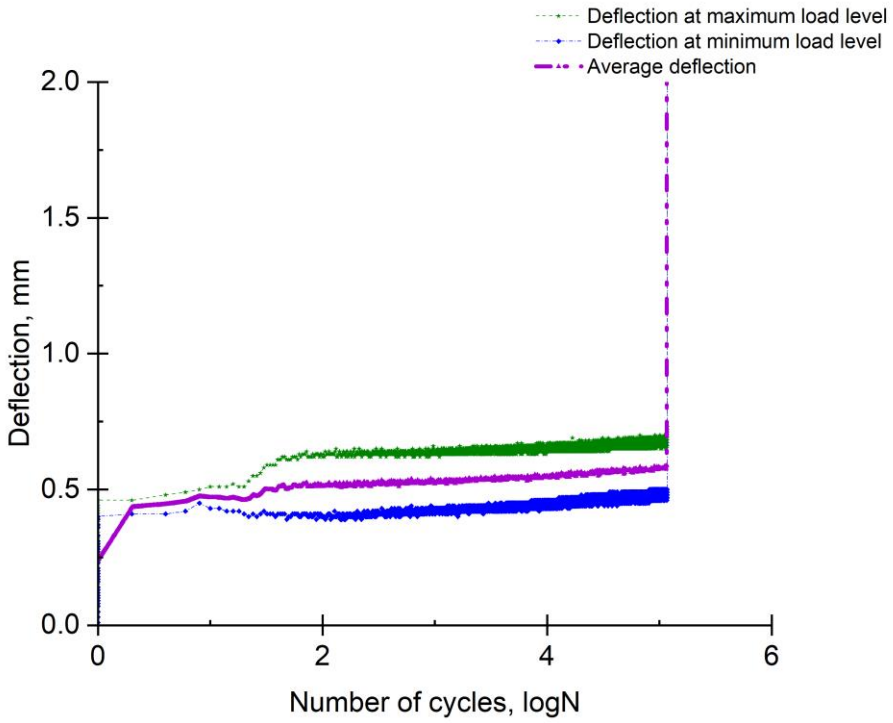

a) Graph illustrating clarity measurements at different load levels

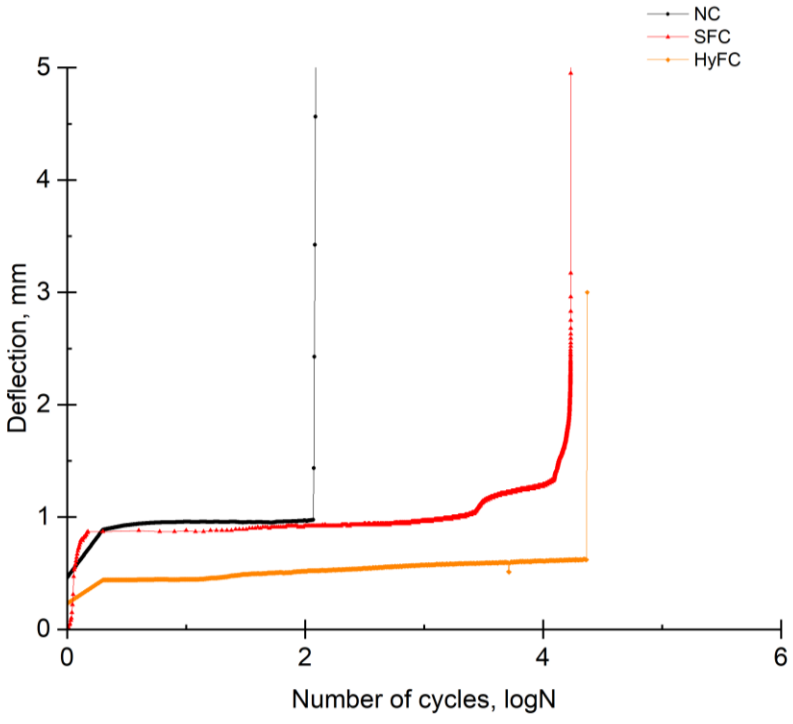

b) Number of cycles versus deflection of test beam for NC, SFC and HyFC beams, load level of 20-80% where the measurements were taken at 50% load level

Figure 4.10: Deflection of test beam for NC, SFC and HyFC beams with number of cycles

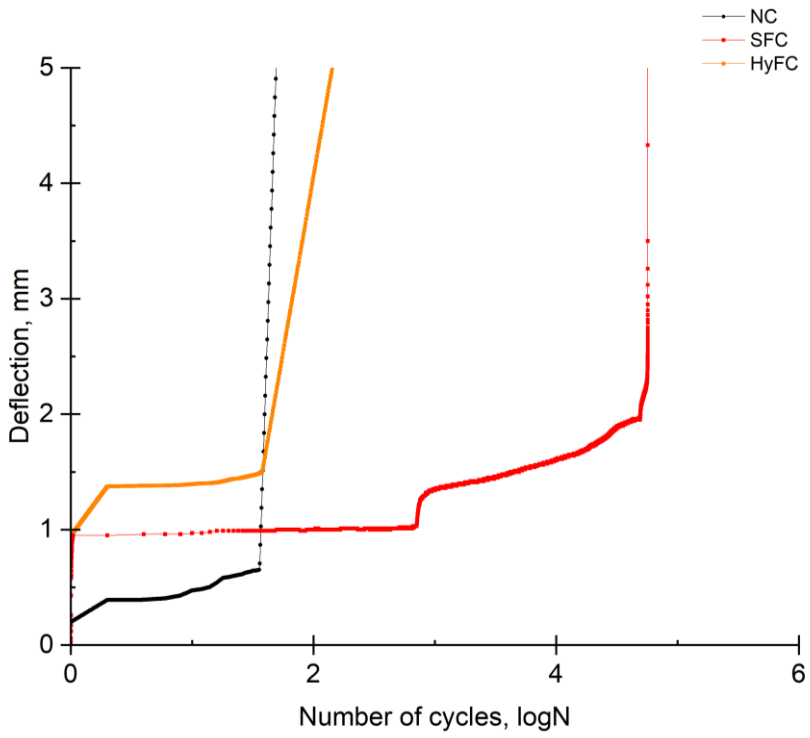

Figure 4.11: Number of cycles versus deflection of test beam for NC, SFC and HyFC beams, load level of 30-70% where the measurements were taken at 50% load level

4.5.4 Crack width behaviour under repeated loads

Figure 4.12 and Figure 4.13 illustrate the development of the crack widths in the NC, SFC and HyFC beams versus the number of cycles under the load levels of 20-80% and 30-70%, but measured when the load level was 50%. All beams exhibited an increase in the primary crack width as the number of cycles increased. This observation is confirmed by the findings of Stephen and Gettu (2020) as well as Tawfiq et al. (1999) who revealed that fatigue cracking occurs in three stages in the presence of one type of fibre (polymer fibres) in reinforced concrete. The growth of crack width with the number of cycles of all of the beams was found to have three distinct stages: the initiation of the crack, the development phase of propagation and the failure stage. Under fatigue testing, cracks were initiated and appeared during the loading process or during the first cycles of fatigue loading. Similar results were observed by Meng et al. (2019) who stated that the initial crack appeared during the loading process or immediately after fatigue loading. After the initiation of cracks, the rate at which the width of the crack propagated was slow as the number of cycles increased. Additionally, Figure 4.12 and Figure 4.13 demonstrate that the crack widths

increased for 20-80% load level of the maximum static test compared to 30-70% load level of the maximum static test whilst comparing the major crack width during the initial loading process.

The second stage refers to gradually increasing the damage of the beams over time. The incorporation of hybrid steel-polypropylene fibres helped to mitigate the propagation of the cracks which became more notable in this stage and this is attributed to the fibre bridging effect of the combination of different types of fibres (Suthiwarapirak et al., 2004; Zhu et al., 2022). When the concrete beams are subjected to higher levels of fatigue loading or stress, cracks develop at an earlier stage and reach a critical size sooner. Consequently, the beams fail after a shorter number of cycles compared to when they are exposed to lower levels of fatigue loading or stress. In summary, higher fatigue loading-stress leads to the formation of cracks earlier and shorter lifespan of the specimens before failure. The more energy applied to the specimen over a shorter period of time, the greater the damage from fibre pull-out and crack propagation in the fracture process zone (FPZ), which can cause a rapid increase in crack width in the second phase of cracking at greater fatigue loading, as reported by Stephen and Gettu (2020).

After the development stage of the crack width, the major crack width starts to widen considerably during the last stage, which ultimately causes the failure. The rate of the crack width rapidly increased in the final stage before the complete failure of the beams. As can be seen in Figure 4.12 and Figure 4.13, the crack width prior to the ultimate failure stage is smaller than the average crack width obtained from static flexural strength testing results for both the normal concrete, steel fibre concrete and hybrid fibre concrete prisms. It is also apparent that the stress ranges have an impact on the development of crack width. Additionally, Figure 4.12 and Figure 4.13 demonstrate that the crack widths increased when the maximum stress level was increased whilst comparing the major crack width during the initial loading process. Moreover, the average crack widths at failure decreased when the maximum load level decreased, especially for HyFC beams. In contrast, the average crack width of NC and SFC beams showed a higher crack width when the maximum load level decreased. Normal concrete exhibited almost the lowest rate of crack opening for each examined load level with a crack width value of 0.01mm. However, the average crack width

at failure exhibited a higher value, indicating a sudden increase in crack width. On the other hand, it can be observed that the inclusion of fibres resulted in an increase in crack width under loading. The crack width showed a gradual increase under load before reaching the point of failure, where the crack width showed a significant increase. The crack width at failure for HyFC beams showed a lower value when compared to SFC beams by approximately 34.48%. Notably, the HyFC beams exhibited a more pronounced effect in reducing the average crack width compared to SFC beams.

Also, beams cast with fibres exhibited no discernible increase in crack length. Beams cast with steel fibre showed a reduction in the crack length compared to NC. On the other hand, the addition of hybrid fibre into test beams showed more notable reduction in the crack length compared to SFC beams. The reduction in the crack length of HyFC beams is attributed to the role of fibres which can bridge micro cracks and slow their propagation, thereby improving performance under cyclic load.

The above discussions suggested that the incorporation of hybrid fibres had a significant impact on reducing crack widths and crack lengths, surpassing the effect observed in SFC beams. The difference in the static test and fatigue test results is more pronounced for beams cast with hybrid fibres when compared to normal concrete and steel fibre concrete beams. The incorporation of hybrid steel-polypropylene fibres helped to mitigate the propagation of the cracks, which become more notable and this is attributed to the fibre bridging effect of the combination of different types of fibres. The positive synergy effect of the different types of fibres in the crack surfaces led to better performance even under these higher stress levels, so the reduction of stress levels with hybrid fibre systems might lead to better and higher resistance to the crack growth.

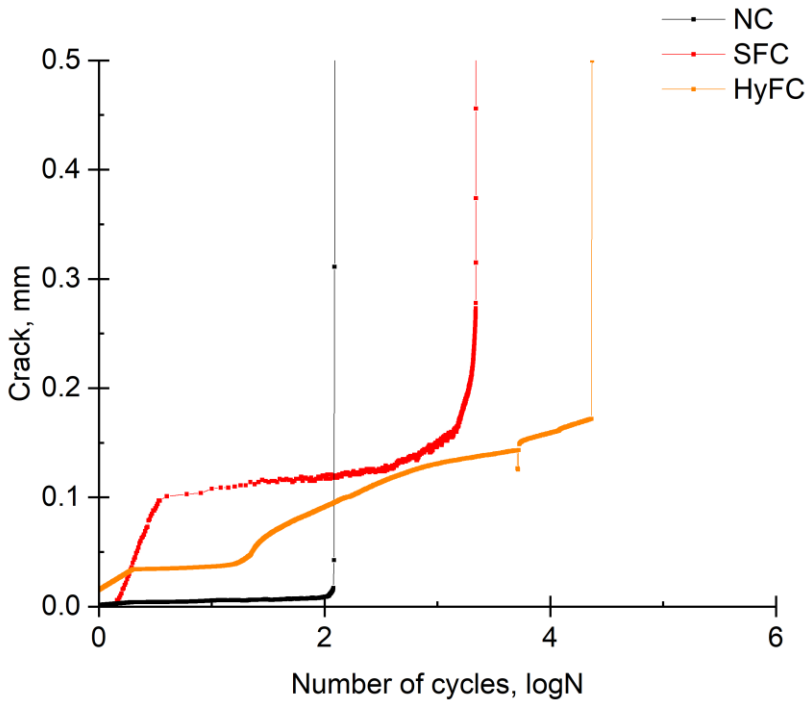

Figure 4.12: Number of cycles versus crack width of test beam for NC, SFC and HyFC beams, load level 20-80% where the measurements were taken at 50% load level

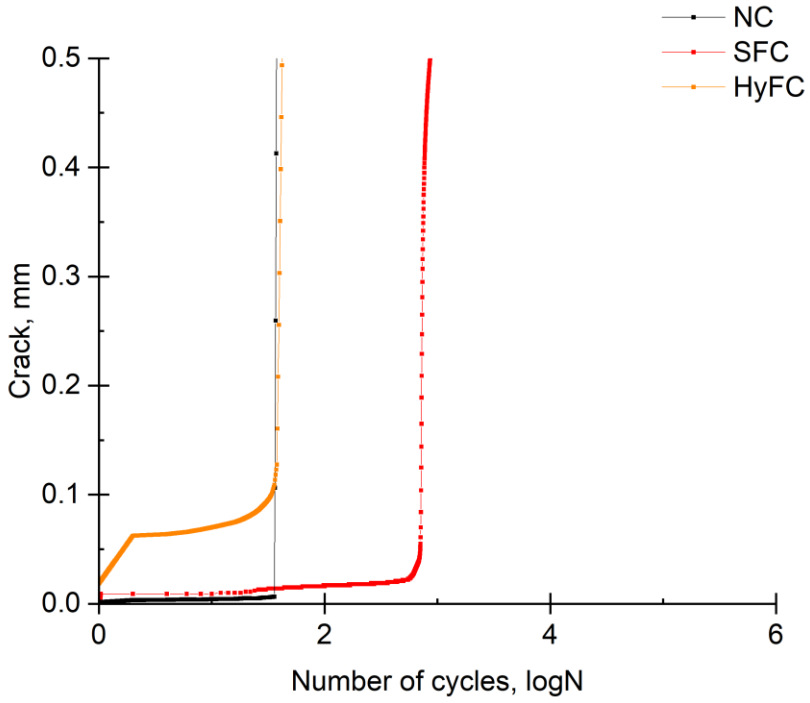

Figure 4.13: Number of cycles versus crack width of test beam for NC, SFC and HyFC beams, load level 30-70% where the measurements were taken at 50% load level

4.6 Time-dependent effects

The results of the long-term experimental tests conducted in the current study are discussed in the following sections. According to Tošic (2020), cited by Ghali et al. (2002), “the measurement of the mechanical behaviour of concrete structures is complicated even without taking into account the effect of fibres because of flaws including drying shrinkage, creep and cracking”. The measured creep and shrinkage were conflicting, preventing them from drawing broad conclusions, as they might not consider all the variability that affect the long-term behaviour. Shrinkage and both compressive and tensile creeps were measured and recorded simultaneously with long-term deflection readings on the full-scale loaded beams. Figure 4.14 illustrates the various characteristics studied using different specimens.

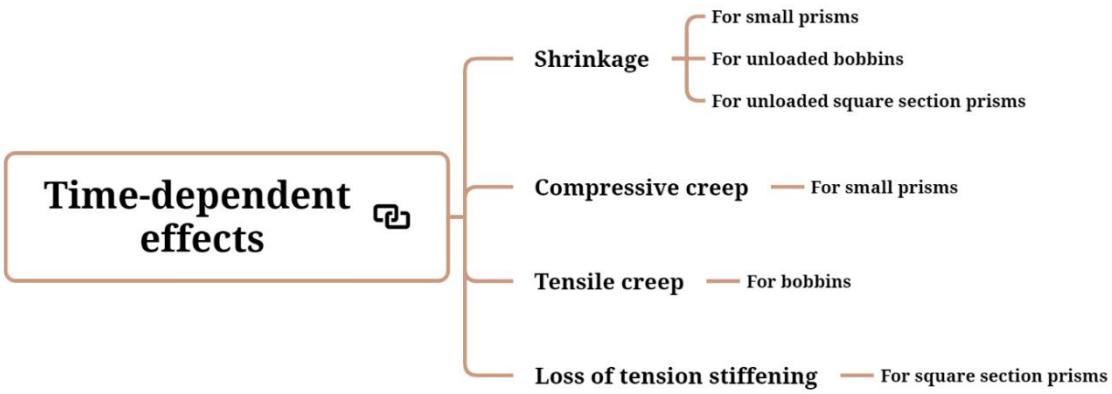

Figure 4.14: Various characteristics for different types of specimens

4.6.1 Shrinkage

As previously mentioned in Chapter 3 and illustrated in Figure 4.14, prisms with different size were used to determine shrinkage for each type of concrete mix.

4.6.1.1 Shrinkage for small prisms

Each concrete mix's shrinkage was determined by averaging the shrinkage values obtained from four prisms; for each prism readings were taken on two opposing vertical surfaces. Figure 4.15 demonstrates the shrinkage strains of the NC and HyFC concrete specimens over 90 days (the measurements started when the specimens reached an age of 28 days, hence what is reported here are the test durations, not the actual age of the specimens). The shrinkage curve for both mix types shows a similar trend over time. The differences in strain due to

shrinkage is not that significant between NC and Hybrid fibre concrete as well. The HyFC showed slightly higher shrinkage until the specimens reached a test age of 68 days (=28+40), but beyond this the difference is not considered to be statistically significant. Even this initial increase could be the experimental variability. The shrinkage of the specimens gradually increased over time for the first 40 days and 50 days of testing for the hybrid fibre and normal concrete specimens, respectively. After that, the shrinkage value of the hybrid fibre concrete specimen showed a slight reduction until the test duration of 50 days, whereas normal concrete showed a higher reduction in its rate than hybrid fibre concrete until 65 days. Then the shrinkage value of hybrid fibre concrete showed a slight increase from 50 days until 65 days, with a rapid increase at 65 to 70 days, while the shrinkage of normal concrete kept on increasing at the test duration of 65 days until the measurements were stopped at the test duration of 90 days.

When the measurements were completed at the test duration of 90 days, both normal and hybrid fibre concrete exhibited the same shrinkage strain. However, their rates differed as the normal concrete remained increasing, whereas the hybrid fibre concrete plateaued out. Normal concrete without fibres was more prone to cracking and deformation, which can cause increased amounts of shrinkage over time. However, most of the time specimens with hybrid fibres experienced greater shrinkage than the corresponding normal concrete without fibres. It was approximately 17.6% larger than the corresponding normal concrete. The presence of fibres creates additional internal stresses within the concrete matrix (Barluenga, 2009), which might lead to higher shrinkage. Hybrid fibres, in particular, may have different compatibility with the matrix, resulting in varying degrees of shrinkage behaviour, as reported by Chen and Liu (2004). The fibre-matrix interface can create stress concentrations, affecting the overall shrinkage response of the concrete according to Barluenga (2009).

As previously mentioned in Chapter 2, researchers were unable to draw broad conclusions about time-dependent properties such as creep and shrinkage of hybrid fibre concretes because they obtained inconsistent test findings. The authors claimed that the higher shrinkage in specimens with fibres might be attributable to the fibre content in the composite degrading the composite‘s characteristics if the fibre was increased beyond an ideal level. This increase

might be attributed to a reduction in the bond between the fibre and the surrounding concrete due to the bundled fibre in small specimens. All the work cited previously, including the current research, has shown that the fibres increased shrinkage. However, none of the studies reviewed mentions the effects and the variability of the amount of superplasticizer added, which correlated with the volume fraction of fibres. So, the amount of superplasticizer and its variability might have also contributed to the increase in shrinkage. Qian et al. (2006) and Afroughsabet and Teng (2020) reported that one of the main reasons identified for the increase in shrinkage when superplasticizer is added is the increase in the volume of micropores.

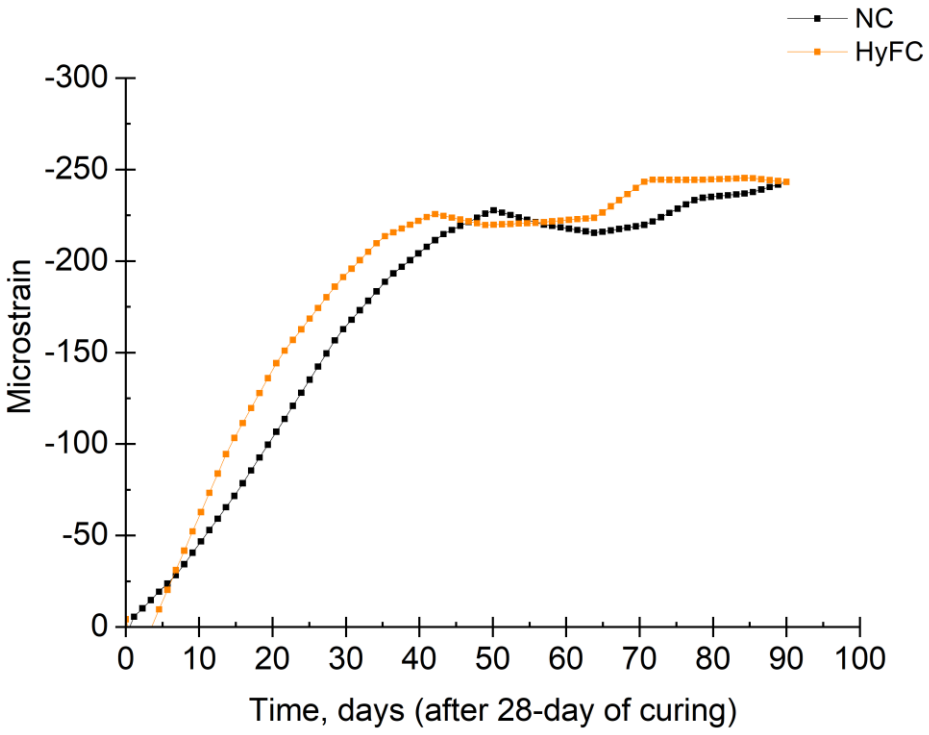

Figure 4.15: Effect of hybrid fibres on shrinkage

4.6.1.2 Shrinkage of not loaded bobbins for determining the tensile creep

The shrinkage of normal and hybrid fibre specimens was also assessed on bobbins. Figure 4.16 illustrates the shrinkage strains of the NC and HyFC concrete bobbin specimens over a period of 90 days. The addition of hybrid fibres to the unloaded bobbin specimens initially resulted in a slight reduction in shrinkage, as shown in Figure 4.16. However, after 21 days, the addition of hybrid fibres to concrete specimens had a significant effect as the strain significantly increased compared to that of NC. Specifically, the shrinkage strain of the hybrid

fibre concrete bobbin specimens reached as high as 60.71% at 90 days, indicating a notable increase due to the inclusion of hybrid fibres. In contrast, the shrinkage of normal concrete levelled out after approximately 30 days, suggesting that the material had likely reached equilibrium with its environment. As shown in Figure 4.16, it is evident that the shrinkage rate of the NC bobbin specimens displayed a reduction after 50 days. This reduction in shrinkage rate could potentially be attributed to the drying environment, as depicted in Figure 4.17, when these tests were carried out.

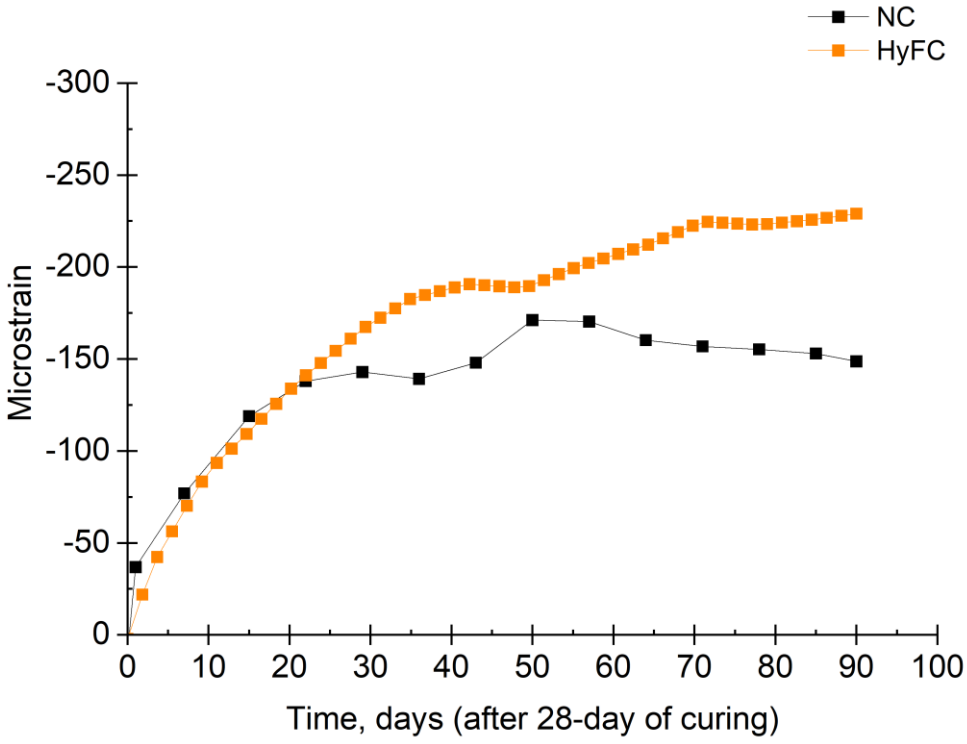

Figure 4.16: Drying shrinkage of NC and HyFC concrete mix for unloaded bobbins

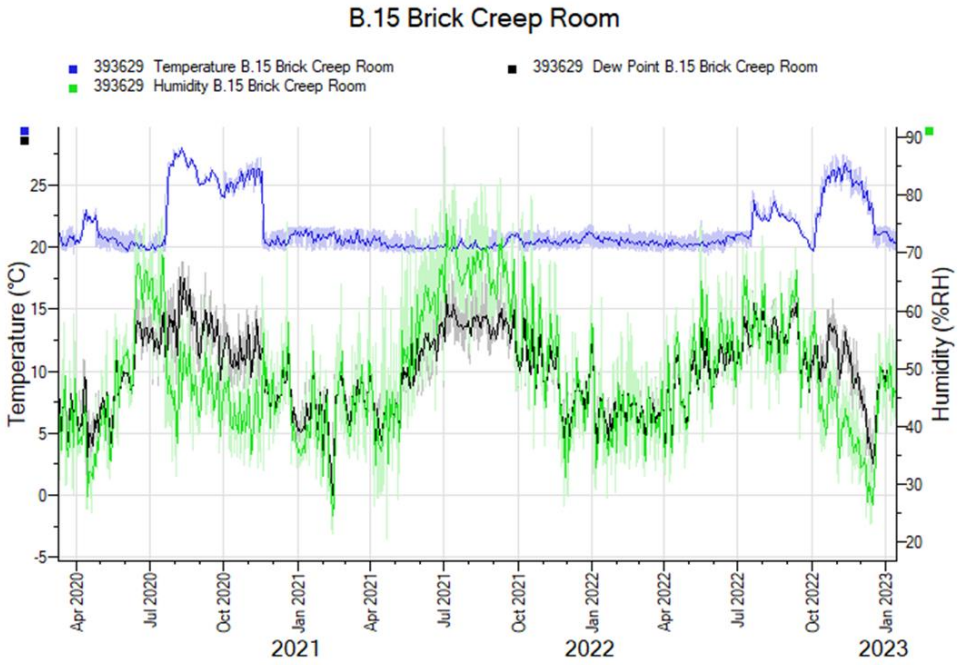

Figure 4.17: The variation of temperature and the relative humidity in the creep room

4.6.1.3 Shrinkage of unloaded prisms for determining the tension stiffening

The shrinkage prisms were prepared and manufactured using the same cross-section and procedure as the testing square section prisms to examine shrinkage strain in unloaded square section prism specimens, as mentioned previously in Chapter 3 (Section 3.8.7). Figure 4.18 illustrates the development of shrinkage for different types of concrete over a period of 35 days. Figure 4.18 highlights the effect of incorporating steel and hybrid steel-polypropylene fibres on the development of shrinkage strain for the duration of the sustained load. As can be seen in Figure 4.18, it was evident that adding hybrid steel-polypropylene fibres reduced the shrinkage strain in unloaded specimens. On the other hand, the inclusion of steel fibres resulted in approximately 67.65% and 28.15% greater shrinkage compared to the corresponding normal concrete after 3 days and 35 days, respectively. This increase in shrinkage might be attributable to a reduction in the bond between the fibre and the surrounding concrete due to fibres bundling. Notably, the composite with 1.5% hybrid steel-polypropylene fibres exhibited the least shrinkage among all the composites, as shown in Figure 4.18. These reductions were approximately 32.35% and 26.67% for HyFC after 3 days and 35 days, respectively, in comparison to the corresponding normal concrete

specimens. The inclusion of more than two different types of fibre demonstrated a significant positive hybrid effect on shrinkage. This reduction might be attributable to the ability of fibres to control the volume variations of concrete by indirectly enhancing the link between the cement matrix and the coarse aggregate, as reported by Sryh (2017).

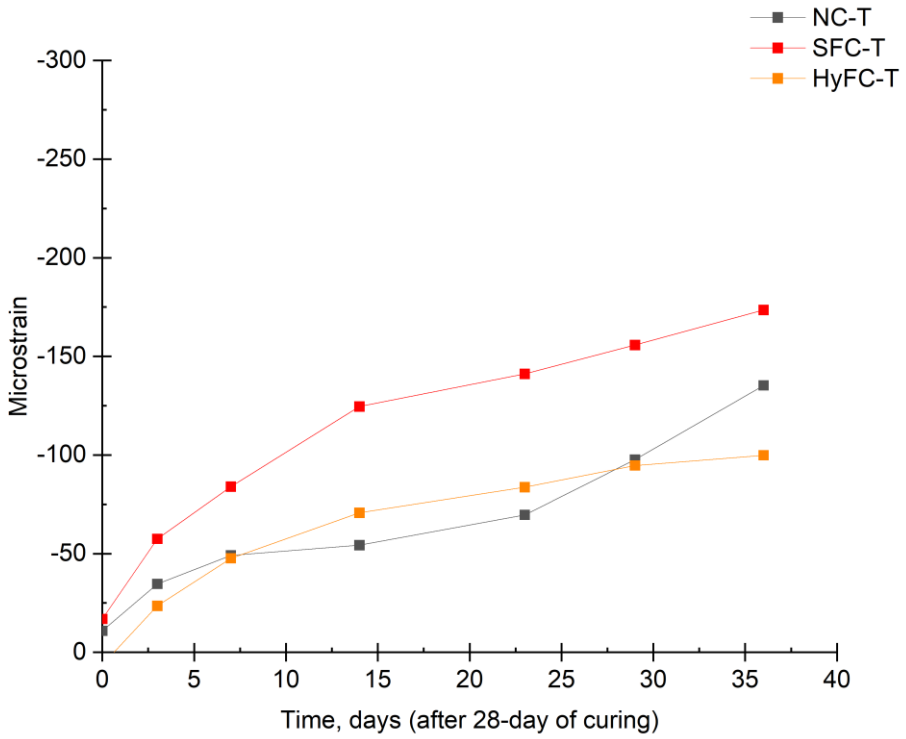

Figure 4.18: Effect of fibres on the drying shrinkage of unloaded specimens

4.6.2 Compressive creep

Figure 4.19 illustrates the development of the compressive creep strains for the NC and HyFC concrete specimens under a constant stress of 23%-25 of 28-day compressive strength over time. Figure 4.20 shows the compressive creep coefficient of NC and HyFC concrete mix. It was found that HyFC concrete specimens exhibited a lower creep coefficient than normal concrete. The compressive creep curve for both specimens shows a similar trend over time. Similar to the results for shrinkage, the addition of 1.5% hybrid fibres caused the strain of the compressive creep samples to record a higher result of strain value than the corresponding normal concrete. The increases were approximately 36% and 46% at the test duration of 30 days and 90 days, respectively. As mentioned earlier, if the NC had a lower compressive strength than the fibre mixes, the applied stress of 20% of the 28-day compressive strength would be lower. As a

result the NC may experience less creep. Also, this increase of strain value with the incorporation of hybrid fibres to concrete specimens on the compressive creep might be attributed to the bundle of fibres, the orientation of fibres during casting and the amount of superplasticizer added.

The findings presented in Chapter 2 and the collective results discussed here indicated that the addition of fibres can indeed result in varying effects on creep behaviour in concrete. These effects are influenced by factors such as the type of fibres used, the dosage of fibres incorporated, and the duration of testing, which is not studied in this research. The studies mentioned earlier provide evidence that different types of fibres, such as short steel fibres, long steel fibres, and the current study with hybrid fibres, can affect creep in different ways. The dosage of fibres also played a role, with varying percentages showing different effects on creep strain. Additionally, the duration of testing can influence the observed creep behaviour, as some studies reported changes in creep over time. Considering these findings collectively emphasised the importance of carefully selecting and controlling the type and dosage of fibres in concrete mixes. In conclusion, the effects of fibre addition on creep behaviour are influenced by multiple factors. Understanding these factors and their interplay is crucial for optimising fibre concrete and ensuring its long-term performance, which is not part of this research.

All of the research in this section, which reports the creep data, has demonstrated that the fibres caused more creep, which might be attributed to the different applied stress to 28-day compressive strengths for samples or the higher amount of applied stress. It is important to understand that the relationship between the modulus of elasticity and creep is not always straightforward and can depend on various variables, such as the material's composition and structure, the amount and duration of the stress or load, and the environmental circumstances. A material with a high modulus of elasticity may occasionally induce significant creep deformation in specific cases. In contrast, a material with a lower modulus of elasticity may only show little creep. The higher creep value might be related to the amount and magnitude of constant load or stress applied to concrete because the applied load or stress was a factor of the compressive strength. However, this effect can be negated by considering the creep coefficient, as shown in Figure 4.20 and discussed in the following section. In

summary, there continues to be uncertainty in the results of the empirical research which sought to identify how dispersed reinforcing fibres affect the creep of concrete; parameters which may have an effect include the orientation of fibres and their shape, the effect of the variability of superplasticizer added to the concrete mix and other variables that have an impact are not fully investigated. However, as can be seen in Figure 4.20, the test results of the creep coefficient should reduce the uncertainty when the fibres are present, as the creep of HyFC showed a lower value when compared to the normal concrete specimens, as the stress-strength ratio is eliminated in terms of the creep coefficient. Considering the creep coefficient in comparing the NC and HyFC made the effect of hybrid fibres more pronounced in reducing the creep. The addition of hybrid fibre showed a reduction in creep coefficient by approximately 49% compared to normal concrete without fibres.

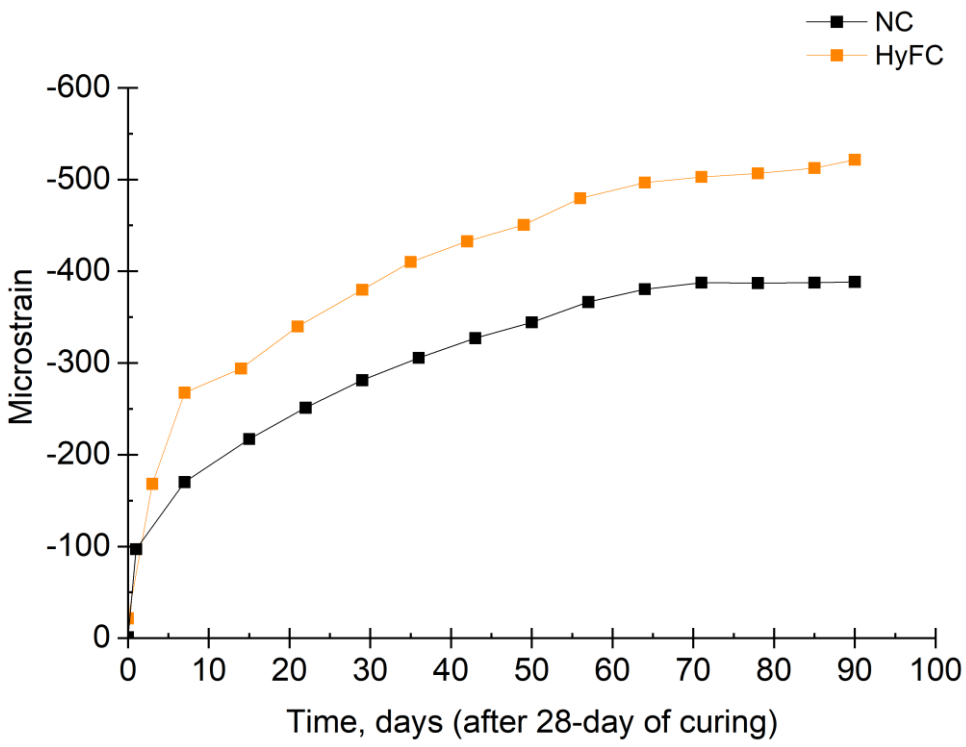

Figure 4.19: Compressive creep of NC and HyFC concrete mix

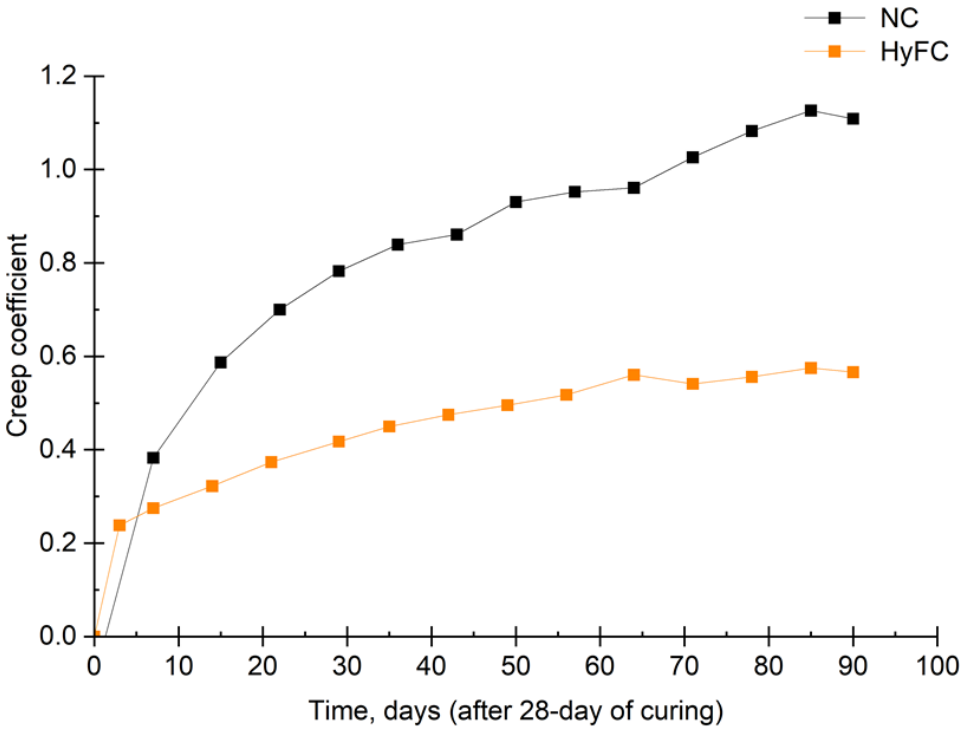

Figure 4.20: Compressive creep coefficient of NC and HyFC concrete mix

4.6.3 Tensile creep

Figure 4.21 illustrates the development of tensile creep strains in concrete specimens made of normal concrete (NC) and hybrid fibre concrete (HyFC) over time under constant stress. The results show that tensile creep increases linearly in the early stages (up to 15 days) for both NC and HyFC concrete specimens, as shown in Figure 4.21. The addition of hybrid fibre concrete did not show any difference in reducing the strain due to tensile creep. The shrinkage of normal concrete specimens reduced at the test duration of 55 days. This reduction in shrinkage affects the calculation of tensile creep since the shrinkage value is considered. Tensile creep is typically measured through a direct tensile test, which involves subjecting a specimen to pure axial tension. In contrast, the splitting tensile strength test is an indirect test that involves less pure tension. This difference in stress field results in the splitting tensile test producing higher values due to the non-pure tension condition. As a result, the presence of fibres has a more significant effect on enhancing the results of the splitting tensile strength test compared to the direct tensile test, where fibres are less active in one direction. Additionally, the reduction in shrinkage after 50 days in normal

concrete affects tensile creep because the shrinkage curves greatly influence the tensile creep curves. The randomness of the fibres means that not all fibres contribute to stiffness in the axial tension direction. Subsequently, tensile creep gradually increased over time until 55 days for the NC specimens and 70 days for the HyFC specimens. It is possible that variations in the quantity of superplasticizer used or its characteristics, casting orientation and fibre alignment could influence the tensile creep behaviour of concrete.

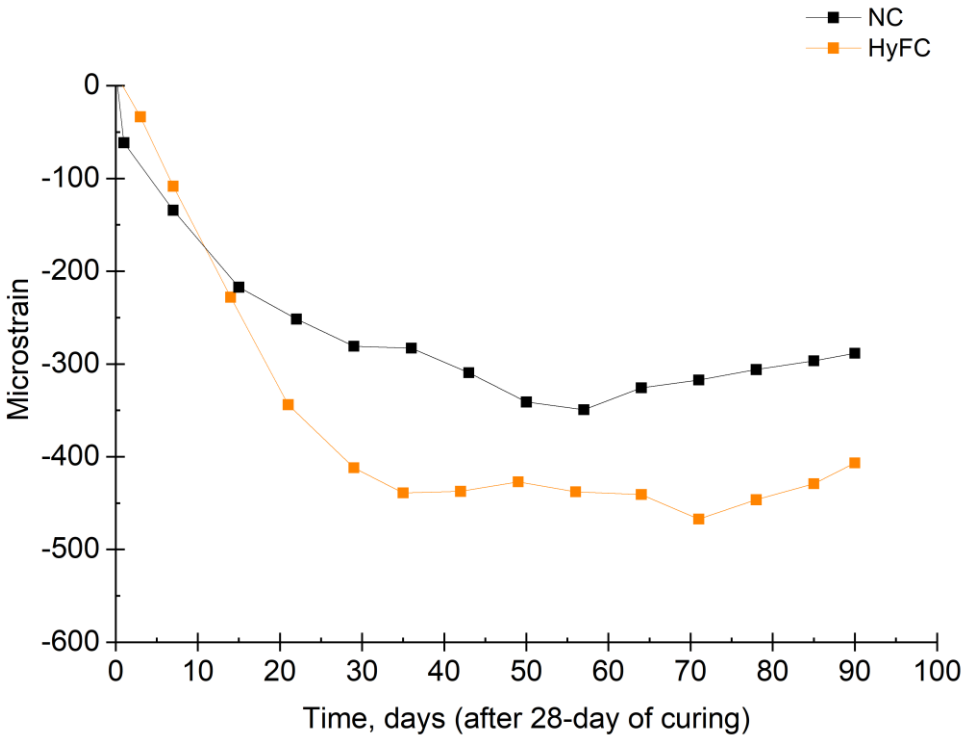

Figure 4.21: Tensile creep of NC and HyFC concrete mix

4.6.4 Long-term loss of tension stiffening tests

The effect of incorporating steel and hybrid steel-polypropylene fibres on the long-term loss of tension stiffening is shown in Figure 4.22. As suggested by Sryh (2017), the shrinkage specimen strain data were added to the tension stiffening specimens' strain readings because they act in different directions. As a result of this, the shrinkage had an effect on the results, so the results are presented without the shrinkage value. This was necessary as the shrinkage data was found to have an adverse effect on tension stiffening, as can be seen in Figure 4.18. It is important to note that when calculating concrete tensile stresses, an average strain value along the entire length of the specimen is utilised to prevent reliance on extreme values, whether they are the highest or lowest strains observed.

This section focuses on the effect of incorporating steel fibres and hybrid fibre systems on the long-term loss of tension stiffening. The loss of tension stiffening over time is represented by the ratio of long-term concrete stresses to the original/initial stresses. Figure 4.22 illustrates the effect of adding different types of fibres, such as steel fibre and hybrid fibre, on the reduction of tension stiffening. The reduction in tension stiffening follows a similar pattern for specimens with and without fibres, as shown in Figure 4.22. However, the presence of steel or hybrid fibres significantly influenced the rate of reduction. The influence of the fibres in terms of minimising the loss of tension stiffening is particularly pronounced during the early stages. After 35 days of loading, the normal concrete specimens experienced a reduction of approximately 45% in long-term tension stiffening. In contrast, the addition of steel fibres resulted in a reduction of around 40%, while the incorporation of hybrid fibres (a combination of steel, micro, and macro polypropylene fibres) led to a reduction of about 32%. The lower reduction in tension stiffening observed with hybrid fibres can be attributed to the combined effect of steel and polypropylene fibres, which possess different characteristics compared to steel fibres alone. The presence of polypropylene fibres contributed to crack resistance and increased the ductility of the concrete, influencing the overall behaviour of tension stiffening.

Furthermore, as can be seen in Figure 4.22, it is noteworthy that the NC-T and SFC-T specimens exhibited tension stiffening behaviour after 30 days, which can be attributed to the stress in the steel bars. It is important to note that some gauges were lost during testing, which could have influenced the observed results.

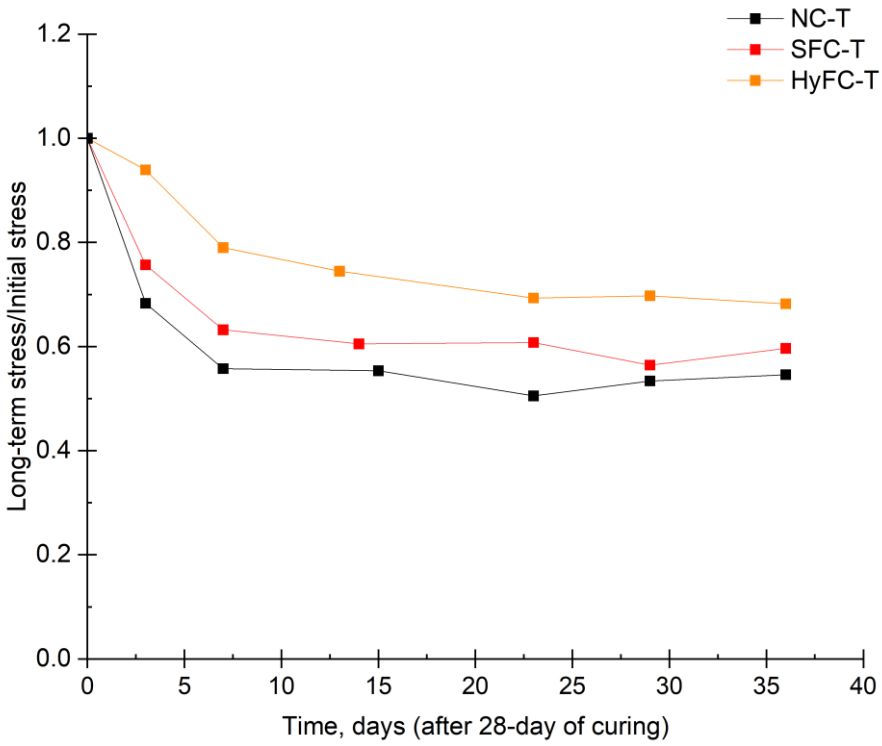

Figure 4.22: Effect of the addition of hybrid fibres on the loss of tension stiffening over time without shrinkage value

4.6.4.1 Surface strain

Figure 4.23 presents the surface strain of all specimens throughout the test duration. It was evident that all specimens exhibited a similar long-term trend in surface strain. The increase in strain can be primarily attributed to the opening and propagation of existing cracks. The compressive strain, as shown in Figure 4.23, displayed a linear increase during the initial loading phase (0-3 days). Subsequently, the compressive strain of all specimens gradually increased throughout the test duration. Notably, the inclusion of steel and hybrid steel-polypropylene fibres led to a greater reduction in surface strain compared to normal concrete. After 3 days, the reductions were approximately 25.20% and 70.40% for SFC and HyFC, respectively, in comparison to normal concrete. Similarly, after 35 days, the reductions were approximately 15.08% and 43.90% for SFC and HyFC, respectively, compared to normal concrete.

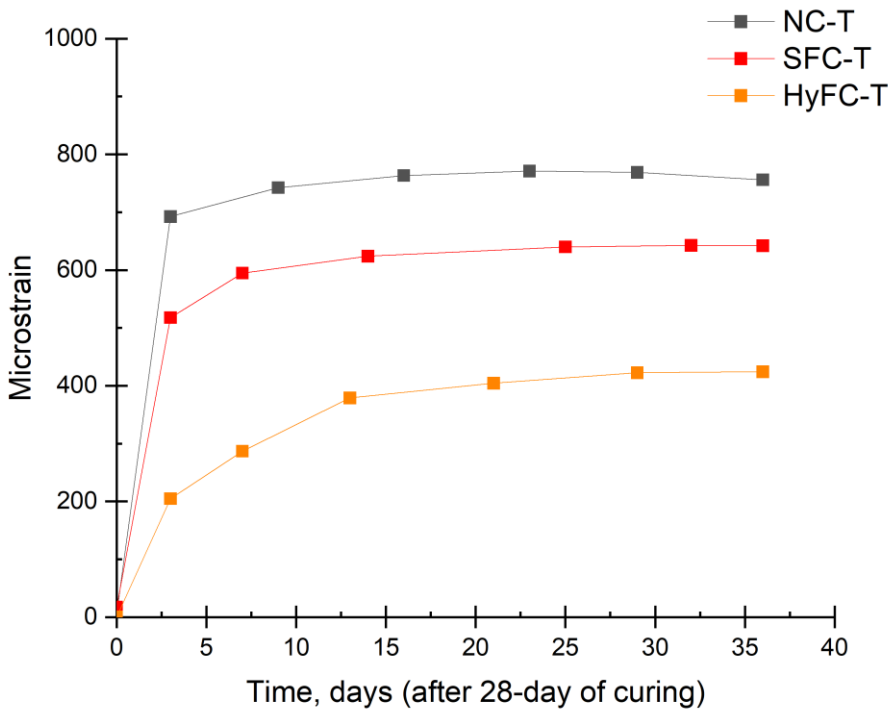

Figure 4.23: Effect of fibres on the concrete surface strains of loaded specimens

4.6.4.2 Steel strain

Figure 4.24 presents the stress in the steel bars over a 35–day period for NC-T, SFC-T and HyFC-T beams under load. Strains in some gauges were not recorded due to the malfunction of the gauges after loading, which affected the average readings of stress in the steel bars. The stress in the steel bars of the normal concrete specimen exhibited an approximate increase of 3% and 7.19% at 3 days and 35 days, respectively. As can be shown in Figure 4.24, the addition of 1.5% of hybrid fibres resulted in a slight reduction in steel bar stress by 3.69% and 14.73% at 3 days and at 35 days under load, respectively. However, the inclusion of 1% steel fibres showed a similar stress after 3 days and an increase in steel bar stress by approximately 16.67% at 35 days. These experimental results indicate that the addition of steel fibres increased the stress in the steel bars, potentially due to the bond strength of hooked-end fibres. It is important to

note that certain fibre types, such as steel fibres, may enhance the stiffness of concrete, leading to higher stress in the steel bars.

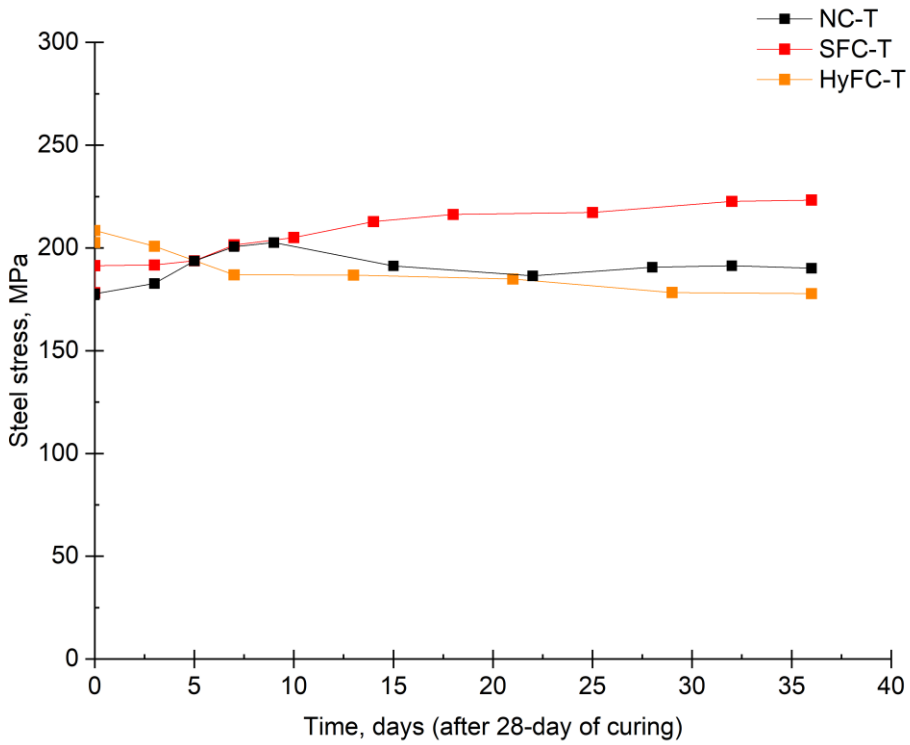

Figure 4.24: Steel stress in the steel bars

4.6.4.3 Crack pattern and crack width

Table 4.12 provides a summary of the crack characteristics, including the location, number, average spacing, and width, for the normal concrete (NC) and fibre concrete (FC) beams. The final crack distributions between the NC, SFC, and HyFC specimens are shown in Figure 4.25. Notably, the different specimens exhibited variations in crack locations. Figure 4.25 clearly shows that the NC specimen had a total of three cracks, while both the SFC and HyFC specimens had four cracks in total. During the loading process, as the specimens were gradually subjected to a load up to 45kN, one or two cracks were initiated in the NC and FC specimens before reaching a constant load level. Subsequently, over the sustained load duration, three additional cracks formed in all beams, primarily due to the restraint imposed by the reinforcing bars on drying shrinkage. Interestingly, the addition of fibres did not have a significant impact on the number of cracks compared to the reference beams without fibres under the same load conditions throughout the test duration. However, the incorporation of fibres

resulted in a significant reduction in crack propagation compared to normal concrete beams without fibres. Moreover, the inclusion of fibres led to a decrease in crack spacing and an increase in the overall number of cracks when compared to normal concrete. The benefits of incorporating fibres, as reported in Table 4.12, include a reduction in crack spacing, which signifies enhanced crack control and improved crack resistance in the concrete specimens.

Table 4.12: Long-term loss of tension stiffening test results

Type of beam	**NC**	**SFC**	**HyFC**
Number of cracks	3	4	4
Location	1-2,3-4,5-6	1-2,2-3,4-5,6-edge	0-1,1-2,3-4,4-5
Average crack spacing (mm)	300	240	240
Crack width (mm)	0.2	0.1	0.1

Normal concrete specimens recorded higher crack widths when subjected to sustained load over time. According to Table 4.12, the crack width for normal concrete was recorded as 0.2mm. However, an increase in fibre volume fractions relative to comparable reference beams resulted in a reduction in crack width for both SFC and HyFC specimens. The SFC and HyFC specimens exhibited a reduction of crack width approximately 50% compared to the reference beams. This reduction is primarily attributed to the "bridging" effect of the fibres across the cracks. It is important to acknowledge the significant role of steel and hybrid steel-polypropylene fibres in narrowing and bridging the cracks. The steel fibres, by reducing tensile stresses across the cracks, effectively reduced the crack widths, thereby arresting further crack propagation, as reported by Tan et al. (1995), Pajak and Ponikiewski (2013) and Deluce and Vecchio (2013). It is noteworthy that both steel and hybrid fibres exhibited excellent abilities in controlling crack width and providing fibre bridging mechanisms.

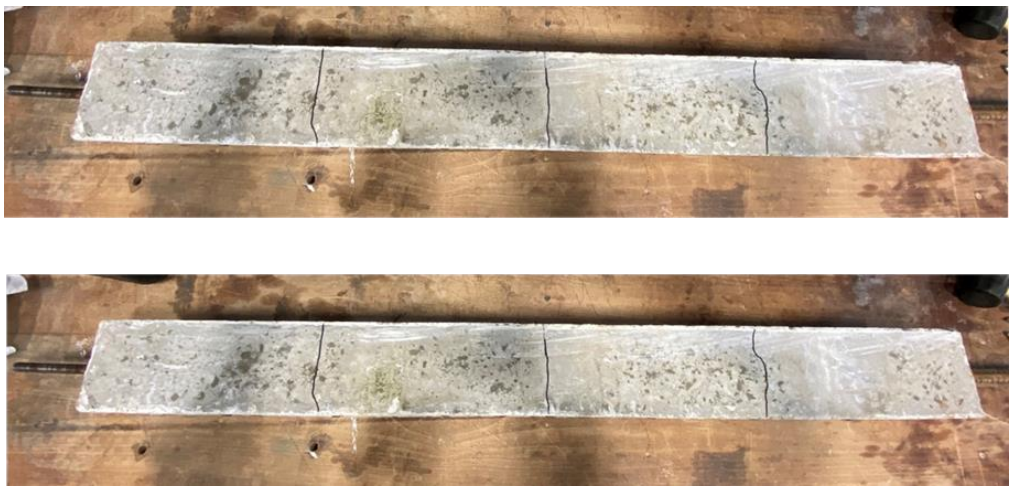

a) NC

b) SFC

c) HyFC

Figure 4.25: Crack pattern for normal and fibre concrete beams

4.7 Summary of observations made

The following key conclusions were drawn from the experimental data presented in this chapter:

Static test

- The incorporation of all of the different types of fibres caused the mode of failure for the prism beams to change to ductile failure.
- The incorporation of fibres had a minor effect on the pre-cracking behaviour of the tested beams and most of the serviceability phases.
- According to the test results, the contribution of fibres can be highlighted in the flexural strength results.
- The incorporation of fibres in test beams produced an increase in both the cracking load and peak load.
- Adding reinforcing fibres to specimens increased the cracking load (taken as average of three specimens) by 17%, 29%, 75% and 142% for micro 0.1PPFC, macro 0.4PPFC, SFC and HyFC, respectively, relative to the reference beams without any fibres (NC).
- The peak load increased with the addition of fibres by 8%, 20%, 74% and 147% for micro 0.1PPFC, macro 0.4PPFC, SFC, HyFC, respectively, relative to the reference beams without fibres (NC).
- Based on the evaluation of the experimental results, it was apparent that the hybrid fibre system increased deflection and reduced crack width at peak load.
- The incorporation of fibres to test beams increased deflection at peak load, which is different in each specimens by 31%, 67%, 85% and 90%, for micro 0.1PPFC, macro 0.4PPFC, SFC and HyFC, respectively, in comparison to the reference specimens.
- The incorporation of hybrid fibre systems also resulted in smaller cracks and a reduction in the visible width of cracks at failure. Hybrid fibres had the most influence in terms of reducing crack widths, followed by the steel and macro propylene fibres.
- Normal concrete beams and beams cast with micro polypropylene fibres had similar crack bridging behaviour.

- Macro polypropylene fibres exhibited an intermediate behaviour between the hybrid fibres and the micro polypropylene fibres.
- The presence of steel, hybrid and macro polypropylene fibres had a greater influence on post cracking behaviour.

Repeated test

- The test results demonstrate that there is a significant scattering in the number of cycles to failure for each loading scenario.
- According to the test results, increasing the fibre content led to an increase in fatigue strength. The incorporation of either steel or hybrid fibres increased the number of cycles when relative to normal concrete.
- The increase in fatigue life is attributed to a combination of the reduction in crack width and shorter length of crack due to the fibre bridging effect.
- The S-N curve indicated that when reducing the stress level, the number of cycles that caused the failure of the specimens kept on increasing.
- The cracking pattern for all beams under different load types is relatively similar. The development of crack propagation under cyclic loads exhibited a similar pattern to that found in the static load.
- Almost all of the NC, SFC and HyFC specimens that failed under fatigue loading had a single major crack that started in the centre of the specimen between the point loads.
- All beams exhibited a rapid increase in mid-span deflection during the loading process and most of the deflection occurred in the early stage.
- It is evident that the mid-span deflection increases gradually and steadily in the second stage. As can be observed, the mid-span deflection of all beams rapidly increased in the last stage before their complete failure.
- All beams exhibited an increase in primary crack width as the number of cycles increased.
- The rate of the crack width increases rapidly in the final stage before the complete failure of the beams.

- The mid-span deflection that can be maintained before the ultimate failure stage is lower than the average mid-span deflection obtained from static flexural strength testing results.

The combination of steel and polypropylene fibre is promising and can be used to improve the performance of prismatic beams under repeated load.

Long-term effect

- It was found that the addition of hybrid fibres to concrete specimens results in longer stabilised shrinkage after 40 days.
- At the age of 90 days when the measurements were complete, both normal and hybrid fibre concrete exhibited the same shrinkage strain, but their rate was different.
- The shrinkage of the hybrid fibre concrete specimens showed a negligible effect.
- Most of the time, specimens with hybrid fibres experienced more shrinkage than the corresponding normal concrete without fibres. It was approximately 17.6% greater than the corresponding normal concrete.
- On the other hand, the addition of hybrid fibres slightly reduced the shrinkage of the bobbins of unloaded specimens.
- The research was unable to draw broad conclusions about time-dependent properties such as creep and shrinkage because inconsistent test findings were obtained.
- It was shown that HyFC concrete specimens exhibited a lower creep coefficient than normal concrete.
- Similar to the results for shrinkage strains, the addition of 1.5% of hybrid fibres caused the strain of the compressive creep to exhibit a higher result than the corresponding normal concrete.
- The impact of hybrid fibre reinforcement on compressive creep is insignificant.
- The addition of hybrid fibres to the concrete specimens had an insignificant effect in terms of reducing tensile creep.

4.8 Conclusions

- The addition of hybrid fibre gave a superior performance compared to the addition of a single type of fibre on the first crack load, peak load, ductility, flexural strength, deflection and crack width.
- In general, the positive synergy effect of the different types of fibres in the crack surfaces led to better performance in terms of deflection and crack patterns under static and repeated load. The inclusion of more than two different fibre types demonstrated a pronounced positive hybrid effect.
- The highest compressive strength was achieved with the addition of 1.5% hybrid steel-polypropylene fibres (i.e., HyFC); these strengths were about 13.01% and 7.65%, respectively, higher compared to the reference specimens without fibres.
- The addition of hybrid steel-polypropylene fibres (also known as HyFC) showed the most significant improvement in splitting tensile strength by about 80.31% higher than the reference specimens without fibres.
- The incorporation of fibres resulted in a significant reduction in the crack propagation relative to the normal concrete beams without fibres. Macro polypropylene fibres showed a reduction in the crack width by about 20% and 48% when the load was at 10 kN and 15 kN, respectively. Beams cast with steel fibres showed a pronounced reduction in crack width compared to specimens cast with micro and macro polypropylene fibres when the load was at 10 kN by about 20%. They also showed a reduction in the crack width of about 51% when the loading was at 15 kN. Hybrid fibres exhibited the most significant reduction in crack width, surpassing specimens with only steel fibres by reducing crack width by approximately 20% at a load of 10 kN and 12% at a load of 15 kN.
- The test results revealed that the incorporation of micro and macro polypropylene fibres resulted in similar stiffness results, which they both showed a reduction in stiffness of approximately 14% and 19%, respectively, compared to NC. On the other hand, the incorporation of SFC and HyFC fibres into test beams showed an increase in stiffness of approximately 10% and 59%, respectively, higher than the reference beams at the formation of first visible crack.

- Beams cast with steel and hybrid steel-polypropylene fibres offered a more pronounced reduction in crack width and exhibited the finest cracks compared to other specimens when the load was 10kN by approximately 20% and 40% respectively. There was a reduction in crack width when loading at 15kN by approximately 51% and 64%, respectively.
- The second stage in repeated tests refers to gradually increasing the damage experienced by the beams over time. The incorporation of hybrid steel-polypropylene fibres helps to mitigate the propagation of cracks, which become more notable in this stage. This is attributed to the fibre bridging effect of the combination of different types of fibres.
- According to test results, the crack width that can be obtained before the ultimate failure stage is lower than the average crack width obtained from static flexural strength testing results for both the normal concrete and hybrid fibre concrete prisms.
- The effect of hybrid fibres is more pronounced in reducing the creep when the stress-strength ratio is eliminated.
- The influence of fibres in terms of minimising the loss of tension stiffening is particularly pronounced during the early stages.
- The presence of either steel or hybrid fibres significantly affects the rate of the reduction in terms of the loss of tension stiffening.
- It seems that the inclusion of hybrid fibre in this study is a novel contribution that has not been previously documented in the literature. These findings highlight the potential superiority of hybrid fibres compared to using a single type of fibre, providing valuable insights to the field.

Chapter 5
Experimental results – Part 2: Long beam (4.2 m Span)

The results of the experimental testing of the 4.2m long beams in this study are discussed in this chapter. The individual performances of different types of load and different reinforcement types are presented first and the effect of the hybrid fibre reinforced concrete beam on the flexural behaviour is then discussed.

5.1 Influence of short-term static load on the performance of the beams

5.1.1 Crack pattern and mode of failure

In all beams, the initial flexural cracks appeared at the bottom of the beams within the constant moment region, which then spread upwards with no specific pattern observed during the test. At each increment of loading, a visual examination was performed to track the progress of cracks on both sides of the beams. Predominantly vertical cracks were formed at the bottom of the beams when the stress in concrete exceeded the tensile strength of the concrete, which extended through the depth of the beam upwards as the load was increased. As a result, a visible crack pattern was obtained for each beam as the load was increased, and the crack width widened until the failure of the beam occurred. These cracks could be described as primary and secondary cracks. Primary cracks are the first cracks to develop in the tension zone of a beam under the flexural load on the beam. Secondary cracks, on the other hand, are cracks which developed after the primary cracks had formed and propagated. Secondary cracks usually have shorter lengths and closer spacing than primary cracks which are often longer. In this work, the secondary cracks occurred when the load was increased beyond the serviceability limit state (SLS) and onto ultimate limit state (ULS), and these cracks formed along the tension side of the beams. The typical flexural failure of each type of beam is shown in Figure 5.1. The failure mode of the normal concrete specimens with only steel reinforcement was as a result of yielding of the tensile steel followed by crushing of the concrete in the compression zone; a similar observation was reported by Kim et al. (2014). Crushing of concrete at the

top of the beam and flexural cracks reaching its upper part resulted in its eventual failure, which is similar to a typical failure pattern of under-reinforced beams.

With the incorporation of either steel fibres or hybrid fibres, the failure mode of the beams changed from a sudden crushing failure of concrete to more ductile failure. The fibres acted as additional reinforcement (Anandan and Alsubih, 2021), distributing the load and preventing the sudden crushing failure of the concrete (Jamsawang et al., 2015; Meda et al., 2012). A more gradual and controlled failure mode resulted from the fibres' assistance in spreading the stress throughout the concrete as the load increased (Jamsawang et al., 2015). This type of failure is desirable in reinforced concrete structures because it showed that the structure can withstand a large load before collapsing and gives a warning with more cracks before the complete failure (Jamsawang et al., 2015). The incorporation of fibres helped to mitigate the propagation of large cracks from tension zone to compression zone but instead formed smaller distributed tension cracks (Kim et al., 2013; Zeng et al., 2022; Jamsawang et al., 2015). Further, this changed the sudden compression failure of the beams to more ductile failure, after giving warning sign before the failure. That is, the presence of fibres in concrete enhanced the toughness and ductility of concrete beams, which resulted in a slower development and spread of cracks both in the tension and compression zones. As a result, the failure of the beams occurred more gradually, and hence it was possible to notice signs that indicate a problem before the complete failure occurred. Fibres also prevented the brittle concrete crushing due to their ability to increase the toughness of concrete in compression, as reported by Meda et al. (2012). The FRC beams had fewer large connected cracks when compared to the reference beams without fibres at the same load level. The extent of crack pattern observed in SFRC is generally less compared to NRC. However, HyFRC, which combined of steel fibres and polypropylene fibres, offered even better crack resistance and improved overall structural behaviour. Previous studies have demonstrated that both polypropylene fibre and steel fibre can enhance the performance of concrete at various stages throughout its lifespan. However, their crack resistance effects operate through different mechanisms, indicating that their abilities to prevent cracking cannot be substituted for one another (Guo et al., 2021). Beams containing steel fibres and hybrid fibres exhibited smaller cracks at the same load levels, when compared to the reference normal reinforced concrete (NRC) beams without fibre.

Consequently, HyFRC is generally considered to have superior performance in terms of crack resistance compared to both SFRC and NRC. The fibres play a dual role. Firstly, they control the crack widths and carry tensile loads at the crack locations. Secondly, they reinforce the strength of the concrete in areas that remain uncracked.

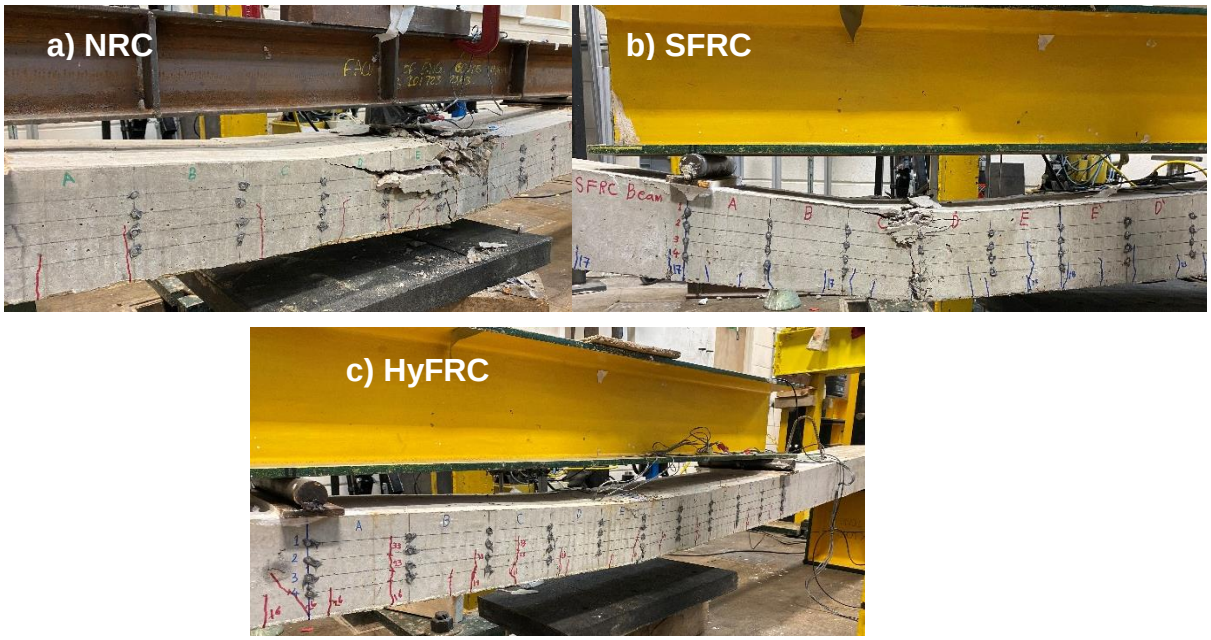

Figure 5.1: Crack pattern and mode of failure for normal and fibre-reinforced concrete beams

5.1.2 Load-deflection curve

Figure 5.2 shows the load-deflection curve of the three types of beams. Each curve is based on the average displacement of two identical beams tested for each type. Table 5.1 summarises the test results. The addition of steel fibre resulted in an increase in cracking load by 29% compared to the reference specimen, which is similar to that reported by Sryh (2017). However, the addition of hybrid fibre had an enhanced effect of increasing the cracking load by 43% compared to the reference specimen. The crack arresting mechanism's efficiency during the crack initiation stage is influenced by the stiffness of the fibres utilised in the FRC (Bhosale and Parkash, 2020). Also, the phenomenon is explained by the crack-bridging and load-carrying capabilities of the fibres, which are directly influenced by the quantity of fibres present at cracks and the strength of the bond between fibres and the concrete matrix (Li et al., 2018. After the formation of the first visible crack, all the beams showed a significant loss in their stiffness, as can be seen in Figure 5.2. The incorporation of steel fibres into the beams showed a

reduction in the deflection at failure of approximately 6.35%. Meda et al. (2012) reported that the fibres' ability to control deflection before the failure load decreased by up to 17% when compared to reference specimens. Whereas, the incorporation of hybrid fibres into the beams showed a higher reduction in the deflection at failure of approximately 14.29% compared to the reference specimens. With an increased post-cracking stiffness, there is a subsequent enhancement in tension stiffening, leading to a notable decrease in the overall deformation and crack control (Meda et al., 2012). The addition of polypropylene fibres in the hybrid fibre system resulted in a 7.94% decrease in the deflection at the failure load compared to the SFRC beams. Both the reduction in deflection and increase in cracking load emphasise that the utilisation of hybrid fibres resulted in superior performance compared to using steel fibres alone.

As reported in Table 5.1, there was an increase in the failure load with the addition of steel fibres and hybrid fibres by 18% and 28%, respectively, compared to the reference beams without fibres. Furthermore, as seen in Figure 5.2 and reported in Table 5.1, the addition of polypropylene fibres in the hybrid fibre system resulted in a 14% increase in load at the formation of the first visible crack and a 10% increase in the failure load compared to the SFRC beams. The incorporation of steel fibres to the beams resulted in an enhancement of both the initial cracking load and the failure load when compared to the reference beams. This is in agreement with other published work (Oh, 1992; Li et al., 2018; Yoo et al., 2014; Pajak and Ponikiewski, 2013). This increase is attributed to the fibres' bridging action at the fracture interfaces, which occurred at the interface between the crack surfaces in the concrete. On the other hand, the utilisation of hybrid fibres has not been extensively studied in the existing literature, it exhibited superior performance when compared to using a single type of steel fibre. This can be explained by that the micro-cracks tend to be attracted to the smaller fibres, while the larger fibres with strong anchorage play a crucial role in bearing the loads after reaching the peak load and delaying the emergence of macro-cracks due to the fibre bridging effect (Pajak and Ponikiewski, 2017). The test results revealed that the addition of single fibres reduced the deformation of the beams, but the addition of hybrid fibres further reduced deformation compared to using a single fibre type. Additionally, the inclusion of hybrid fibres resulted in increased strength, as evidenced by the data presented in Table 5.1 and Figure

5.2. This demonstrates the effectiveness of fibres in enhancing the flexural stiffness, which can be attributed to the ability of hybrid fibres to carry tensile load and increase the stiffness of the concrete. Sryh (2017) reported that the significant capability of steel fibres to improve the concrete's stiffness under flexural conditions is regarded as the primary reason for the increases in flexural strength, as reported in previous studies.

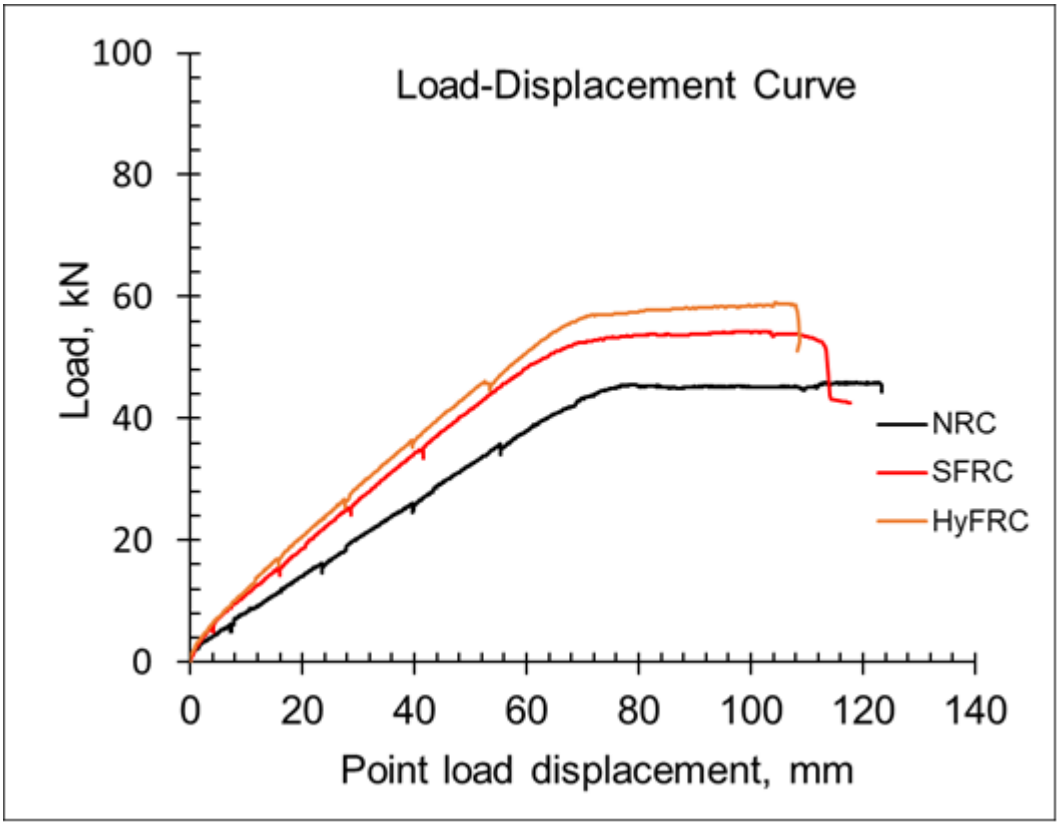

Figure 5.2: Load-deflection curve for beams

Table 5.1: Test results for normal and fibre reinforced concrete beams

Type of beam	Load at the formation of first visible crack		Deflection at the formation of first visible crack	Failure load		Crack width at Failure	Deflection just before reaching the failure load	
	In (kN)	Percentage* (%)	(mm)	In (kN)	Percentage** (%)	In (mm)	In (mm)	Percentage*** (%)
NRC-ST-0	8.5	-	9.08	45.91	-	4.5	126.47	-
SFRC-ST-1	12	29%	11.12	54.25	18.17%	3.85	118.63	6.35
HyFRC-ST-1.5	15	43%	14.32	58.92	28.34%	3.5	108.31	14.29

*Increase in load at first crack compared to NRC, **Increase in failure load compared to NRC and ***Decrease in deflection at failure load.

5.1.3 Load-strain responses

Figure 5.3 shows the surface strain of the concrete on the side of the beams in the tension region along the reinforcement and the strain response of the tension steel reinforcement bars at mid-span of the beams. The data presented in Figure 5.3(a) demonstrated that incorporating 1% steel fibres reduced the surface strain of the concrete in the tension zone by 36% at the failure load. Sryh (2017) reported that the addition of 0.5% and 1% steel fibres reduced the strains in the tension zone by approximately 13% and 25%, respectively. However, the incorporation of 1.5% hybrid fibres further reduced the surface strain of the concrete in the tension zone by 43% at the failure load, as shown in Figure 5.3(a). This indicates that the addition of hybrid fibre provides an additional 7% reduction in surface strain when compared to the addition of steel fibres alone, thereby highlighting the extra benefit offered by hybrid fibres. The addition of hybrid fibres to concrete can reduce the surface strain because they act as a bridge across cracks, enhancing the bond between the concrete matrix and the reinforcing steel bars, and enhancing the member's ductility. The data demonstrates that during the serviceability limit state, the addition of steel fibres enhances the flexural stiffness of reinforced concrete beams. Further, the addition of hybrid fibres exhibited even higher flexural stiffness compared to the addition of steel fibre only.

The incorporation of steel fibres into beams initially exhibited a similar strain pattern to normal reinforced concrete (NRC) beams, up until reaching a load of 32 kN. However, beyond this point, the addition of steel fibres led to a decrease in tensile reinforcement strains. The reduction of the strain in the reinforcing bars can be the result of the contribution of the steel fibres to carrying the tensile load and thereby increasing the concrete’s tension stiffening (Sryh, 2017). In contrast, the inclusion of hybrid fibres in the beams exhibited a higher reduction in tensile reinforcement strain when compared to both NRC and SFRC beams. Beam cast with hybrid steel-polypropylene fibres exhibited a more noticeable reduction in the tensile reinforcement strain when compared to NRC and SFRC at lower loads. This reduction was approximately 60% at a load of 20 kN. The addition of steel fibre resulted in an approximately 8.7% reduction in tensile reinforcement strains at a load of 40 kN compared to the NRC beam. Furthermore, the incorporation of hybrid fibres into beams led to roughly 33.33% reduction in tensile reinforcement strain at a load of 40 kN. Both types of beams

with fibres exhibited nearly identical tensile reinforcement strain at the failure load, as shown in Figure 5.3(b).

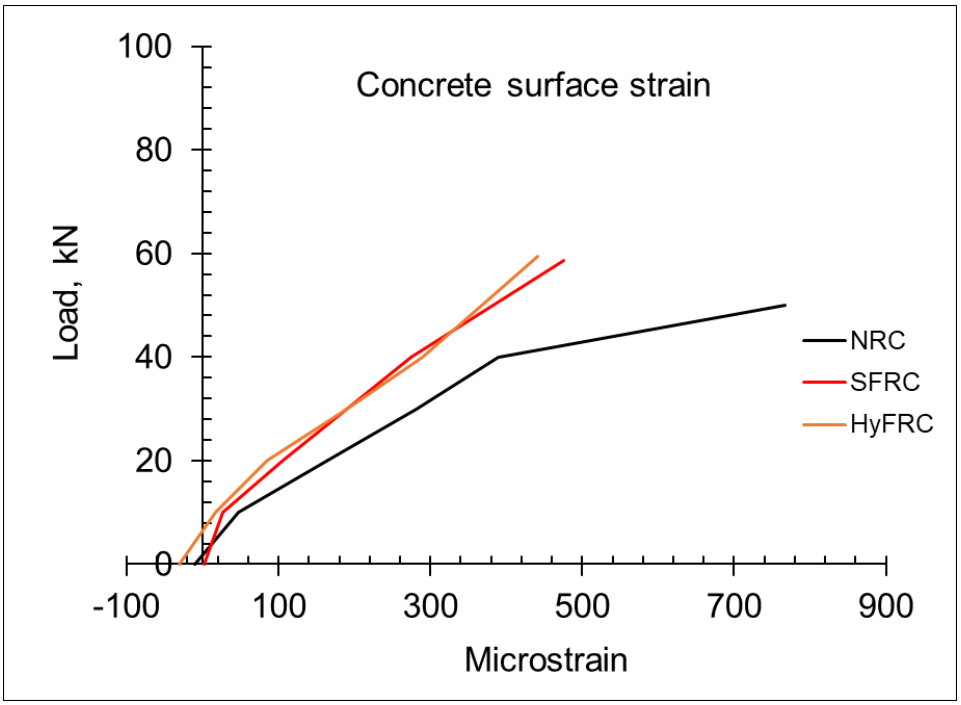

a) Concrete surface strain recorded until the failure load

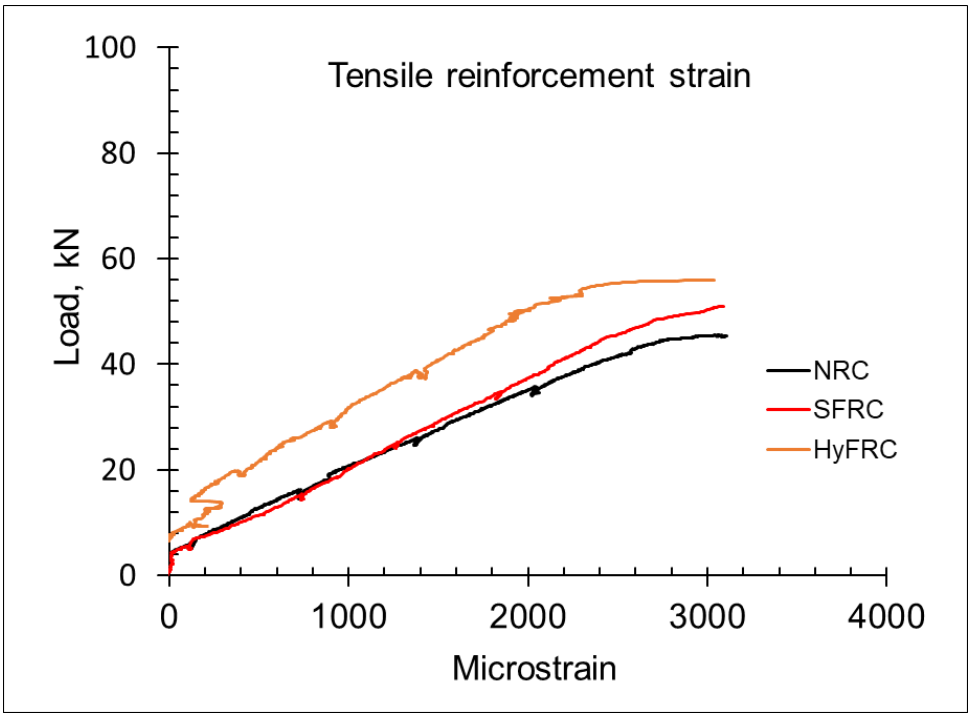

b) Tensile reinforcement strain

Figure 5.3: Load vs strain behaviour

5.1.4 Crack width and crack spacing

(a) Crack width

As reported in Table 5.1, a decrease in the crack width was observed in the SFRC and HyFRC beams; this decrease is mainly credited to fibres 'bridging' across the cracks (Oh, 1992; Fantilli et al., 2021; Chiaia et al., 2009). The addition of fibres might have helped to mitigate crack openings and reduce their widths significantly. As reported in Table 5.1, there was a decrease in the crack width with the addition of steel fibres alone and hybrid fibres (i.e. 0.1% micro polypropylene fibre and 0.4% macro polypropylene fibre to 1% steel fibre). These decreases were about 14% and 22% for SFRC and HyFRC, respectively. Moreover, the addition of polypropylene fibres in the hybrid fibre system resulted in an 8% lower crack width compared to 1% steel fibre alone. The ability of steel fibres to minimise beam crack widths might be due to their excellent characteristics in terms of high modulus, yielding capacity, and the presence of hooked-ends, which could improve the bond between the fibre and the surrounding concrete, as reported by Abbadi (2018) and Bhosale and Prakash (2020). As a result of the steel fibre's ability to reduce tensile stresses across cracks, which indicated that the stress from the cracked region can be distributed by fibres to the surrounding intact concrete, so preventing further cracking in concrete by bridging the crack faces and providing additional reinforcement to the surrounding concrete, crack widths are reduced, which in turn arrest further propagation of cracks, as reported by Tan et al. (1995), Pajak and Ponikiewski (2013) and Deluce and Vecchio (2013). In addition to the benefits of steel fibres, the additional contribution of 0.5% polypropylene fibres in reducing crack width can be attributed to their abundance and strong flexibility (Guo et al., 2021). Polypropylene fibres primarily prevent the formation of micro cracks, as reported by Guo et al. (2021).This highlights the role of polypropylene fibres in further reducing crack widths and enhancing the overall performance of the hybrid fibre-reinforced concrete system. Pakravan et al. (2017) stated that the inclusion of fibres in the concrete decreased the stresses and enhanced the overall toughness and durability of the material.

(b) Crack spacing

The reduction in the crack spacing, which reflects one of the significant benefits of adding fibres, can be observed in Table 5.2. The addition of steel fibres led to a reduction in crack spacing of approximately 24.77% compared to NRC beams, which agrees with findings reported by Tiberti et al. (2014) and Vandwalle (2000). On the other hand, the addition of hybrid fibres into beams resulted in a reduction

in crack spacing of approximately 22.58% when compared to NRC beam. That is, the addition of hybrid fibres did not have a noticeable effect on crack spacing when compared to SFRC beams.

Table 5.2: Comparison of predicted crack spacing values with experimental results

Type of beams	Experimental results	Experimental/Predicted		
	Exp (mm)	EC2	fib MC2010	RILEM TC 162-TDF
NRC-ST-0	114.32	1.41	1.31	1.41
SFRC-ST-1	86.00	1.06	0.99	1.17
HyFRC-ST-1.5	88.52	1.09	1.02	1.32

The crack spacing is reduced, leading to a smaller distance between cracks. This, in turn, can result in larger crack widths. This observation highlights the importance of crack spacing in understanding crack propagation behaviour. Smaller crack spacing can accelerate crack growth due to the larger plastic zone sizes near the crack tips according to Gao et al. (2019). This observation is evident in the test results, where SFRC exhibited a lower crack spacing value but higher crack width. On the other hand, HyFRC showed a higher crack spacing but lower crack width when compared to SFRC.

In this research, the three different values of crack spacing as per EC2 (1992) design code, *fib* Model Code (2010) and a RILEM recommendation (2003) were determined. These values are compared with the experimental results in Table 5.2. The mean, standard deviation, and coefficient of variation of the cracking properties for each beam type were determined and summarised in Table 5.2. The crack spacing was measured when the stress in the tensile steel reinforcement was about 200 MPa, which is associated with the formation of the stabilised crack pattern in NRC and FRC beams.

The data in this table indicates that the current crack spacing formulae underestimated the value of crack spacing for NRC beams compared to their experimental data. The use of the EC2 design code and RILEM recommendation for predicting the crack spacing of NRC beams resulted in a deviation of 41% compared to the experimental results. On the other hand, the fib MC2010 exhibited a deviation of 31% when compared to the experimental results.

On the other hand, for SFRC beams, the EC2 prediction method resulted in a deviation of 6%, which closely aligned with the experimental results. Similarly, the fib MC2010 prediction method showed a ratio of experimental to prediction (Exp/Pred) of 0.99, which was in better agreement with the experimental data. However, the RILEM recommendation underestimated the actual crack spacing, exhibiting a deviation of about 17%.

Furthermore, when applying the same prediction formulae to HyFRC beams, the fib MC2010 method showed a ratio of (Exp/Pred) equal to 1.02, indicating a close match with the experimental result. The EC2 showed a relatively small difference with a deviation of 9% compared to the experimental results in terms of crack spacing. In contrast, the RILEM recommendation significantly underestimated the crack spacing, showing a deviation of about 32% compared to the results obtained from the experiments. This provides a clear and concise summary of the performance of each prediction method for HyFRC beams.

In summary, the prediction methods exhibited varying degrees of accuracy in estimating crack spacing for different types of beams. The EC2 method showed good predictions for both SFRC and HyFRC beams. EC 2 showed better predictions of the crack spacing for SFRC and HyFRC beams, which was a surprise as the code equations do not consider the effect of using fibres in beams in the equations. However, the fib MC2010 method displayed relatively better results for SFRC and HyFRC beams. The fib MC2010 predicted the crack spacing of SFRC and HyFRC beams closer to that obtained from the experiment, which is considered to be due to the fact that the fib MC2010 takes into account the contribution of the fibres. However, the RILEM recommendation consistently underestimated the crack spacing values across all beam types. However, it should be mentioned that there is no stirrups in the mid-span of the beam, which could potentially reduce the crack spacing.

However, the findings of the present study suggest that the current design formulae in EC 2 fail to take the effect of the fibres into account in their equations to predict the crack spacing, whereas the fib Model Code 2010 formula and RILEM recommendation incorporate factors associated with fibres. The prediction method of RILEM tends to underestimate the crack spacing, even though the effect of length and diameter of fibres were included in the calculation. However, this prediction method does not fully account for the effect of the volume fraction of fibres, which is considered to be the main parameter

influencing the crack spacing. The prediction methods in RILEM recommendation typically relied on simplified assumptions and average material properties. The interaction between fibres and surrounding matrix is frequently simplified in prediction methods, which may not fully represent the complicated behaviour, leading to underestimating crack spacing.

5.2 Influence of repeated test on the performance of full-scale beams

5.2.1 S-N curves

As previously detailed in Section 4.5 (repeated test for 0.5m beams), a similar procedure was followed for testing the full-scale beams (4.2m span) subjected to repeated load. Higher fatigue load can simulate real-world situations and test the resilience and dependability of materials or structures under more severe conditions in engineering or materials science. Engineers can assess a material or structure's fatigue resistance and establish its fatigue strength by subjecting it to increasing degrees of cyclic stress. This information is crucial for building products that are secure and long-lasting. Higher fatigue load may also be utilised in research and development to examine how materials behave in difficult situations and to find potential failure processes. It is important to note, however, that higher fatigue load stress must be used under close control and monitored to guarantee the integrity and safety of the materials and structures being tested. The applied frequency for the full-scale beams was chosen to be 2 Hz, but as the hydraulic system used in the lab was not suitable for conducting higher frequency for full-scale beams, so the applied frequency was 1 Hz.

The results in Table 5.3 present the fatigue test data for NRC and HyFRC beams at different stress levels. It is apparent from Table 5.3 that the data obtained from fatigue tests are widely scattered. A similar observation was found with the small beams (0.5m), which was discussed in detail in the previous chapter. The relationship between maximum and minimum flexural stress to fatigue life for NRC and HyFRC beams is illustrated in Figure 5.4 in the form of logN vs number of cycles, which is called S-N curves. As the applied stress level decreased, the number of cycles that caused fatigue failure of the specimens notably kept on increasing, as shown in Table 5.3 and Figure 5.4. The highest limit of the fatigue load had an impact on the fatigue life. As a result, the beams

in this investigation had a shorter fatigue life when the stress level was high. This observation is confirmed by other researchers, e.g. Qu et al. (2019) and Gao et al. (2021) for normal reinforced concrete and steel fibre-reinforced concrete beams. However, the effect of hybrid fibre reinforcement on a material's fatigue life is a complicated topic that depends on a number of variables, such as the type, orientation, and fibre volume fraction, the characteristics of the matrix material and the loading conditions. The fatigue life of a material may be decreased by the addition of fibre reinforcement. This may happen when stress concentrations at the fibre-matrix interface cause crack initiation and propagation. This phenomenon can be more noticeable at higher levels of stress or in materials with higher stiffness or brittleness. Moreover, the mechanical characteristics of the fibres themselves may contribute to the shortening of the fatigue life. However, HyFRC beams resisted thousands of cycles even after the beams were subjected to high fluctuation in the loading regime (about 90% of the ultimate load) during the repeated test when the loading machine lost its control for all beams when subjected to the load levels of 20-80% and 30-70%. The S-N curve showed that the number of cycles required to cause the specimens to fail increased when the maximum applied load level decreased. These increases were also reported in Table 5.3. NRC beams exhibited an increase of approximately 76.31%, whereas HyFRC showed a noticeable increase of about 144% when the maximum load level reduced from 80% to 70%.

Table 5.3: Repeated test results for full-scale beams

Type of beam		**NRC**		**HyFRC**		
Stress level		**20-80**	**30-70**	**20-80**	**30-70**	**30-70**
Crack width (mm)	Long-term	0.24	0.51	0.30	0.10	0.12
	After failure	3.46	10.00	2.50	4.73	8.00
Numbers of cracks	Long-term	17	16	16	15	15
	After failure	20	20	19	18	18
Total crack length (mm)	Long-term	70	72.50	65.00	68.33	61.67
	After failure	102.73	101.47	90.00	93.83	97.67
Crack spacing (mm)	Long-term	83.00	89.00	96.01	95.63	96.63
	After failure	65.83	71.43	76.25	75.00	77.00
First crack (kN)	-	12.00	13.00	15.00	16.00	16.00
Deflection (mm)	-	57.19	89.63	69.16	73.20	90.66
Number of cycles	-	725550	1279200	178080	513600	357600

Overall, the fatigue life of FRC beams can vary significantly depending on the type of fibre, geometry and fibre volume fraction (Banjara and

Ramanjaneyulu, 2018). It is important to consider these factors when designing and constructing FRC beams in order to achieve the desired level of performance and durability. As reported in Table 5.3, there was no increase in the number of cycles at failure with the addition of hybrid fibres compared to the reference beams without fibres, which might be related to the greater increase in the applied load during the repeated test, as mentioned earlier. Higher deflection, higher initial crack length and considerable bridging deterioration caused by higher initial crack width could be the factors which contributed to this low fatigue life when loads were applied.

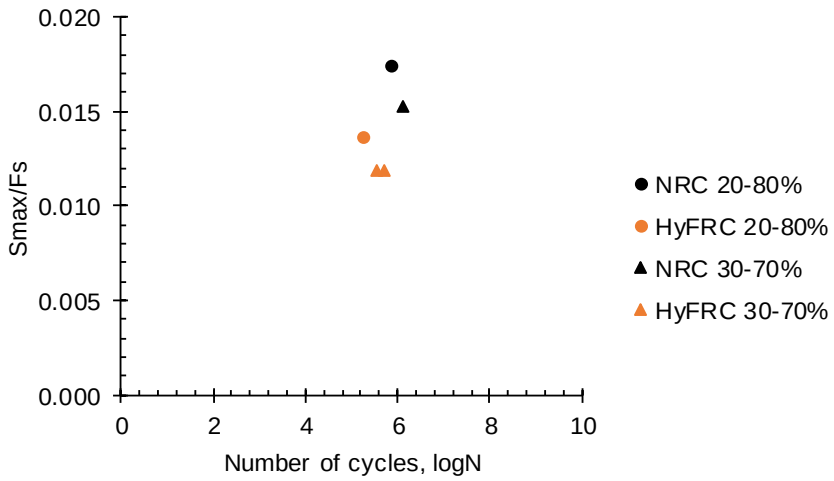

a) The relationship between (S_{max}/F_s) and the logarithm of the number of cycles to failury

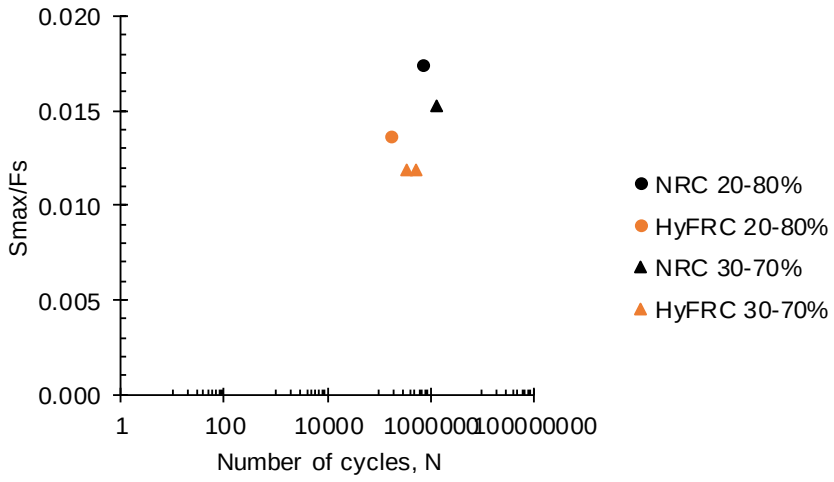

b) The relationship between (S_{max}/F_s)and the number of cycles to failure

Figure 5.4: S-N for all beams

5.2.2 Crack pattern and mode of failure under repeated loads

The crack patterns observed in all beams were relatively similar under different load types. The distribution and crack patterns of all beams before and after fatigue failure are shown in Figure 5.5(b), Figure 5.6(b), Figure 5.7(b) and Figure 5.8(b). Several primary cracks at pure bending sections nearly appeared during the static loading process until the stabilised crack pattern reached. Several primary and secondary cracks were observed during the first loading cycles of fatigue load, as summarised in Table 5.3 and will be discussed in the next paragraph. However, even after reaching the stabilised crack pattern, repeated loading caused existing cracks to widen and new cracks initiated as the number of cycles increased, as can be seen in Table 5.3. Gao et al. (2021) also reported that all of the cracks for each beam formed in the first few cycles due to the higher fatigue load limit. As the number of loading cycles increased, the cracks in the long beams grew and merged, resulting in the formation of multiple cracks. This was attributed to the increased span and the larger area over which the load was distributed, leading to a more distributed crack pattern. Before failure, secondary cracks developed and propagated.

The failure behaviour of the long beams differed from that of the short beams in terms of the failure mode and the extent of cracking. The long beams, due to their larger span, experienced more pronounced cracking and exhibited a different failure mode compared to the short beams. Conversely, the short beams had a smaller span, which led to a more localised distribution of cracks. While there were notable differences in their failure mechanisms.

The typical flexural failure of each type of full-scale beam is shown in Figure 5.5(a), Figure 5.6(a), Figure 5.7(a) and Figure 5.8(a). The failure mode observed in the full-scale beams was primarily a crushing failure of concrete for beams subjected to a repeated load of 20-80% of the ultimate load, as shown in Figure 5.5(a). This involved crushing of concrete at the top of the specimen and flexural cracks reaching its upper part, ultimately leading to failure. On the other hand, the NRC beams subjected to a repeated load of 30-70% of the ultimate load exhibited a cover spalling of concrete due to the excessive number of repeated loads, as can be seen in Figure 5.6(a). Also, this concrete cover spalling could be attributed to the higher level of loading.

In summary, the main difference between the full-scale beams and short beams' failure behaviour lies in the extent and distribution of cracking. The long beams experienced more widespread cracking due to their larger span, while the short beams showed localized cracking patterns. These differences can be attributed to the varying load distributions and span lengths, resulting in different failure modes for the two sets of beams.

a) Mode of failure

b) Crack pattern

Figure 5.5: NRC; load level of 20-80%

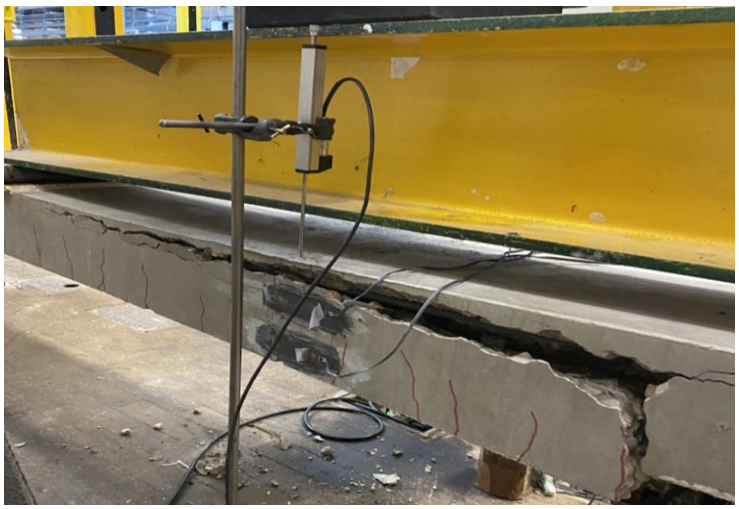

a) Mode of failure

b) Crack pattern

Figure 5.6: NRC; load level of 30-70%

With the incorporation of hybrid fibres, the failure mode of the beams changed from the sudden crushing failure to more ductile failure of the concrete, as shown in Figure 5.7(a) and Figure 5.8(a). Single type of fibres can prevent the sudden concrete crushing due to their ability to increase concrete toughness in compression or tension, as reported by Meda et al. (2012). Hybrid fibre-reinforced beams exhibited enhanced ductility and improved behaviour at failure, providing warning signs through slower crack development and spread compared to NRC beams. This was attributed to the synergetic effect between steel and polypropylene fibres, improving concrete's mechanical properties through crack restraint and bridging. The distribution and orientation of the fibres also played a crucial role in influencing the mode of failure. While Qu et al. (2019) observed that the addition of steel fibres alone increased the toughness of failure and

altered the mode of failure to some extent, the results of the current study revealed an additional significant contribution with the incorporation of hybrid fibres.

a) Mode of failure

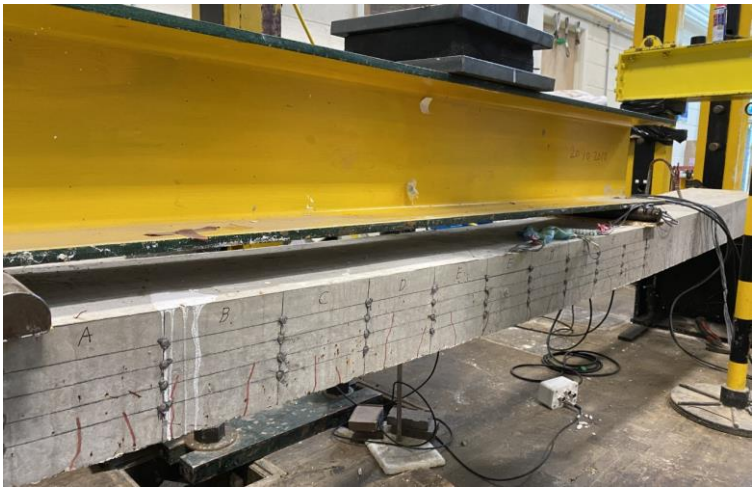

b) Crack pattern

Figure 5.7: HyFRC; load level of 20-80%

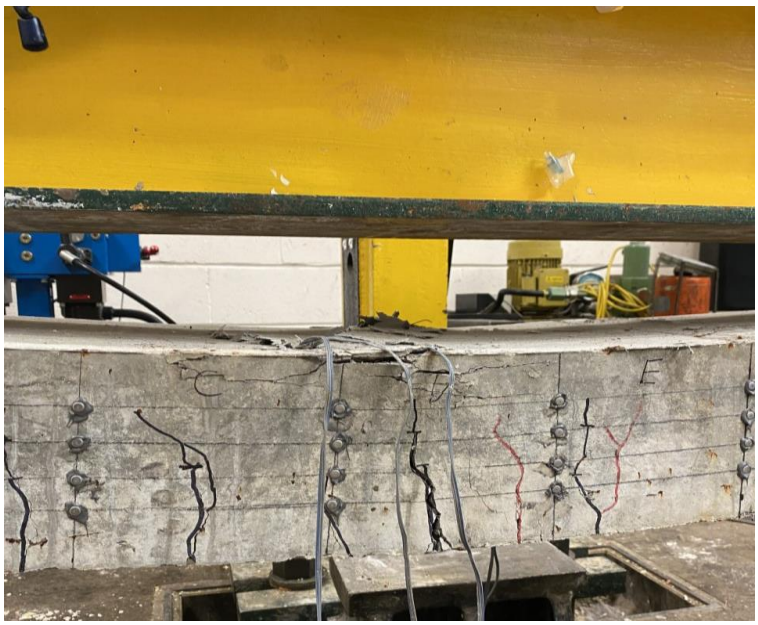

a) Mode of failure

b) Crack pattern

Figure 5.8: HyFRC; load level of 30-70%:

The HyFRC beams had fewer cracks when compared to the reference beams without fibres at the same number of cycles, as reported in Table 5.3. The incorporation of Hybrid fibres to beams resulted in a reduction of approximately 5.88% and 6.67% in the number of cracks at load levels of 20-80% and 30-70%, respectively. These reductions can be attributed to the role of fibres, which helped to resist the formation and initiation due to the higher increase in tensile strength. However, the number of cracks increased before the failure of the beams occurred with the addition of the hybrid fibres.

With a decrease in load level/stress range compared to static loading, the observed number of cracks decreased by about 5.88% and 6.25% for NRC and HyFRC, respectively, when the maximum load levels were reduced from 80% to 70%. As the number of cycles increased until beam failure, both NRC and HyFRC beams showed an increase in the number of cracks. For load levels of 20-80% and 30-70%, the increase at failure was approximately 17.65% and 25% for NRC beams and about 18.75% and 20% for HyFRC beams, respectively.

Incorporating hybrid steel-polypropylene fibres in concrete can lead to a significant reduction in the crack's propagation and result in better performance compared to normal reinforced concrete beams without fibres, possibly due to the fibre bridging effect. Bhosale et al. (2020) reported that the increase in the volume fraction of fibres primarily results in a higher number of fibres participating in crack bridging. This increase in fibre crack bridging contributes to maintaining the shape of the stress-crack width relationship in FRC. Consequently, it leads to an enhancement in the material's fracture energy, particularly through improved second peak resistance. This enhanced performance means that reinforced concrete made with hybrid steel-polypropylene fibres can better withstand the impacts of repetitive loads, such as those encountered in seismic events or high traffic regions.

5.2.3 Load deflection behaviour under repeated loads

Figure 5.9(a) Figure 5.10(a) show the number of cycles vs deflection curve of the NRC and HyFRC beams when subjected to load levels of 20-80% and 30-70%, respectively. The number of cycles in Figure 5.9(b) and Figure 5.10(b) is represented by a log scale plot, which enables easier analysis and comparison of different concrete types. Table 5.3 reports the test results. The number of cycles-deflection curve of the specimens is found to have three distinct stages, especially for the load level of 30-70%. In the first stage, all of the beams responded linearly up until the formation of the first visible crack, with increasing loading displacement, as shown in Figure 5.9(b) and Figure 5.10(b). The mid-span deflection of all beams as shown in Figure 5.9(b) and Figure 5.10(b) gradually increased with the increase in the number of cycles during the early stages due to stiffness degradation (Parvez and Foster, 2015). When subjected to the load level of 20-80%, NRC beams showed a linear increase in the mid-span deflection followed by a rapid increase and then a linear increase, as shown

in Figure 5.9(b). Finally, the mid-span deflection showed a fluctuated value before the failure of the beam occurred, as shown in Figure 5.9(b). In comparison, the mid-span deflection of NRC beams, when subjected to a 30-70% load level, showed three different stages, as shown in Figure 5.10(b). As shown in Figure 5.10(b), NRC beams responded linearly in the early loading stage. Figure 5.10(b) shows how the mid-span deflection increased steadily and gradually during the second stage. Then the mid-span deflection exhibited fluctuated values before it exhibited a rapid rate of growth until the failure of the beam occurred, as shown in Figure 5.10(b). Meanwhile, increasing the load level of NRC beam had no impact on mid-span deflection, as shown in Figure 5.9(a) and Figure 5.10(a). In contrast, Gao et al. (2021) indicated that increasing the load levels led to an increase in mid-span deflection. As can be shown in and Figure 5.10(a) and Figure 5.10(b), after the gradual increase in mid-span deflection, it showed a rapid rate of growth. As a result, the deflection rapidly increased in the last stage before the complete failure of the beams occurred.

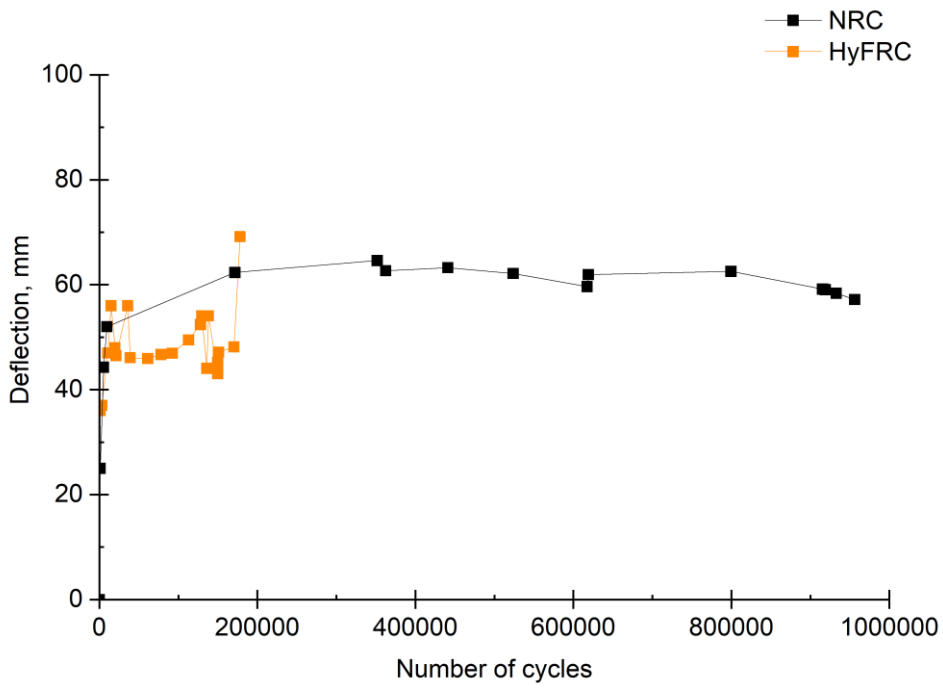

a) Number of cycles versus deflection of beams

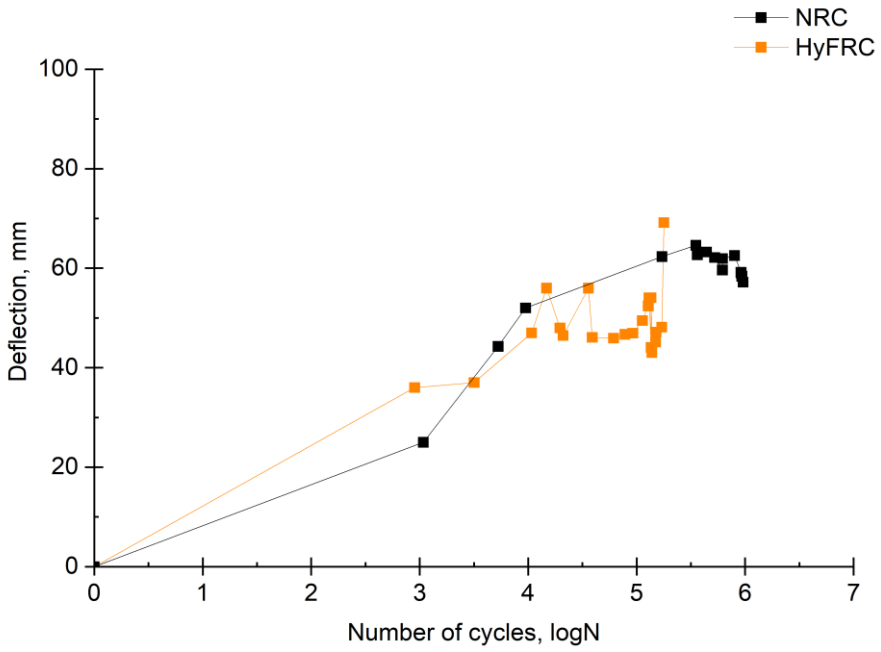

b) LogN with mid-span deflection

Figure 5.9: Load level of 20-80% where the measurements were taken at 50% of load

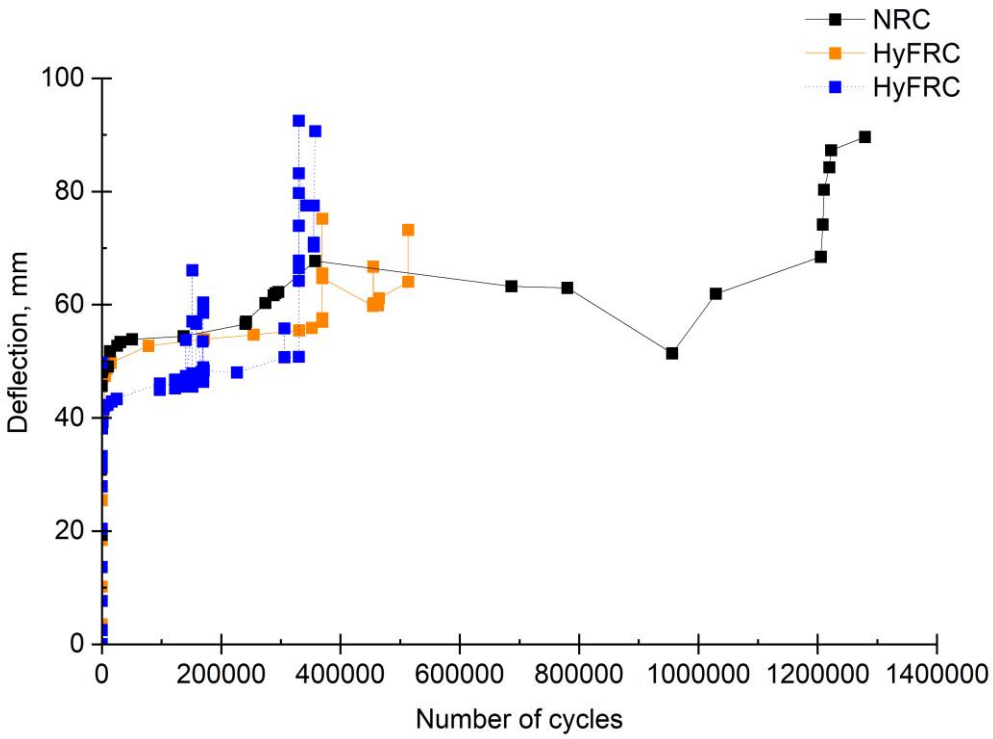

a) Number of cycles versus deflection of beams (Two beams were conducted for HyFRC beams with the same load level)

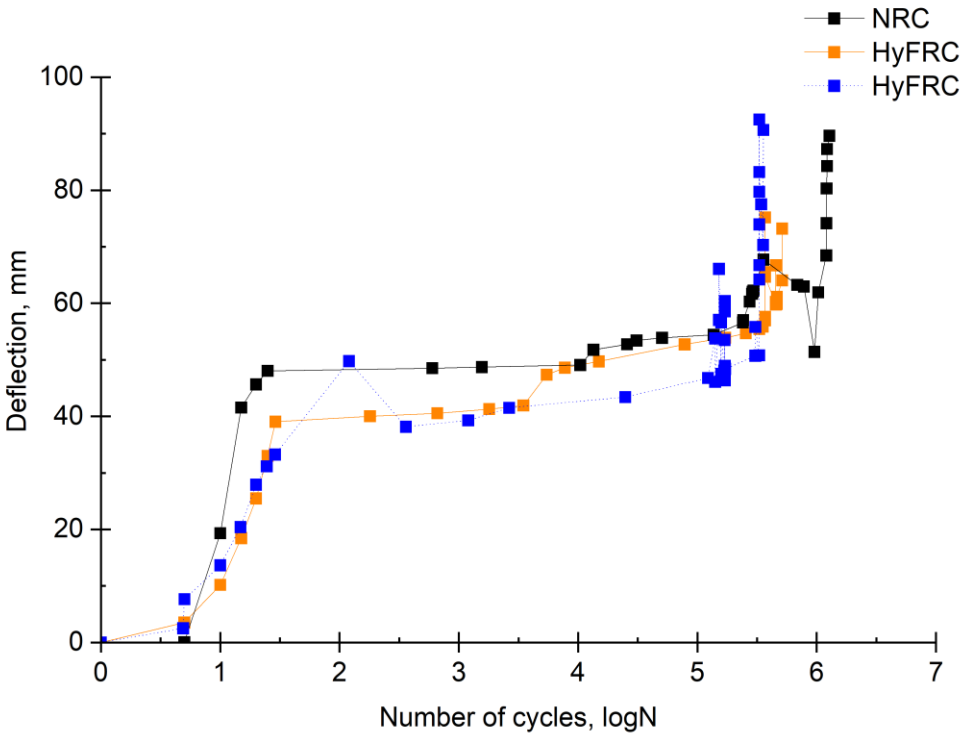

b) LogN with mid-span deflection

Figure 5.10: Load level of 30-70%; where the measurements were taken at 50% of load

The incorporation of hybrid fibres into beams of load level 30-70% produced a reduction in the deflection at the failure of approximately 8.59%, as reported in Table 5.3 based on the average of the two specimens. The mid-span deflection of all beams showed a linear response in the early stages, as can be seen in Figure 5.9(b) and Figure 5.10(b). The mid-span deflection of HyFRC beams, when subjected to a load level of 30-70%, showed a reduction for the average of two specimens in comparison to the reference beams without fibres. It is observed that in the second stage, the mid-span deflection increased gradually and steadily. It was evident that in the final phase before the failure of the beams, the mid-span deflection of all beams increased rapidly, as can be seen in Figure 5.10. HyFRC beams showed lower deflection even if they were subjected to higher load because the machine lost its control, which demonstrated the benefit of adding hybrid fibres to beams, as can be seen in Figure 5.10(a) and Figure 5.10(b) for the load level of 30-70%.

As can be seen in Figure 5.9(b) when the load level was 20-80%, the addition of hybrid fibres exhibited a higher deflection in the early stage of loading when the beams responded linearly. The incorporation of fibres proved to be

highly effective in reducing the mid-span deflection, even under higher loads, which can be attributed to the enhanced stiffness resulting from the addition of fibre (Parvez and Foster, 2014). During the second stage, the mid-span deflection exhibited fluctuating values, as shown in Figure 5.9(a). However, the incorporation of hybrid fibres into beams of load level 20-80% had an increase on the deflection when compared to the reference beams without fibres at ultimate by approximately 20%, as shown in Figure 5.9(a) and Figure 5.9(b).

The cracking load of the concrete can be greatly increased when three types of fibres are combined to form as a hybrid mix, which results in a more effective reinforcement system. As reported in Table 5.3, the addition of the hybrid fibre system resulted in a 15 kN and 16 kN load increase at the formation of the first visible crack when the applied load level was 20-80% and 30-70%, respectively, representing a 25% and 23.08% increase compared to the reference specimens. The incorporation of hybrid fibres to the beams produced an increase in the initial cracking load. In general, hybrid fibre-reinforced concrete beams outperformed beams made without any fibres. This is because the combination of steel and polypropylene fibres can provide both tensile and flexural strength to the beam (Li et al., 2018; Guo et al., 2021; Yap et al., 2014; Wu et al., 2022; Zhu et al., 2022), which can help to reduce the number of cracks and the overall deformation of the beam (Meda et al., 2012) .

5.2.4 Crack width and length under repeated loads

(a) Crack width

Figure 5.11 and Figure 5.12 show the development of the crack width of the NRC and HyFRC beams versus the number of cycles under the load levels of 20-80% and 30-70%.The primary crack width gradually increased as the number of cycles increased, indicating fatigue damage caused by repeated loading. The crack width development and propagation showed three distinct stages: crack initiation, development phase, and failure stage, as shown in Figure 5.11 and Figure 5.12 for the load levels of 20-80% and 30-70%, respectively. Cracks initiated in high-stress areas with significant bending moments and propagated with increasing cycles (Meng et al., 2018). The fatigue crack propagation process exhibited two main phases, with crack width increasing linearly in the first stage and gradually and steadily in the second stage, as can be observed in Figure 5.11 and Figure

5.12. In the final stage, the crack width experienced rapid growth due to spalling or breaking of concrete at the crack tips, leading to complete failure of the beams. Notably, the major crack width significantly widened during the last stage, ultimately causing failure (see Figure 5.11 and Figure 5.12).

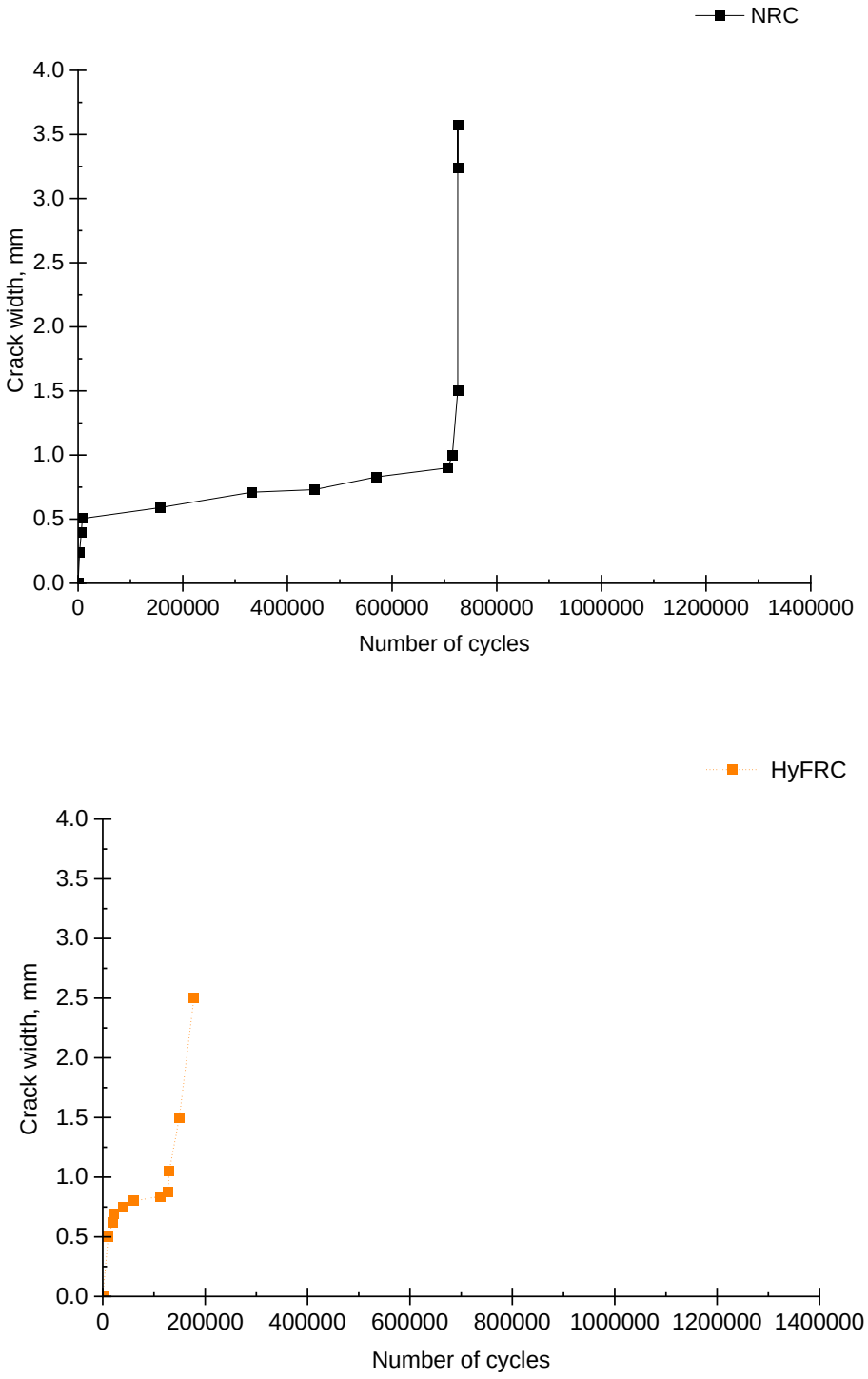

Figure 5.11: Load level of 20-80% where the measurements were taken at the median load; Number of cycles versus crack width of beams

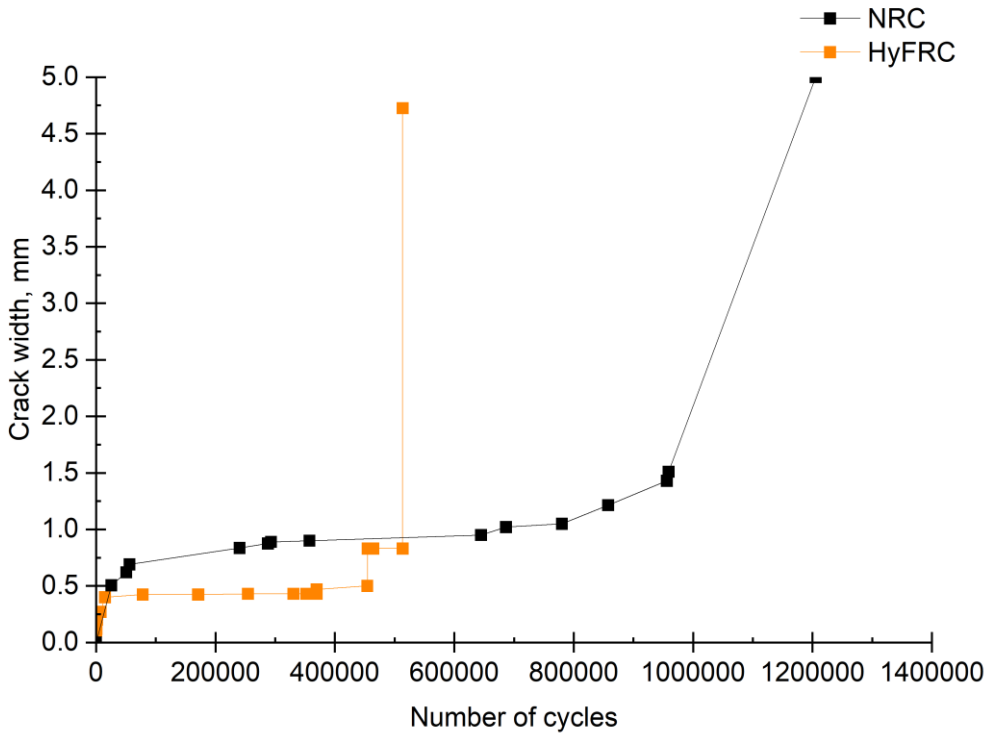

Figure 5.12: Load level of 30-70% where the measurements were taken at the median load; Number of cycles versus crack width of beams

Additionally, Table 5.3 demonstrates that the crack width for HyFRC was 0.3mm and 0.11mm for load levels of 20-80% and 30-70%, respectively. Conversely, the reference beams showed the opposite crack width value to HyFRC for different load levels of 0.24mm and 0.51mm for load levels of 20-80% and 30-70%, respectively. This increase might be attributed to the initiation of cracks in the weak regions within the concrete, which is referred to as flaw initiation (Germano et al., 2015; Lee and Barr, 2002), and it can be observed that the crack undergoes rapid growth during its early stages (Meng et al., 2018). On the other hand, the average crack widths at failure increased when the maximum load level decreased; this increase in the crack width might be attributed to a reduction in the bond between the fibre and the surrounding concrete due to the bundled fibres (Gao et al., 2021). Reference concrete specimens recorded the highest crack width after failure for different maximum load levels as the specimens had a wider crack at failure. HyFRC beams showed smaller crack widths when compared to the reference beams without fibres. This reduction in crack width was observed in HyFRC beams and is mainly attributed to the fibres 'bridging' across the cracks, as the presence of fibrous reinforcement effectively slowed down and hindered the progression of the flaws (Germano et al., 2015).

As reported in Table 5.3, there was a reduction in the crack width with different maximum load levels for HyFRC; these decreases were approximately 27.75% and 36.35% for 20-80% and 30-70%, respectively when the crack width values decreased from 3.46 mm to 2.50 mm and from 10.00 mm to 6.365 mm. This reduction demonstrates the hybrid fibre system's positive influence in reducing the crack's width. In the current investigation, the aim was to assess the influence of hybrid fibre reinforcement on the flexural performance of concrete beams under different types of loadings. It is important to note that HyFRC beams exhibited good crack width controlling abilities across all evaluated loading levels and stress ranges.

(b) Crack length

Table 5.3 shows the development of the crack length of the NRC and HyFRC beams after the stabilised crack pattern was reached and at failure. NRC beams exhibited longer primary cracks in both cases. The crack growth rate was influenced by stress, load cycles, concrete characteristics (strength, stiffness, toughness) and was faster with higher stress and more load cycles. The inclusion of steel and polypropylene fibres in HyFRC acted as bridges, reducing stress concentration at crack tips and resulting in shorter crack lengths. Consequently, HyFRC demonstrated better crack resistance and overall structural behaviour, with approximately 8.77% and 8.09% reduction in crack length after reaching the stabilised crack pattern and at failure, respectively. On the other hand, beams cast with hybrid fibres did not exhibit any noticeable increase in crack length. The reduction in crack length of HyFRC beams can be attributed to the role of fibres, which can bridge micro cracks and slow down their propagation, thereby enhancing performance under repeated loads (Meng et al., 2018).

5.3 Influence of sustained test on the performance of full-scale beams

This section presents the findings on the long-term crack patterns, deflections, strain, crack width and crack length of NRC and HyFRC beams. The study also examined the impact of using hybrid fibres on the long-term deflection of the beams. The findings of the experiments are presented and discussed in this section, and are summarised in Table 5.4.

Table 5.4: Sustained test results for full-scale beams

Type of the beam		NRC	HyFRC	Percentage*
Crack width (mm)	Long-term	0.2	0.1	-50%
Number of cracks	Long-term	18	15	-16.67%
Total crack length (mm)	Instantaneous	55.9	32.9	-41.14%
	Long-term	93.05	67.90	-27.03%
Developed crack length (mm)	Long-term	37.15	35.00	-5.79%
Crack spacing	Long-term	84.22	107.14	27.21%
Deflection (mm)	-	36.33	33.99	-6.45%
First crack (kN)	-	15	16	6.67%
Failure load after unloaded (kN)	-	55.98	56.73	1.34%
Recovery deflection** (mm)	-	17.82	18.83	-5.66%

* Percentage of the difference between the NRC and HyFRC to demonstrate the effect of the addition of hybrid fibres into beams compared to reference beam without fibre. **Recovery deflection refers to the residual deflection or deformation that remains in a material or structure after it has been subjected to a load and then unloaded.

5.3.1 Long-term crack pattern of full-scale beams

Figure 5.13 displays the crack pattern and distribution along the beam in the constant moment region at the stabilised crack pattern, where no more cracks formed. Cracks initiated and propagated in the constant moment region until 50% of ultimate load (around 200 MPa of steel stress) at which stage they got stabilised and no further new cracks were formed. However, new flexural cracks initiated and propagated vertically outside the constant moment region. The creep deformation of the concrete and shrinkage over time can contribute to the formation of these new cracks by affecting stress distribution. This finding is consistent with some of the studies in the empirical literature for NRC beams, which stated that when the sustained load reaches a certain level, no new cracks

form, but the existing crack widen and flexural cracks form along the beam (Choi and Yun, 2013).

a) NRC

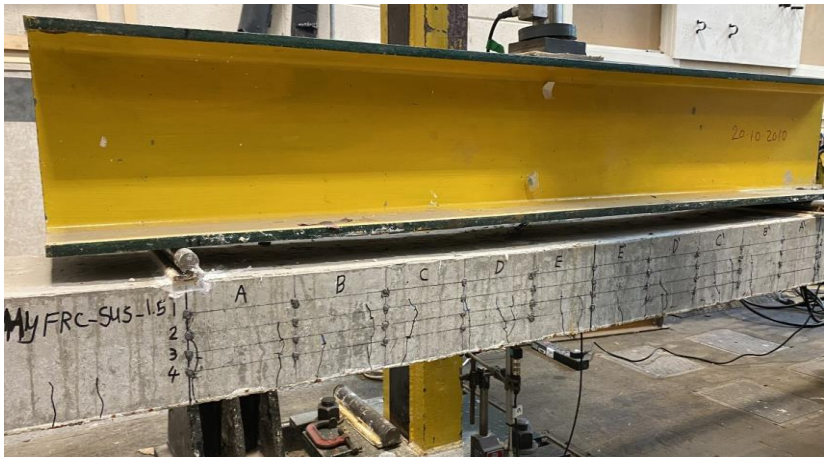

b) HyFRC

Figure 5.13: Crack pattern

NRC and HyFRC exhibited different performances at long-term loading. HyFRC beams displayed fewer compared to NRC beams, indicating that the incorporation of hybrid fibres significantly reduced crack propagation, as summarised in Table 5.4. Similar results were reported by Sryh (2017) with steel fibre only, which can be explained by the fact that steel fibres act as crack inhibitors, controlling the spread of cracks. The presence of fibres in HyFRC beams acted as crack arrestors and bridged across the crack surface, leading to approximately 16.67% fewer cracks at the stabilised crack pattern compared to NRC beams. The inclusion of fibres also contributed to more uniform stress distribution and increased total tensile strength of the concrete in HyFRC, potentially delaying or preventing crack progression (Parvez and Foster, 2014).

In summary, HyFRC outperformed NRC in terms of crack control and long-term performance. Additionally, fibres contribute to load transfer from the matrix to the fibres, increasing the total tensile strength of the concrete (Smarzewski, 2018) and potentially leading to increased stresses within the uncracked concrete.

5.3.2 Long-term deflection of full-scale beams

Figure 5.14 illustrates the load-deflection curve of the NRC and HyFRC beams under long-term deflection. As reported in Table 5.4, there is a significant difference between the NRC and HyFRC beams in term of recovery deflection. However, the load at the first visible crack and mid-span deflection showed only a slight effect with the addition of hybrid fibres. The mid-span deflection of the beams gradually increased with the increase in load until it reached 50% of the ultimate load, with a stress of 200MPa in the steel bars. The load-deflection curve for beams under long-term deflection shows a similar trend over time. Figure 5.15 shows the long-term deflection-time curves derived as the difference between total deflection and instantaneous deflection. The growth in mid-span deflection over time for beams was found to have two distinct stages. Initially, beams exhibited a rapid increase and responded linearly after reaching the stabilised pattern in the early stage between 0 and 20 days, as reported by Sryh (2017), Daud et al. (2018) and Higgins et al. (2013). It is worth mentioning that the aforementioned studies were conducted on normal concrete beams as well as steel fibre-reinforced concrete beams. In contrast, the current study specifically examined the effects of incorporating hybrid fibres, consisting of both steel and polypropylene fibre, on the observed findings. In the second stage, the mid-span deflection exhibited a somewhat gradual and steady behaviour, as can be observed in Figure 5.15. Smaller increases were observed and they tended to stabilise over time. Smaller increases were observed and they tended to stabilise over time except some undulations due to variations in load application.

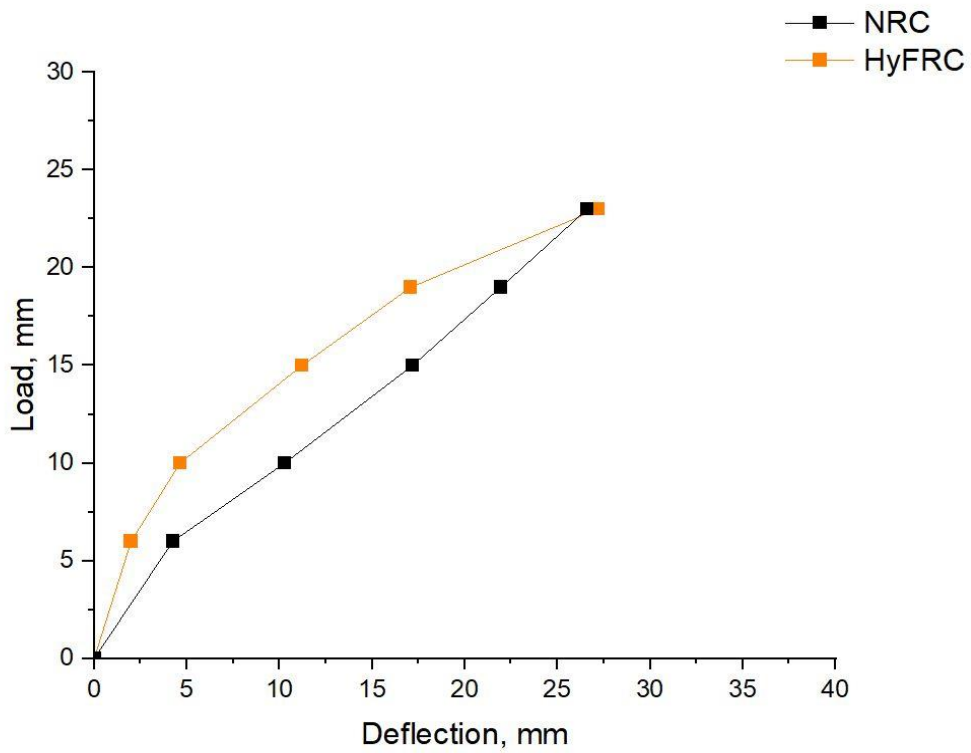

Figure 5.14: Comparison of load and instantaneous deflection curve of NRC and HyFRC beams

The addition of hybrid fibres to the beams produced a 6.66% increase in the cracking load compared to the reference specimen, without any fibres. In Figure 5.15, it is evident that the mid-span deflection is noticeably lower for the HyFRC. The findings indicated that adding hybrid fibres decreased the deformation of the beams, highlighting the effectiveness of fibres in enhancing flexural stiffness, similar to that obtained for the static beams. Overall, the long-term deflection of beams showed a difference between two types of beams over time in terms of the maximum value and change over time, as can be seen in Figure 5.15. A similar observation was reported by Sryh (2017) with the addition of only steel fibre content of 0.5% and 1.0%.

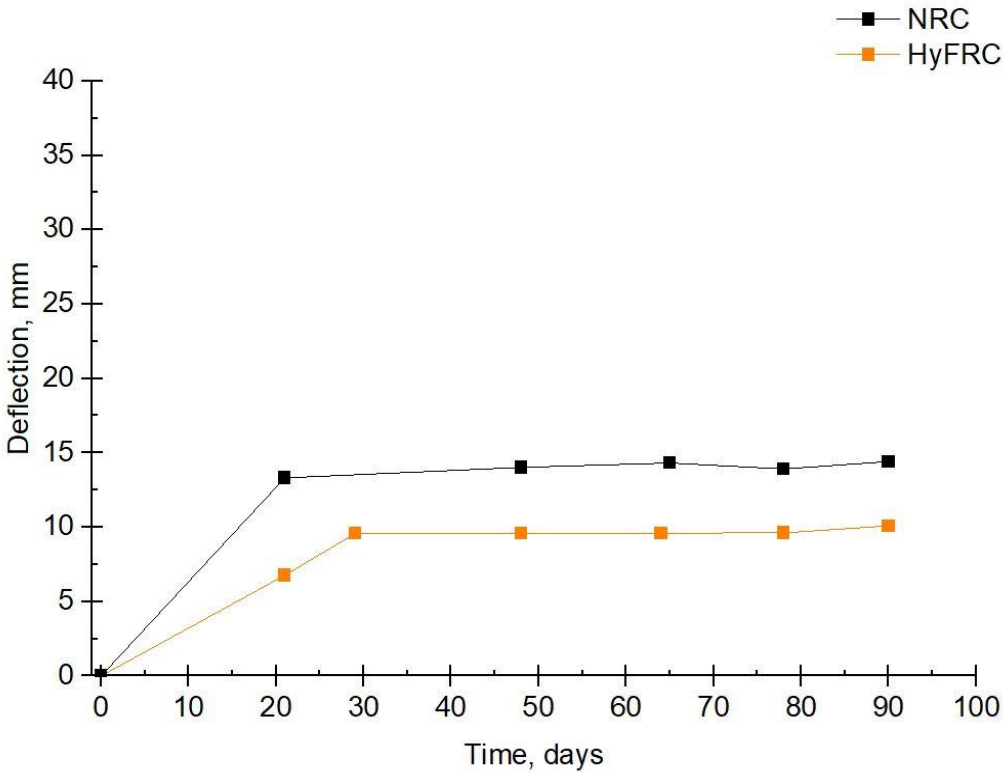

Figure 5.15: Comparison of deflections between NRC and HyFRC beams when subjected to long-term loading

The incorporation of hybrid fibres appeared to offer an effective means of reducing the initial deflection, as reported in Table 5.5. The reduction in long-term deflection in HyFRC beams was approximately 29.98% compared to the reference specimens without fibres.

The data in Table 5.5 indicates that the inclusion of hybrid fibres had a notable effect on the long-term deflection of NRC beams. Specifically, when hybrid fibres were added at a concentration of 1.5%, there was a significant 6.45% reduction in long-term mid-span deflection. This reduction suggests that the addition of hybrid fibres helped to stabilise the mid-span deflection after 30 days under load.

However, it is essential to note that the effect of hybrid fibres on long-term deflection became less pronounced with longer loading times. This could be attributed to the long-term creep tendency of concrete. Creep is the gradual deformation of concrete that occurs when it is subjected to sustained loading. Over time, this creep leads to increased deflection in the concrete. One reason for the diminishing effect of hybrid fibres over time is that some of the fibres degraded or lost their efficiency due to factors like bond issues between the fibres

and the matrix. As a result, the fibres became less effective in preventing deflection.

Recovery deflection refers to the residual deflection or deformation that remains in a material or structure after it has been subjected to a load and then unloaded. In many cases, some amount of deformation remains even after unloading. This residual deflection is what is referred to as recovery deflection. From the data in Figure 5.16, it was apparent that the addition of hybrid fibres showed a recovery deflection by 5.66% after the sustained load was released when compared to the reference beams without fibres. This indicates that the use of hybrid fibres resulted in better deflection recovery compared to traditional concrete beams.

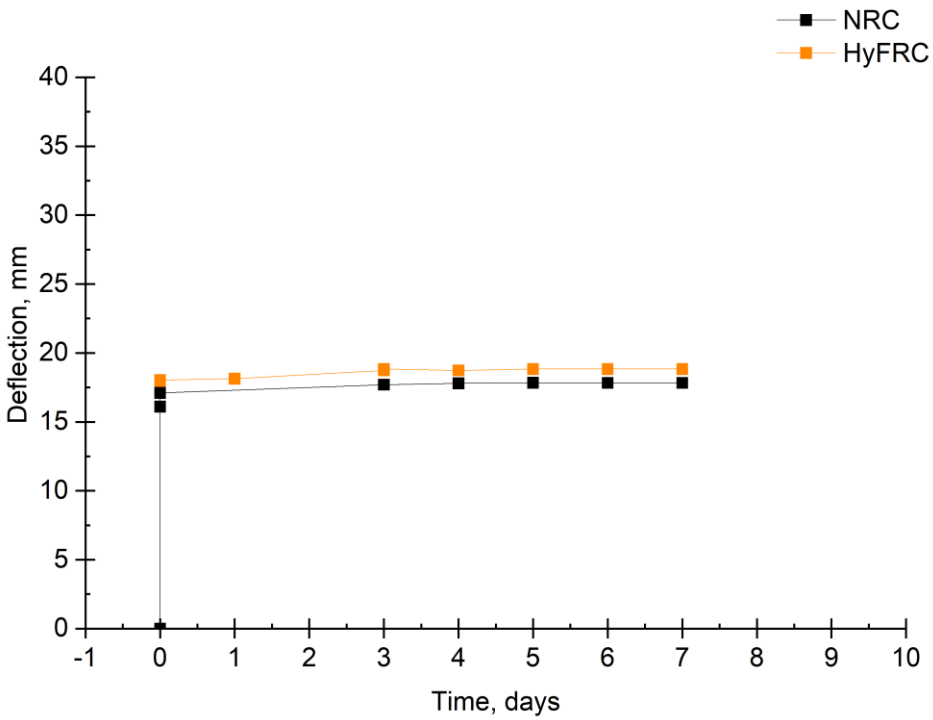

Figure 5.16: Comparison of recovery deflection between NRC and HyFRC after unloading the beams

Comparison between experimental long-term deflection and design code long-term deflection

This section discussed the Eurocode 2 (EC2) method for predicting the long-term deflection of NRC and HyFRC beams. As can be seen in Figure 5.17, the test results of this study demonstrated that the design code predictions for the long-term deflection of NRC beams were accurate during the initial 15-day period.

However, after this period, the code predictions were found to over-predict the long-term deflection until the end of the measurement under load. The degree of overestimation was measured to be approximately 20% in deviation, which indicated a moderate level of discrepancy between the code predictions and NRC experimental results.

Considering the stabilisation of the experimental results after 15 days, a possible factor contributing to the observed discrepancy between the design code predictions and the experimental results is the structural changes and hydration of the concrete in the beams. These changes could have influenced their behaviour under load, potentially leading to shifts in the position of the neutral axis, as explained in the following section (5.3.4) and a reduction in the rate of deflection, which in turn could impact the accuracy of the code predictions beyond this point. Additionally, other factors such as shrinkage, compressive and tensile creep of concrete, and environmental conditions might have also played a role in the observed discrepancy. To comprehensively understand the reasons behind this discrepancy, further investigations are necessary.

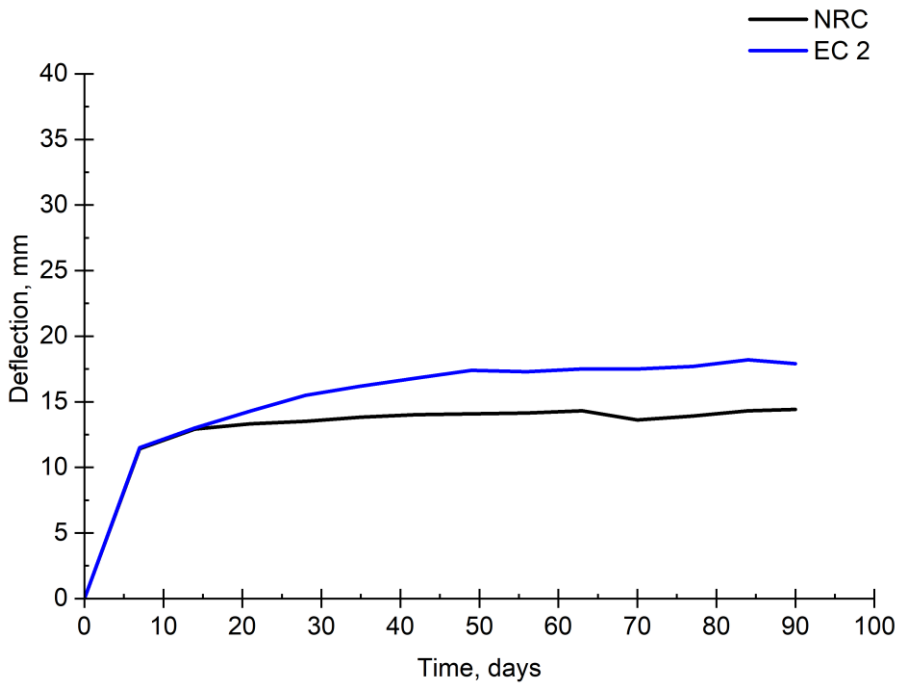

Figure 5.17: Comparison between the experimental results of NRC beams and code prediction

Figure 5.18 shows the comparison of the experimental results and the code predictions for the HyFRC beams. The Figure clearly indicates that the

predictions for long-term deflections of FRC beams according to Eurocode 2 significantly overestimated the experimental results throughout the entire duration of the load. Similarly, Sryh (2017) found that the code prediction highly over-predicted the long term-deflection for beams incorporating steel fibres only. This observation from the current study suggested that the code does not adequately account for the effect of fibres on the long-term deflection of HyFRC beams. The overestimation of deflection by the code may be attributed to its failure to consider the influence of fibres on cracking behaviour and tensile properties of concrete, which have a significant impact on the deflection behaviour of FRC beams.

Furthermore, the existing formula used in Eurocode 2 to calculate long-term deflection does not incorporate the influence of tensile creep. However, it acknowledges that while the tension stiffening factor may indirectly account for certain aspects of tensile creep, it does not fully encompass all the effects associated with tensile creep. This omission of tensile creep in the current formula could potentially explain why the code predictions tend to overestimate long-term deflection. Forth (2014) emphasised the discrepancy between tensile and compressive creep in concrete and stressed the importance of addressing this inequality when considering the position or change in curvature of the neutral axis, as well as the loss of tension stiffening over time. Neglecting the inequality between tensile and compressive creep can lead to inaccurate predictions of the beam's behaviour under load.

Therefore, it is crucial to modify the Eurocode 2 method to incorporate the influence of fibres and consider the effects of tensile creep in order to accurately predict the long-term deflection behaviour of FRC beams. These findings highlighted the importance of further research and refinement to improve the accuracy of design codes in predicting the long-term behaviour of concrete beams under load. It was also concluded from the comparison between the experimental and the code equations do not consider the effect of using FRC in their equations to predict the long-term deflection. It's essential to understand how FRC can impact long-term deflection. FRC typically offers improved durability and reduced cracking due to the presence of fibres. It needs to incorporate FRC-specific parameters or modification factors into the equations to account for this effect. A proposed equation model should be considered with a

modification factor and an exponent to be used to account for fibre effect. These adjustments will ensure that the equations accurately represent the real-world behaviour of structures with FRC components.

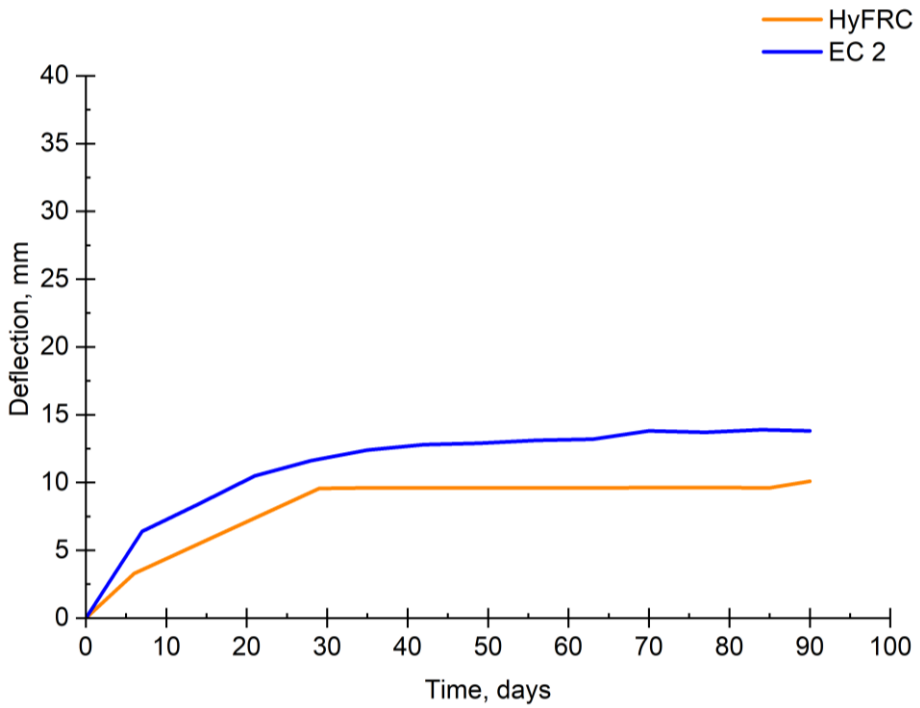

Figure 5.18: Comparison between the experimental results of HyFRC beams and code prediction

5.3.3 Long-term strain response of concrete and steel reinforcement

(a) Concrete surface strain

The surface strain of the concrete in the compression and tension zone is illustrated in Figure 5.19(a-c). The difference between the strain recorded at t days and the instantaneous strain recorded at t0 days was used to compute long-term strains. The compressive concrete strains observed in NRC and HyFRC beams followed a similar pattern over time. The concrete strains gradually increased as the load increased until reaching 50% of the ultimate load. During the early stage (between 0 and 15 days), NRC and HyFRC beams exhibited a linear and rapid response. As can be seen Figure 5.19(a), the majority of compressive concrete strain occurred within the first 50 days. Subsequently, the concrete strain experienced a slight increase until 85 days, after which it tended to stabilise. The addition of hybrid fibres had no noticeable effect on reducing the compressive concrete strains.

As can be seen in Figure 5.19(b), the primary occurrence of tension concrete strain is observed within the first 15 days for both NRC and HyFRC beams. Notably, the increase in tensile strain at the reinforcement level in the tension zone is primarily attributed to the opening and propagation of existing primary cracks, rather than the formation of new cracks.

For NRC beams, a gradual decrease in concrete strains in tension was observed from 15 days to 35 days, followed by a period of stabilisation from 35 to 50 days. Subsequently, there was a continued reduction in concrete strains from 50 days to 90 days. In the case of HyFRC beams, the tension zone's concrete strain also exhibited stabilisation from 15 to 45 days. Subsequently, there is a slight reduction in concrete strains from 45 days to 85 days, where the strains tend to stabilise.

The observed reduction in concrete strain over time is believed to be influenced by the gradual redistribution of stresses inside the beam while the load is sustained. Additionally, creep deformation over time may also contribute to the reduction in strain.

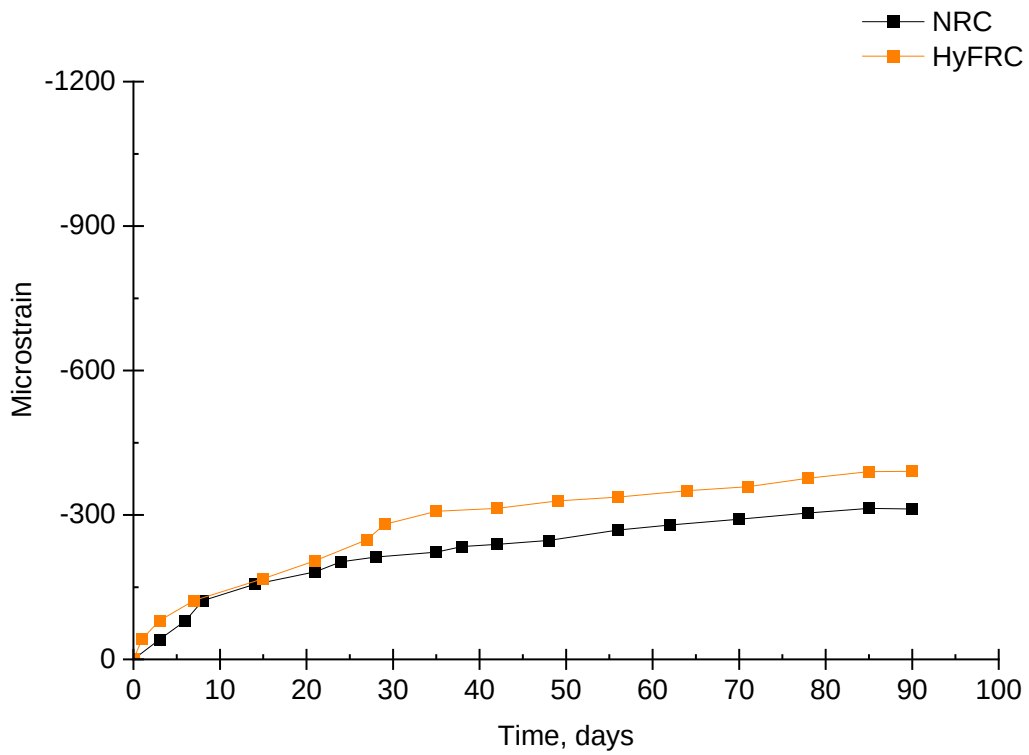

a) Top row align with compression reinforcement

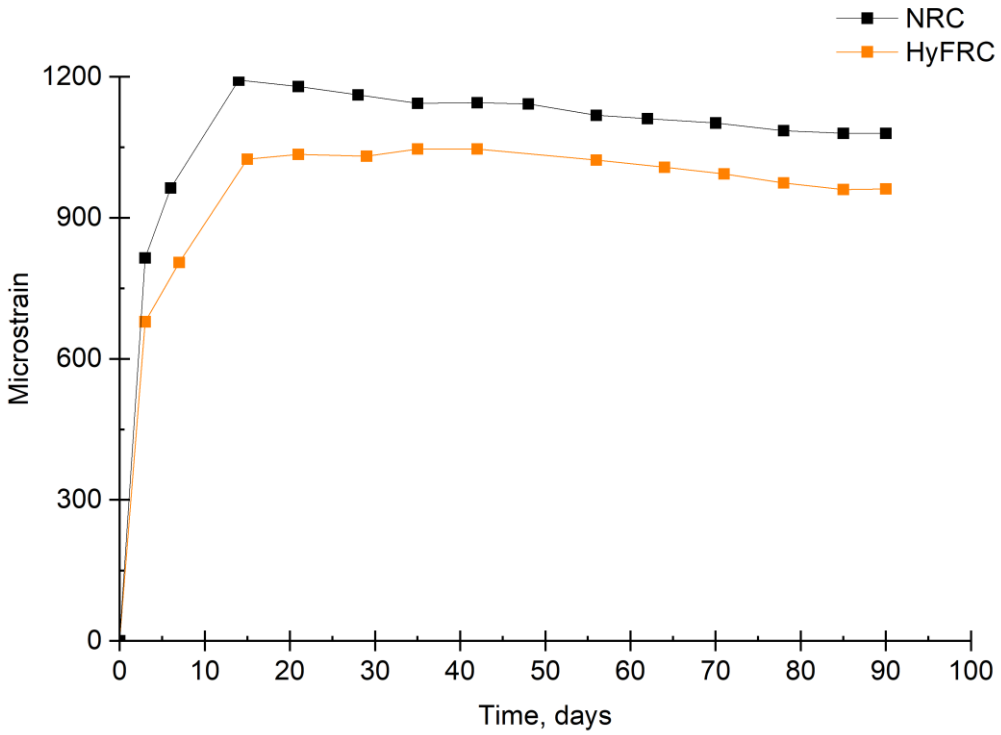

b) Bottom row with tensile reinforcement

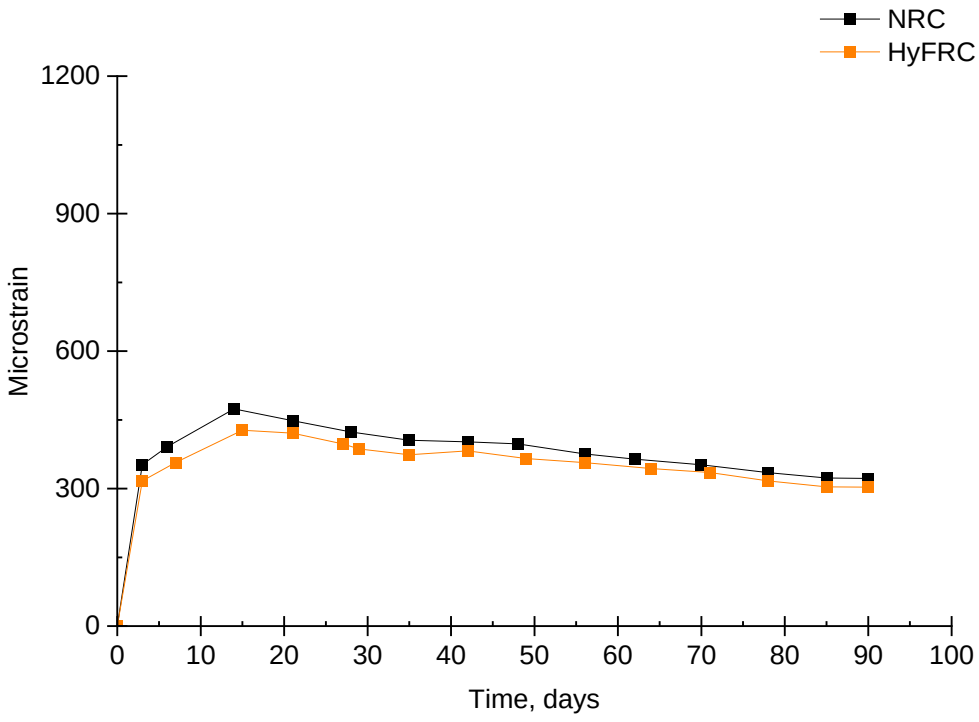

c) Average of all rows for surface strain

Figure 5.19: Concrete surface strain

(b) Steel strain

The stress in the steel bars of NRC and HyFRC beams are plotted in Figure 5.20 with time for a period of 90 days under load. Initially, both of NRC and HyFRC beams exhibited a similar trend of steel stress over time in the early stage, as shown in Figure 5.20. All of the beams exhibited a rapid increase and responded linearly in stress after reaching the stabilised pattern in the early stage between 0 and 15 days. Figure 5.20 shows that the addition of 1.5% hybrid fibres reduced the stress in the tensile reinforcement of the concrete in the tension zone by 10% and 4.42% at 3 days and at 15 days under load, respectively.

The steel stress of HyFRC beams tended to stabilise from 15 to 45 days, whereas the stress of NRC beams exhibited a significant reduction over time. This phenomenon may be associated with changes in loading conditions, as the loads were monitored and manually adjusted during the test. NRC beams exhibited an approximately 33.33% reduction in the stress of steel bars after 90 days relative to HyFRC beams and this reduction might be related to the bond loss between the steel and concrete. Figure 5.20 illustrates how the reduction in steel stress over time is affected by the addition of hybrid fibres (e.g., steel and polypropylene fibres) to concrete. The presence of steel fibres significantly affects the rate of reduction in steel stress, as the steel fibres have a high elastic modulus. Meanwhile, steel stress of HyFRC beams decreased gradually from 40 to 90 days. The stress rate in the steel bars was affected by the addition of hybrid fibres to the concrete beams, which might be related to a good bonding between the matrix and fibre and the distribution of fibre within the concrete mix.

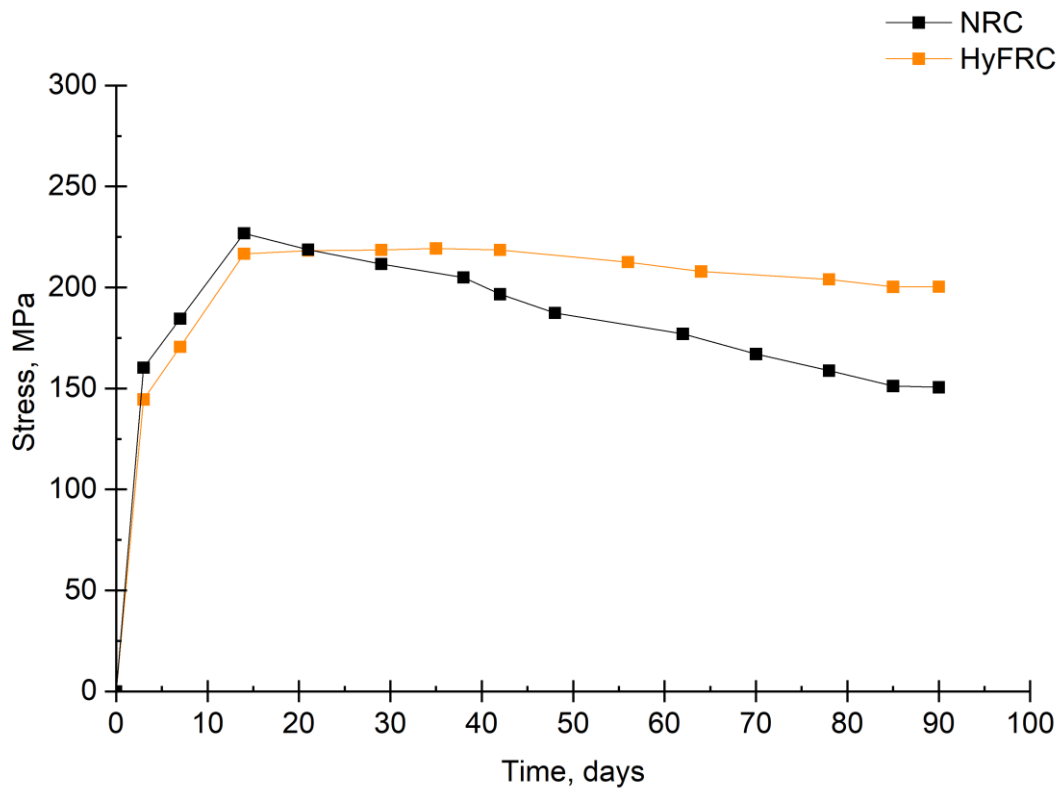

Figure 5.20: Steel stress in tensile reinforcement

5.3.4 Long-term crack width and length of full-scale beams

(a) Crack width

Figure 5.21 and Figure 5.22 show the development of the crack width of NRC and HyFRC beams for the short- and long-term test. Figure 5.21 demonstrates that both NRC and HyFRC beams exhibited a rapid rate of crack width growth during the loading process until they reached a stabilised crack pattern. In the case of NRC beams, the crack width remained relatively constant in the stabilised pattern from the first day to 20 days. Afterward, there was a linear increase in crack width from 21 to 55 days, followed by stabilisation from 55 to 90 days under load.

On the other hand, HyFRC beams showed a slight increase in crack width during the initial load, ranging from 0mm to 0.05mm. This increase can be attributed to the tensile stresses acting on the concrete and reinforcing steel, resulting in concrete cracking and steel elongation. However, the addition of hybrid fibres effectively reduced the propagation of cracks at early ages when concrete is more susceptible to cracking compared to NRC beams. The addition of hybrid fibres to the beams appeared to stabilise the crack width after 7 days

under load, whereas the normal reinforced concrete beams appeared to stabilise after 55 days under load.

As the loading continued, NRC beams exhibited a significant increase in crack width at 90 days, approximately two times greater than that recorded on the first day. Similar results were observed by Mias et al. (2015) who stated that crack widths after 250 days were up to approximately 2.4 and 2.9 times higher when compared with other concrete beams.

HyFRC beams showed a 50% reduction in crack width after reaching the stabilised crack pattern and after 90 days under load compared to NRC beams. This reduction is attributed to the ductile behaviour of the hybrid fibre system, which distributes stress across the cracked section of the beam and decreases stress concentration at the crack tip. This reduction also is generally attributed to the fibres' ‘bridging’ activity across the cracks. Vasanelli et al. (2014) stated that the inclusion of FRC led to a reduction in crack width compared to plain concrete, while Tan et al. (1995) observed that the addition of steel fibres resulted in smaller cracks as the fibre content increased.

The current study was designed to determine the effect of hybrid fibre reinforcement on the flexural performance of concrete beams under different types of loadings. The current study indicated that the hybrid fibre system, consisting of both steel, micro, and macro polypropylene fibres, provides improved crack width control and reduced crack propagation compared to plain concrete or the use of steel fibres alone. This finding highlights the potential benefits of using hybrid fibres in enhancing the durability and long-term performance of concrete structures.

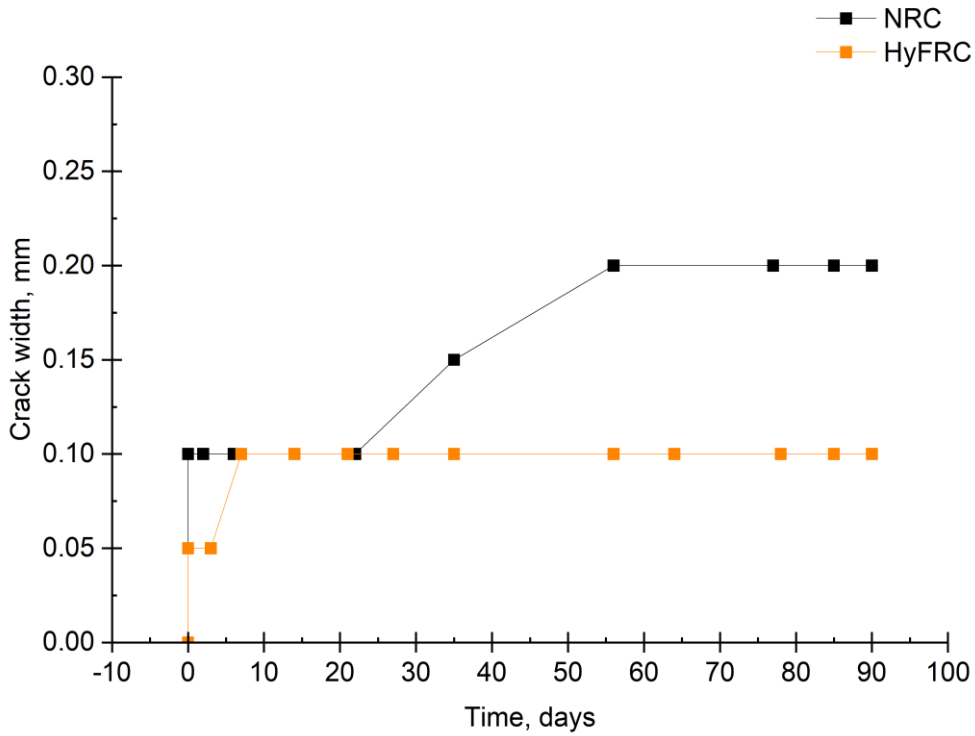

Figure 5.21: Effect of hybrid fibres on short- and average long-term crack width

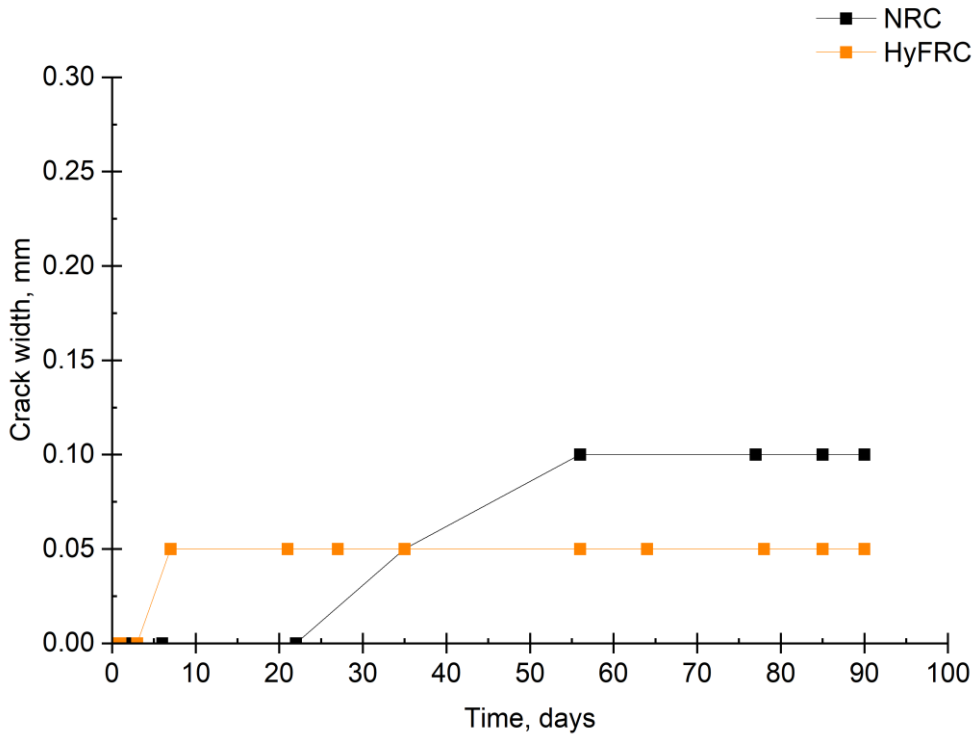

Figure 5.22: Effect of hybrid fibres on average long-term crack width

Comparison between crack width of experimental and design code

Table 5.5 presents a summary of the experimental crack width results and the corresponding predictions based on the design code. The purpose of comparing the crack width data with the limits specified in the design code was to evaluate the accuracy and reliability of the code in predicting the behaviour of NRC and HyFRC specimens. The average crack width obtained from the long-term bending tests was compared to the values predicted by the design code provisions.

Table 5.5: Comparison between the crack width results of experimental and design code

Type of the beam	Experimental result	Experimental/Predicted			Mean	S.D
	EXP (mm)	EC2	fib MC2010	RILEM TC-162-TDF		
NRC-SUS-0	0.1	1.11	1.08	0.77	0.99	0.19
HyFRC-SUS-1.5	0.05	0.71	0.83	0.83	0.79	0.07

As summarised in Table 5.5, the design code specified in EC2 and the provisions of MC 2010 slightly underestimated the average crack width prediction for NRC beams when measured at the stabilised crack pattern. The predicted values were close to the experimental values, with only a 10% and 7% difference, respectively. Considering that the experimental crack width data fell within the limits set by the code, it suggests that the code can reasonably predict the behaviour of the NRC specimens.

On the other hand, the results obtained from RILEM TC-162 significantly over-predicted the average crack width, with an overestimation of approximately 30%. This discrepancy by RILEM TC-162 in normal reinforced concrete beams can be attributed to its reliance on the crack spacing formula, which may not accurately account for the specific characteristics and behaviour of normal reinforced concrete, leading to an overestimation of crack width.

However, in the case of the HyFRC beam, the experimental data for the crack width showed values lower than the predicted limit specified by the EC2 design code, with a difference of approximately 40%. Since the EC2 design code does not consider the influence of fibres on crack width, it is possible that the code's prediction may not accurately reflect the behaviour of the hybrid fibre-reinforced concrete beam, thus explaining the lower crack width observed in the experimental data compared to the predicted design code limit.

Additionally, other provisions, such as RILEM TC-162 and MC2010, overestimated the average crack width by approximately 20%. While the results obtained from the code provisions initially provided an indication of the average crack width, further investigations were necessary to achieve accurate predictions of crack width.

Existing crack width prediction formulas for concrete structures primarily rely on crack spacing as a main parameter, often overlooking the influence of fibre volume fraction. Consequently, incorporating fibre reinforcement into concrete structures may lead to inaccurate crack width predictions, despite the positive effects on durability and long-term performance.

Research by Vasanelli et al. (2014), which focused on single-type fibres, emphasised the crucial role of fibres in the long-term condition and overall structural durability, highlighting a gap in existing code regulations that do not adequately account for fibre influences. However, it is important to note that the current study utilised hybrid fibres, including steel, micro polypropylene, and macro polypropylene fibres, emphasising the significance of considering multiple fibre types.

Despite extensive research on the mechanical behaviour of FRC structural elements, accurately calculating crack width and spacing in FRC flexural elements remains an unresolved issue. The relationships used to predict crack widths in FRC elements still require further validation and assessment (Micelli et al., 2019).

The current approach for predicting crack width tends to overestimate the values by relying solely on the length and diameter of the fibres, without fully considering the effect of the volume fraction of fibres on crack width. This discrepancy could be attributed to the limitations of the prediction method and the failure to account

for the specific influence of the volume fraction of fibres. This discrepancy can lead to potential durability and long-term performance issues for the structure, as the existing formulas fail to account for the bridging effect of fibres across cracks, which effectively reduces the crack width.

The experimental results clearly demonstrated the significant role of fibres in enhancing the long-term condition and overall structural durability of HyFRC material. Despite this evident contribution, the provisions outlined in the existing design codes did not adequately account for the effects of hybrid fibres. The crack width limits specified in the design code were based on assumptions and simplifications that may not accurately represent the actual behaviour of the HyFRC specimens. As a result, it becomes crucial to consider updating or modifying the design code to incorporate the specific effects of hybrid fibres on crack width.

To achieve this, further research and a comprehensive range of experiments are necessary to develop new models capable of accurately predicting the behaviour of hybrid fibre-reinforced concrete beams over the long-term. Gaining a better understanding of the behaviour of these structures will ensure that the design code accurately reflects the behaviour of the materials used, thereby ensuring the safety and reliability of the structure.

In conclusion, recognising the significant contribution of fibres in HyFRC and improving design code provisions to account for their effects will lead to more accurate predictions and better design practices, ensuring the long-term durability and performance of fibre-reinforced concrete beams.

(b) Long-term crack length of full-scale beams

Table 5.4, Figure 5.23 and Figure 5.24 show the growth of the crack length in the NRC and HyFRC beams over time, once the stabilised crack pattern was reached. In the case of NRC beams, the crack length rapidly increased as the load was applied during the loading process. NRC beams, in particular, exhibited longer crack lengths after reaching the stabilised crack pattern. Initially, the crack length for NRC beams remained unchanged at 55.9mm from 0 to 3 days, followed by a linear increase from 73.25mm to 79.50mm between 3 and 7 days. Subsequently, the crack length showed gradual growth, reaching 93.05mm between the 7th and 90th days.

On the other hand, the incorporation of hybrid fibres in HyFRC beams resulted in shorter initial crack length, as can be seen in Figure 5.23 and Figure 5.24. The presence of fibres can result in varied crack heights in FRC beams compared to conventional reinforced concrete beams, which might be attributed to the irregular distribution and orientation of the fibres relative to the direction of crack propagation (Caggiano et al., 2016; Raju et al., 2020; Sarmiento et al., 2016). The rate of crack length growth in HyFRC beams was slower than that of conventional concrete beams. Sryh (2017) reported that the crack length observed in SFRC beams were smaller compared to NRC beams without fibres. However, no specific percentages or quantitative differences were mentioned regarding the effect of fibres on crack length. The addition of hybrid fibres effectively reduced crack length propagation due to increased stiffness of the concrete members and the ability of fibres to govern crack development.

Moreover, Figure 5.23 demonstrates that the average crack length increased over time under load for the HyFRC beams over 90–day period. Compared to the behaviour exhibited by NRC beams without fibres, the addition of hybrid fibres appeared to slow the propagation of cracks after the load was applied. The instant crack length in HyFRC beams after load application was 32.9mm and remained constant from 0 to 3 days, showing a 41.14% reduction compared to reference beams. The crack length in HyFRC beams increased linearly from 32.90mm to 51.55mm between 3 and 7 days, slightly increased to 53.05mm between 7 and 29 days, and then linearly increased to 63.15mm between 29 and 35 days. Subsequently, the crack length increased linearly from 63.15mm to 67.90mm between 54 and 64 days. The addition of hybrid fibres appeared to stabilise the crack length after 65 days under load at a value of 67.90mm. HyFRC beams exhibited a significant 27.03% reduction in crack length after 90 days under sustained load.

These findings enhance our understanding of the influence of fibres on the crack propagation over the long-term when compared to NRC beams without fibres. The use of hybrid fibre with different mechanical properties contributed to resisting and bridging crack development under sustained load, which is particularly evident in HyFRC beams.

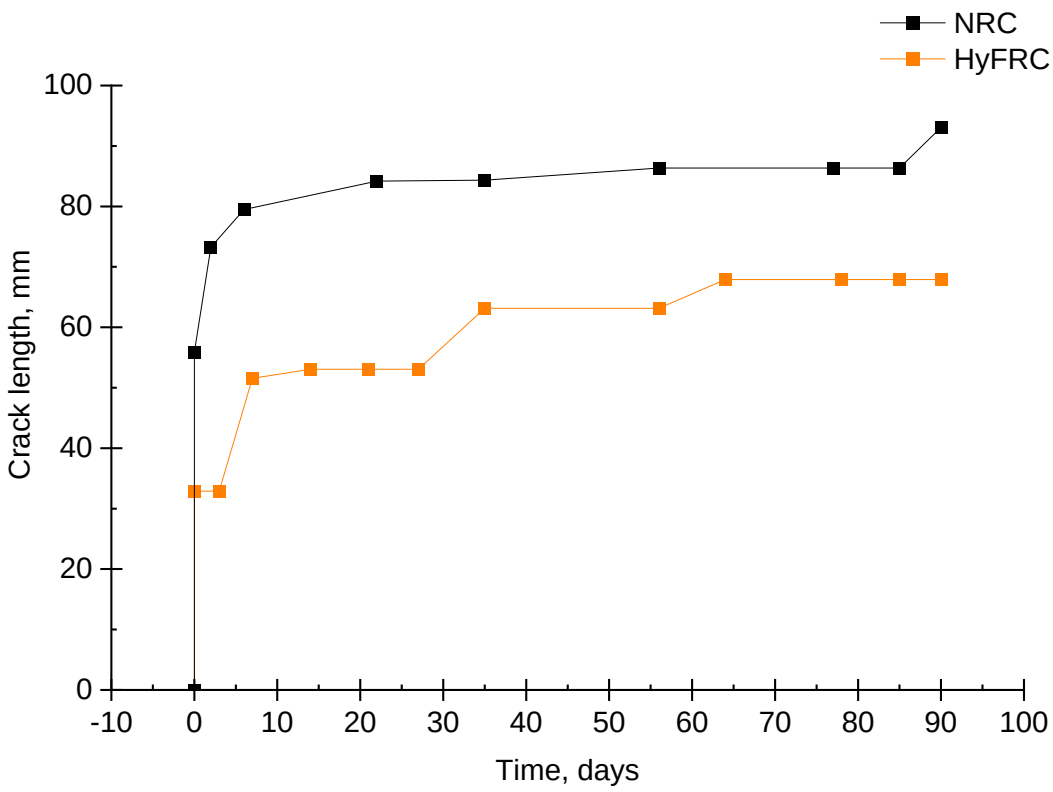

Figure 5.23: Effect of hybrid fibres on short- and average long-term crack length

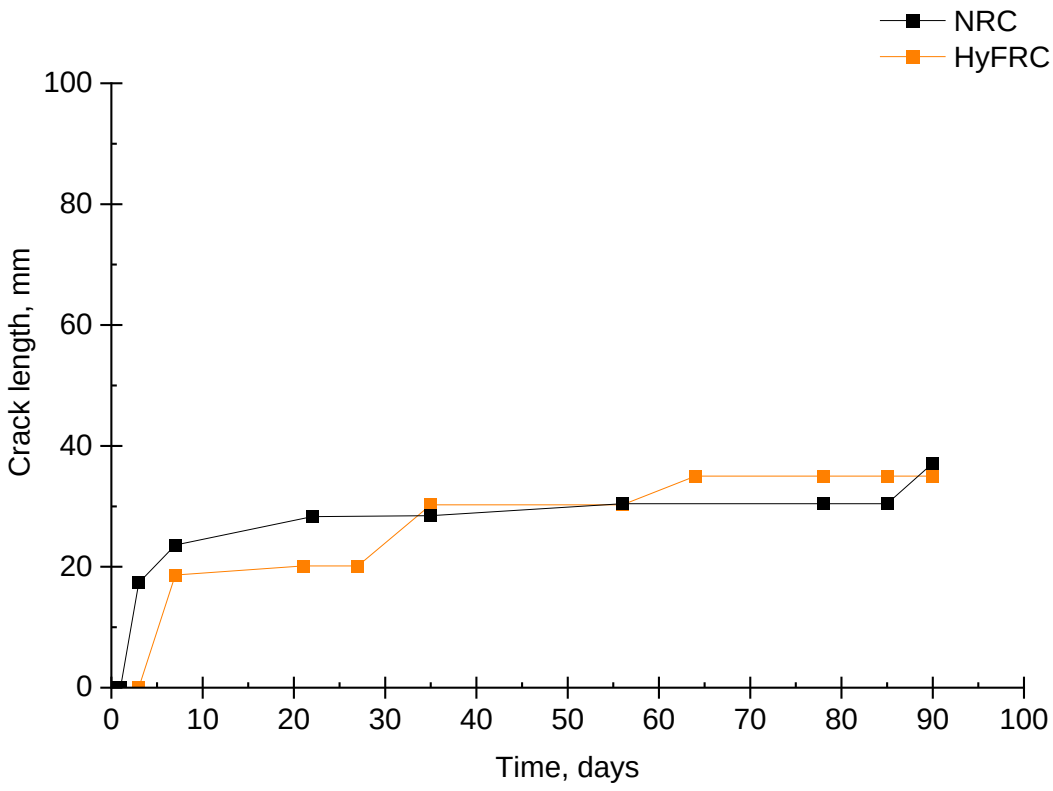

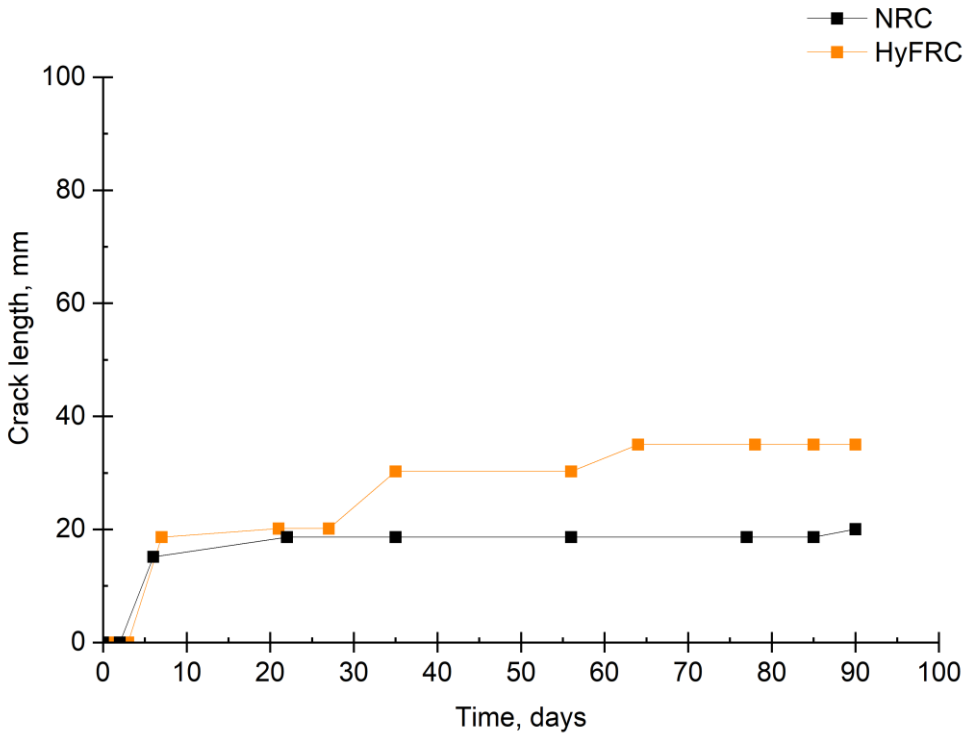

Figure 5.24: Effect of hybrid fibres on average long-term crack length

Comparison between crack length and the change of neutral axis

The behaviour of the neutral axis and crack length over time in NRC and HyFRC beams is shown in Figure 5.25(a) and Figure 5.25(b). Figure 5.25(a) and Figure 5.25(b) show the neutral axis and the crack length curves, which were derived by subtracting the instantaneous depth from the total depth. The development of cracks changed the distribution of stresses and affect the position of the neutral axis. As the crack length increased, the position of the neutral axis shifted, leading to changes in the load-carrying capacity of the structure. The formation of cracks created damaged areas with distinct mechanical characteristics from the undamaged material, leading to changes in stress distribution and shifts in the position of the neutral axis.

Both NRC and HyFRC beams showed a linear increase in crack depth and neutral axis position during the initial days of the test, as shown in Figure 5.25(a) Figure 5.25(b). This indicated that the crack in the beam expanded over time, causing a corresponding shift in the position of the neutral axis. The steady increase in both curves suggested that the rate of crack growth and the shift in the neutral axis position remained relatively constant throughout this period.

However, as the loading time increased, environmental factors like creep and shrinkage began to have a more pronounced impact, resulting in complex and non-linear trends in the curves depicting the position of the neutral axis and crack depth. These factors influenced the stress distribution within the structure.

The effects of creep and shrinkage caused changes in crack width and development over time, leading to differences between crack length and NA position. The time-dependent behaviour could be more pronounced in NRC beams, resulting in larger differences over time. The addition of fibres in the beams enhanced the tensile strength and crack resistance of the concrete. The presence of fibres influenced crack formation, propagation, and overall behaviour, contributing to variations between crack length and NA position.

These variations could be attributed to the use of different fibre types in the HyFRC, causing a non-uniform distribution of fibres within the concrete matrix. Each fibre type exhibited different mechanical properties, including tensile strength and stiffness, leading to varied behaviour regarding crack bridging and the stress transfer. Moreover, the random distribution of fibres in HyFRC resulted in varying degrees of fibre alignment and clustering, influencing the propagation pattern of cracks and the location of the neutral axis, leading to a larger difference between the recorded data for crack length and the position of the neutral axis.

Additionally, changes in loading conditions, such as increasing or decreasing loads monitored and adjusted manually during the test, could contribute to non-linear and intricate patterns in the curves. Furthermore, the development of new cracks or the propagation of existing ones could alter the stress distribution and consequently affect the position of the neutral axis, introducing non-linear behaviour in the curves. When combined with other environmental conditions, these factors could induce long-term changes in the mechanical properties of the concrete, leading to increasingly complex behaviour of the structure over time.

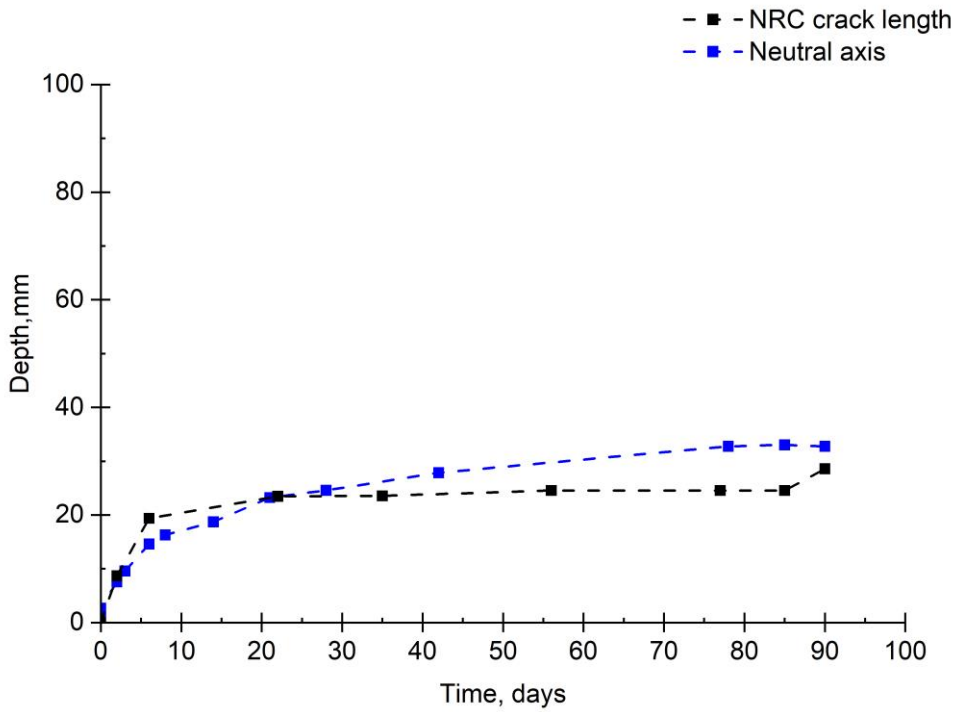

a) NRC crack length vs neutral axis

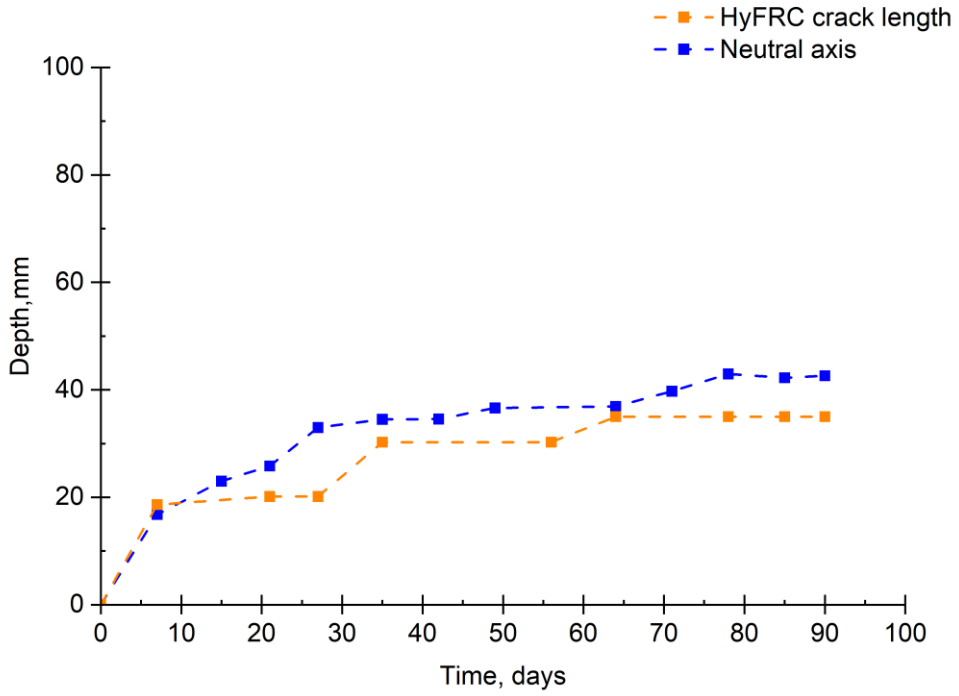

b) HyFRC crack length vs neutral axis

Figure 5.25: Change in the neutral axis and depth of crack with time

5.4 Summary and conclusions

This section presented the findings of the conducted experimental investigations on the behaviour of hybrid fibre-reinforced concrete (HyFRC) beams. The experiments focused on crack pattern and crack width, deflections, strains and long-term performance under different types of load.

The outcomes of the experimental data presented in this chapter can be summarised as follows:

- It was observed that the use of fibre reinforcement in concrete beams led to fewer cracks compared to reference beams without fibres at the same load level under different types of load. Steel fibres contributed to smaller cracks and increased the initial cracking load and failure load of the beams, while hybrid fibres showed higher contribution compared to the addition of steel fibres. Furthermore, the incorporation of steel and hybrid fibres resulted in a reduction in deflection at failure, with the HyFRC beams exhibiting a greater reduction compared to SFRC beams.
- The experimental results demonstrated that the presence of hybrid fibres contributed to a decrease in crack length and improved performance under different types of load by bridging micro cracks and impeding their propagation. These findings highlight the effectiveness of hybrid fibres in enhancing the flexural stiffness and crack resistance of concrete beams.
- The test results showed that incorporating hybrid fibres into concrete beams resulted in increased resistance to failure at lower stress levels, reduced deflection at failure, smaller crack widths, and decreased crack lengths compared to reference beams without fibres. These findings demonstrate the beneficial effects of hybrid fibres in enhancing the structural performance and durability of the concrete beams under load.
- It was observed from the analysis of the test results that the current crack spacing formulae in the design codes (such as EC 2, fib Model Code 2010) and other guidance documents (RILEM TC 162-TDF) underestimate the value of crack spacing in comparison to the experimental results for NRC beams. On the other hand, for SFRC and HyFRC beams, the EC 2 and fib Model Code 2010 gave reasonable predictions compared to the

experimental results, while RILEM considerably underestimated the crack spacing.

- The measured degree of overestimation for long-term deflection of NRC beams was around 20%, suggesting a moderate level of disparity between the predictions provided by the code and the actual experimental outcome.
- In terms of long-term deflection, the experimental results showed a reduction in deflections compared to predicted values from the Eurocode 2 (EC2). However, the EC2 predictions overestimated the long-term deflections of the HyFRC beams throughout the duration of the load. This discrepancy highlights the need for modifications in the design code to accurately predict the long-term deflection behaviour of HyFRC beams.
- Regarding crack width, the crack width predictions based on the design code provisions, such as EC2, exhibited a reasonable accuracy for NRC beams with differences of only 10% and 7% compared to the experimental results. However, the crack width predictions derived from RILEM TC-162 showed a substantial overestimation, with an approximate 30% difference from the average crack width observed in the experiments.
- It was observed that the values measured in the HyFRC beams were lower than the predicted values by the EC2 design code, showing a significant difference of approximately 40%. This indicates that the current design code may not adequately account for the effect of hybrid fibres on crack width.
- Furthermore, the study compared the crack width predictions from different provisions, including RILEM TC-162 and MC2010. It was found that these provisions overestimated the average crack width by approximately 20%. These results emphasise the importance of revisiting and refining the crack width prediction models to account for the influence of hybrid fibres.

Overall, the findings of this study indicated the significant contribution of hybrid fibres to crack width reduction and improved long-term performance of concrete structures. However, further research and revisions in design codes are necessary to fully incorporate the effects of hybrid fibres and accurately predict the behaviour of HyFRC beams. These results contribute to the understanding of

fibre-reinforced concrete behaviour and provide valuable insights for the design and construction industry.

Chapter 6 Finite Element Analysis Modelling

The main aim of this chapter is to compare and validate the experimental results with both the FEA and available design provisions.

6.1 Finite Element modelling (FEA)

6.1.1 Introduction

Experimental tests offer more accurate and reliable outcomes, still, it is a very costly and time-consuming process. The scope of tests performed in laboratories remains constrained, and restraints are imposed by the time constraints associated with the tests, and restrictions on the specimen size, the number of specimens, the cost of producing them and different parameters that may be tested. Furthermore, it is not always possible to cover a wide range of parameters in experimental work, which is needed for a comprehensive investigation. Consequently, a FEA was developed to replicate the flexural behaviour of the experimental response of the full-sale beams under four-point bending, which was then used to conduct a parametric study to explore its structural performance in further detail.

In this chapter, the creation of a three-dimensional finite element model is detailed, which has the capability to simulate the flexural behaviour of the full-scale prefabricated beams under static and repeated four-point bending. The finite element model was created utilising Abaqus 6.14, which is a software widely employed for finite element analysis. The selection of Abaqus for this research project was based on the researcher's familiarity and expertise with the software. Choosing Abaqus, a software with which the researcher is well-versed, it ensures a seamless integration of the software into the research methodology. The accuracy and reliability of the three-dimensional finite element model were verified by comparing its results with the experimental findings outlined in Chapter 5. The finite element model successfully demonstrated its capability to replicate the overall behaviour of the full-scale beams. As a result, a parametric study was conducted in this chapter utilising the validated finite element model to examine various parameters, including varying concrete strengths, as well as comparing with results of previous studies, in order to investigate their effects on the structural performance and the flexural behaviour of the full-scale beams.

6.1.2 Choosing Abaqus as the modelling tool

Abaqus is a versatile software program commonly employed to model structural responses for finite element analysis (FEA). Stress-related issues can be classified into two categories, static and dynamic responses, based on the significance of inertial effects. It is specifically designed to be user-friendly for complex problems, featuring a straightforward input language, robust data-checking capabilities, and a wide array of pre-processing and post-processing options for displaying output results. Abaqus offers a diverse selection of element types, including continuum elements, which encompass one-dimensional, two-dimensional, and three-dimensional beams, membranes, and shells. In this study, Abaqus/standard was utilised as it is an optimal solution technology for static and repeated analyses where precise stress solutions are crucial, such as in the flexural behaviour tests.

6.1.3 Modelling process

A variety of input options are available for modelling in Abaqus/CAE, including geometry parameters, properties of materials, element types, loads, solution controls, graphic user interfaces, the meshing process, boundary conditions, interaction and constraints, and post-processing controls. Modern FEA software is usually divided into three components: the pre-processor, the processor, and the post-processor. During the pre-processor phase, the model was constructed, and the geometry, material properties, and element type are defined. Additionally, loads and boundary conditions are specified in the pre-processor. Using the information provided, the processor is capable of calculating the stiffness matrix and force vectors. Various results are derived in the final block, known as the post-processor, such as stress, strain, and failure ratios.

Different main steps may be identified in the Abaqus process:

- Step 1 – Parts modelling that includes specifying geometric, material properties and element types (i.e., solid, shell...Etc.,).
- Step 2 - Boundary and constraint conditions
- Step 3 - Output analysis
- Step 4 - Post-processing of the results

The first step of the model involves defining the element types and then the geometry of its parts. This is followed by assigning material properties for the

different parts. Once this is completed, the parts are assembled, and contact/interaction, loads, and boundary conditions are applied to the model. Next, the model is meshed by dividing into smaller elements, and these are defined based on the nodes and element connectivity. After this, the model is solved, and finally, the results are computed and visualised.

6.1.3.1 Model geometry

The geometrical and cross-sectional details of the specimens used to develop the finite element model were discussed in Chapter 3, which are shown in Figure 6.1. The concrete beam and loading plate were modelled using eight noded solid elements with reduced integration (C3D8R). The steel reinforcement in tension and compression and shear links were adapted using a truss element (2-node linear, T3D2), which can carry only tensile and compression loads and exclude any resistance to bending.

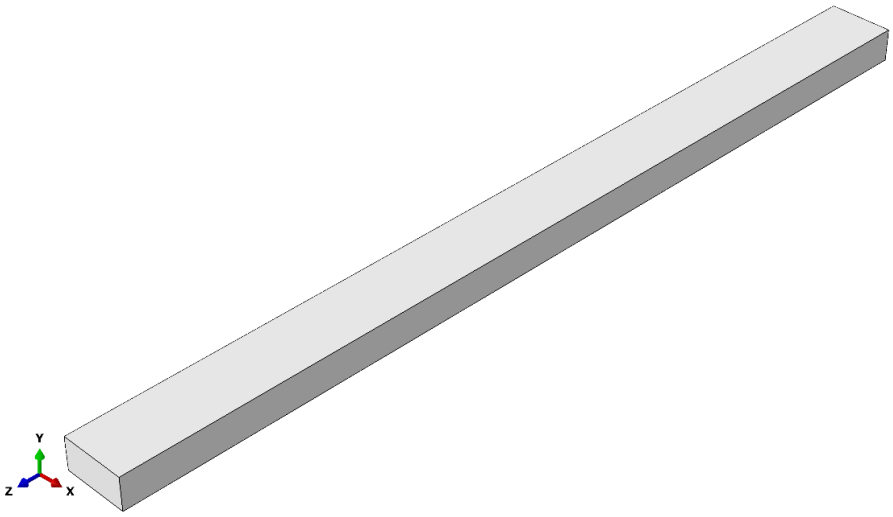

a) Beam cross-section

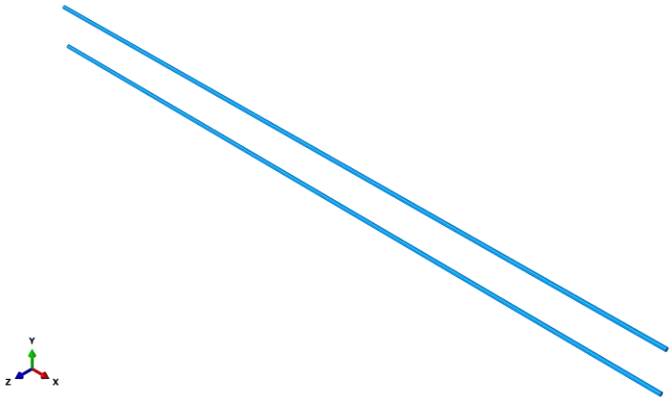

b) Compressive reinforcement

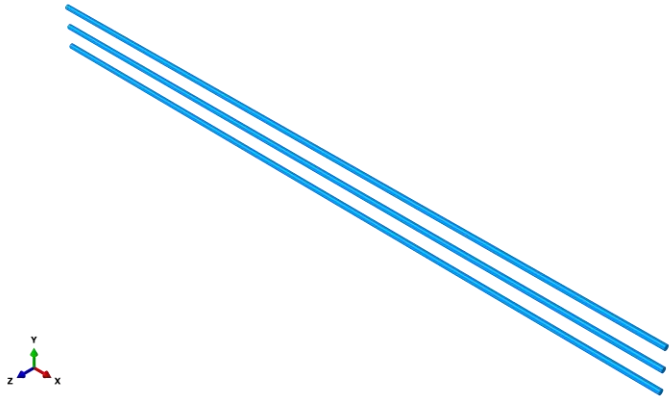

c) Tensile reinforcement

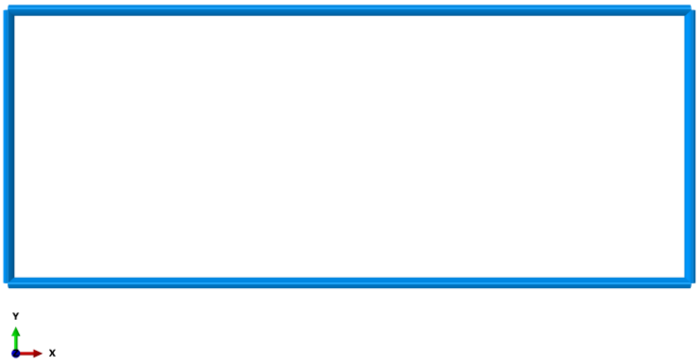

d) Shear links

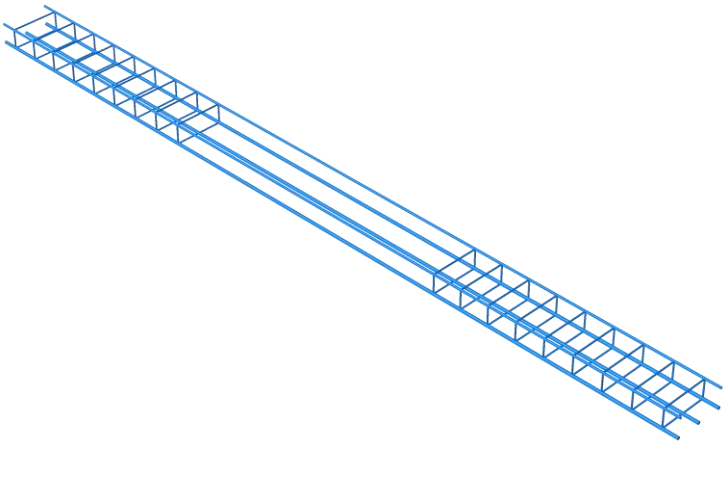

e) Reinforcement cage

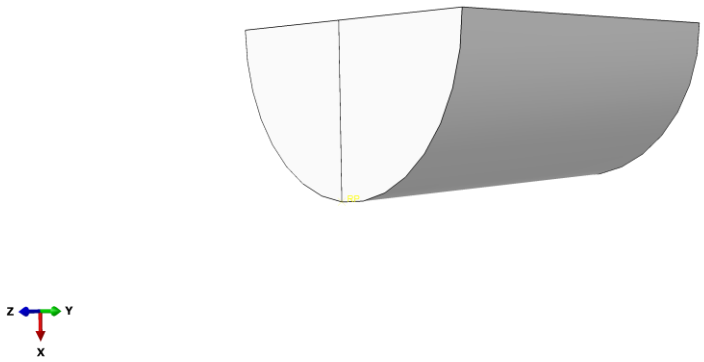

f) Supports

Figure 6.1: Beam geometry and cross-section details

6.1.3.2 General Principles of Material modelling

The nonlinear material stress-strain curves of each constituent in the part section were introduced into the material property field. The commonly used materials are isotropic, which means they have an infinite number of symmetry planes, making their properties independent of orientation. To represent their elastic properties, only two constants are required, typically Young's modulus, E and the Poisson's ratio, v, although other pairs of constants may be used when more convenient.

The stress-strain behaviour of each material in Abaqus was defined using constitutive material laws. Accurately modelling material behaviour for finite element analysis is an important and challenging task. Many constitutive models are available to define the characteristics and behaviour of materials. There are two methods for defining the input parameters utilised as properties of materials. One is to use the empirical equations for estimating the properties, like tensile strength, compressive strength and modulus of elasticity of concrete etc., and the other is to obtain these properties by experimental testing in the laboratory. The experimental test results in this investigation were used in the empirical equations available in the literature to obtain the stress-strain curve for all of the different mixes.

The accuracy of the analysis heavily relies on the appropriate selection and definition of these constitutive laws, as they dictate the mechanical properties

of the components in the simulation. Concrete beams, reinforcing steel bars and the position of loading plates are the main factors influencing the behaviour of flexural specimens. It is crucial to accurately model these elements in the finite element analysis in order to obtain precise and reliable results. Thus, material nonlinearity was used with a bilinear stress-strain relationship adopted using a combined isotropic and kinematic material-hardening model from Abaqus for the steel reinforcement in tension and compression, and shear links.

Table 6.1: Material parameters for concrete

Type of concrete*	**Concrete strength**		**Modulus of elasticity E_c (MPa)**
	f_c (MPa)*	**f_{ct} (MPa)***	
NRC	40.51	3.25	30,172
Micro 0.1PPFC	40.46	3.16	31,241
Macro 0.4PPFC	41.42	3.38	31,444
SFRC	43.48	5.03	31,069
HyFRC	43.61	5.86	31,916

*These were discussed in section 4.3.1 and 4.3.2.

6.1.3.3 Modelling concrete

Components must be linked to specific materials. Material properties can be linear or nonlinear, isotropic or orthotropic and may be either constant or temperature-dependent, depending on the type of analysis being conducted (e.g. linear elastic analysis or damage mechanics analysis). It is crucial to enter the appropriate material properties to analyse composite materials successfully. In order to obtain realistic results, the simulation of accurate concrete materials plays a vital role, as stated by Genikomsou and Polak, (2015). Table 6.1 lists the material parameters for concrete which were obtained through the experimental investigation. The material properties of the concrete, such as compressive and tensile strengths, can be obtained from tests such as concrete cylinder compression and splitting tests according to the EN BS 1881-116 (1983). However, these tests only provide average values for the concrete properties. To fully input the stress-strain behaviour of the concrete into Abaqus, a concrete

property model is necessary to capture the complete material response, as discussed in the next section.

Concrete damage plasticity model

The concrete beam was simulated using a concrete damage plasticity (CDP) model, which was based on a constitutive law from EC2, and incorporated exponential tension softening to replicate the processes of concrete crushing and cracking. The reason for utilising the CDP model in the present study is because it is more effective in accurately depicting the inelastic behaviour of concrete. The model is a continuum, plasticity-based, damage model for concrete. It assumes that the main two failure mechanisms are tensile cracking and compressive crushing of the concrete material. The CDP model in Abaqus employs a combination of isotropic damaged elasticity, as well as isotropic tensile and compressive plasticity. This particular option was utilised to define parameters such as yield function, flow potential, and viscosity. Different parameters were involved in this study for the CDP model, as summarised in Table 6.2, such as, the ratio of initial equibiaxial compressive yield stress to initial uniaxial compressive yield stress (f_{b0}/f_{c0}), the ratio of the second stress invariant to the tensile meridian to that of the compressive meridian (K_c), dilation angle is the direction of the plastic strain (ψ), and flow potential eccentricity (e).

Table 6.2: Concrete damage plasticity

Concrete type	Dilation Angle (ψ)	Eccentricity (e)	f_{b0}/f_{c0}*	K_c**
NRC HyFRC	31	0.1	1.16	0.667

*The default value is 1.16 based on Abaqus manual, **The default value is 0.667 based on Abaqus manual.

Modelling concrete in compression

The compressive response of normal concrete can be represented using a stress-strain curve in a uniaxial direction, as depicted in Figure 6.2. This curve is derived from Eq. 6-1 in Eurocode 2 (EN 1992-1-1, 2004), which describes the behaviour of concrete under compression.

$$\frac{\sigma_c}{f_{cm}} = \left(\frac{kh - h^2}{1 + (k-2)h}\right) \qquad \text{Eq. 6-1}$$

Where:

σ_c: is the compressive stress of the normal concrete

f_{cm}: is the characteristics compressive cylinder strength of normal concrete

$$f_{cm} = f_{ck} + 8 \quad \text{Eq. 6-2}$$

$$h = \frac{\varepsilon_c}{\varepsilon_{c1}} \quad \text{Eq. 6-3}$$

ε_{c1}: is the compressive strain of the normal concrete at the peak stress f_{cm}

$$\varepsilon_{c1} = 0.7 {f_{cm}}^{0.31} \leq 2.8 \quad \text{Eq. 6-4}$$

$$k = \frac{1.05 f_{cm} \times |\varepsilon_{c1}}{f_{cm}} \quad \text{Eq. 6-5}$$

$$E_{cm} = 22 \times \left(\frac{f_{cm}}{10}\right)^{0.3} \quad \text{Eq. 6-6}$$

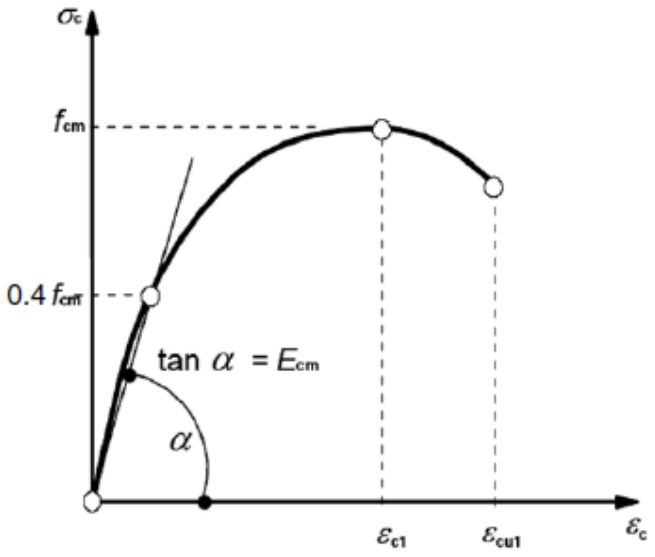

Figure 6.2: A graphical representation illustrating the relationship between stress and strain in concrete material, based on Eurocode 2 (EN 1992-1-1, 2004)

Equation 6-1 is applicable when the absolute value of compressive strain ($|\varepsilon_c|$) is between zero and the nominal ultimate strain ($|\varepsilon_{cu1}|$). For concrete having a characteristic compressive cylinder strength between 12-50 MPa, the nominal

ultimate strain (ε_{cu1}) can be assumed as 0.0035, according to Eurocode 2 (EN 1992-1-1, 2004). However, if the characteristic compressive strength of concrete is higher than 50 MPa, the ultimate compressive strain can be determined using the following expression Eq. 6-7.

$$\varepsilon_{cu} = 2.8 + 27\left[\frac{(98 - f_{cm})}{100}\right]^4 \qquad \text{Eq. 6-7}$$

It is assumed that the stiffness reduction caused by concrete crushing is zero. Therefore, there is no requirement for specifying compression damage data in the input. As per the Abaqus manual, when compression damage is not present, the plastic strain of concrete can be considered equivalent to the inelastic strain (Dassault Systemes, 2014). Figure 6.3 shows the compressive stress-strain curve and this data which was used as the material property for concrete.

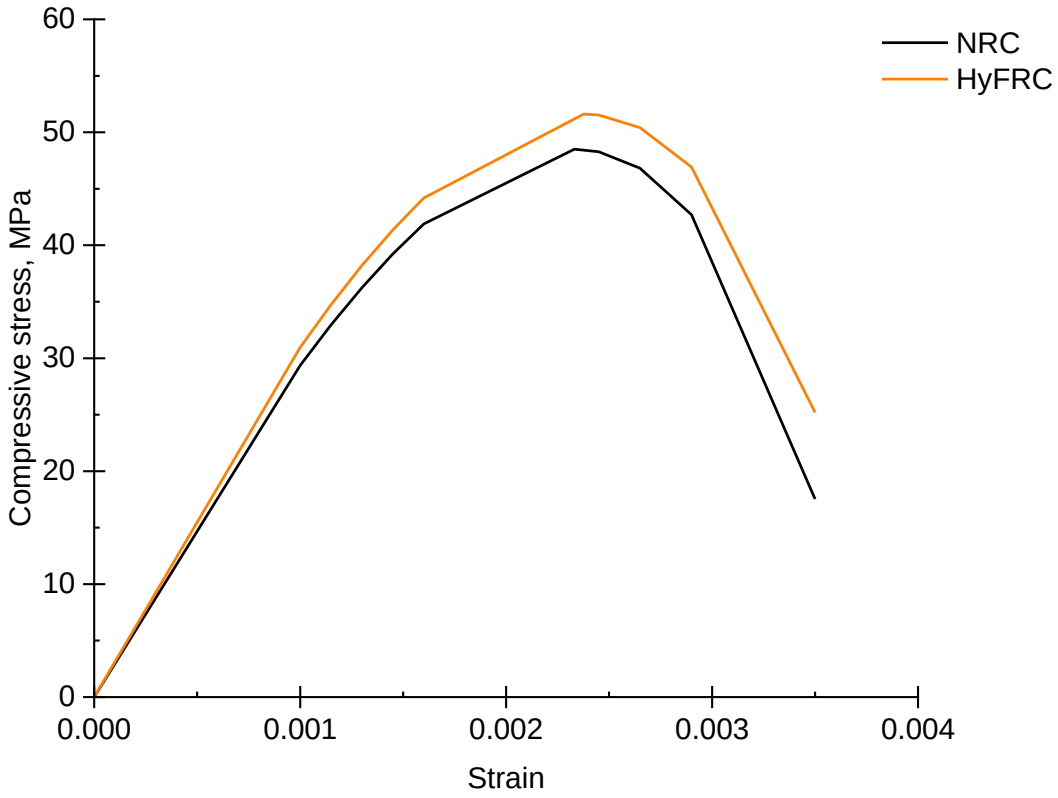

Figure 6.3: A graphical representation illustrating the relationship between stress and strain under compression for normal concrete material

Modelling Concrete in Tension

When considering concrete under tension, it is assumed that the tensile stress increases proportionally with the strain until the concrete eventually cracks. Introducing tension stiffening into the concrete modelling is to simulate load transfer across cracks through the rebar. Tension stiffening can be characterised by defining a post-failure stress-strain relationship or using a fracture energy cracking criterion. The post-failure behaviour for direct straining is modelled with tension stiffening, which allows to define the strain-softening behaviour for cracked concrete. This behaviour also allows for the effects of the reinforcement interaction with concrete to be simulated in a simple manner. Tension stiffening is required in the concrete damaged plasticity model. The appearance of cracks in concrete occurs at specific locations, and the concrete away from the cracks can still carry some tensile load. As a result, the reinforcement bars experience reduced deformation, and the overall deformation of the reinforced concrete member decreases, making the member stiffer than anticipated based on the assumption of concrete not carrying tensile loads. This additional stiffness is termed "tension stiffening" (Scott and Beeby, 2012). The choice of tension stiffening parameters is important since, generally, more tension stiffening makes it easier to obtain numerical solutions.

This approach represents the concrete's brittle behaviour using a stress-displacement relationship instead of a stress-strain relationship. There are different techniques for defining concrete's brittle behaviour using the fracture energy concept. The more accurate method of defining brittle behaviour uses an exponential expression, as experimentally established by Cornelissen et al., (1986) and illustrated in Figure 6.4. This can be calculated using the following equations:

$$\frac{\sigma_c}{f_t} = f(w) - \frac{w}{w_c} f(w_c) \qquad \text{Eq. 6-8}$$

$$(w) = \left[1 + \left(\frac{c_1 w}{w_c}\right)^3\right] exp\left(-\frac{c_2 w}{w_c}\right) \qquad \text{Eq. 6-9}$$

Where:

w: is the crack opening displacement.

w_c: is the crack opening displacement at which stress can no longer be transferred.

w_c: 5.14G_f/f_t for normal weight concrete.

c_1: for normal weight concrete, the constant c_1 is a material constant and its value is 3.0.

c_2: for normal weight concrete, the constant c_2 is a material constant and its value is 6.93.

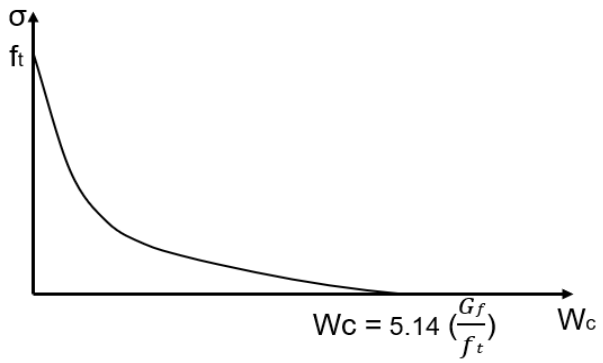

Figure 6.4: Exponential concrete tension softening model (Cornelissen et al., 1986)

The material model accounts for concrete damaged in tension. When a concrete crack appears, the elastic stiffness of the material is reduced. The reduction in elastic stiffness is determined by two damage parameters, namely d_c and d_t, which are considered as functions of the plastic strains. These damage parameters can vary between 0 (representing an undamaged state) and 1 (representing complete strength loss). The cracking displacement curve for normal concrete material is presented in Figure 6.5(a) and Figure 6.5(b), depicting the relationship between tensile stresses and cracking displacement, and tensile damage and cracking displacement, respectively. For the parametric study, the same formulae were utilised to represent the properties of normal concrete in both compression and tension.

$$G_f = 73 \times {f_{cm}}^{0.18} \qquad \text{Eq. 6-10}$$

G_f: fracture energy

f_{cm}: is the characteristics compressive cylinder strength of normal concrete

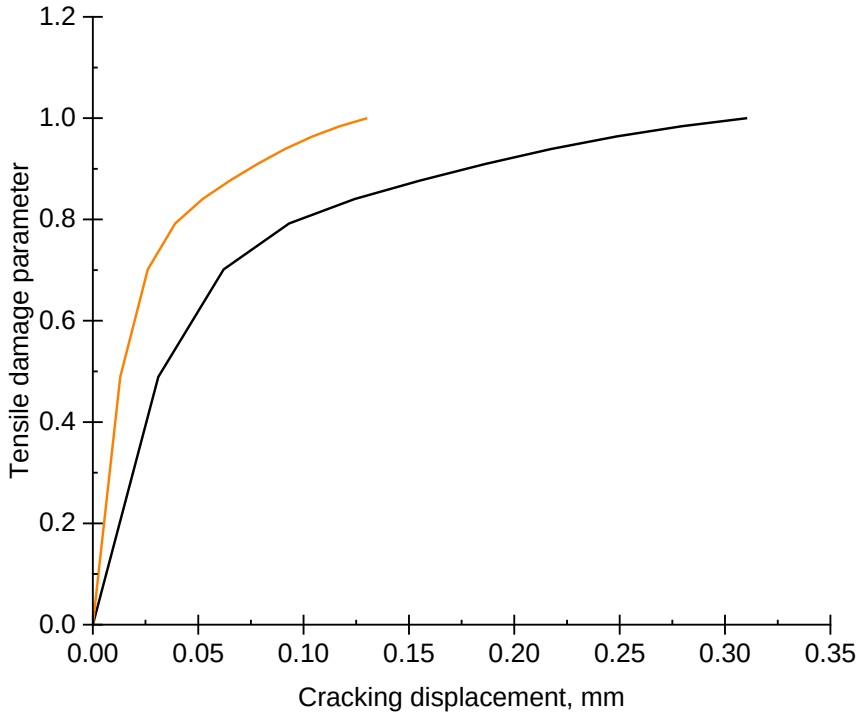

a) The relationship between tensile stresses and cracking displacement

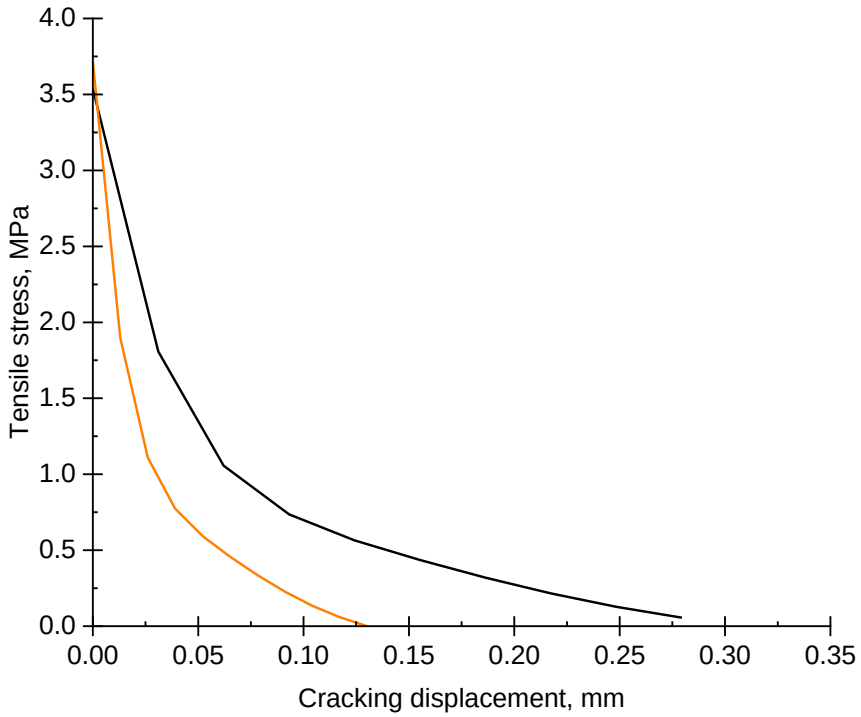

b) Tensile damage and cracking displacement

Figure 6.5: The cracking displacement curve for normal concrete material

6.1.3.4 Material modelling of steel reinforcement

The key elements of the model include the material properties of the reinforcing steel. The stress-strain curves for this material can be derived from steel tensile tests according to EN ISO 6892-1 (2009). Steel reinforcement and the surrounding concrete are bonded together in reinforced concrete members. Effects associated with the rebar/concrete interface, such as bond slip and dowel action, are modelled approximately by introducing some “tension stiffening” into the concrete modelling to simulate load transfer across cracks through the rebar. Material nonlinearity was used with a bilinear stress-strain relationship adopted using a combined isotropic and kinematic material-hardening model from Abaqus for the steel reinforcement in tension and compression and shear links, as shown in Figure 6.6. The true stress-true plastic strain relationships were established by modifying the engineering stress-strain curves for steel reinforcement.

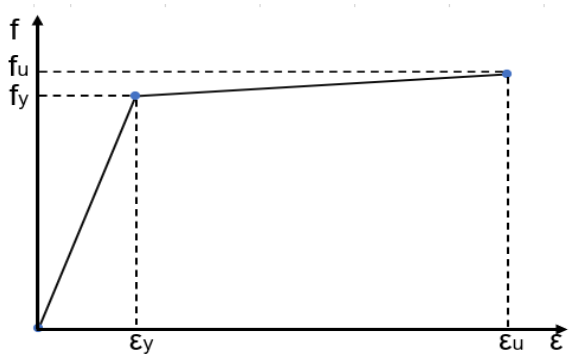

Figure 6.6: Material stress–strain curves

All the mechanical properties obtained from the manufacturer were used to define all the characteristics and behaviour of steel. The information was input into the Abaqus software, specifically into the elastic and plastic options, to define two different material behaviours. Table 6.3 provides a summary of the properties of the steel components. Each type of bar had a distinct definition for the cross-sectional area because they have different sizes of bars (8mm,10mm and 16mm) which were used in the tested beams, as summarised in Table 6.3.

Table 6.3: Properties of steel bars

Nominal diameter (mm)	Area (mm^2)	Modulus of elasticity (MPa)	Yielding stress (MPa)
8	50		
10	78.6	200,000	500
16	201.06		

6.1.3.5 Assembly and step field for defining the load case

If there are multiple components, it is necessary to assemble them into what is known as an assembly to create the physical object to be analysed, as shown in Figure 6.7. After that, the analysis process is usually divided into several stages, each representing distinct loading and constraint conditions. There must be a minimum of two stages: an initial stage and at least one additional stage. The applied loads cannot be applied during the initial stage, whereas the boundary conditions are only applied.

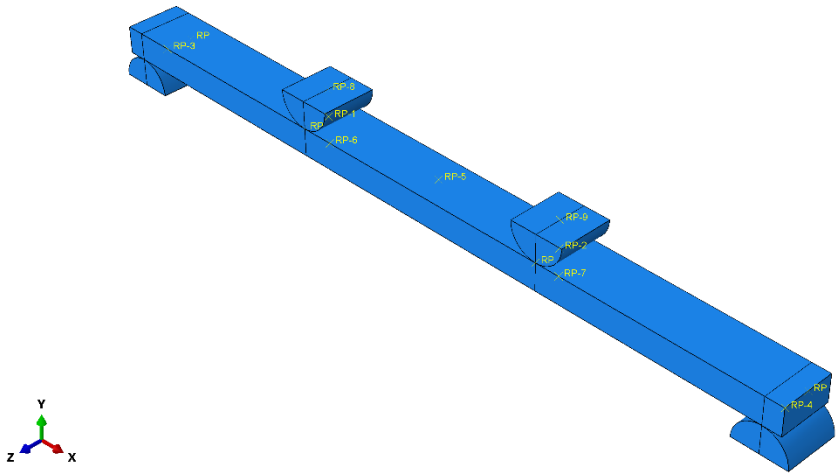

Figure 6.7: Model Assembly

6.1.3.6 Loads

When conducting structural analysis, the model is subjected to a range of loads, which include forces, pressures, inertial forces such as gravity, and specified displacements. The loading points and the support points were each secured by two rigid steel plates on the top and the bottom of the specimens, respectively. In this investigation, displacement control was utilised, where a downward enforced displacement was applied to the top surface of the loading steel plate, as illustrated in Figure 6.8(b). In this research, a time-controlled method known as dynamic explicit analysis was employed. Also, the gravity load was applied to the model. Regarding repeated test in FEA, the only difference between the static and repeated test, was that the load-controlled was applied to simulate the scenario of the experimental tests.

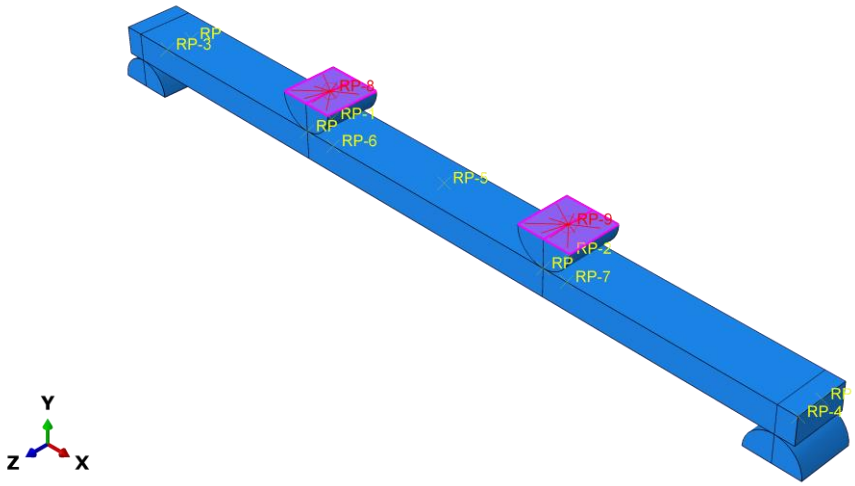

a) Coupling of loading plate

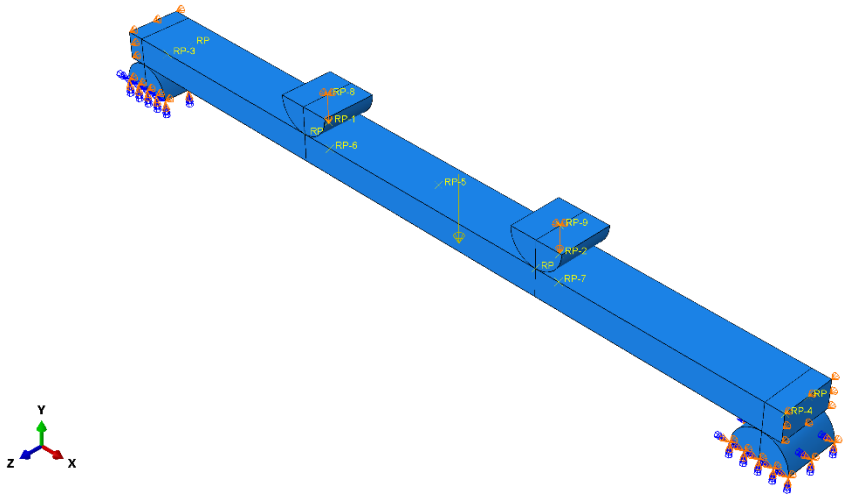

b) Boundary condition for both supports: hinge and roller

Figure 6.8: Applied load and boundary conditions

6.1.3.7 Contact interaction and boundary conditions

In the FEA, contact interactions and boundary conditions play crucial roles as they involve the representation of physical processes related to surface-to-surface interactions and boundary conditions in numerical simulations. The structures considered in the analysis can be either two-dimensional (2-D) or three-dimensional (3-D) and may involve small or finite sliding. The boundary conditions are shown in Figure 6.8.

Constraints were employed to limit the movement of certain parts of the model in several ways to mimic the experimental test. As a Coupling Constraint links the movement of a surface to the movement of a single point, such a constraint was used to connect the surface of the loading plate to the point where the load was applied. In order to define the contact interaction between the loading plates and the concrete beams, the Abaqus software utilised a surface-to-surface contact feature. The desired contact behaviour was achieved by implementing a "Hard" contact in the normal direction. This prevented the loading plates from penetrating into the concrete beams. In order to maintain the structural integrity and absorb some stresses, the contact was made stiffer in the finite element analysis (FE). Furthermore, the effect of contact was evaluated by applying the load using a point load. Similar results were obtained between hard and soft contact point, confirming the validity and reliability of the modelling approach. The contact interactions for the finite element (FE) model are illustrated in Figure 6.9. The contact interaction was implemented at the interface between the concrete beam and the loading plate, as shown in Figure 6.9. In this interaction, a friction coefficient of 0.35 was assumed on the basis of a sensitivity analysis. In this analysis, the friction coefficient was varied within the range of 0.15 to 0.35. Despite the variation in the friction coefficient, the obtained results remained consistent and comparable. This indicates that the outcomes were not significantly influenced by changes in the friction coefficient within the specified range.

The connection between the surrounding concrete and the steel reinforcement is present in reinforced concrete members. The analysis assumes that there is no slip occurring between the reinforcing steel bars and the concrete beams. As a result, it was necessary to assume that the steel reinforcement and concrete had a perfect bond, and the steel reinforcement was represented using one-dimensional bar components.

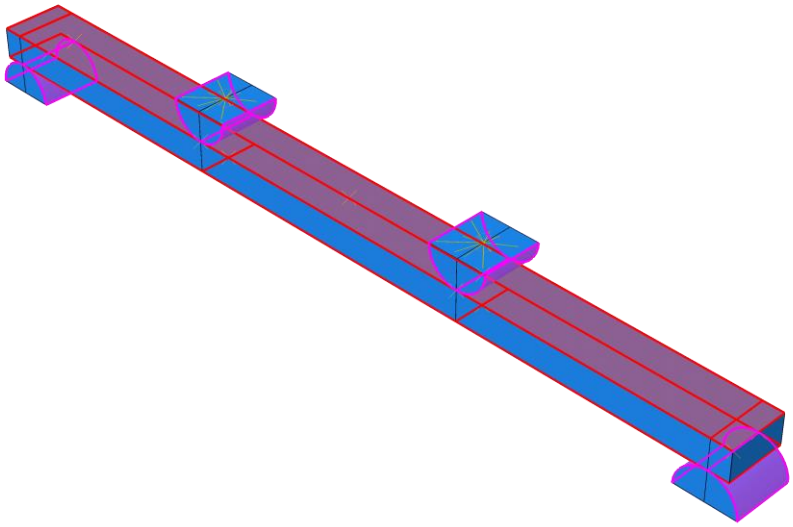

Figure 6.9: Interaction between concrete and loading plates

In this research, it was noted that a perfect bond is implemented using "embedded constraint" to describe the relationship between concrete and reinforcement. The bond between the concrete and steel reinforcement is represented by the symbol shown as a yellow circle, which in Abaqus represents the bond, as shown in Figure 6.10. This means that there is no slip between the embedded region (i.e., reinforcement) and the host region (i.e., concrete beam). In other words, two bodies are in perfect contact with each other, and their relative motion is zero. This technique of embedded constraint (perfect bonding) could have some limitations. For instance, under excessive load, the concrete might crack and cause a separation from the rebar which might not be represented in the model with a perfect bond assumption. In this case, the perfect bond assumption may become unpractical. However, in reality, there is some slippage between concrete and rebars, but this is usually very small. In this FEA validation, the load-deflection behaviour in the tested concrete beams were the area of interest to avoid computationally expensive. Thus, utilising an 'Embedded' command for modelling simplicity, where the presumption is that the inner bars are perfectly bonded to the concrete, the concrete and internal reinforcements were combined. Thus, this embedded element technique can be used to model rebar reinforcement. (Dassault Systemes, 2014).

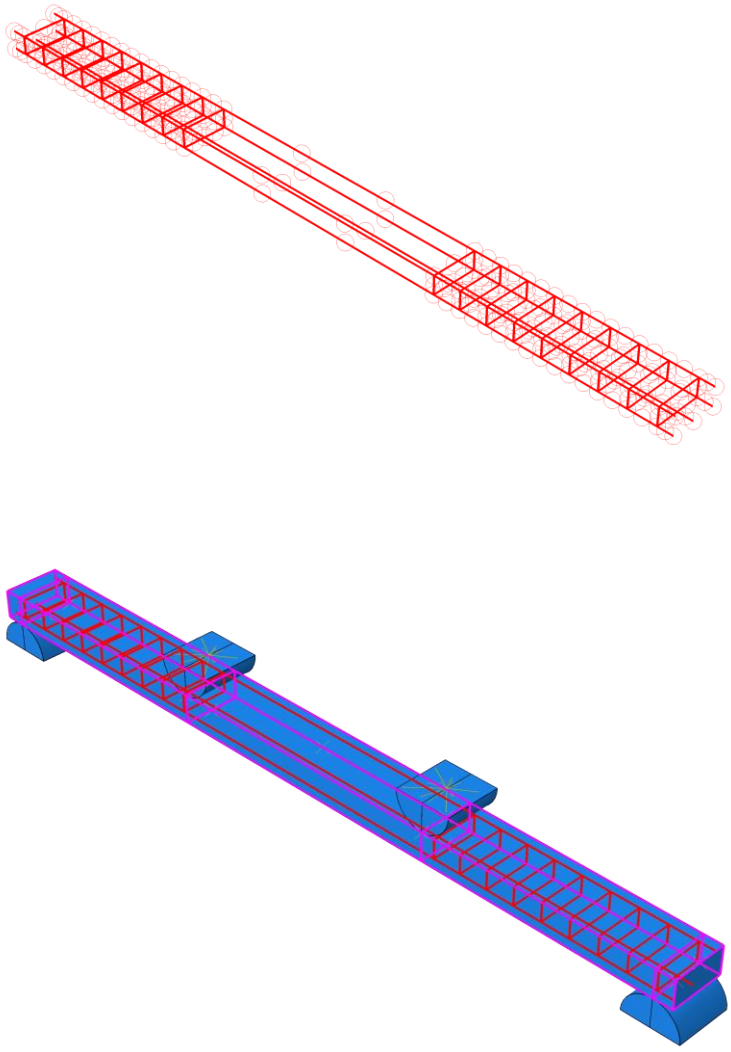

Figure 6.10: Embedded constraint of reinforcement

6.1.3.8 Mesh generation

The fundamental modelling concepts, including the definition of nodes and surfaces, conventions and input formats for using Abaqus, are thoroughly explained by Karlsson and Sorensen, (2006a). Once the material properties of the individual components are inputted, the model is assembled accordingly. Ultimately, the next stage in the process is to create a mesh for the assembled model. To proceed with the analysis, the assembly needs to be divided into smaller elements, which is referred to as meshing.

There are various methods of meshing a model. In finite element modelling, creating a high-quality mesh is critical to obtain accurate results. Generally, a finer mesh will yield better results, but the number of elements in the model will increase computation time. The number of seeds depend on the

desired size of the element or the number of elements that is required throughout the length of the edge, and Abaqus/CAE will, wherever possible, place the mesh nodes on the seeds. All the elements in the model were intentionally allocated the same size of the mesh to ensure that each of the two different materials shares the same node in order to achieve precise results from the FEA model. An ideal mesh should have well-shaped elements with minimal distortion and aspect ratios that are not too extreme. This helps to ensure accurate and reliable numerical results. A well-shaped mesh allows for a more precise representation of the physical problem and reduces the introduction of errors due to element distortion. Additionally, maintaining moderate aspect ratios helps to prevent numerical instabilities and improves the convergence behaviour of the FEA solution. To minimise analysis time, the model with the intermediate mesh size was used because it needed less time and computer storage than the one with the finer mesh for the overall size of the model. As discussed in the next section, a convergence sensitivity study was performed to determine the optimal mesh size. For the concrete components and steel reinforcement, a mesh size of 20 mm was chosen for the whole beam to avoid convergence with different components. Figure 6.11 illustrates the mesh that was employed for the finite element investigation. The overall mesh size was set to 20mm, with the smallest size being approximately 20mm. The finite element mesh of the specimen is shown in Figure 6.11.

To model reinforcing bars and reinforcing stirrups parts, a linear approximation of displacement, two nodes, and three translational degrees of freedom were used in a 2-D two-node truss element (T3D2). The steel bar portion was modelled as a truss element (T3D2) and the concrete part was modelled with a brick element (C3D8R).

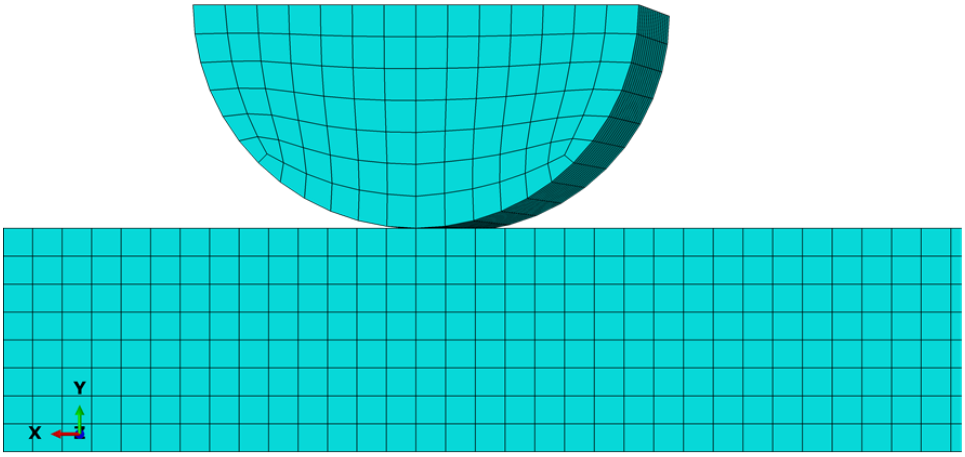

a) XY view

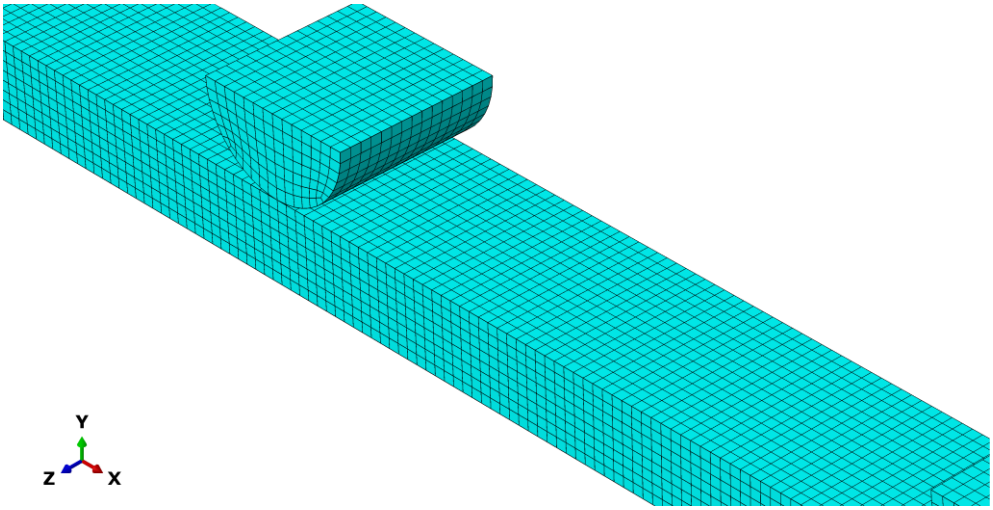

b) XYZ view

Figure 6.11: Clarity of the mesh size for the whole model

6.1.3.9 Convergence problems

Mesh sensitivity analysis in Abaqus refers to the process of examining the impact of mesh size on the accuracy of finite element analysis (FEA) results. It involves systematically varying the number of elements and/or nodes in the mesh to determine the optimal mesh size for the FEA model. It is important to perform mesh sensitivity analysis because an excessively coarse mesh can lead to inaccurate results. In contrast, an overly fine mesh can be computationally time-consuming and need more storage for storing data and may not significantly improve the accuracy of the solution. As shown in Figure 6.12, the number of elements and nodes in the mesh increased with a decrease in the mesh size. The number of elements and nodes in the mesh has a direct impact on the accuracy

of FEA results. Generally, an increased number of elements and nodes can result in more accurate results, but it also increases the computational time required to run the simulation. Therefore, selecting an appropriate mesh size for an FEA model requires balancing accuracy and computational efficiency.

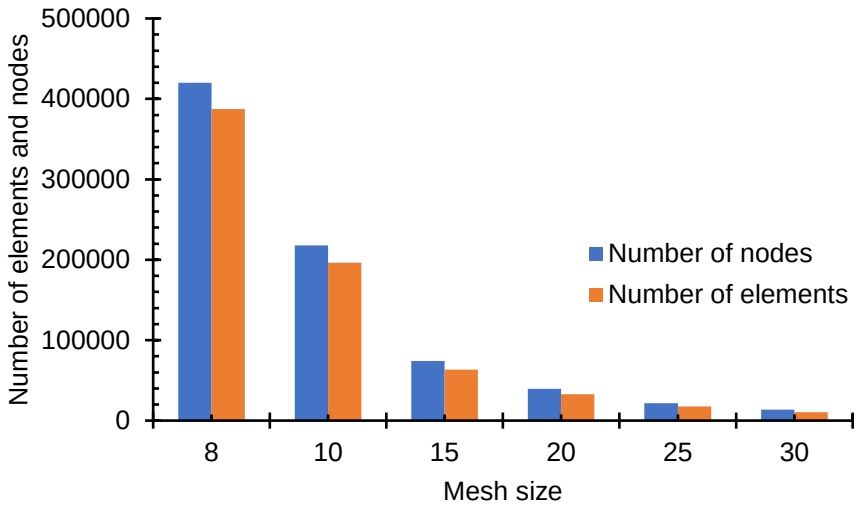

Figure 6.12: Change on the number of elements and nodes with different mesh size in (mm)

The effect of mesh size on accuracy can differ based on the type of analysis and geometry of the model. In general, smaller mesh sizes can provide more accurate results for linear statically analysis. The required number of elements and nodes for accurate FEA results can also depend on the geometry's complexity and areas of high strain or stress concentration. In such cases, mesh refinement may be required in these areas to obtain precise outcomes. Four different element sizes were employed to determine the best size for the full-scale specimen in FEA. The three smallest element sizes were 8mm, 10mm, and 15mm, while the other mesh sizes were 20mm, 25mm and 30mm. However, the mesh size of 8mm was not tested because the Academic Teaching Licence for Abaqus restricts the number of nodes to 250000. Additionally, the mesh size of 10mm was not completed and stopped prematurely for unknown reasons during the analysis. According to Figure 6.13, the mesh size of 15mm and 20mm showed almost the same behaviour and the same values for load-deflection. Therefore, a mesh size of 20mm was selected for further analysis based on the computational time and storage data.

6.1.3.10 Post-processing and visualisation

The process of post-processing and visualisation involves analysing the simulation results and presenting them in a graphical format that is easy to comprehend. After the solution has been computed, the post-processor can be utilised to examine and analyse the outcomes, which can be reviewed either graphically or by presenting the numerical values in a list. Due to the large volume of results that a model typically produces, it is often more efficient to use graphical tools for analysis.

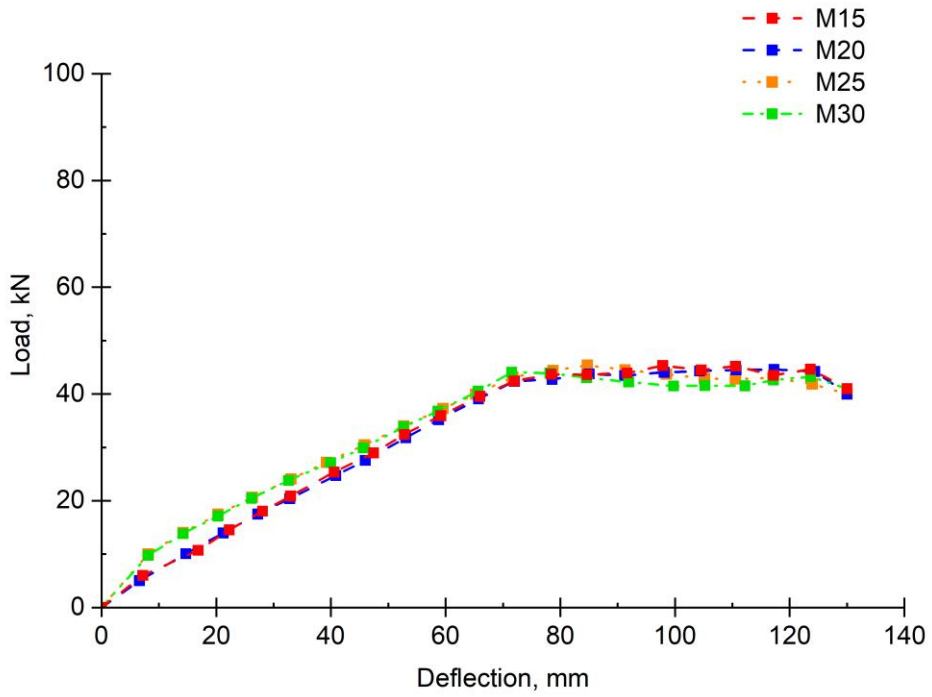

Figure 6.13: Mesh convergence

6.1.4 Validation study results

One common approach to compare and validate the results is to report the data in a table and create a graph to visually compare the data patterns and use statistical analysis to evaluate the degree of correlation between the experimental outcomes and FEA simulations. Table 6.4 and Table 6.5 summarise the results of the FEA and experimental results for different types of concrete under static and repeated loads. Based on the results of the experimental and FEA models for the normal concrete, Figure 6.14 displays the best fit for predicting the visually observed load-deflection curve of the FEA models.

Table 6.4: Comparison between the static results of FEA models and experimental results (maximum deflection and failure loads)

Type of the model beam	Concrete strength		Modulus of elasticity	Experimental		FEA model		Ratio	Ratio
	f_c (MPa)	f_{sp} (MPa)	E_c (MPa)	Max. load (kN)	Max. deflection (mm)	Max. load (kN)	Max. deflection (mm)	Max. load (EXP/FEA)	Max. deflection (EXP/FEA)
NRC-ST**	40.51	3.25	30,172	45.91	126.47	44.60	130	1.03	0.97
SFRC-ST	43.48	5.03	31,069	54.25	118.63	55.97	118.63	0.97	1.00
HyFRC-ST	43.61	5.86	31,916	58.92	108.31	58.30	110.98	1.01	0.98
Mean	**-**	**-**	**-**	**-**	**-**	**-**	**-**	**1.00**	**0.98**
S.D	**-**	**-**	**-**	**-**	**-**	**-**	**-**	**1.00**	**0.99**

* The reason for not testing all the five types of concretes was because restrictions were imposed on lab utilisation for each research project following the Covid-19 related closure of the labs in 2020 and 2021. **ST stand for static test.

Table 6.5: Comparison between the repeated loading results of FEA models and experimental results (maximum deflection)

Type of the model beam	**Concrete strength** f_c **(MPa)**	f_{sp} **(MPa)**	**Modulus of elasticity** E_c **(MPa)**	**Experimental Deflection (mm)**	**FEA model Deflection (mm)**	**Ratio (EXP/FEA)**
NRC-RP* (20%-80%)	40.51	3.25	30,172	57.19	61.60	0.93
HyFRC-RP (20%-80%)	43.61	5.86	31,916	69.16	75.92	0.91
HyFRC-RP (30%-70%)				81.93	86.36	0.94

*RP stand for repeated test.

The prediction model of FEA underestimated the maximum load value of NRC beam by 2.85% compared to the experimental results. Similarly, the prediction model for the HyFRC beam showed a slight reduction when compared to the experimental results and this reduction was only 1.05%. However, in the case of SFRC, the prediction model for the SFRC beam slightly overestimated the maximum load by 3.17% compared to the experimental results. The values of the maximum deflection from the FEA model and experimental results are also reported in Table 6.4. The FEA model over-predicted the maximum deflection of the NRC and HyFRC models when compared to the experimental results by approximately 2.79% and 2.47%, respectively. However, the prediction value for the maximum deflection of the SFRC model was in good agreement with the experimental results.

Similarly, the deflections for the repeated load test were obtained from the FEA, which were compared with the experimental results, as summarised in Table 6.5. Load level of 20-80% was conducted in FEA only for the NRC beams as it was time-consuming for conducting other load levels. In contrast, FEA analysis was conducted both load levels of 20-80% and 30-70% for HyFRC beams. As reported in Table 6.5, the ratio of experimental results of NRC beam to FEA results showed a value of 0.93. The ratio of experimental results to FEA results of HyFRC beams for load levels of 20-80% and 30-70% showed a value of 0.91 and 0.94, respectively. However, these results gave an indication that the results of FEA showed more conservative value compared to the experimental results.

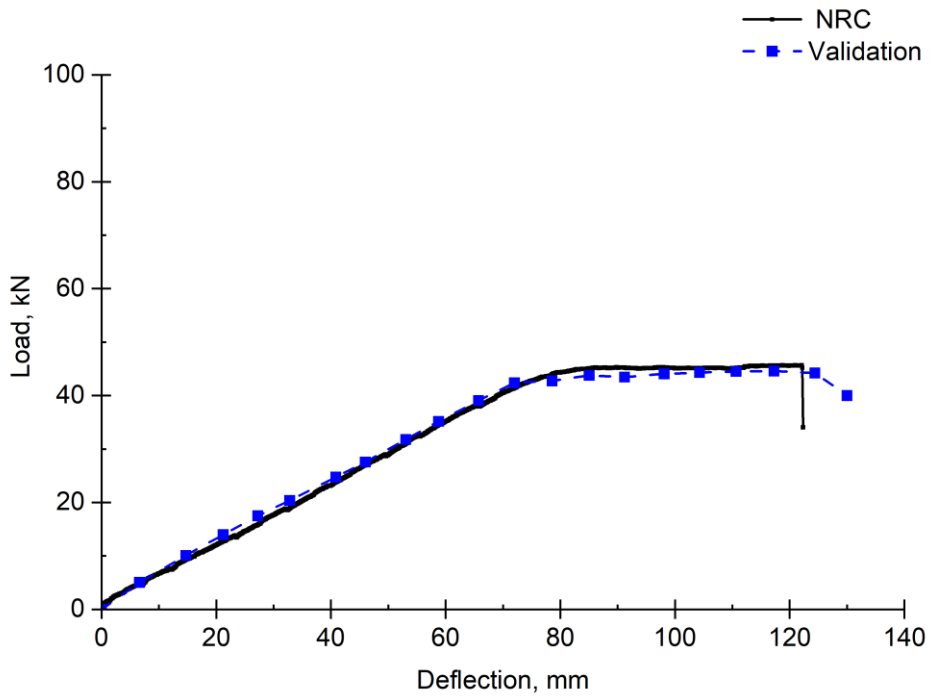

a) Comparison between experimental and FEA results of NRC beam

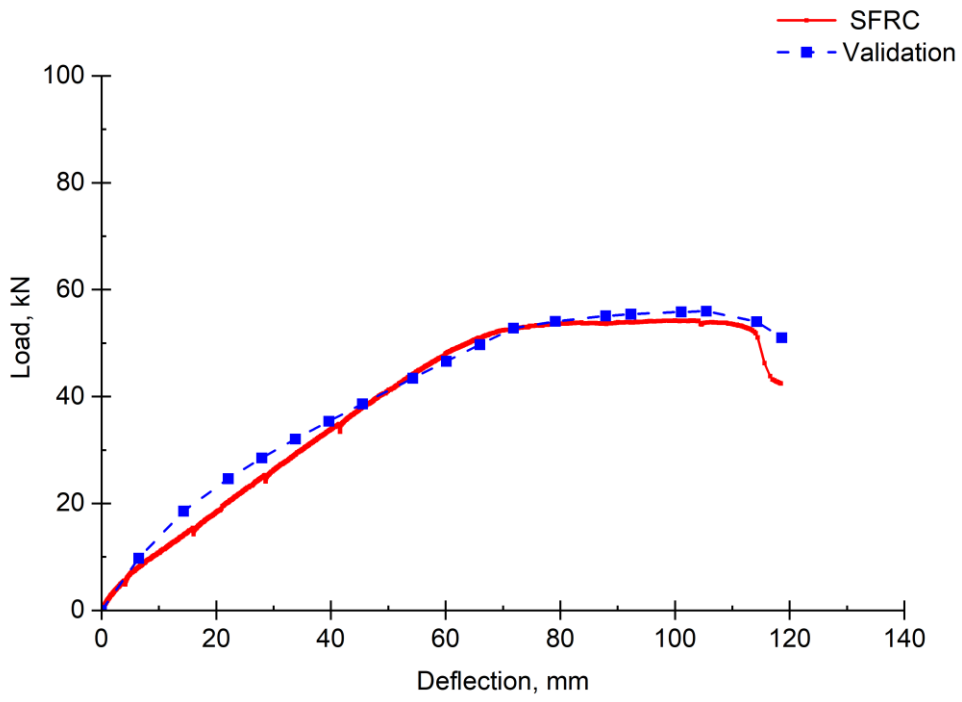

b) Comparison between experimental and FEA results of SFRC beam

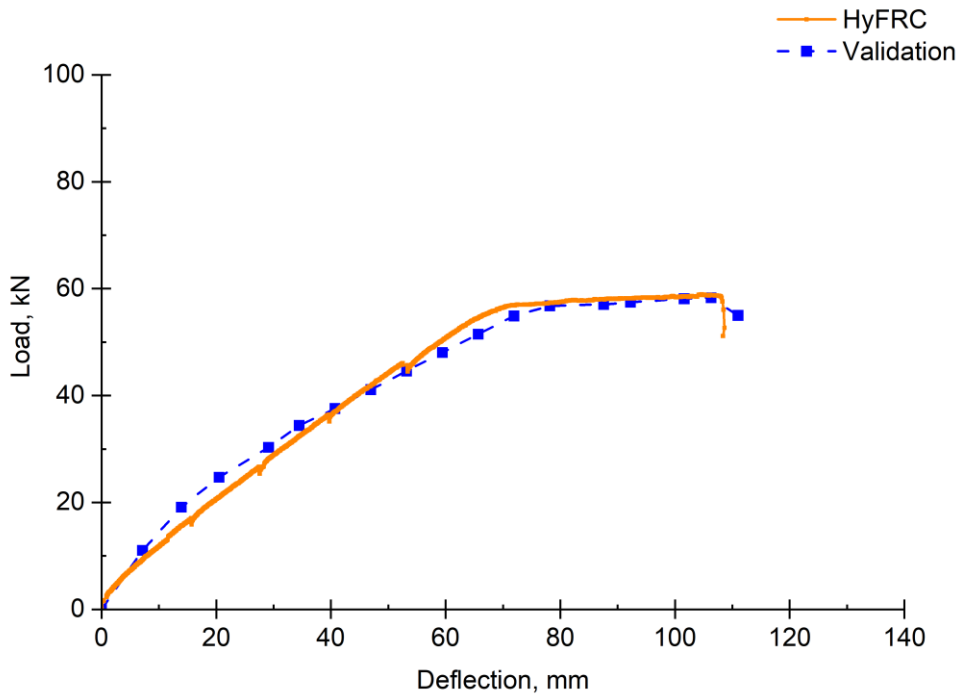

c) Comparison between experimental and FEA results of HyFRC beam

Figure 6.14: Comparison between experimental results and FEA models: a) NRC, b) SFRC and c) HyFRC beam

The maximum load and deflection results from all the experimental results and FEA models were found to have a correlation coefficient of 0.959 and 0.963, respectively, indicating a strong relationship in regression analysis between the experimental results and FEA model predictions.

The maximum load for all experimental results and FEA models was accurately predicted, with a mean value of 1.0 and a standard deviation (SD) of 1.0. Furthermore, the fact that the mean value for the maximum load was 1.0 with a standard deviation of 1.0 suggests that, on average, the FEA model accurately predicted the behaviour of the experimental specimens. The standard deviation of 1.0 indicates that the predictions have some variability around the mean, which is expected due to factors such as the assumption on bond failure and modelling assumptions. Overall, the level of accuracy appears to be reasonable, indicating that the FEA model predictions were similar to the maximum load for the experimental specimens.

Similarly, the maximum deflection results from both the experimental results and FEA models show a mean value of 0.98 and a standard deviation

(SD) of 0.99. This indicates that, on average, the FEA model predictions were closely similar to the maximum deflection of the experimental specimens. The close similarity between the mean value of the FEA predictions (0.98) and the average behaviour of the experimental specimens suggests that the FEA model captured the overall deflection trends well. However, the standard deviation of 0.99 indicates some variability around the mean, which could be due to factors such as the assumption on bond failure and modelling assumptions. Overall, the provided results indicate a reasonably good agreement between the FEA model predictions and the experimental data for maximum deflection.

The lack of smoothness in the validation curve of the FEA model, as shown in Figure 6.14, compared to the experimental results, could be attributed to several factors. One possible reason is in relation to the stress-strain curve defined in the CDP model. The CDP model was utilised to simulate the behaviour of concrete, including its cracking and softening response. The stress-strain curve defined within the CDP model plays a crucial role in capturing the material's behaviour, particularly during the post-cracking stage. If the stress-strain curve is not accurately calibrated or fails to fully capture the material's response, discrepancies between the FEA model predictions and the experimental results may arise.

In the stress-strain curve, there are elastic and plastic regions. In the elastic regions, the behaviour of the specimen depends not only on the material and cross-sectional geometry but also on the boundary conditions. Therefore, it can be observed in Figure 6.14(a) that the FEA model accurately captures the behaviour of the NRC specimen in the elastic zone and the plastic behaviour well. However, in SFRC specimens, as shown in Figure 6.14(b) and Figure 6.14(c), the FEA models exhibit minor differences in the elastic zone. The current equations used in FEA modelling are based on normal concrete, so new equations are needed to account for the effect of fibres. Therefore, this lack of smoothness can be attributed to strains recorded up to the first cracking of the SFRC and HyFRC specimens, for which the strain gauge functioned, plotted against their corresponding stress.

Regarding the behaviour at the end of the test, the failure mode of the normal concrete specimens was indeed observed to be a brittle flexural failure. However, the FEA model exhibited a different behaviour, showing a softening

response in the post-cracking stage. This softening behaviour was achieved through the implementation of the CDP formulation in the model. This formulation allowed for the representation of the material's response beyond the initial cracking, preventing rapid failure and capturing the softening behaviour typically observed in real-world concrete structures. The failure mode of the SFRC beams showed a softening behaviour in the post-cracking stage, which was found in the FEA model as well. Figure 6.15 shows the area where the initiation of cracks and crack patterns are likely to form based on the stress profile and the steel stress of the FEA model results. This figure showed concentrations of stress forming where the crack will be forming in this area. Figure 6.15(a) shows the crack patterns at the end of experimental test. While Figure 6.15(b) proves the ability of proposed FEA model to predict the crack pattern. Also, it indicates the presence of high peaks along this region. The presence of peaks in Figure 6.15 indicates the likely locations of cracks and offers insights into the position of the neutral axis. Notably, the finite element analysis predicts more cracks compared to the experimental results. Regarding the crack formation, it is important to note that at the location of a crack, there is no tension capacity present.

The crack patterns showcased in Figure 6.15 depict the observed or simulated crack formations resulting from the analysis conducted using the FEA model. Figure 6.15 relates to the distribution and magnitude of stress within the concrete beam and steel material. It also indicates that the stresses were concentrated in concrete beams rather than in the supports. This means that the supports were in the elastic region. In the FEA model results, the steel stress is a significant parameter that was examined. Figure 6.15 provides visual representation or data related to the steel stress in the context of the analysis. It indicates regions where the steel experiences higher stress concentrations and regions with lower stress. Understanding the steel stress distribution is crucial for evaluating the behaviour and performance of the reinforced concrete under various loading conditions. Overall, Figure 6.15 displays the initiation of cracks, crack patterns, and steel stress obtained from the results of an FEA model. It serves as a visual or graphical representation of the analysed data, to gain insights into the crack behaviour and steel stress distribution in the studied system.

a) The final crack pattern of the experimental results before the failure occurred

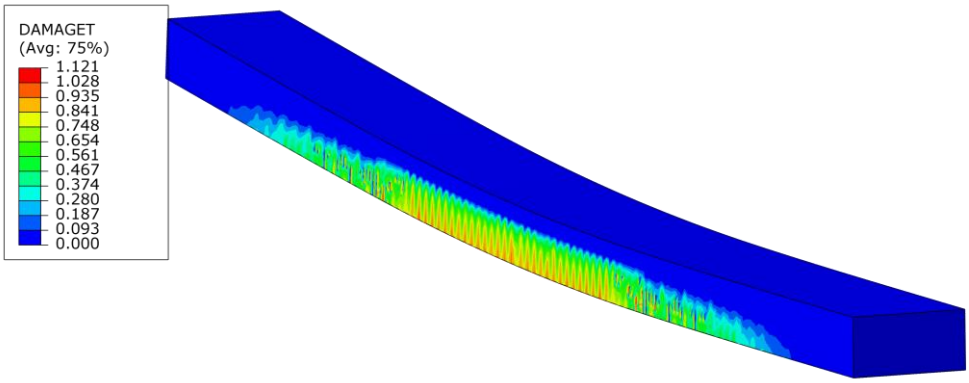

b) Concrete tensile damage -crack pattern- in FEA model

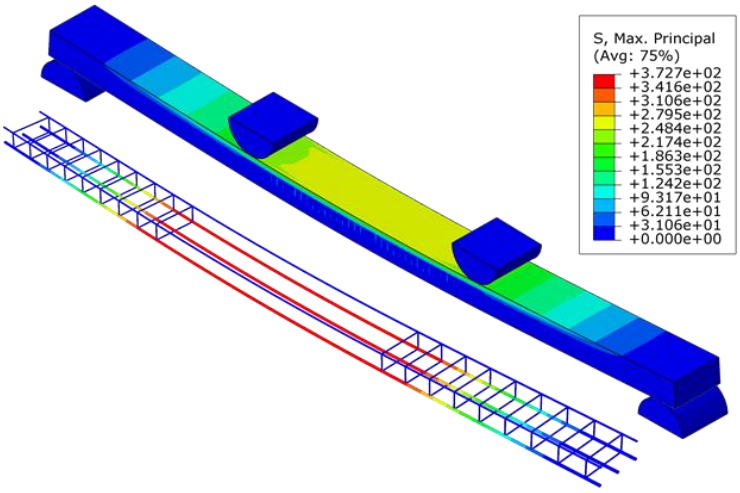

c) Von Mises stresses of concrete beam and the embedded steel rebars

Figure 6.15: FEA model results: crack pattern and steel stress

The validation carried out above has demonstrated a remarkable consistency between the experimental test results and FEA results in terms of

the maximum failure load, maximum deflection, and crack pattern. The observed load-deflection curve of the experimental results and FEA models perfectly match, indicating that the FEA model has been properly calibrated and can accurately replicate the behaviour of the experimental specimens. This confirms the reliability of the FEA model used in the validation process, and it can be employed for a parametric study on the behaviour of the flexural strength of full-scale beams. Based on the comparison and the results of the FEA, the outcomes are consistent, and it is probable that the FEA model is reliable and can be applied for further examination in parametric study of full-scale beams with and without fibres when subjected to the static load.

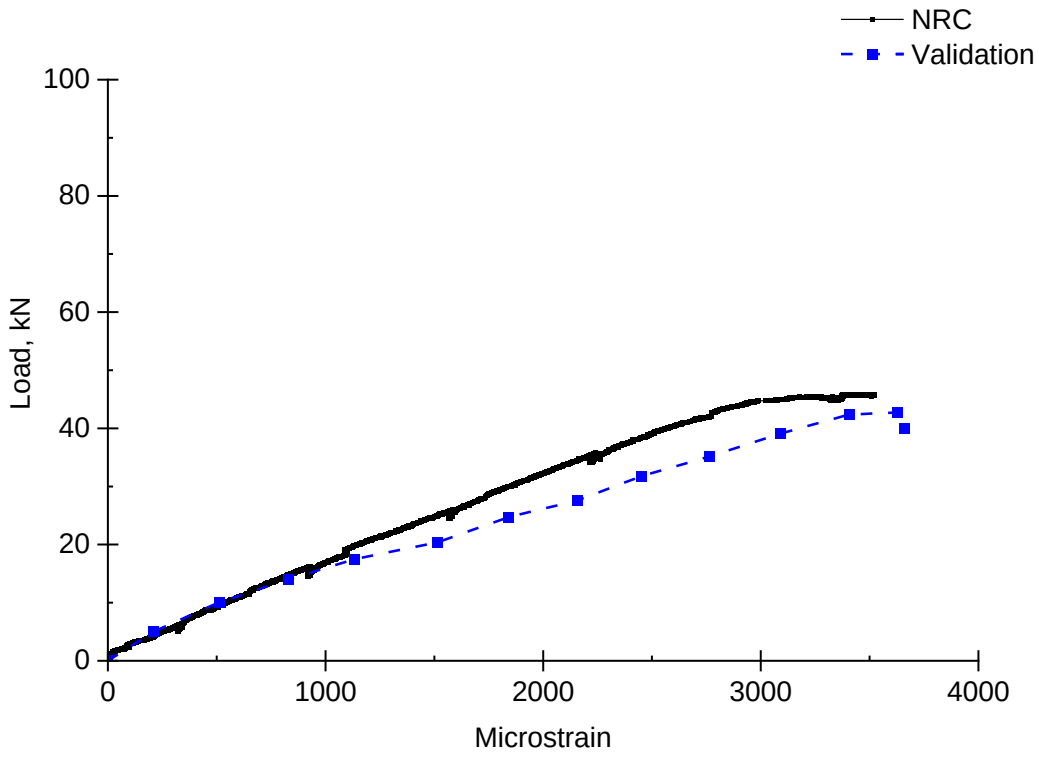

a) NRC

Figure 6.16(a) reveals a notable alignment with the strain in the steel reinforcement concerning the experimental results, particularly up to a load of 45% of the ultimate load, indicative of proximity to the applied load required to establish a stabilized crack pattern. However, beyond this point, it begins to overestimate the results until the experiment's ultimate failure. This overestimation amounted to approximately 27%, signifying a conservative prediction by the FEA method in comparison to the experimental results.

Figure 6.16(b) displays a similar trend in results obtained from the FEA prediction when compared to the experimental results. The FEA results initially underestimated the strain in the steel reinforcement until reaching a load of 30 kN, where the two curves intersected. Beyond this point, the FEA began to overestimate the experimental results. The underestimation percentage was approximately 13%, while the overestimation percentage after 30 kN was about 11.89% in comparison to the strain in the steel reinforcement of the experimental results.

In the case of HyFRC, Figure 6.16(c) demonstrates that the strain in the steel reinforcement was nearly identical with only a small variation, approximately 6% difference between the experimental and FEA prediction results. However, the FEA prediction displayed an overestimation of the experimental results by approximately 21%. It can be concluded from the NRC and HyFRC predictions that the strain in the steel reinforcement exhibits similar results that approach the applied load required to induce a stabilized crack pattern.

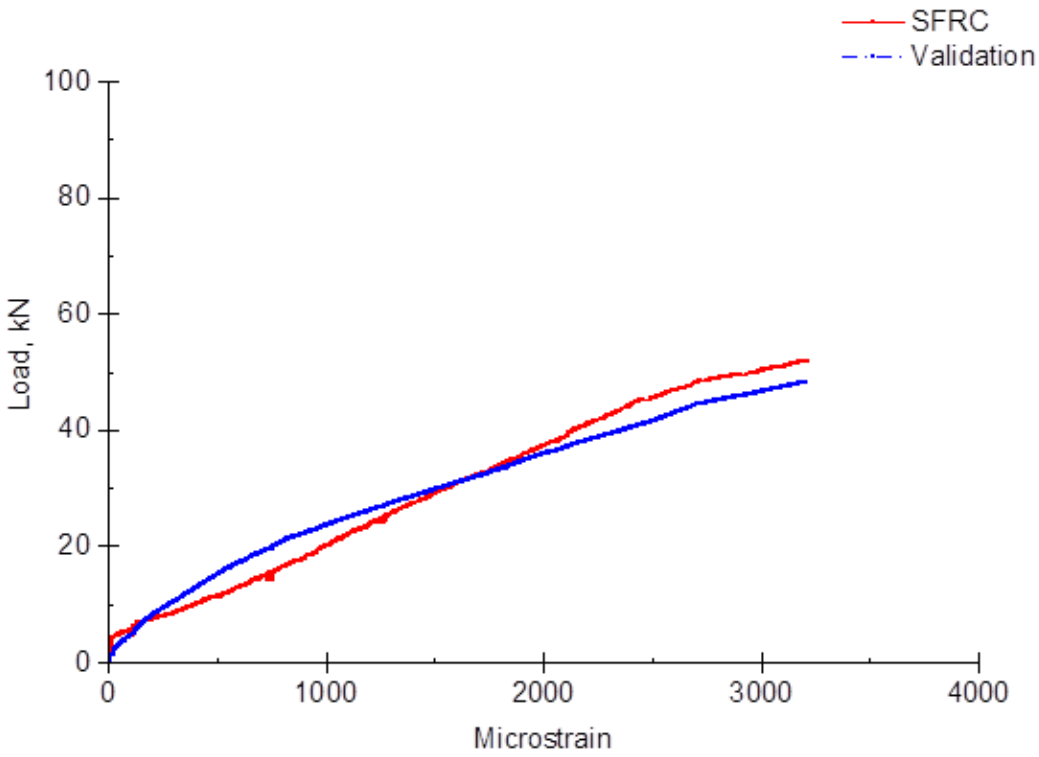

b) SFRC

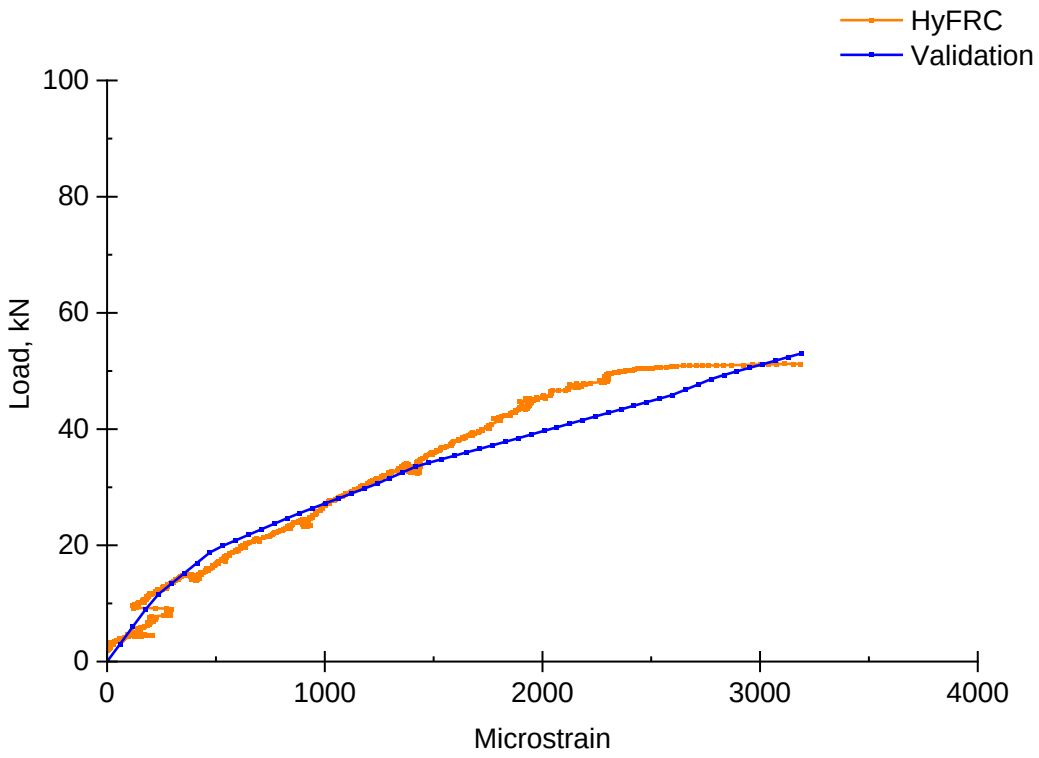

c) HyFRC

Figure 6.16: Load vs strain behaviour of the embedded steel rebars of the experimental results and FEA models

6.1.5 The parametric analysis

This section describes the parametric research using FEA. The purpose of the parametric study was to assess the applicability of the current model with specimens that could not be tested experimentally in this research, viz. 0.1% micro polypropylene fibre (0.1PPFC) and 0.4% macro polypropylene fibre (0.4PPFC). In addition, a detailed finite element analysis (FEA) model of the flexural behaviour of a set of beams reported in a previous study by Sryh, (2017) was utilised. The previous type of models were validated using the experimental results, so these can be used to predict the performance of experiments that were not studied experimentally in this research, especially 0.1PPFC and 0.4PPFC. The FEA parametric study investigated varying parameters, including the strength of concrete with and without fibres, viz. 0.1PPFC and 0.4PPFC, as shown in Figure 6.17. Additionally, the study considered NRC, 0.5% SFRC and 1.0% SFRC, as shown in Figure 6.18 and reported in Table 6.6. These modelling parameters were sourced from the current research study and were not

experimentally tested. Furthermore, to validate the models, some of these parameters were adopted from a previous study conducted by Sryh (2017).

The result obtained from the FEA and the findings by Sryh (2017) suggest that the model exhibited similar results for NRC followed by 1.0% SFRC, while a reduction was observed in the case of 0.5% SFRC, as shown in Figure 6.18. The validation model showed a ratio of 0.98, 0.93, and 0.96 for NRC, 0.5% SFRC, and 1.0% SFRC beams, respectively, when comparing the experimental results to the model predictions, as reported in Table 6.6. The parametric study conducted in this research, based on the test results reported by Sryh (2017), demonstrated that the FEA model provided accurate predictions for NRC, 0.5% SFRC and 1.0% SFRC. These findings indicate that the model performed very well for NRC, followed by 1.0% SFRC, while there was a reduction in accuracy for the 0.5% SFRC case. The variation in accuracy could be attributed to the different mechanical properties and behaviours of the materials used. The NRC beams may exhibit more predictable behaviour, potentially leading to slightly better model performance compared to the SFRC beams. The presence of steel fibres in the SFRC beams, especially at a lower percentage (0.5% SFRC), could introduce some complexity and uncertainty in the material response, which may have contributed to a relatively small reduction in prediction accuracy. However, it's essential to note that the differences in accuracy between NRC and SFRC models are not substantial, and the overall predictive capabilities of the FEA model appear reasonable for both cases.

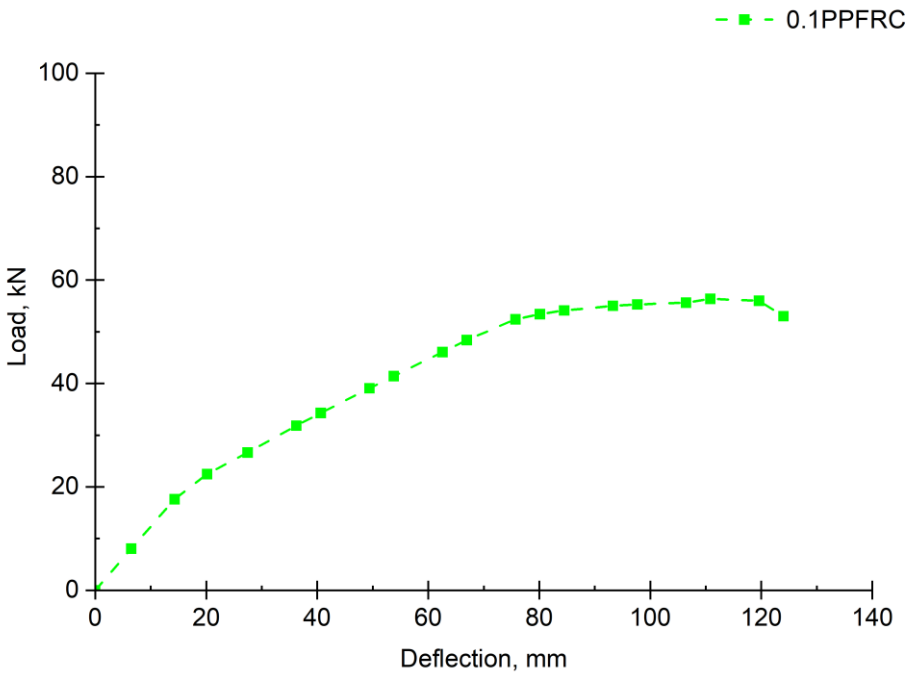

a) 0.1PPFC

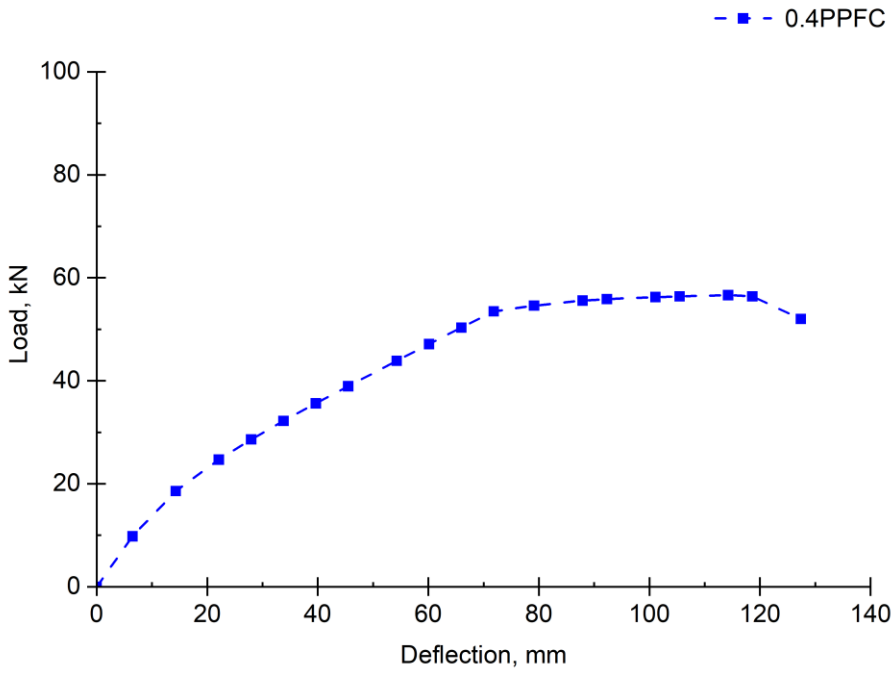

b) 0.4PPFC

Figure 6.17: Comparison between parametric study and FEA model

Table 6.6: Comparison between the results of FEA models and parametric study

Type of the model beam	Reference	Concrete strength		Modulus of elasticity	Validated experimental tests of Sryh (2017)		FEA model		Ratio
		f_c (MPa)	f_{spt} (MPa)	E_c (MPa)	Load (kN)	Deflection (mm)	Load (kN)	Deflection (mm)	Deflection (EXP/FEA)
NRC	Sryh (2017)	41.50	4.17	30,550	-	30.49	-	31.19	0.98
SFRC-0.5%		43.72	4.68	31,840	-	27.15	-	29.05	0.93
SFRC-1.0%		47.12	5.62	33,470	-	24.68	-	25.68	0.96
Micro PP	Current study	40.46	3.16	31,241	-	-	56.36	123.98	-
Macro PP		41.42	3.38	31,444	-	-	56.62	127.4	-

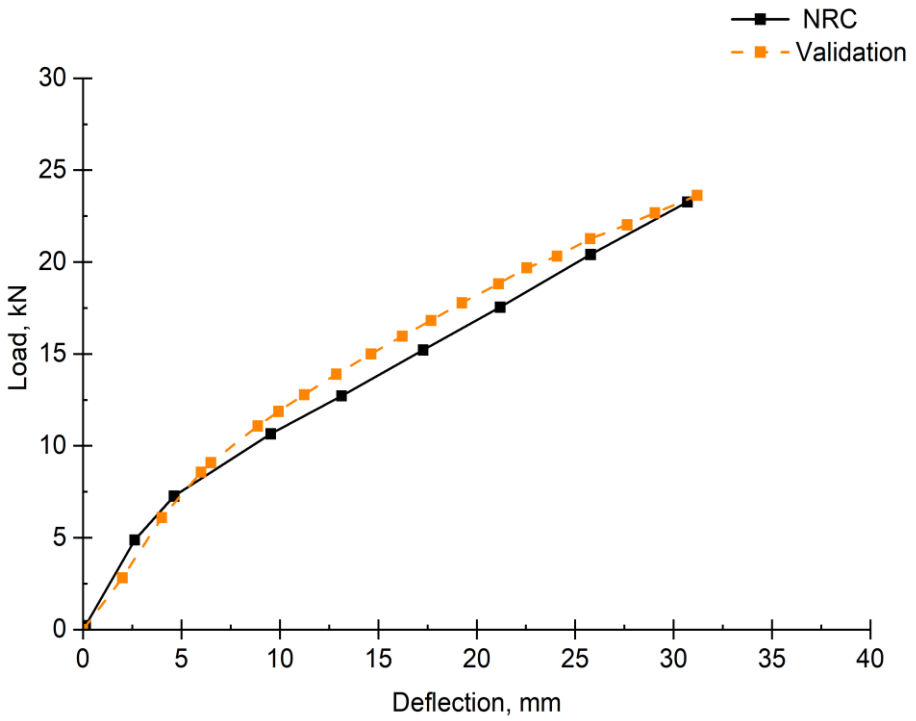

a) NRC beam (from Sryh, 2017) vs FEA

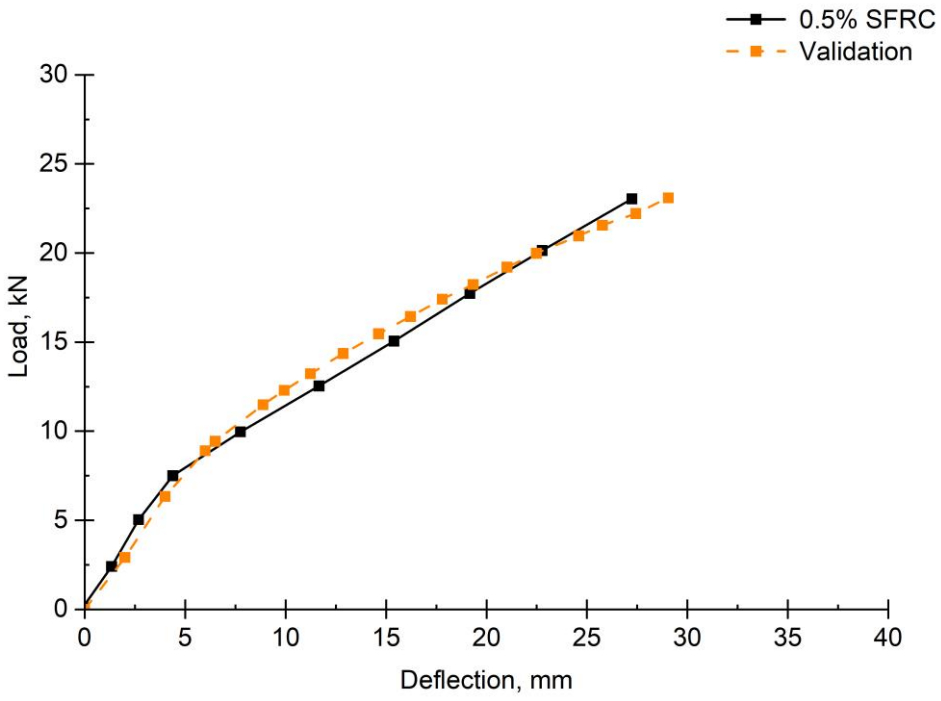

b) 0.5% SFRC beam (from Sryh, 2017) vs FEA

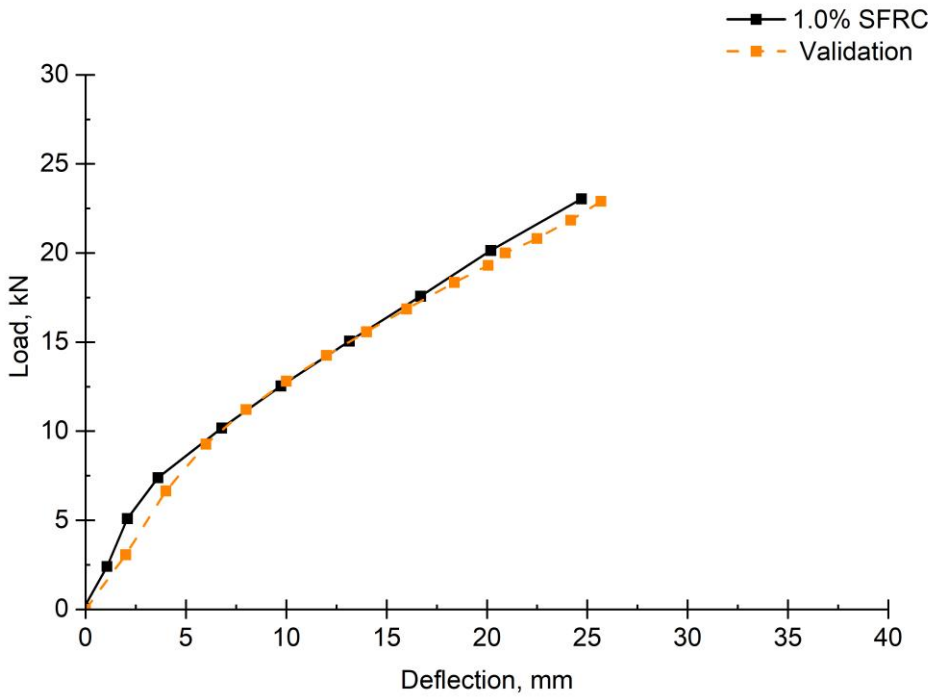

c) 1.0% SFRC beam (from Sryh, 2017) vs FEA

Figure 6.18: Comparison between parametric study and FEA mode

6.2 Summary

This chapter has highlighted the four distinct steps involved in classifying the FEA: geometry and material modelling, boundary and constraint conditions, output analysis, and post-processing of results. It emphasised the significance of accurate material properties and appropriate selection of element and mesh types for various components of the full-scale prefabricated beams under static and repeated four-point bending. Furthermore, the boundary and constraint conditions in the FEA were designed to replicate the external environments observed in the experimental test series. Detailed explanations of the contact interactions between each component were provided in this chapter to enable accurate modelling of their interactions during analysis.

The 3-D finite element model proposed in this study has undergone validation using the experimental results discussed in Chapter 5. It has been successfully demonstrated to accurately and reliably simulate the overall behaviour of the full-scale prefabricated beams when subjected to static and repeated tests. A parametric study was conducted to explore the system's

behaviour of varying parameters by including the strength of concrete with and without fibres (NC, 0.5% SFRC, 1.0% SFRC, 0.1PPFC and 0.4PPFC).

6.3 Conclusions

The present work has primarily focused on the validation of load-deflection behaviour in concrete beams. The study concentrated on two specific parameters, deflection and cracking under load, primarily due to the constraints of the software used. While this investigation provides valuable insights into the structural performance of NRC, SFRC, and HyFRC beams under specific loading conditions.

In this chapter, the experimental results of full-scale beams subjected to both static and repeated tests were compared with finite element (FE) models. The calculated results closely matched the outcomes of both the finite element analysis (FEA) and the parametric study. From the obtained results, the following key conclusions have been drawn:

- The predicted value for the maximum deflection of the SFRC model exhibited good agreement with the experimental results. The maximum deflection values of the FEA model and experimental results were compared for static test. The FEA model slightly over-predicted the maximum deflection of the NRC and HyFRC models by approximately 2.79% and 2.47%, respectively, when compared to the experimental results.
- The FEA prediction model exhibited a slightly underestimation of the maximum load value by 2.85% compared to the experimental results of the static test. Similarly, the HyFRC model beam prediction model showed a slight reduction of only 1.05% compared to the experimental results. However, in the case of the SFRC model, the predicted models slightly overestimated the maximum load by 3.17%.
- The ratio of experimental to the FEA results for NRC showed a value of 0.93. Similarly, for HyFRC beams at load levels of 20-80% and 30-70%, the ratios were 0.91 and 0.94, respectively. These findings suggest that the FEA results tended to be more conservative compared to the experimental results.

- The validation model exhibited ratios of 0.98, 0.93, and 0.96 for NRC, 0.5% SFRC, and 1.0% SFRC beams, respectively, when comparing the experimental results to the model predictions for parametric study.

Chapter 7
Conclusions and recommendations

7.1 Introduction

This research examined the effects of hybrid fibre systems, consisting of micro and macro polypropylene fibres as along with steel fibres, on the flexural performance of concrete beams under static, sustained, and cyclic loads. The aim was to mitigate the development of both micro-cracks and macro-cracks in flexural members by using hybrid fibre systems in concrete. This was achieved by investigating the effect of hybrid fibre systems on prismatic concrete beams (0.5 m span) and full-scale concrete beams (4.2 m span) using both experimental and analytical investigations. On the basis of the results presented and discussed in Chapters 4 to 6, conclusions drawn are given in section 7.2 and recommendations for further research are given in section 7.3.

7.2 Conclusions

- The influence of the combination of steel, micro and macro polypropylene fibres resulted in the most significant enhancement in the terms of compressive strength, splitting tensile strength and modulus of elasticity surpassed the addition of single type of fibre.
- The addition of combination of steel, micro and macro polypropylene fibres had a superior performance compared to the addition of a single type of fibre in terms of the first crack load, peak load, ductility, flexural strength, deflection and post cracking behaviour.
- Additionally, this combination offered a more pronounced positive synergy effect of the different types of fibres in the crack surfaces led to better performance in terms of crack patterns, which mitigate the propagation of cracks with fewer and smaller cracks due to the fibre bridging effect under static, repeated and sustained loadings.
- The results of the long-term deflections of HyFRC beams provide clear evidence that the predictions from EC2 consistently and significantly overestimated the experimental results throughout the entire duration of the applied load. This effect should be taken into account, as it might outweigh

the benefits of using hybrid fibres in comparison to the existing EC2, which is not the case.

- The experimental results for the crack width of the HyFRC beam demonstrated a notable deviation from the predicted value prescribed by the EC2 design code, showing a significant difference of around 40%. Furthermore, alternative provisions such as RILEM TC-162 and MC2010 exhibited an overestimation of the average crack width by approximately 20%.
- Further investigations should incorporate the effect of fibre volume fraction in calculating the crack spacing value, which affects the crack width prediction
- The effect of the hybrid fibre on time dependant effect is fluctuated in terms of shrinkage, both compressive and tensile creeps and loss of tension stiffening.
- The addition of hybrid fibre concrete specimens showed a negligible effect on shrinkage and tensile creep. The effect of hybrid fibres is more pronounced in reducing the creep when the stress-strength ratio was eliminated. It was shown that HyFC concrete specimens exhibited a lower creep coefficient than normal concrete.
- The presence of hybrid fibres significantly affects the rate of the reduction in terms of the loss of tension stiffening, which was particularly pronounced during the early stages.

The proposed FEA models are capable of reproducing the load-deflection curves of experimental tests accurately. Therefore, they can be adopted to predict the performance of HyFRC beams, enabling engineers to design with confidence and researchers to conduct further investigations.

Finally, adding a combination of steel, micro and macro polypropylene fibres to concrete when subjected to static, repeated, and sustained loads enhances several of its characteristics, particularly ductility, crack propagation, crack resistance, and crack width. The results of this study reveal that incorporating hybrid fibres into the concrete effectively counters the adverse impact of multi-level cracking with different combinations of hybrid fibre systems at various levels/scales under different types of loads.

It is evident that the inclusion of hybrid fibres in this study constitutes a novel contribution that has not been previously documented in the literature. These

findings highlight the potential superiority of hybrid fibres compared to using a single type of fibre, providing valuable insights to the field. Furthermore, the extensive experimental findings, analytical and finite element investigations, and advancements presented in this research offer significant value to researchers and engineers. They aid in enhancing code guidelines and extending the applicability of HyFC and HyFRC for various structural applications.

7.3 Recommendations from the current work and for future work

7.3.1 Limitations of the study

The current study's limitations need to be acknowledged to understand the applicability of its findings to real-world civil engineering structures. Due to time constraints and Covid-19 restrictions, the number of specimens in the experimental programme was reduced, and the full-scale beam tests were limited. Additionally, the hydraulic system available in the lab was not suitable for performing long-term repeated tests, specifically for full-scale beams when the maximum load exceeds 70% of the static load. Consequently, the accuracy of predicting how hybrid fibres affect the flexural fatigue strength in civil engineering structures may be limited. It is also important to acknowledge that certain aspects were not explored in the FEA study due to the time constraint. Additionally, time-dependent behaviour, which could be significant for certain applications, has not been addressed in this study due to limitations in the software used.

7.3.2 Recommendations

The research findings have yielded valuable insights into improving the performance of hybrid fibre systems in concrete beams under various loadings. However, it is essential to note that the focus was primarily on crack propagation and deflection at the macro-scale of structural components, rather than at the microstructure level of the concrete. The extensive experimental tests and finite element analysis have shed light on how hybrid fibre systems can effectively limit the development of micro-cracks and macro-cracks, enhancing concrete beam performance. Nonetheless, there is still potential for further improvement in the performance of hybrid fibre systems in concrete beams. To address this, the following recommendations for future research are proposed:

- A number of interesting future studies using the same experimental set up is apparent. It would be interesting to assess the effects of other types of fibres with different volume fractions under sustained and repeated load, especially for full-scale beams to establish a potentially stable relationship.
- Conduct additional investigation and experimentation of fatigue tests with hybrid fibre systems, considering different loading frequencies and different stress levels is strongly recommended to demonstrate the clear benefits of hybrid beneficial effects and draw S-N curves using the same experimental setup.
- Additionally, a study to investigate on how hybrid fibre reinforcement can restrict the development of micro and macro cracks in RC elements subjected to sustained load with longer period and different size of fibres would be very interesting. Furthermore, more research on the time-dependent deformation of hybrid fibre concrete (HyFC) should be examined.
- For future FEA studies, expanding the modelling to include other parameters and phenomena relevant to concrete behaviour, such as time dependent modelling, strain predictions and more complex cracking analysis, would be beneficial. This could lead to a deeper understanding of the structural response for example, in terms of cracks propagation, and contribute to improved design methodologies for concrete structures.

These recommendations provide a comprehensive roadmap for future research endeavours in the field, aiming to further enhance the understanding and application of hybrid fibre systems in concrete structures.

References

ABAQUS 2008. Documentation, version 6.8.1. Dassault system, USA.

Abbadi, A. 2018. Shear contribution of fibre-reinforced lightweight concrete (FRLWC) reinforced with basalt fibre reinforced polymer (BFRP) bars [Master Thesis]. Laval University.

Abbadi, A., Basheer, P.A.M., and Forth, J.P. 2022. Effect of hybrid fibres on the static load performance of concrete beams. *Materials Today: Proceedings*.

Abd-Elhady, A. A., Sallam, H. E. D. M. and Mubaraki, M. A. (2017) 'Failure Analysis of Composite Repaired Pipelines with an Inclined Crack under Static Internal Pressure', *Procedia Structural Integrity*. Elsevier B.V., 5, pp. 123–130. doi: 10.1016/j.prostr.2017.07.077

Abd-elhady, A. A. *et al.* (2020) 'Investigation of fatigue crack propagation in steel pipeline repaired by glass fiber reinforced polymer', *Composite Structures*. Elsevier, 242(February), p. 112189. doi: 10.1016/j.compstruct.2020.112189.

Afroughsabet, V. and Teng, S. 2020. Experiments on drying shrinkage and creep of high-performance hybrid-fiber-reinforced concrete. *Cement and Concrete Composites.* 106, pp.103481.

Afroughsabet, V., Biolzi, L., Ozbakkaloglu, T. 2016. High-performance fiber-reinforced concrete: a review, *J. Mater. Sci*. 51 (14), pp.6517–6551.

Afroughsabet, V., Ozbakkaloglu, T. 2015. Mechanical and durability properties of high-strength concrete containing steel and polypropylene fibers. *Construction and Building Materials*, 94, pp.73-82.

American Concrete Institute (ACI) Committee 209. 1997. Prediction of Creep, Shrinkage and Temperature Effects in Concrete Structures. ACI Committee 209 Report, 92(Reapproved), p.47.

American Concrete Institute (ACI) Committee 215, A. C., 1997. 'Considerations for Design of Concrete Structures Subjected to Fatigue Loading Reported', ACI Committee 215.

Anandan, S. and Alsubih, M. 2021. Mechanical strength characterization of plastic fiber reinforced cement concrete composites. *Applied Sciences* 11(2), p. 852.

Arora, S., Singh, S.P. 2016. Analysis of flexural fatigue failure of concrete made with 100% coarse recycled concrete aggregates. *Construction and Building Materials*, 102, pp.782-791.

Bajaj, Vineet et al. 2012. Flexural fatigue analysis of hybrid fibre-reinforced con-crete. *Magazine of Concrete Research* 64(4), pp.361-373.

Balaguru, P., and Ramakrishnan, V.J.M.J. 1988. Properties of fiber reinforced con-crete: workability, behavior under long-term loading, and air-void characteris-tics. *Materials Journal* 85(3), pp.189-196.

Banjara, N.K. and Ramanjaneyulu, K. 2018. Experimental investigations and numerical simulations on the flexural fatigue behavior of plain and fiber-reinforced concrete. *Journal of Materials in Civil Engineering* 30(8), p.04018151.

Banthia, N. and Gupta, R. 2004. Hybrid fiber reinforced concrete (HyFRC): fiber synergy in high strength matrices. *Materials and Structures* 37, pp.707-716.

Barluenga, G. 2010. Fiber–matrix interaction at early ages of concrete with short fibers. *Cement and Concrete Research* 40(5), pp.802-809.

Barr, B. and El-Baden. A. 2003. Shrinkage properties of normal and high strength fibre reinforced concrete. Proceedings of the Institution of Civil Engineers-Structures and Buildings 156(1), pp.15-25.

Bawa, S. and Singh, S.P. 2020. Flexural fatigue strength prediction of hybrid-fibre-reinforced self-compacting concrete. Proceedings of the Institution of Civil Engineers-Construction Materials 173(5), pp.234-250.

Behfarnia, K. and Behravan, A. 2014. Application of high performance polypropylene fibers in concrete lining of water tunnels. *Materials & Design* 55, pp.274-279.

Bhosale, A.B., Prakash, S.S. 2020. Crack propagation analysis of synthetic vs. steel vs. hybrid fibre-reinforced concrete beams using digital image correlation technique. *International Journal of Concrete, Struct. Mater*. 14(1), pp.1–19.

Bhowmik, S. and Ray, S. 2018. An improved crack propagation model for plain concrete under fatigue loading. *Engineering Fracture Mechanics* 191, pp.365-382.

Bissonnette, B., Pigeon, M. and Vaysburd, A.M. (2007) Tensile creep of concrete: study of its sensitivity to basic parameters. *ACI Materials Journal* 104(4), p.360.

Błyszko, J. 2017. Comparative analysis of creep in standard and fibre reinforced concretes under different load conditions. *Procedia Engineering* 193, pp.478-485.

Branston, J. et al. 2016. Mechanical behaviour of basalt fibre reinforced concrete. *Construction and Building Materials* 124, pp.878-886.

British Standards Institution (BSI), 1983. BS 1881-116. Testing concrete-Part 116: method for determination of compressive strength of concrete cubes. BS 116. (1881): 36.

British Standards Institution (BSI), 2000. BS EN 12390-2. Testing hardened concrete, Part 2: Making and curing specimens for strength tests.

British Standards Institution (BSI), 2001. BS EN 10002-1. Tensile testing of metallic materials, Part 1: Method of test at ambient temperature.

British Standards Institution (BSI), 2002. BS EN 1008. Mixing Water for Concrete. Specification for Sampling, Testing and Assessing the Suitability of Water, Including Water Recovered from Processes in the Concrete Industry, as Mixing Water in Concrete.

British Standards Institution (BSI), 2004. BS EN 1992-1-1: Eurocode 2: Design of Concrete Structures: Part 1-1: General Rules and Rules for Buildings.

British Standards Institution (BSI), 2005. BS EN 1990:2002+A1: Eurocode - Basis of structural design.

British Standards Institution (BSI), 2006. BS EN 14889-1. Fibres for concrete.

British Standards Institution (BSI), 2006. BS EN 206-1, Part 1: Method of Specifying and Guidance for the Specifier.

British Standards Institution (BSI), 2009. BS EN 12350-2. Testing Fresh Concrete Part 2: Slump Test.

British Standards Institution (BSI), 2009. BS EN 12390-3. Testing hardened concrete Part 3. Compressive Strength of Test, Specimens.

British Standards Institution (BSI), 2009. BS EN 12390-5. Testing hardened concrete, Part 5: Flexural strength of test specimens.

British Standards Institution (BSI), 2009. BS EN 12390–6. Testing hardened concrete Part 6: Tensile splitting strength of test specimens.

British Standards Institution (BSI), 2009. BS ISO 1920-8 'Testing of concrete, Part 8: Determination of drying shrinkage of concrete for samples prepared in the field or in the laboratory Essais', 4(4), p.221.

British Standards Institution (BSI), 2009. BS ISO 1920-9 'Testing of concrete, Part 9: Determination of creep of concrete cylinders in compression', 4(4), p.221.

British Standards Institution (BSI), 2012. BS EN 934-2. Admixtures for concrete, mortar and grout. Concrete admixtures. Definitions, requirements, conformity, marking and labelling.

British Standards Institution (BSI), 2013. BS 1881-125. Testing Concrete. Methods for Mixing and Sampling Fresh Concrete in the Laboratory.

British Standards Institution (BSI), 2013. BS EN 12390-13. Testing hardened concrete, Part 13: Determination of secant modulus of elasticity in compression.

British Standards Institution (BSI). 1992. BS882: Specification for aggregates from natural sources for concrete, London.

British Standards Institution (BSI). 2011. BS EN 197-1: Cement, composition, specifications and conformity criteria for common cements.

Cachim, P.B., Figueiras, J.A., and Pereira, P.A.A. 2002. Fatigue behavior of fiber-reinforced concrete in compression. *Cement and Concrete Composites* 24(2), pp.211-217.

Caggiano, A., Cremona, M., Faella, C., Lima, C., Martinelli, E. 2012. Fracture behavior of concrete beams reinforced with mixed long/short steel fibers. *Construction and Building Materials* 37, pp.832-840.

Chen, B. and Liu, J. 2005. Contribution of hybrid fibers on the properties of the high-strength lightweight concrete having good workability. *Cement and Concrete Research* 35(5), pp.913-917.

Chen, B., Liu, J. 2005. Contribution of hybrid fibers on the properties of the high-strength lightweight concrete having good workability. *Cement and Concrete Research*, 35(5), pp.913-917.

Chern, J.C. and Young, C.H. 1989. Compressive creep and shrinkage of steel fibre reinforced concrete. *International Journal of Cement Composites and Lightweight Concrete* 11(4), pp.205-214.

Chiaia, B., Fantilli, A.P., Vallini, P. 2009. Evaluation of crack width in FRC structures and application to tunnel linings, *Mater. Struct*. 42(3), pp.339–351.

Choi, W.C., and Yun, H.D. 2013. Long-term deflection and flexural behavior of reinforced concrete beams with recycled aggregate. *Materials & Design* 51, pp.742-750.

Conforti, A., Minelli, F., and Plizzari, G.A. 2013. Wide-shallow beams with and without steel fibres: a peculiar behaviour in shear and flexure. Composites Part B: Engineering 51, pp.282-290.

Cornelissen, H., Hordijk, D., and Reinhardt, H. 1986. Experimental determination of crack softening characteristics of normalweight and lightweight. Heron 31(2), pp.45-46.

Crump, T. et al. (2017) 'Dynamic fracture analysis by explicit solid dynamics and implicit crack propagation', International Journal of Solids and Structures. Elsevier Ltd, 110–111, pp. 113–126. doi: 10.1016/j.ijsolstr.2017.01.035.

Cucchiara, C., La Mendola, L., and Papia, M. 2004. Effectiveness of stirrups and steel fibres as shear reinforcement. *Cement and Concrete Composites* 26(7), pp.777-786.

Dassault Systèmes. 2014. Abaqus user subroutines reference guide, Version 6.14. Dassault Systemes Simulia Corp., Providence, RI, USA.

Daud, S.A., Forth, J.P. and Nikitas, N. 2018. Time-dependent behaviour of cracked, partially bonded reinforced concrete beams under repeated and sustained loads. *Engineering Structures* 163, pp.267-280.

Deluce, J.R., Vecchio, F.J. 2013. Cracking Behavior of Steel Fiber-Reinforced Con-crete Members Containing Conventional Reinforcement, *ACI Struct. J*. 110(3).

Deshpande, S.S. 2007. Evaluating free shrinkage of concrete for control of cracking in bridge decks. University of Kansas.

El-Mal, A., Sherbini, A.S. and Sallam, H.E.M. 2015. Mode II fracture toughness of hybrid FRCs. *International Journal of Concrete Structures and Materials* 9(4), pp.475-486.

Fallah, S., Nematzadeh, M. 2017. Mechanical properties and durability of high-strength concrete containing macro-polymeric and polypropylene fibers with nano-silica and silica fume. *Construction and Building Materials*, 132, pp.170-187.

Fantilli, A.P., Orfeo, B., Caldentey, A.P. 2021. The deflection of reinforced concrete beams containing recycled steel fibers, *Struct. Concr*. 22(4), pp.2089–2104.

Fib (International Federation for Structural Concrete). 2010. FIB model code for concrete structures.

Forth, J.P. 2015. Predicting the tensile creep of concrete. *Cement and Concrete Composites* 55, pp.70-80.

Gao, D. et al. 2021. Effects of fiber clustering on fatigue behavior of steel fiber reinforced concrete beams. *Construction and Building Materials* 301, p.124070.

Gao, W. et al. 2019. Theoretical study on extension of crack tip plastic zone by remote simple tensile considering crack interaction. *European Journal of Mechanics-A/Solids* 77, p.103814.

Garas, V.Y., Kahn, L.F., and Kurtis, K.E. 2009. Short-term tensile creep and shrinkage of ultra-high performance concrete. *Cement and Concrete Composites* 31(3), pp.147-152.

Genikomsou, A.S. and Polak, M.A. 2015. Finite element analysis of punching shear of concrete slabs using damaged plasticity model in ABAQUS. *Engineering Structures* 98, pp.38-48.

Germano, F., Tiberti, G., and Plizzari, G. 2016. Post-peak fatigue performance of steel fiber reinforced concrete under flexure. *Materials and Structures* 49, pp.4229-4245.

Goel, S. and S. P. Singh 2014. Fatigue performance of plain and steel fibre reinforced self-compacting concrete using S–N relationship. *Engineering Structures* 74, pp.65-73.

Goel, S., Singh, S.P. and Singh, P. 2012. Flexural fatigue analysis of self-compacting concrete beams. *Proceedings of the Institution of Civil Engineers-Construction Materials* 165(6), pp.367-376.

Guo, H., Jiang, L., Tao, J., Chen, Y., Zheng, Z., Jia, B. 2021. Influence of a hybrid combination of steel and polypropylene fibers on concrete toughness. *Construction and Building Materials* 275, p.122132.

Hamoush, S., Abu-Lebdeh, T., Cummins, T. 2010. Deflection behavior of concrete beams reinforced with PVA micro-fibers. *Construction and Building Materials* 24(11), pp.2285-2293.

Hasan-Nattaj, F., and Nematzadeh, M. 2017. The effect of forta-ferro and steel fibers on mechanical properties of high-strength concrete with and without silica fume and nano-silica. *Construction and Building Materials* 137, pp.557-572.

Hassanpour, M., Shafigh, P., and Mahmud, H.B. 2012. Lightweight aggregate concrete fiber reinforcement–A review. *Construction and Building Materials* 37, pp.452-46.

Higgins, L. et al. 2013. Behaviour of cracked reinforced concrete beams under repeated and sustained load types. *Engineering Structures* 56, pp.457-465.

Hillerborg, A. 1985. The theoretical basis of a method to determine the fracture energy GF of concrete. *Materials and Structures* 18, pp.291-296.

Houde, J., Prezeau, A., and Roux, R. Creep of concrete containing fibers and silica fume. *Special Publication* 105, pp.101-118.

Huang, C., and Zhao, G. 1995. Properties of steel fibre reinforced concrete containing larger coarse aggregate. *Cement and Concrete Composites* 17(3), pp.199-206.

Iqbal Khan, M., and Abadel, A.A. 2013. Numerical modeling of steel fiber-reinforced beam. *Applied Mechanics and Materials* 377, pp.22-27.

ISO, EN. 2009. Metallic materials-Tensile testing-Part 1: Method of test at room temperature. ISO, Switzerland, Eroupe, ISO: 6892-1.

Jamsawang, P., Voottipruex, P., and Horpibulsuk, S. 2015. Flexural strength characteristics of compacted cement-polypropylene fiber sand. *Journal of Materials in Civil Engineering* 27.9: 04014243.

Jebli, M. et al. 2018. Experimental characterization of mechanical properties of the cement-aggregate interface in concrete. *Construction and Building Materials* 161, pp.16-25.

Jiang, C. et al. 2018. Modeling the effects of fatigue damage on concrete carbonation. *Construction and Building Materials* 191, pp.942-962.

Johnston, C.D. and Zemp, R.W. 1991. Flexural fatigue performance of steel fiber reinforced concrete--influence of fiber content, aspect ratio, and type. *Materials Journal* 88(4), pp.374-383.

Juárez, C. et al. 2007. The diagonal tension behavior of fiber reinforced concrete beams. *Cement and Concrete Composites* 29(5), pp.402-408.

Jun, Z., and Stang, H. 1998. Fatigue performance in flexure of fiber reinforced concrete. *Materials Journal* 95(1), pp.58-67.

Kang, T.H.K. et al. 2011. Shear testing of steel fiber-reinforced lightweight concrete beams without web reinforcement. *ACI Structural Journal* 108(5), p.553.

Karlsson, B.I. and Sorensen, E.P. 2006a. ABAQUS: Analysis user's manual version6.5, Pawtucket, Rhode Island, Hibbitt Publication.

Kim, B., Boyd, A.J. and Lee, J.Y. 2011. Durability performance of fiber-reinforced concrete in severe environments. *Journal of Composite Materials* 45(23), pp.2379-2389.

Kim, D.J. et al. 2011. Comparative flexural behavior of hybrid ultra-high performance fiber reinforced concrete with different macro fibers. *Construction and Building Materials* 25(11), pp.4144-4155.

Kim, Y.Y. et al. 2014. Flexural performance of reinforced concrete beams strengthened with strain-hardening cementitious composite and high strength reinforcing steel bar. *Composites Part B: Engineering* 56, pp.512-519.

Kiviste, K., Ryabchikov, A. and Lille, H. 2011. Determination of shrinkage of fibre-reinforced concrete. *Civil Engineering* 11, pp.113-116.

Kovler, K., and Bentur, A. 1997. Shrinkage of early age steel fiber reinforced concrete. *Archives of Civil Engineering* 43(4), pp.431-439.

Kytinou, V.K., Chalioris, C.E. and Karayannis, C.G. 2020. Analysis of residual flexural stiffness of steel fiber-reinforced concrete beams with steel reinforcement. *Materials* 13(12), p.2698.

Li, B., Chi, Y., Xu, L., Shi, Y., Li, C. 2018. Experimental investigation on the flexural be-havior of steel-polypropylene hybrid fiber reinforced concrete, *Constr. Build. Mater.* 191, pp.80–94.

Mangat, P.S. and Azari, M.M. 1985. A theory for the creep of steel fibre reinforced cement matrices under compression. *Journal of Materials Science* 20, pp.1119-1133.

Mangat, P.S. and Azari, M.M. 1988. Shrinkage of steel fibre reinforced cement composites. *Materials and Structures* 21, pp.163-171.

Mangat, P.S., and Azari, M.M. 1984. A theory for the free shrinkage of steel fibre reinforced cement matrices. *Journal of Materials Science* 19, pp.2183-2194.

Meda, A., Minelli, F. and Plizzari, G.A. 2012. Flexural behaviour of RC beams in fibre rein-forced concrete, *Compos. B Eng*. 43 (8), pp.2930–2937.

Medeiros, Arthur et al. 2015. Effect of the loading frequency on the compressive fatigue behavior of plain and fiber reinforced concrete. *International Journal of Fatigue* 70, pp.342-350.

Mehta, P.K., Monteiro, P.J. 2014. Concrete: microstructure, properties, and materials. McGraw-Hill Education.

Meng, D., Lee, C. and Zhang, Y. 2019. Flexural fatigue properties of a polyvinyl alcohol-engineered cementitious composite. *Magazine of Concrete Research* 71(21), pp.1130-1141.

Meza, A., and Siddique, S. 2019. Effect of aspect ratio and dosage on the flexural response of FRC with recycled fiber. *Construction and Building Materials* 213, pp.286-291.

Mias, C. et al. 2015. Short and long-term cracking behaviour of GFRP reinforced concrete beams. *Composites Part B: Engineering* 77, pp.223-231.

Micelli, F. et al. 2019. Effects of short fibers on the long-term behavior of RC/FRC beams aged under service loading. *Applied Sciences* 9(12), pp.2540.

Mobasher, B., Yao, Y. and Soranakom, C. 2015. Analytical solutions for flexural design of hybrid steel fiber reinforced concrete beams. *Engineering Structures* 100, pp.164-177.

Moës, N., Dolbow, J. and Belytschko, T. (1999) 'A finite element method for crack growth without remeshing', *International Journal for Numerical Methods in Engineering*, 46(1), pp. 131–150. doi: 10.1002/(SICI)1097-0207(19990910)46:1<131::AID-NME726>3.0.CO;2-J.

Mohamadi, M.R., Mohandesi, J.A. and Homayonifar, M. 2013. Fatigue behavior of polypropylene fiber reinforced concrete under constant and variable amplitude loading. *Journal of Composite Materials* 47(26), pp.3331-3342.

Mohammadi, S. (2012) 'XFEM Fracture Analysis of Composites Soheil Mohammadi', *WILEY*, p. 368.

Mohammadi, Y. and Kaushik, S.K. 2005. Flexural fatigue-life distributions of plain and fibrous concrete at various stress levels. *Journal of Materials in Civil Engineering* 17(6), pp.650-658.

Mohammadi, Y., Singh, S.P., Kaushik, S.K. 2008. Properties of steel fibrous concrete containing mixed fibres in fresh and hardened state. *Construction and Building Materials,* 22(5), pp.956-965.

Naaman, A.E. and Hammoud, H. 1998. Fatigue characteristics of high performance fiber-reinforced concrete. *Cement and Concrete Composites* 20(5), pp.353-363.

Nagabhushanam, M., Ramakrishnan, V. and Vondran, G. 1989. Fatigue strength of fibrillated polypropylene fiber reinforced concretes. *Transportation Research Record* 1226, pp.36-47.

Nakov, D. et al. 2017. Experimental and analytical analysis of creep of steel fibre reinforced concrete. *Periodica Polytechnica Civil Engineering*.

Neville, A.M. and Brooks, J.J. 1987. Concrete technology. Vol. 438. England: Longman Scientific & Technical.

Ng, P.L. et al. 2019. Tension stiffening approach for deformation assessment of flexural reinforced concrete members under compressive axial load. *Structural Concrete* 20(6), pp.2056-2068.

Nia, A.A., Hedayatian, M., Nili, M., Sabet, V.A. 2012. An experimental and numerical study on how steel and polypropylene fibers affect the impact resistance in fiber-reinforced concrete. *International Journal of Impact Engineering*, 46, pp.62-73.

Nili, M. and Afroughsabet, V. 2012. The long-term compressive strength and durability properties of silica fume fiber-reinforced concrete. *Materials Science and Engineering*: A 531, pp.107-111.

Nogueira L.V., Cardoso, D.C.T. and de Andrade Silva, F. 2021. Creep mechanisms in precracked polypropylene and steel fiber–reinforced concrete. *Journal of Materials in Civil Engineering* 33(8), p.04021187.

Oh, B.H. 1992. Flexural analysis of reinforced concrete beams containing steel fibers, *J. Struct. Eng*. 118(10), pp.2821–2835.

Okuyucu, D. et al. 2011. Some characteristics of fibre-reinforced semi-lightweight concrete with unexpanded perlite. *Magazine of Concrete Research* 63(11), pp.837-846.

Pająk, M. and Ponikiewski, T. 2017. Experimental investigation on hybrid steel fibers reinforced self-compacting concrete under flexure. *Procedia Engineering* 193, pp.218-225.

Pajak¸ M., Ponikiewski, K.T. 2013. Flexural behavior of self-compacting concrete rein-forced with different types of steel fibers, *Constr. Build. Mater.* 47, pp.397–408.

Pakravan, H.R., Latifi, M. and Jamshidi, M. 2017. Hybrid short fiber reinforcement system in concrete: A review. *Construction and Building Materials* 142, pp.280-294.

Parvez, A. and Foster, S.J. 2015. Fatigue behavior of steel-fiber-reinforced concrete beams. *Journal of Structural Engineering* 141(4), p.04014117.

Paskova, T. and Meyer, C. 1997. Low-cycle fatigue of plain and fiber-reinforced concrete. *Materials Journal* 94(4), pp.273-286.

Qian K.L. 2006. Influence of Relative Humidity on Shrinkage of Mortar and Concrete. *Journal of Shenyang Jianzhu University*.

Qian, X.Q., Meng, T., Zhan, S.L. and Qian, K.L. 2006. Influence of relative humidity on shrinkage of mortar and concrete, *Journal of Shenyang Jianzhu University*, pp.268-271.

Qu, F. et al. 2019. Flexural Fatigue Performance of Steel Fiber Reinforced Expanded-Shales Lightweight Concrete Superposed Beams with Initial Static-Load Cracks. *Materials* 12(19), p.3261

Raju, R. A. et al. 2020. Effects of concrete flow on the distribution and orientation of fibers and flexural behavior of steel fiber-reinforced self-compacting concrete beams. *Construction and Building Materials* 262, p.119963.

Ramakrishnan, V., Gollapudi, S.P., Zellers, R.C. 1987. Performance characteristics and fatigue strength of polypropylene fiber reinforced concrete. *Special Publication*, 105, pp.159-178.

Ramakrishnan, V., Wu, G.Y., Hosalli, G. 1989. Flexural fatigue strength, endurance limit and impact strength of fiber reinforced concretes. *Transportation Research Record*, 1226, pp.17-24, ISO 690.

RILEM TC 162-TDF. 2003. Test and design methods for steel fibre reinforced concrete' r-e-design method, *Mater. Struct. Constr*. 36(262), pp.560–567.

Sadrinejad, I., Madandoust, R., Ranjbar, M.M. 2018. The mechanical and durability properties of concrete containing hybrid synthetic fibers, *Constr. Build. Mater*. 178, pp.72–82.

Sahoo, D.R., Solanki, A. and Kumar, A. 2015. Influence of steel and polypropylene fibers on flexural behavior of RC beams. *Journal of Materials in Civil Engineering* 27(8), p.04014232.

Saje, D. et al. 2013. Shrinkage and creep of steel fiber reinforced normal strength concrete. ASTM International.

Schäfer, N. et al. 2019. Fatigue behavior of HPC and FRC under cyclic tensile loading: Experiments and modelling. *Structural Concrete* 20(4), pp.1265-1278.

Scott, R.H. and Beeby, A.W. 2005. Long-term tension-stiffening effects in concrete. *ACI Structural Journal* 102(1), p.31.

Scott, R.H. and Beeby, A.W. 2012. Evaluation and management of tension stiffening. *Special Publication* 284, pp.1-18.

Singh, S.P. and Kaushik, S.K. 2003. Fatigue strength of steel fibre reinforced concrete in flexure. *Cement and Concrete Composites* 25(7), pp.779-786.

Singh, S.P., Mohammadi, Y. and Madan, S.K. 2006. Flexural fatigue strength of steel fibrous concrete containing mixed steel fibres. *Journal of Zhejiang University-Science A* 7(8), pp.1329-1335.

Smarzewski, P. 2018. Flexural toughness of high-performance concrete with basalt and polypropylene short fibres. Advances in Civil Engineering.

Soutsos, M.N., Le, T.T. and Lampropoulos, A.P. 2012. Flexural performance of fibre reinforced concrete made with steel and synthetic fibres. *Construction and Building Materials* 36, pp.704-710.

Sryh, L. and Forth, J. 2022. Long-Term Flexural Behaviour of Cracked Reinforced Concrete Beams with Recycled Aggregate. *International Journal of Concrete Structures and Materials* 16(1), p.19.

Stephen, S.J. and Gettu, R. 2020. Fatigue fracture of fibre reinforced concrete in flexure. *Materials and Structures* 53(3), p.56.

Suthiwarapirak, P., Matsumoto, T. and Kanda, T. 2004. Multiple cracking and fiber bridging characteristics of engineered cementitious composites under fatigue flexure. *Journal of Materials in Civil Engineering* 16(5), pp.433-443.

Tailhan, J.L., Rossi, P. and Daviau-Desnoyers, D. 2015. Probabilistic numerical modelling of cracking in steel fibre reinforced concretes (SFRC) structures. *Cement and Concrete Composites* 55, pp.315-321.

Tan, K.H., Paramasivam, P. and Tan, K.H. 1994. Creep and shrinkage deflections of RC beams with steel fibers. *Journal of Materials in Civil Engineering* 6(4), pp.474-494.

Tawfiq, K., Amaghani, J. and Ruiz, R. 1999. Fatigue cracking of polypropylene fiber reinforced concrete. *Materials Journal* 96(2), pp.226-233.

Taylor, P. and Wang, X. 2014. Concrete pavement mixture design and analysis (MDA): factors influencing drying shrinkage.

Tiberti, G., Minelli, F., Plizzari, G.A., Vecchio, F.J. 2014. Influence of concrete strength on crack development in SFRC members, *Cem. Concr. Compos.* 45, pp.176–185.

Tošić, N., Aidarov, S. and de la Fuente, D. 2020. Systematic review on the creep of fiber-reinforced concrete. *Materials* 13(22), p.5098.

Tülin, A., Tokyay, M. and Çelik, T. 2004. Effect of coarse aggregate size and matrix quality on ITZ and failure behavior of concrete under uniaxial compression. *Cement and Concrete Composites* 26(6), pp.633-638.

Uygunoğlu, T. 2008. Investigation of microstructure and flexural behavior of steel-fiber reinforced concrete. *Materials and Structures* 41, pp.1441-1449.

Vandewalle, L. 2000. Cracking behaviour of concrete beams reinforced with a com-bination of ordinary reinforcement and steel fibers, *Mater. Struct*. 33(3), pp.164–170.

Vasanelli, E. et al. 2014. Crack width prediction of FRC beams in short and long term bending condition. *Materials and structures* 47(1), pp.39-54.

Waqas, A., Khan, M., and Smarzewski, P. 2021. Effect of short fiber reinforcements on fracture performance of cement-based materials: a systematic review approach. *Materials* 14(7), p.1745.

Wang, Z. et al. (2012) 'Progressive failure analysis of bolted single-lap composite joint based on extended finite element method', Materials and Design. Elsevier Ltd, 37, pp. 582–588. doi: 10.1016/j.matdes.2011.08.039.

Wang, H. and Wang, J. (2014) 'Numerical Analysis of Surface Crack Propagation in Flexible Pavements Using XFEM and Cohesive Zone Model', *International Journal of Pavement Research and Technology*, 7(3), pp. 178–184

Wu, W. et al. 2022. Flexural fatigue behaviors of high-content hybrid fiber-polymer concrete. *Construction and Building Materials* 349, p.128772.

Xiao, J., Li, H. and Yang, Z. 2013. Fatigue behavior of recycled aggregate concrete under compression and bending cyclic loadings. *Construction and Building Materials* 38, pp.681-688.

Yan, H., Sun, W., Chen, H. 1999. The effect of silica fume and steel fiber on the dynamic mechanical performance of high-strength concrete. *Cement and Concrete Research,* 29(3), pp.423-426.

Yang, K.H. 2011. Tests on Concrete Reinforced with Hybrid or Monolithic Steel and Polyvinyl Alcohol Fibers. *ACI Materials Journal* 108(6).

Yap, S.P., Bu, C.H., Alengaram, U.J., Mo, K.H., Jumaat, M.Z. 2014. Flexural toughness characteristics of steel–polypropylene hybrid fibre-reinforced oil palm shell concrete. *Materials & Design* 57, pp.652-659.

Yazıcı, Ş., İnan, G., Tabak, V. 2007. Effect of aspect ratio and volume fraction of steel fiber on the mechanical properties of SFRC. *Construction and Building Materials*, 21(6), pp.1250-1253.

Yin, S., Tuladhar, R., Shi, F., Combe, M., Collister, T., Sivakugan, N. 2015. Use of macro plastic fibres in concrete: A review. *Construction and Building Materials*, 93, pp.180-188.

Yoo, D.Y., Kang, S.T., Yoon, Y.S. 2014. Effect of fiber length and placement method on flexural behavior, tension-softening curve, and fiber distribution characteristics of UHPFRC. *Construction and Building Materials* 64, pp.67-81.

Yoo, D.Y., Lee, J.H., Yoon, Y.S. 2013. Effect of fiber content on mechanical and fracture properties of ultra high-performance fiber reinforced cementitious composites. *Composite Structures* 106, pp.742-753.

Yoo, D.Y., Yoon, Y.S., Banthia, N. 2015. Flexural response of steel-fiber-reinforced concrete beams: Effects of strength, fiber content, and strain-rate. *Cement and Concrete Composites* 64, pp.84-92.

Yuan, H., Weijian, Y. and Chao, H. 2018. Corroded reinforced concrete beams under low-speed and low-cycle fatigue loads. *Construction and Building Materials* 186, pp.644-651.

Zainal, S.M., Iqbal S. et al. 2022. The synergistic effects of different types of hybridized synthetic fibers on concrete post-crack residual strength. *KSCE Journal of Civil Engineering* 26(1), pp.131-142.

Zeng, J.J. et al. 2022. Flexural behavior of FRP grid reinforced ultra-high-performance concrete composite plates with different types of fibers. *Engineering Structures* 272, p.115020.

Zhang, J., Stang, H. and Li, V.C. 1999. Fatigue life prediction of fiber reinforced concrete under flexural load. International *Journal of Fatigue* 21(10), pp.1033-1049.

Zheng, J.J., Li, C.Q. and Zhou, X.Z. 2005. Thickness of interfacial transition zone and cement content profiles around aggregates. *Magazine of Concrete Research* 57(7), pp.397-406.

Zhu, S., Zhang, Y.X. and Lee, C.K. 2022. Experimental investigation of flexural behaviours of hybrid engineered cementitious composite beams under static and fatigue loading. *Engineering Structures* 262, p.114369.

Appendix

The secant modulus represents the gradient of a line that starts at the origin of the stress-strain diagram and intersects the curve at a specific point. Figure A.1 illustrates that the secant modulus is plotted from the origin to any location on the stress-strain curve. This approach is highly favoured because it eliminates uncertainties when determining its value from the diagram.

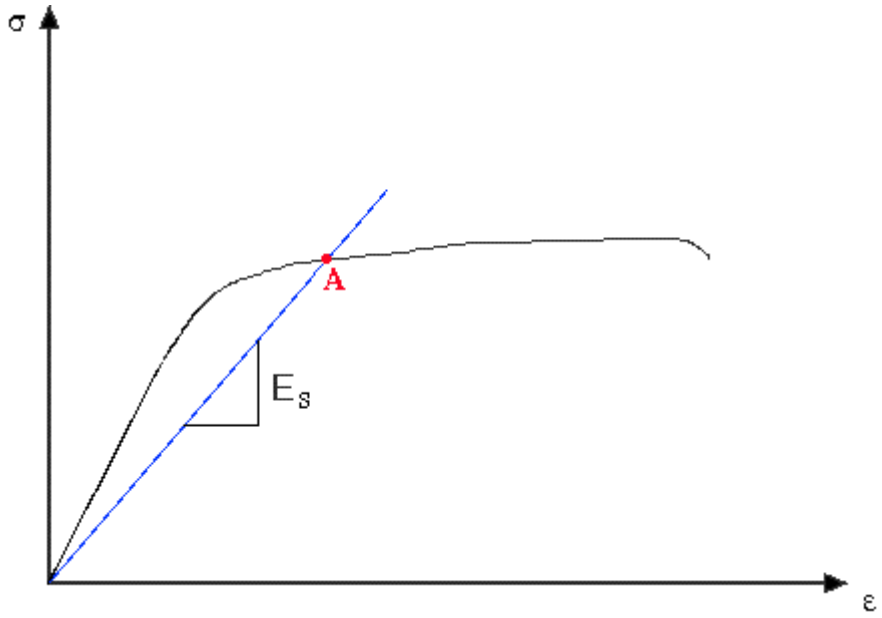

Figure A.1: How the secant modulus is determined

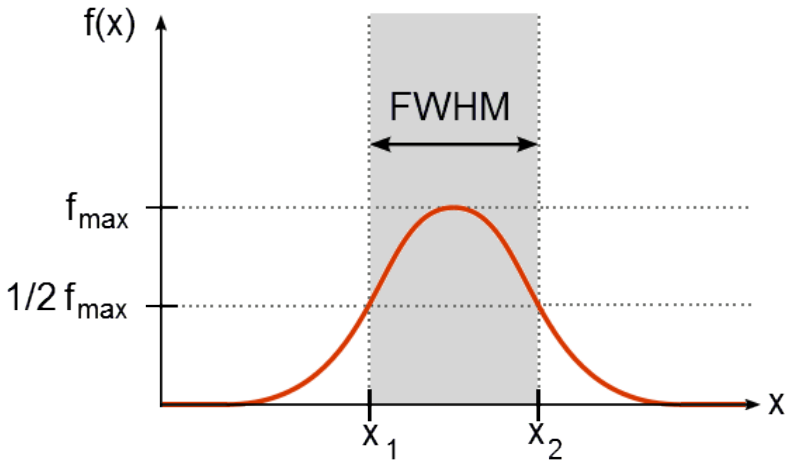

Figure A.2: Illustration of FWHM (Full Width at Half Maximum, which refers to the width of a peak or curve at half of its maximum height)

Load-deflection curve for small specimens

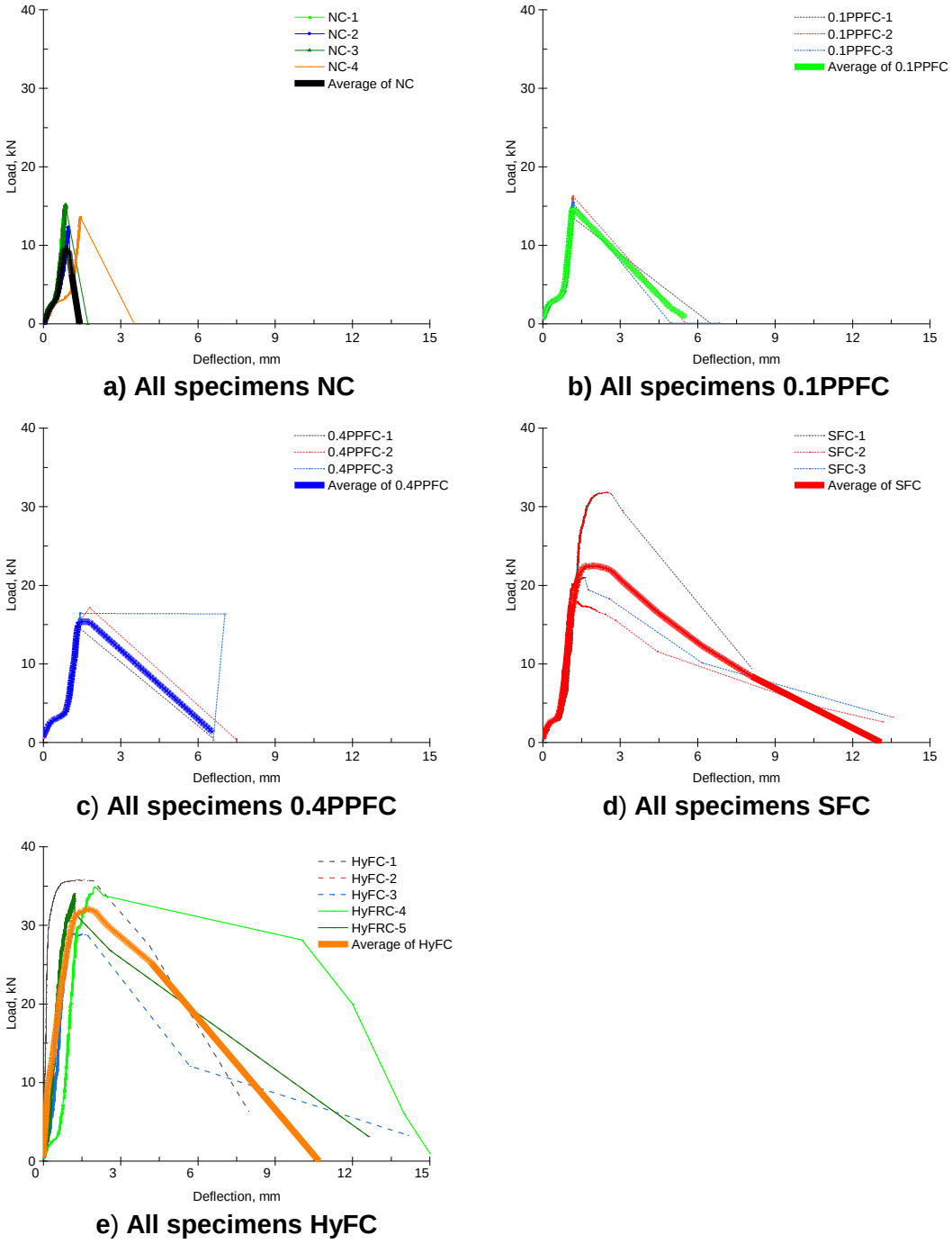

Figure A.3: Individual results of load-deflection curves for test beams (Deflection up to 2 mm)

Load-crack width curves for small specimens

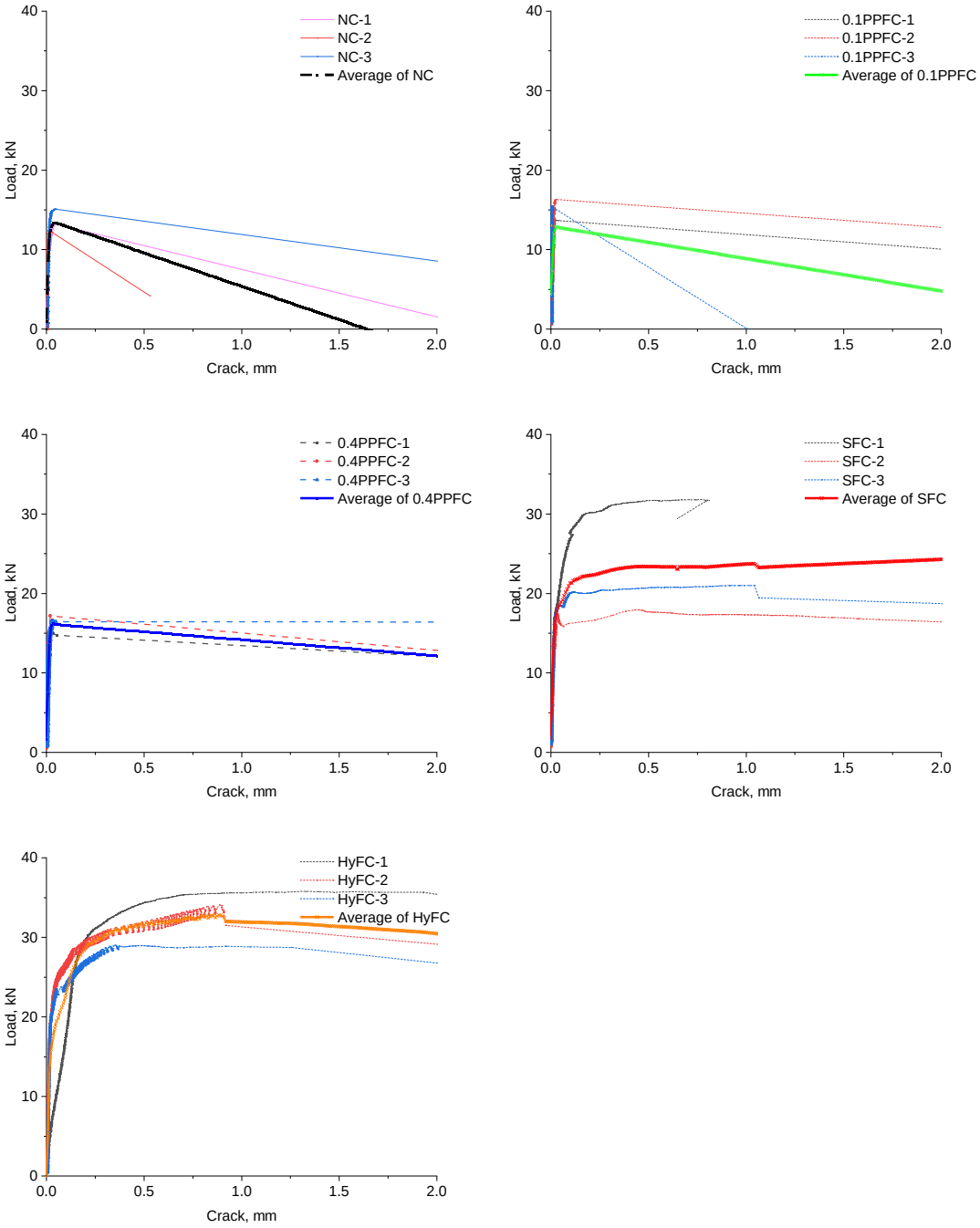

Figure A.4: Individual results of load-crack width curves for test beams (Crack width up to 2 mm)

Deflection-cycles curves under different load levels

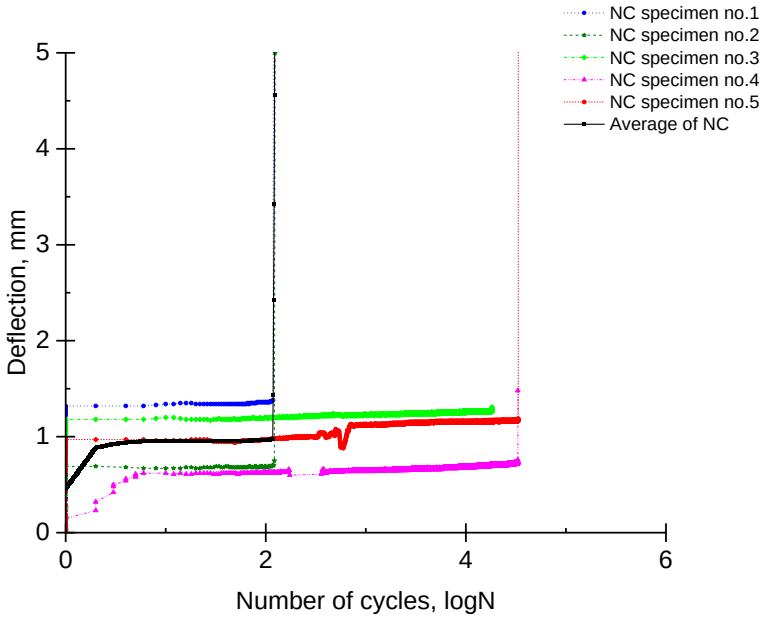

a) NC specimens for the load level of 20-80% of the maximum load

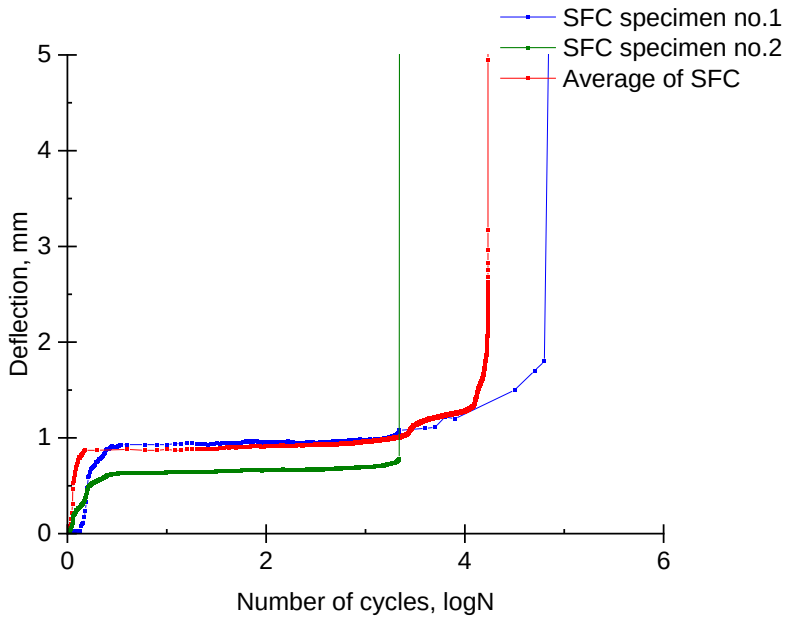

b) SFC specimens for the load level of 20-80% of the maximum load

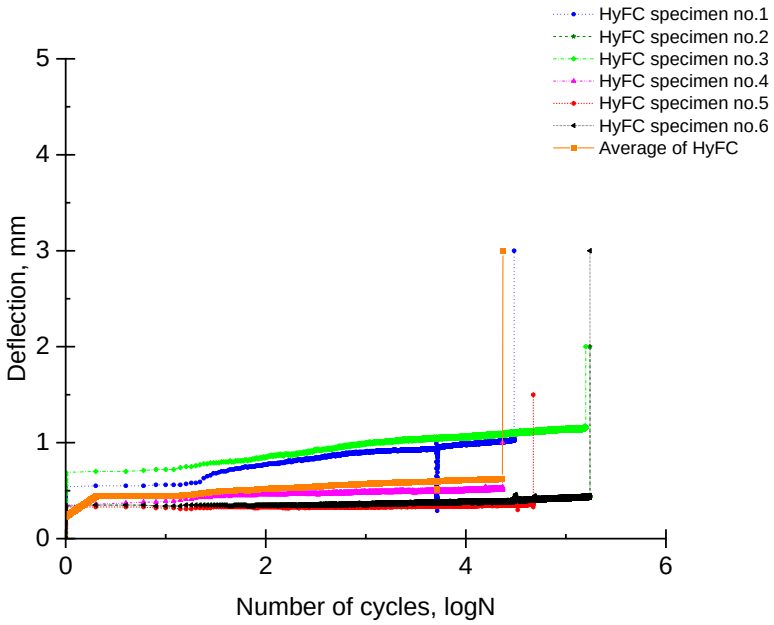

c) HyFC specimens for the load level of 20-80% of the maximum load

Figure A.5: Individual results of deflection of test beam for NC, SFC and HyFC beams with number of cycles, load level of 20-80% where the measurements were taken at 50% load level

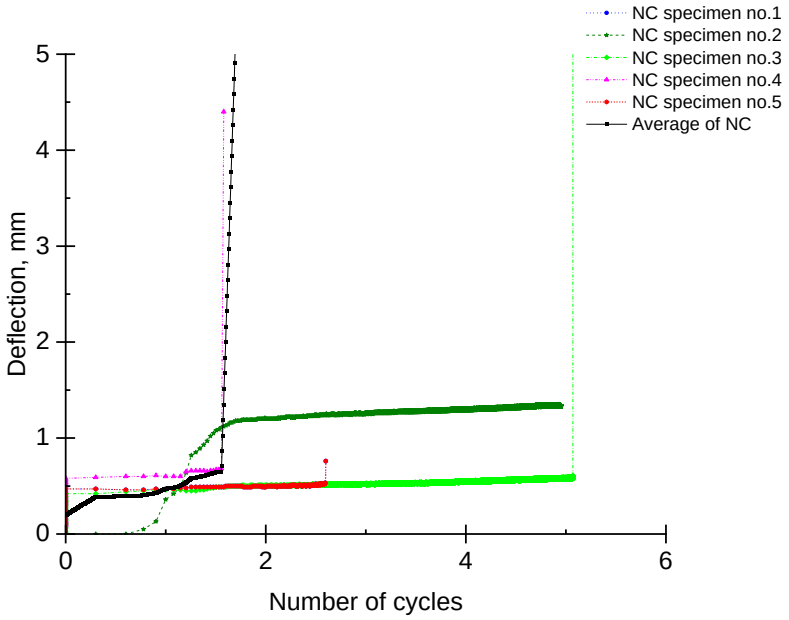

a) NC specimens for the load level of 30-70% of the maximum load

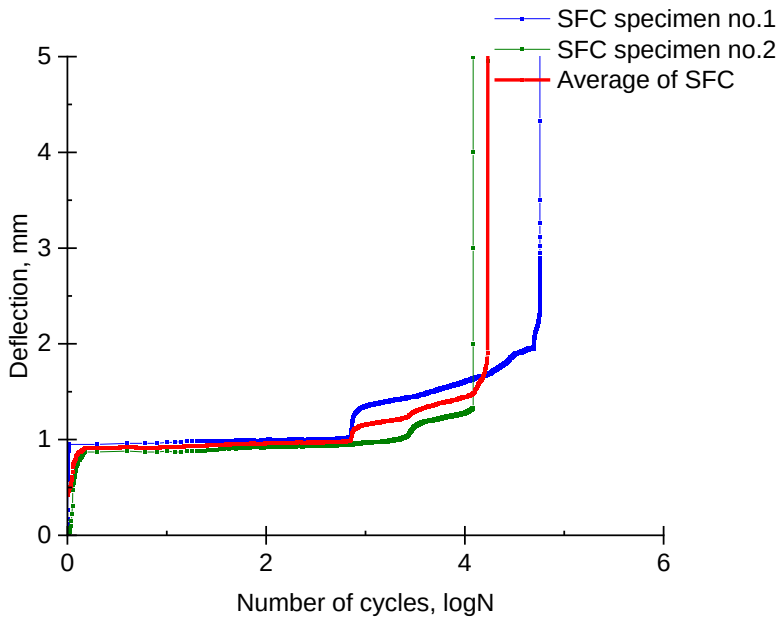

b) SFC specimens for the load level of 30-70% of the maximum load

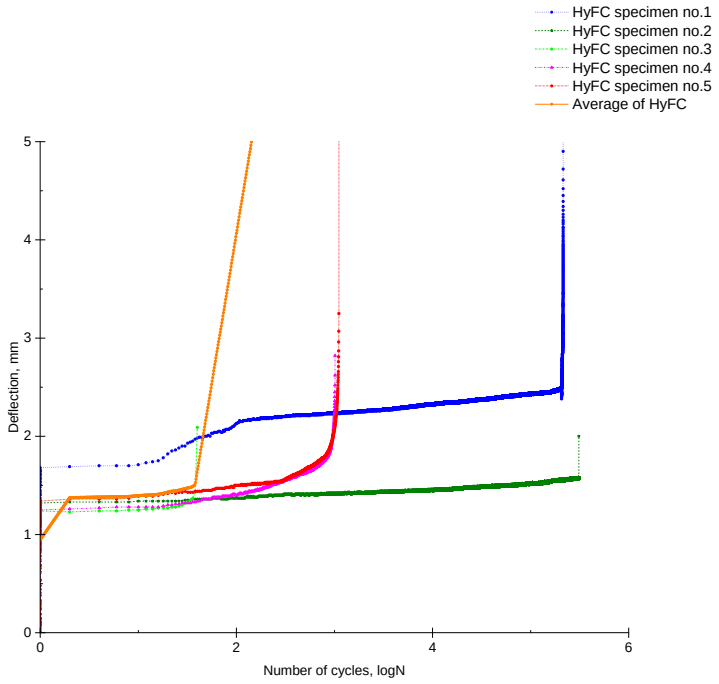

c) HyFC specimens for the load level of 30-70% of the maximum load

Figure A.6: Individual results of umber of cycles versus deflection of test beam for NC, SFC and HyFC beams, load level of 30-70% where the measurements were taken at 50% load level

Crack width behaviour under repeated loads

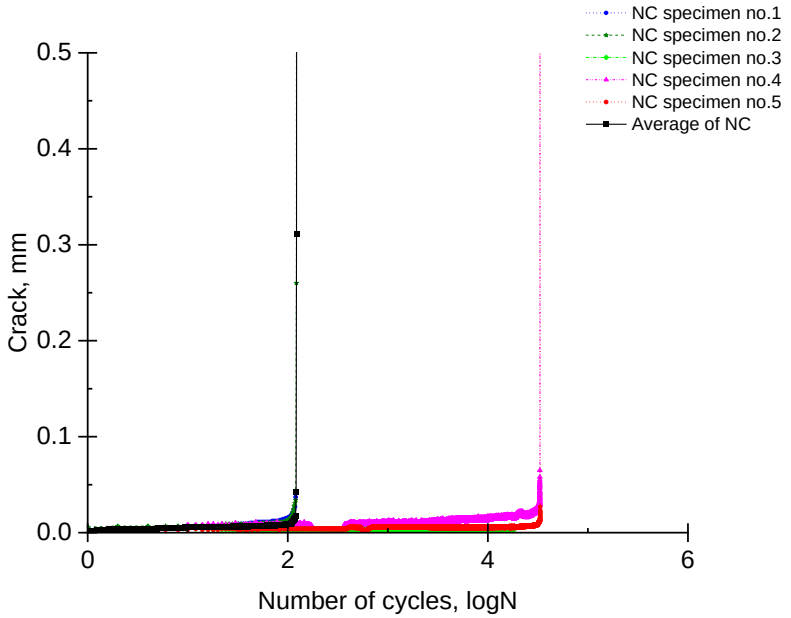

a) NC specimens for the load level of 20-80% of the maximum load

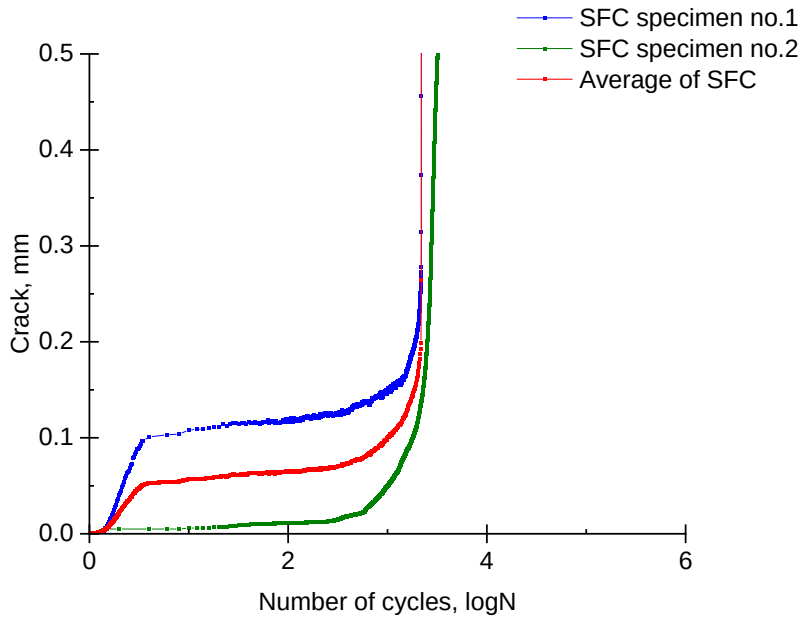

b) SFC specimens for the load level of 20-80% of the maximum load

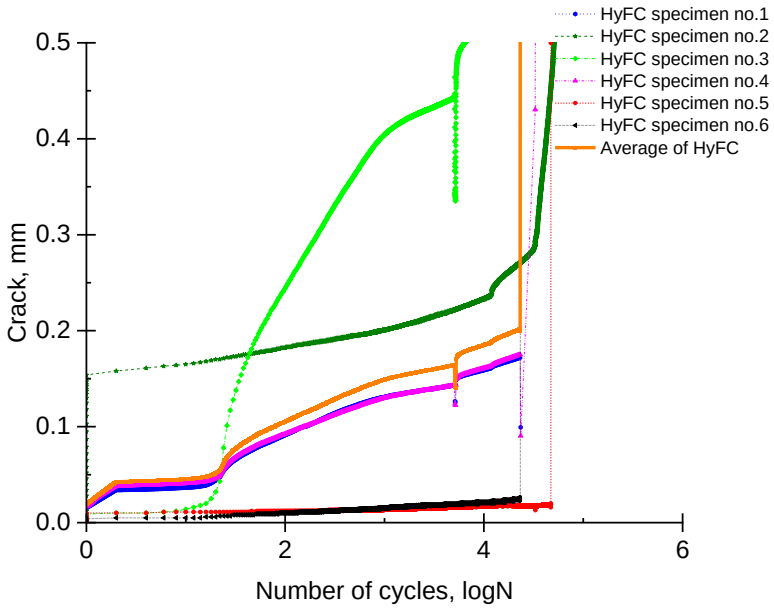

c) HyFC specimens for the load level of 20-80% of the maximum load

Figure A.7: Individual results of number of cycles versus crack width of test beam for NC, SFC and HyFC beams, load level 20-80% where the measurements were taken at 50% load level

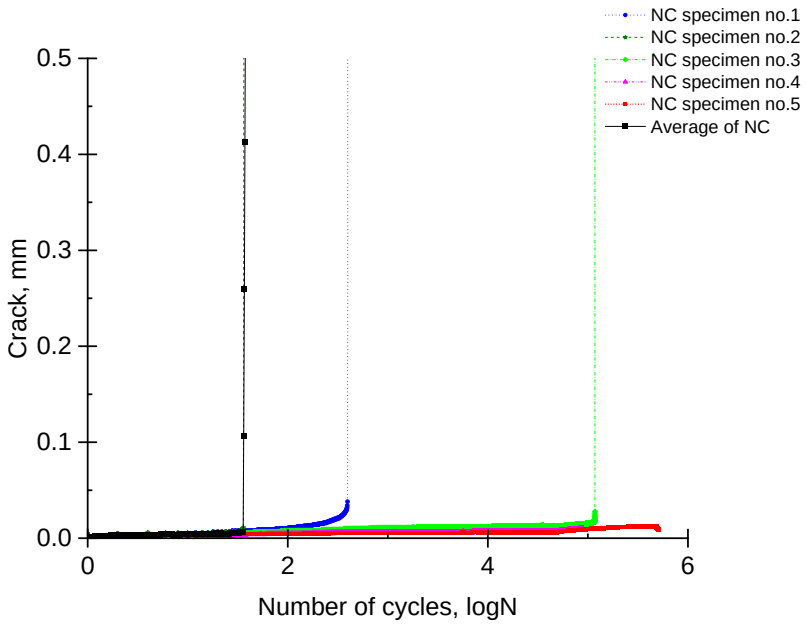

a) NC specimens for the load level of 30-70% of the maximum load

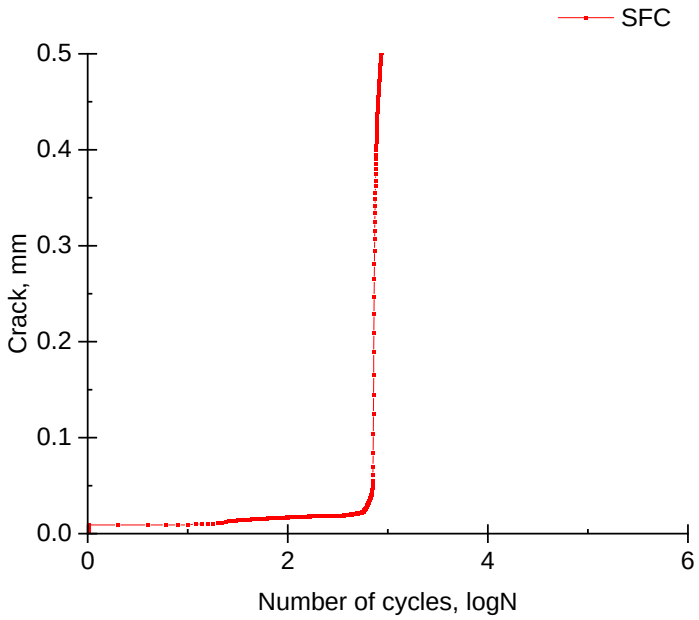

b) SFC specimens for the load level of 30-70% of the maximum load

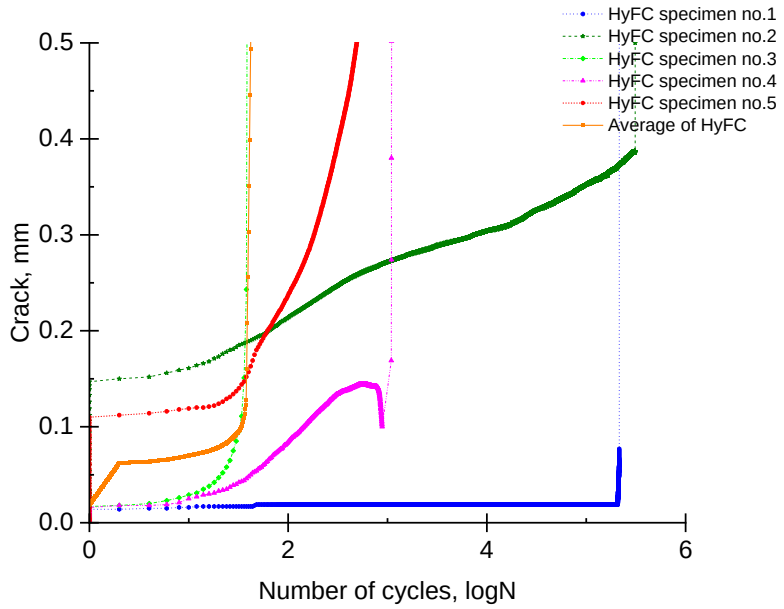

c) HyFC specimens for the load level of 30-70% of the maximum load

Figure A.8: Individual results of number of cycles versus crack width of test beam for NC, SFC and HyFC beams, load level 30-70% where the measurements were taken at 50% load level

Shrinkage

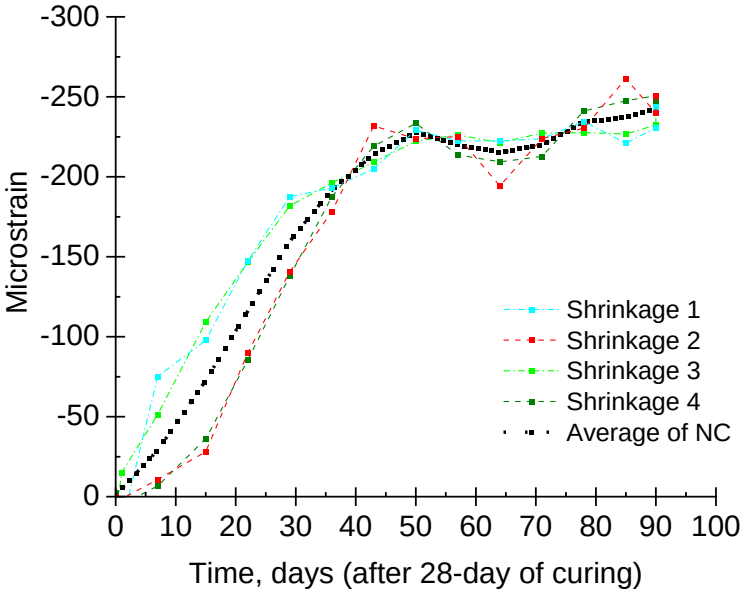

a) NC specimens

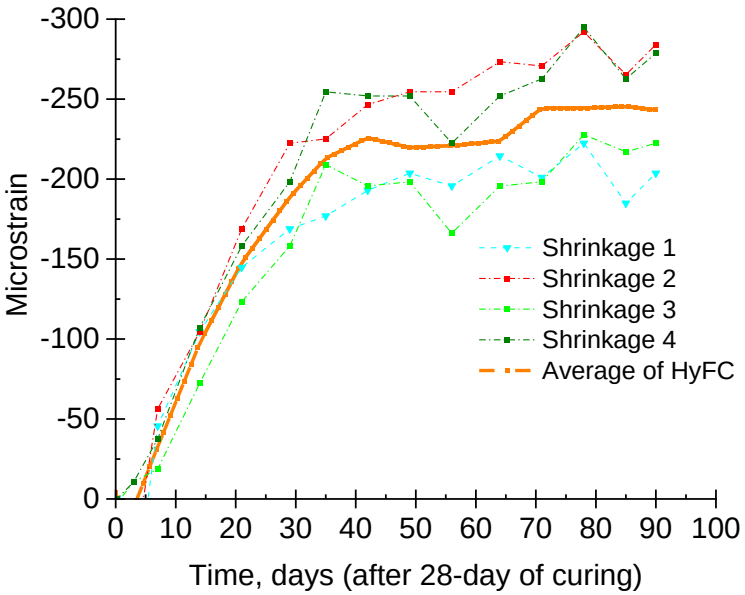

b) HyFC specimens

Figure A.9: Individual results of the effect of hybrid fibres on shrinkage

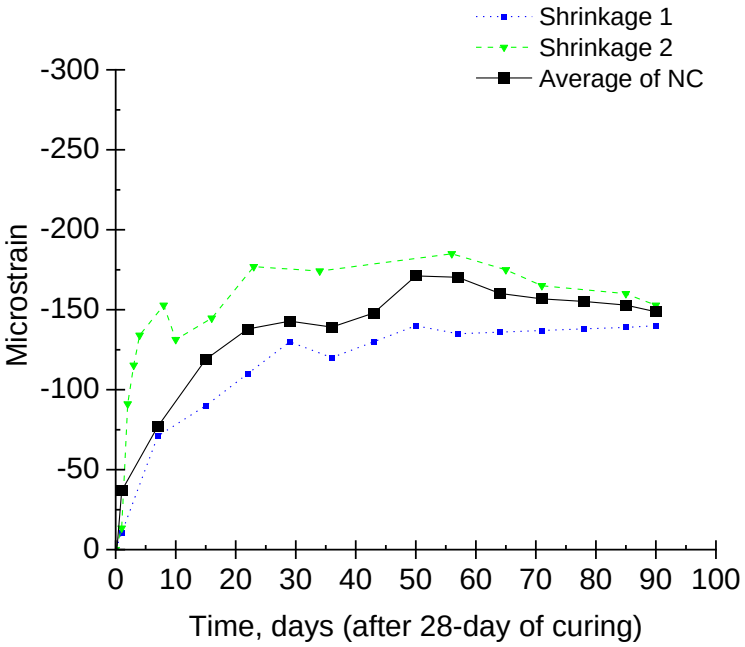

a) NC specimens

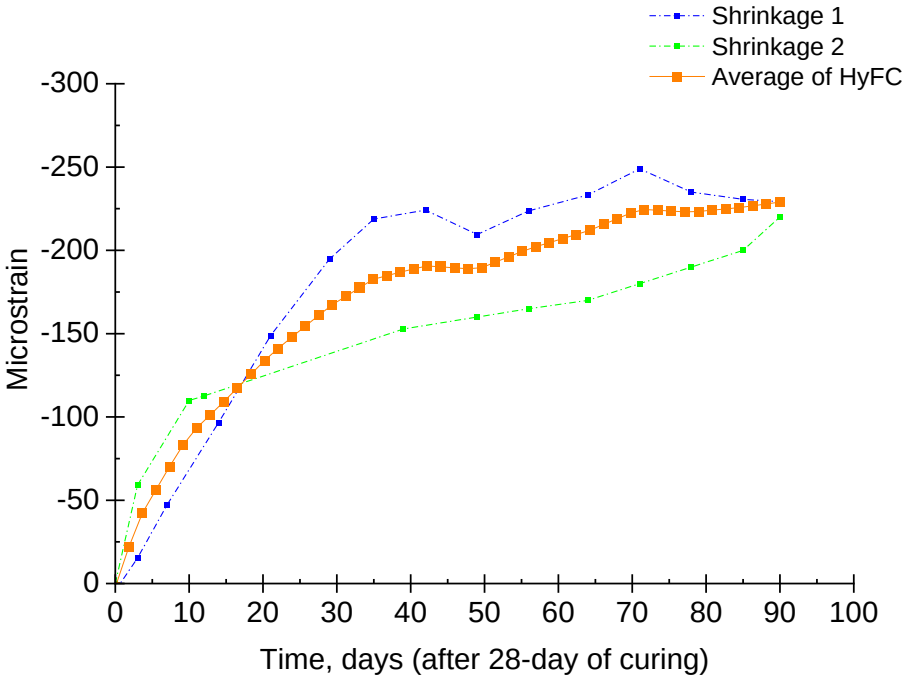

Figure A.10: Individual results of drying shrinkage of NC and HyFC concrete mix for unloaded bobbins

Compressive creep

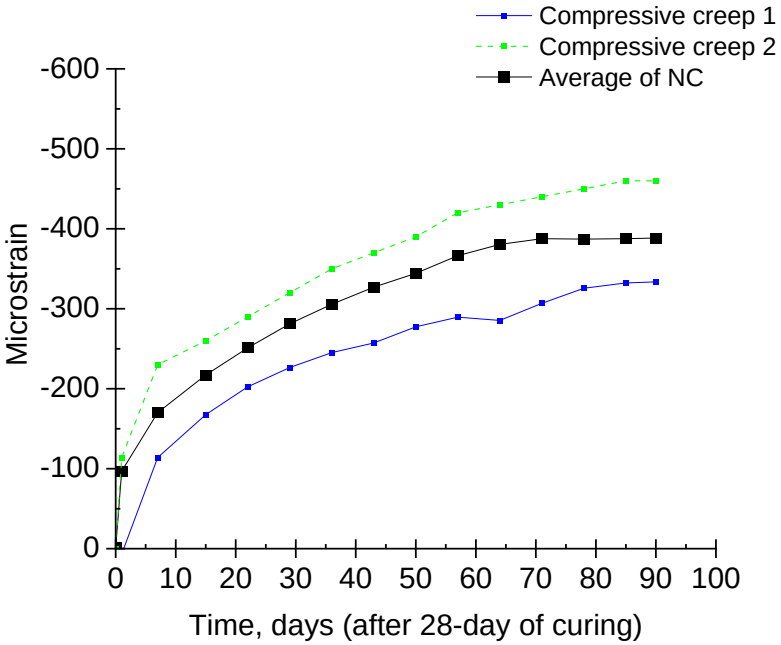

a) NC specimens

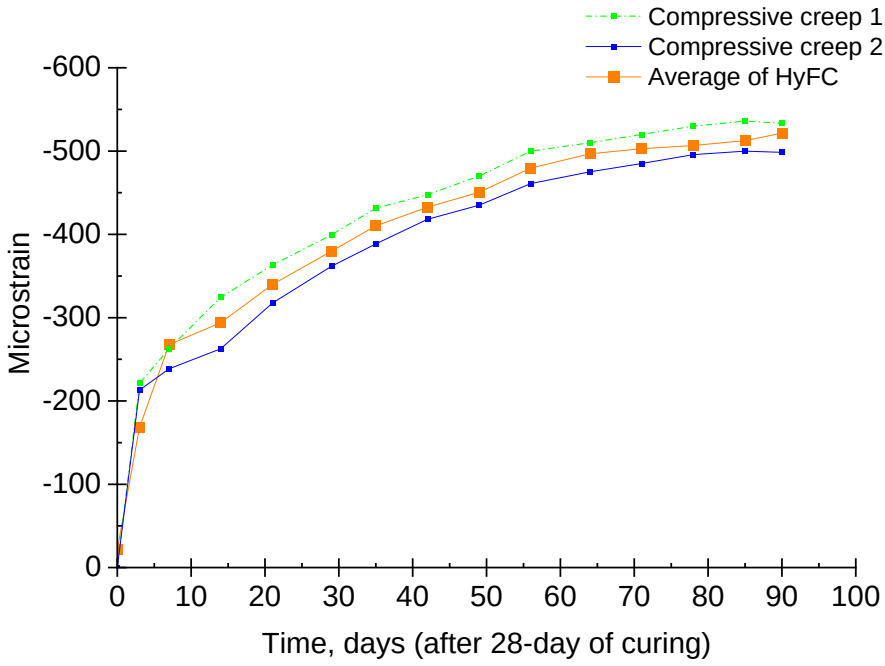

b) HyFC specimens

Figure A.11: Individual results of compressive creep of NC and HyFC concrete mix

Tensile creep

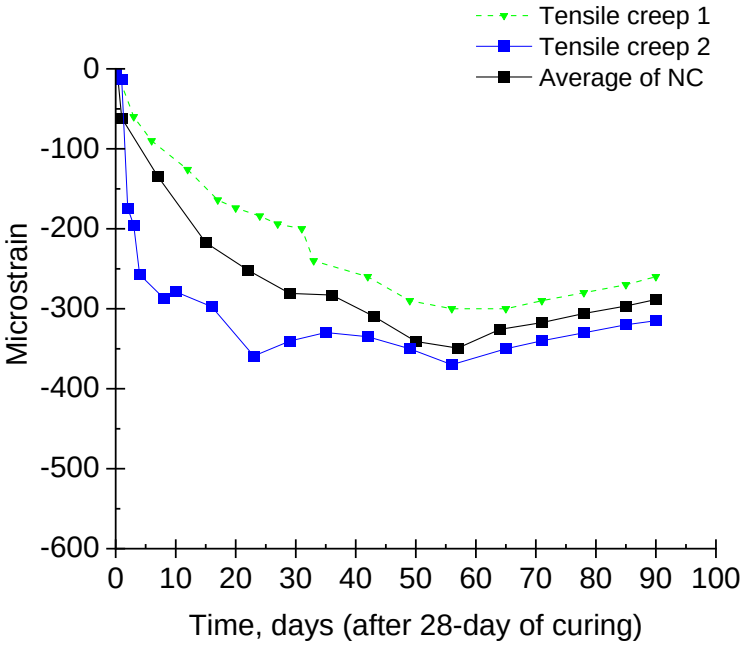

a) NC specimens

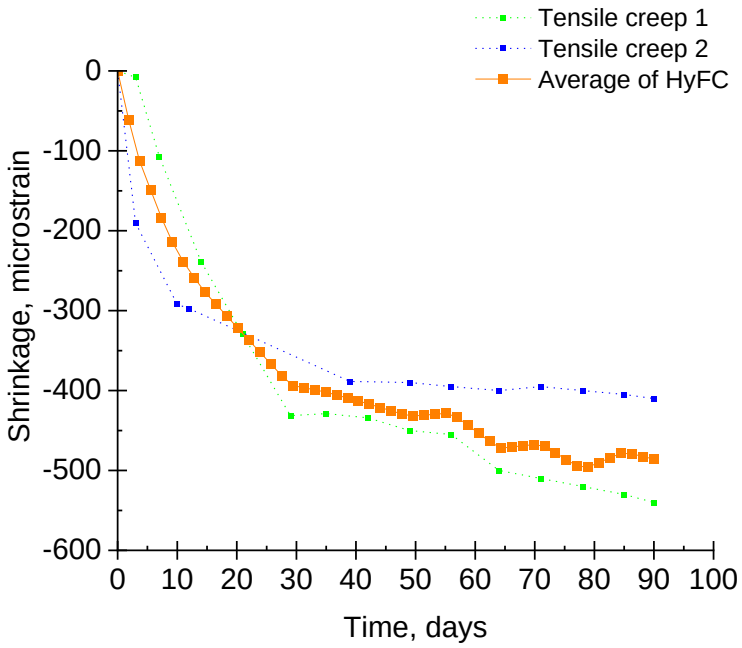

b) HyFC specimens

Figure A.12: Individual results of tensile creep of NC and HyFC concrete mix

Load-deflection curve for long beams

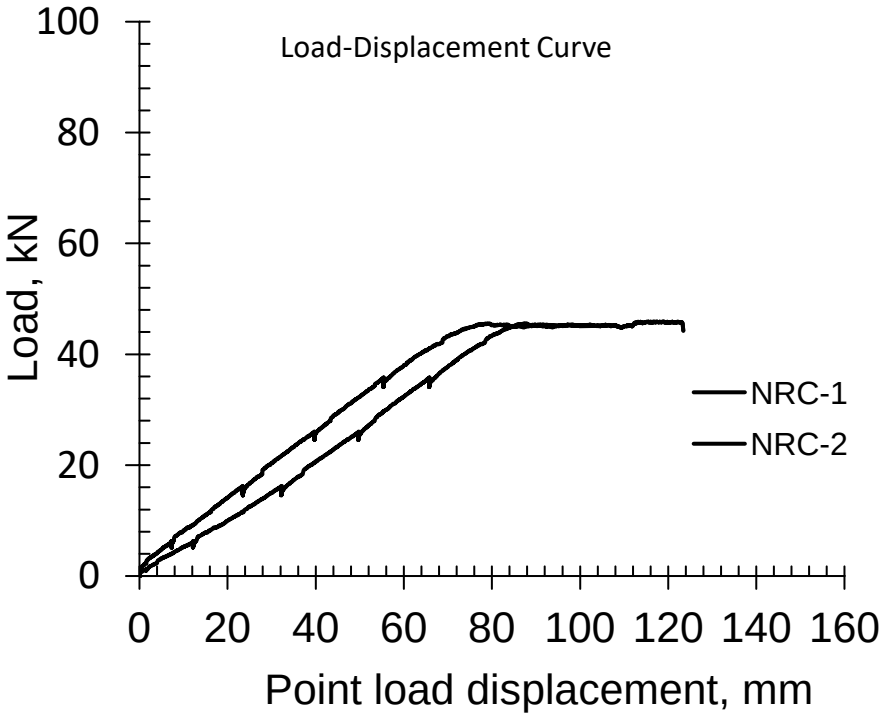

b) NRC specimens

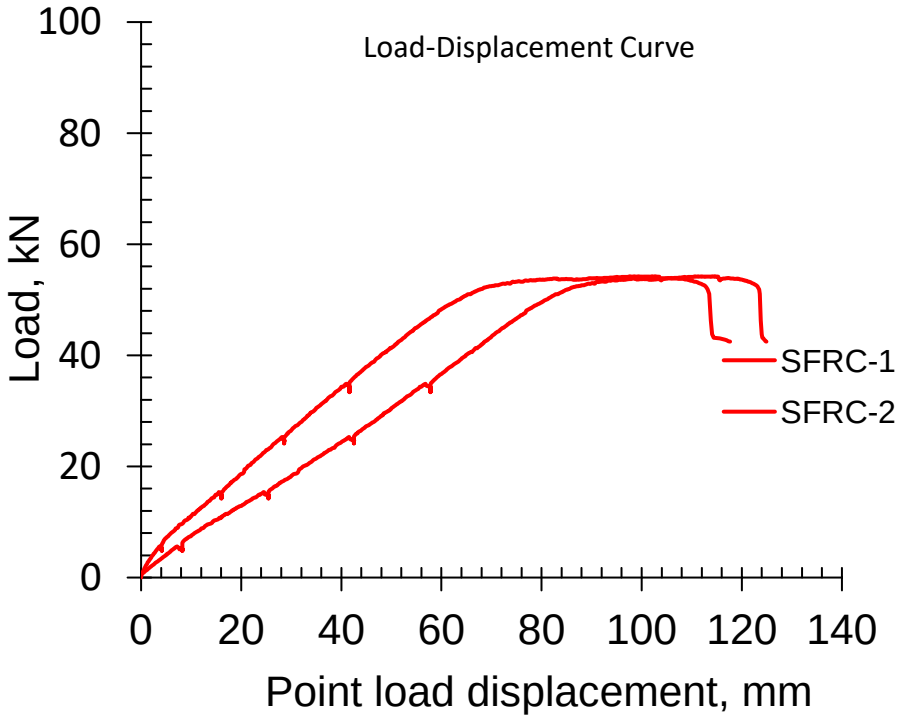

b) SFRC specimens

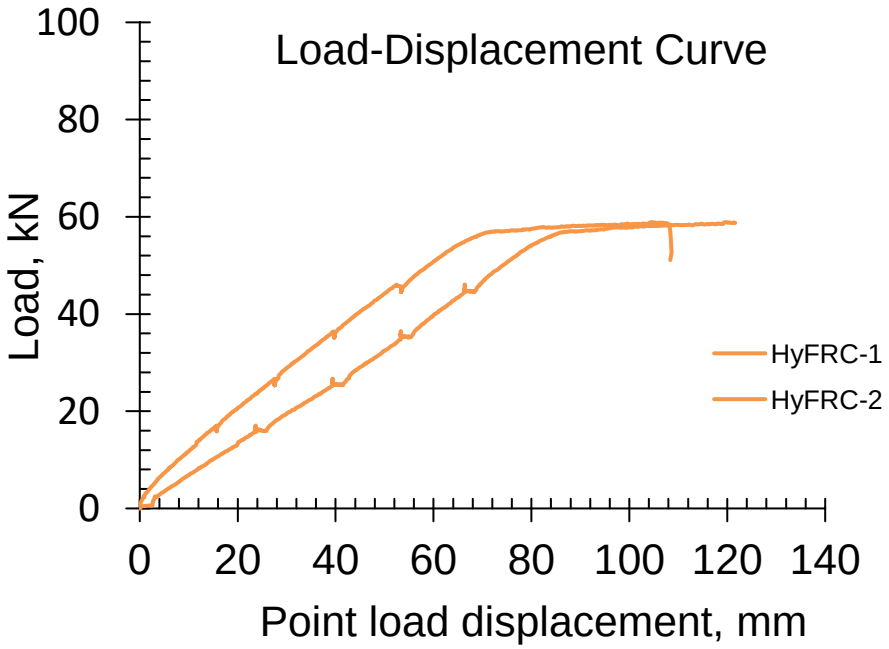

b) HyFRC specimens

Figure A.13: Individual results of load-deflection curve for beams

Calculation of long-term deflection

Structural elements that are not expected to experience loads surpassing the point at which concrete's tensile strength would be exceeded anywhere within the element should be categorised as "un-cracked." On the other hand, elements expected to develop cracks, though not necessarily completely, will exhibit behaviour falling between the "un-cracked" and "fully cracked" states. For elements primarily subjected to flexural forces, Expression (7.18) provides a reliable prediction of their behaviour.

$$\alpha = \zeta\alpha_{11} + (1-\zeta)\alpha_1 \qquad \text{Eq. A-1}$$

α is the deformation parameter considered which may be, for example, a strain, a curvature, or a rotation. (As a simplification, a may also be taken as a deflection.

α_1 and α_{11}= the distribution coefficient which takes into account the tension stiffening of the section. The factor ζ can be calculated from Expression 7.19 of EC2 as follows:

$$\zeta = 1 - \beta\left(\frac{M_{cr}}{M_a}\right)^2 \text{ when } M_a > M_{cr} \text{ (section is cracked)} \qquad \text{Eq. A-2}$$

ζ= 0 for uncracked sections.

β is a coefficient taking account of the influence of the duration of the loading or of repeated loading on the average strain (1.0 for a single short-term loading, 0.5 for sustained loads or many cycles of repeated loading).

M_a = the applied moment.

M_{cr}= the first cracking moment.

$$M_{cr}= \frac{f_{ctm} I_{unc}}{y_{tunc}} \quad \text{Eq. A-3}$$

The Eurocode 2 approach is applicable for estimating the overall long-term curvature of beams subjected to sustained loads, taking into account both creep and shrinkage effects independently. The impact of tension stiffening loss over time is factored in through the inclusion of a distribution factor,ζ, in the computations. Furthermore, the influence of creep is considered by adjusting the concrete's modulus of elasticity using the Effective Modulus Method (EMM), which relies on the creep coefficient's value over time, as illustrated below:

When dealing with loads of a duration that induces creep, the comprehensive deformation, which incorporates creep, can be determined by utilising an effective concrete modulus of elasticity, as defined in EC2 (Expression 7.20).

$$E_{c,eff}(t_0, t)= \frac{E_{c28}}{1+\varphi(\infty,t_0)} \quad \text{Eq. A-4}$$

$\varphi(\infty, t_0)$ is the creep coefficient relevant for the load and time interval.

t_0 is the age of the concrete at time of loading in days.

$$\frac{1}{r_c} = \zeta \frac{M_a}{E_{c,eff} I_c} + (1- \zeta) \frac{M_a}{E_{c,eff} I_u} \quad \text{Eq. A-5}$$

E_{c28} is the tangent modulus of elasticity at 28 days.

$$y_{tunc}= \frac{\frac{bh^2}{2}+(\alpha-1)(A_s d+A_{s2} d_2)}{bh+ (\alpha-1)(A_s+A_{s2})} \quad \text{Eq. A-6}$$

$$I_{unc} = \frac{bh^3}{12} + bh(\frac{h}{2} - y_{tunc})^2 + (\alpha - 1) A_s(\mathrm{d} - y_{tunc})^2 + (\alpha - 1) A_{s2}(y_{tunc} - d_2)^2 \quad \text{Eq. A-7}$$

$$y_{tc} = \frac{[(\alpha_e A_s+(\alpha_e-1)A_{s2})^2 + 2\mathrm{b}((\alpha_e A_s \mathrm{d}+(\alpha_e-1)A_{s2} d_2)]^{0.5} - (\alpha_e A_s+(\alpha_e-1)A_{s2})}{b} \quad \text{Eq. A-8}$$

$$I_c = \frac{b y_{tc}^3}{12} + \alpha_e A_s(\mathrm{d} - y_{tc})^2 + (\alpha_e - 1) A_{s2}(y_{tc} - d_2)^2 \quad \text{Eq. A-9}$$

d is the distance between the centroid of the area of tension reinforcement and the maximum compressive fibre in a reinforced concrete beam.

d_2 is the distance between the centroid of the area of compression reinforcement and the maximum compressive fibre in a reinforced concrete beam.

α is the ratio of modulus ratio ($\frac{E_s}{E_c}$).

A_s is the area of steel in the tension zone.

A_{s2} is the area of steel in the compression zone.

I_{unc} & I_c the second moments of area of the un-cracked and cracked sections.

$$S_{unc} = A_s(\mathrm{d} - y_{tunc}) - A_{s2}(y_{tunc} - d_2) \qquad \text{Eq. A-10}$$

$$S_c = A_s(\mathrm{d} - y_{tc}) - A_{s2}(y_{tc} - d_2) \qquad \text{Eq. A-11}$$

S_{unc} & S_c is the initial moments of area of the reinforcement around the centroid of both the un-cracked and cracked sections.

Shrinkage curvatures can be assessed using the expression provided in EC2 (Equation 7.21).

$$\frac{1}{r_{cs}} = \zeta\ \varepsilon_{cs}\ \alpha_e\ \frac{S}{I} \qquad \text{Eq. A-12}$$

$\frac{1}{r_{cs}}$ is the curvature due to shrinkage

ε_{cs} is the free shrinkage strain.

I is the second moment of area of the section.

α_e = the effective modulus ratio ($\frac{E_s}{E_{c,eff}}$).

S and I should be calculated for the uncracked condition and the fully cracked condition, the final curvature being assessed by use of Expression (7.18) (first equation)

So the calculation for the curvature resulting from the shrinkage effect is as follows:

$$\frac{1}{r_{sh}} = \zeta\ \varepsilon_{sh}(t_0, t)\ \alpha_e\ \frac{S_c}{I_c} + (1-\zeta)\ \varepsilon_{sh}(t_0, t)\alpha_e\ \frac{S_u}{I_u} \qquad \text{Eq. A-13}$$

$\varepsilon_{sh}(t_0, t)$ = the shrinkage strain at time t.

α_e = the effective modulus ratio ($\frac{E_s}{E_{c,eff}}$).

I_u & I_c the second moments of area of the un-cracked and cracked sections.

The development of the drying shrinkage strain in time follows from:

$$\varepsilon_{cd}(t) = \beta_{ds}(t, t_s).\, k_h.\, \varepsilon_{cd,0} \qquad \text{Eq. A-14}$$

k_h is a coefficient depending on the notional size h_0 according to Table 3.3

$$\beta_{ds}(t, t_s) = \frac{(t - t_s)}{(t - t_s) + 0.04\sqrt{{h_0}^3}} \qquad \text{Eq. A-15}$$

t is the age of the concrete at the moment considered, in days.

t_s is the age of the concrete (days) at the beginning of drying shrinkage (or swelling). Normally this is at the end of curing.

h_0 is the notional size (mm) of the cross-section = $2A_c/u$

Where:

A_c is the concrete cross-sectional area.

u is the perimeter of that part of the cross section which is exposed to drying

The total long-term curvature is calculated using the expression:

$$\frac{1}{r} = \frac{1}{r_{sh}} + \frac{1}{r_c} \qquad \text{Eq. A-16}$$

$\frac{1}{r}$ is the total long-term curvature.

$\frac{1}{r_{sh}}$ is the curvature due to shrinkage.

$\frac{1}{r_c}$ is the curvature due to creep .

So, the total long-term deflection is:

$$\Delta = \mathrm{K}L^2 \frac{1}{r} \qquad \text{Eq. A-17}$$

K is the

L is the length of the beam in mm

The creep coefficient and shrinkage strain at time can be obtained from the method in FIB Model Code (2010) for normal concrete and are given by:

$$\varphi(\infty, t_0) = \phi_{c,RH}(\mathrm{h})\ \beta_c(\mathrm{f}_{cm28})\ \beta_c(\mathrm{t}_0)\ \beta_c(\mathrm{t}, \mathrm{t}_0) \qquad \text{Eq. A-18}$$

$$\varepsilon_{sh} = \phi_{S,RH}(\mathrm{h})\ \beta_s(\mathrm{f}_{cm28})\ \beta_s(\mathrm{t}, \mathrm{t}_0) \qquad \text{Eq. A-19}$$

ϕ_{RH}(h) is the correction factor for ambient relative humidity.

$\beta(\mathrm{f}_{cm28})$ is the correction factor for compressive strength.

$\beta_c(\mathrm{t}_0)$ is the correction factor for loading age.

$\beta(\mathrm{t}, \mathrm{t}_0)$ is the time function.

The change of neutral axis

The neutral axis was determined by calculating the ratio of strain values from the top and bottom of the maximum compressive strain (ε_c) and maximum tensile strain (ε_t) to the ratio of the neutral axis (x or c) and the depth of the section (d) as shown in Figure A.14 (a and b).

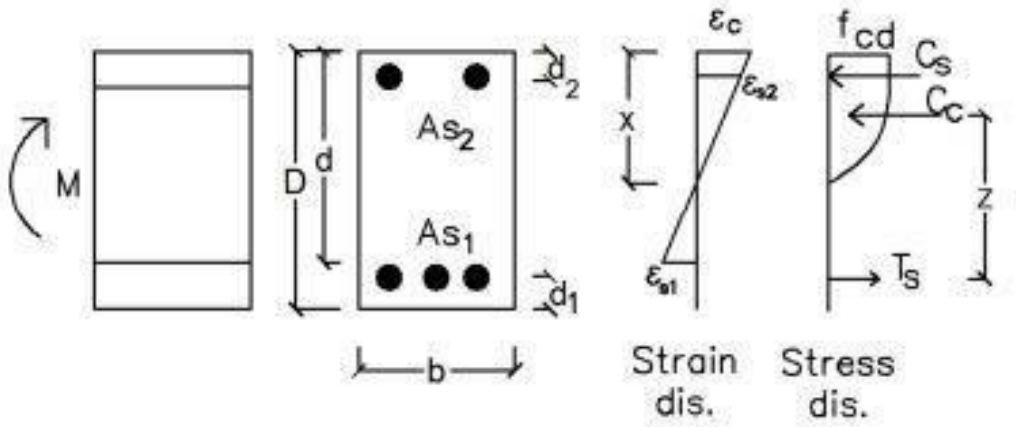

a)

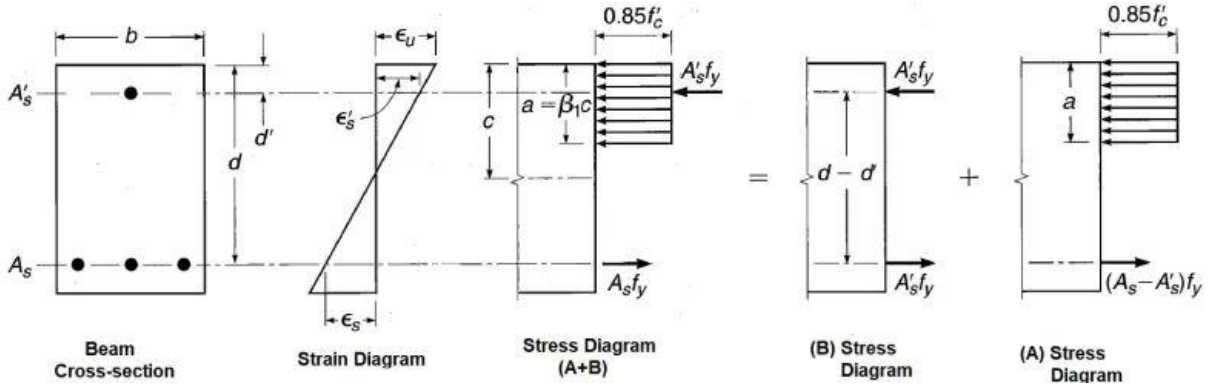

b)

Figure A.14: Calculation of the change of neutral axis

Modelling of the unreinforced beam

Introduction

Crack propagation kinetics are of significant interest in a wide variety of areas from forecasting crack arrest duration in engineering systems, earthquakes, and bone fracture, to affecting spacecraft fragmentation defence and military armour (Crump et al., 2017).

Fracture mechanics defines as the science of anticipating and predicting the capability of structures on carrying load and elements that contain cracks. Fracture mechanics is the subject of the research, characterizing the fracture resistance of the materials. Among other words, the 'tolerance' of propagation of a substance to crack is analysed. The restrictions and inflexible nature of analytical approaches in handling arbitrary complex issues, particularly in anisotropic dynamic problems, have led to the widespread use of various numerical methods over the past decades to resolve problems of composite fracture mechanics (Mohammadi, 2012) .The key types of numerical approach to solve general problems of crack stability and propagation problems are categorized into different types, the method of boundary elements (BEM), meshless methods, the method of finite elements (FEM), the method of extended finite elements (XFEM) and, more recently, various multi-scale techniques. (Mohammadi, 2012).

In the context of static testing in the Finite Element Analysis (FEA) of unreinforced beams, the sole distinction between the full-scale beam and unreinforced beam tests was the application of load control. This was done to simulate the experimental tests under a general static step scenario. In order to model the crack, the eXtended Finite Element Method (XFEM) was used to simulate the crack growth.

A lot of researches on concrete fracture behaviour have developed many effectual concrete fracture models. The traditional finite element model (FEM) with cohesive zone model can therefore not predict the crack and its propagation path that has been randomly formed (Wang and Wang (2014)). However, the XFEM offers significant advantages in numerical modelling of crack propagation as opposed to the traditional finite-element method. The crack geometry in the XFEM, does not need to be matched with the edges of the components, which offers flexibility and versatility in modelling. XFEM does not demand on the mesh

to match the geometry of the discontinuities, which is considered to be functional and effective way to simulate and illustrate the initiation and spread of an individual and separate crack along an arbitrary path as reported by Wang (2011). XFEM is generated independently of the crack, Thus, the direction and position of the crack are not defined (Huang, 2011). XFEM has been the major comprehensive hunt for solving a number of discontinuity issues in under a decade. Consequently, the XFEM model simulated failure is simpler to detect than the standard model of finite elements.

Extended Finite Element Method (XFEM) concept

The eXtended Finite Element Method (XFEM) is a partition-of-unity-cantered technique that is well-suited for simulating crack propagation phenomena, even when the crack path is not known in advance. Typically, it is implemented numerically using dedicated, independent software.

There is also space for the use of advanced techniques such as the Extended Finite Element Method (XFEM), which does not take into account the matching of mesh with discontinuities and is desirable and useful in the study of discrete crack initiation and propagation. XFEM has a tremendous potential for simulating the complex composite material structure. Furthermore, in XFEM, the direction of crack propagation and growth is independent of the presumed mesh size (Wang (2012)). The benefits of using the XFEM include prediction of the path of crack without remeshing and no need for a specific element size or mesh refining close to the crack tip as stated by Moes et al. (1999). Further, in the numerical simulation of crack growth, XFEM has significant advantages since the XFEM does not demand to know the site of crack initiation and the path of the crack as reported by Mahmoud et al. (2014). In various research under static and dynamic loading, the XFEM precisely predicted the initiation of the crack site and crack direction as reported by Wang (2012); Elhady et al. (2017); Elhady et al. (2020); Dirik and Yalçinkaya (2016).

Model process and geometry

Similar procedure was followed for conducting the modelling process for unreinforced beam same as modelling of full-scale beams (section 6.1.3), as can be seen in Figure A.15. Different main steps may be identified in the Abaqus process:

- ❖ Step 1 – Parts modelling that includes specifying geometric, material properties and element types (i.e., solid, shell...Etc.,).
- ❖ Step 2 - Boundary and constraint conditions
- ❖ Step 3 - Output analysis
- ❖ Step 4 - Post-processing of the results

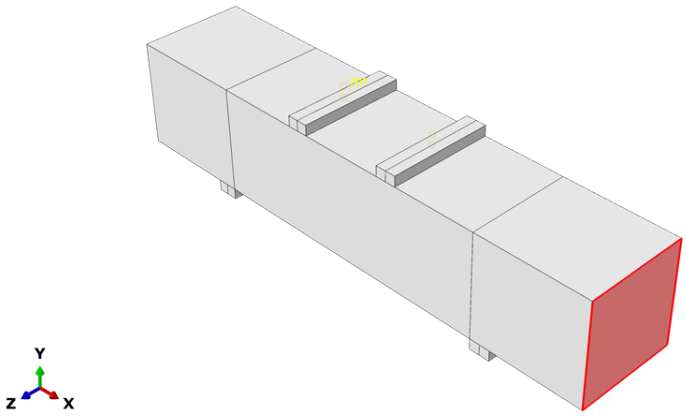

a) Model geometry

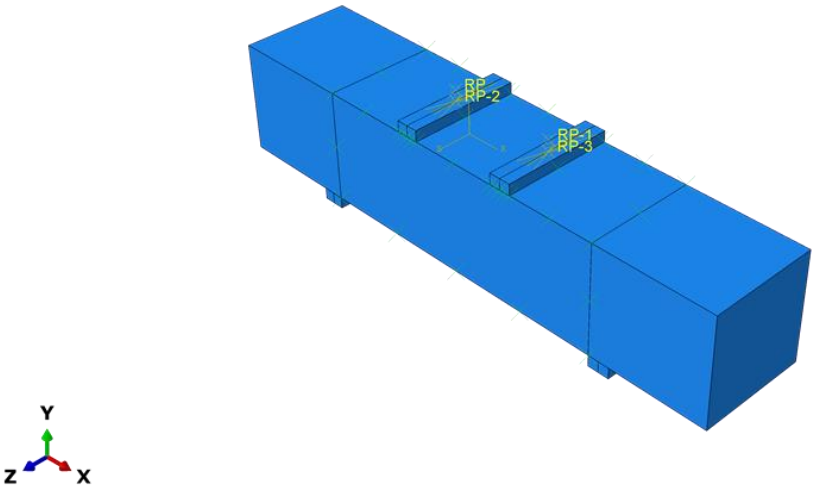

b) Crosses indicate the area where the XFEM is defined

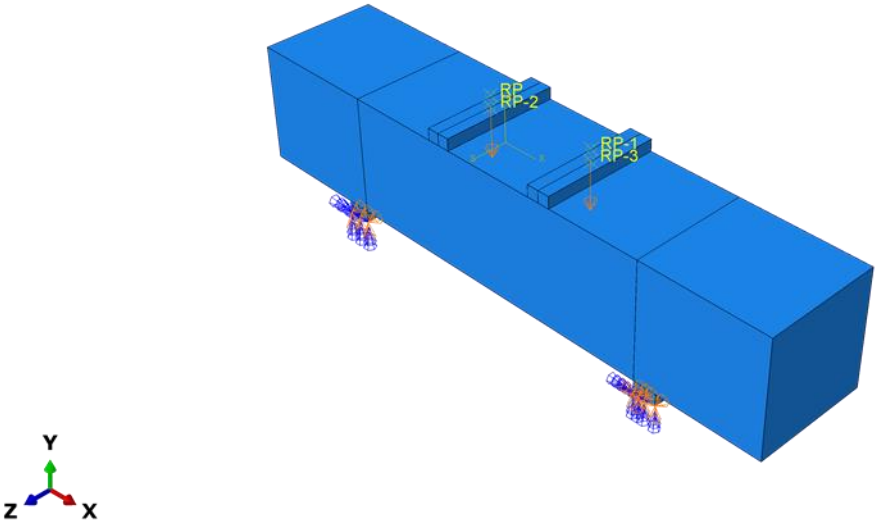

c) Loads and boundary conditions

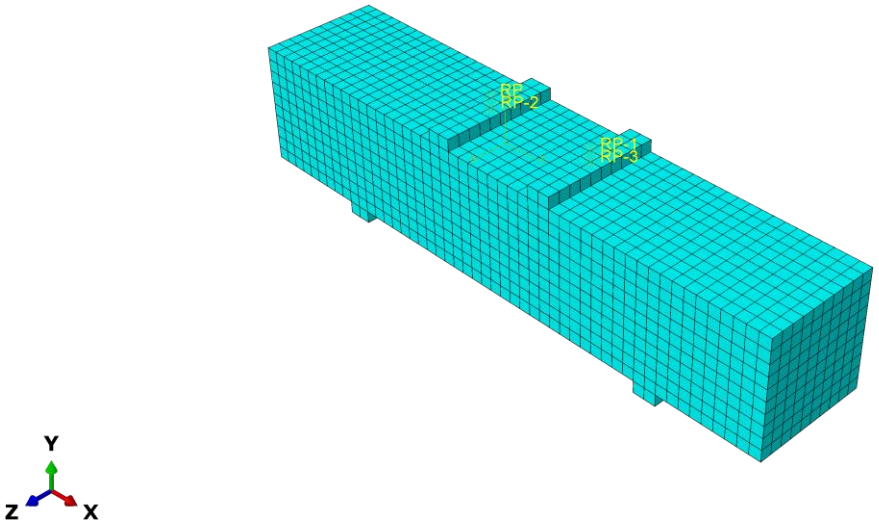

d) Mesh of the specimen

Figure A.15: Modelling process

Validation study results

Tables Table A.1 and Table A.2 provide a concise overview of the outcomes obtained from both FEA and experimental testing for various concrete types when subjected to static loads. From the findings of the experimental and FEA analyses for HyFC, Figure A.16(c) showcases the most accurate representation for forecasting the visually observed load-deflection curve within the FEA models.

The FEA predictive model underestimated the NC beam's maximum load by 11.36% when contrasted with the experimental findings with a ratio of EXP/FEA equal to 1.12. Likewise, for the SFC and HyFC beam, the predictive model exhibited a slight reduction, specifically 5.46% and less than 1% a ratio of EXP/FEA equal to 1.05 and 1.01, respectively, compared to the experimental results.

However, in the context of maximum deflection, the predictive model underestimated the maximum deflection at the peak load by 34.5%, 69% and 11.5% for NC, SFC and HyFC, respectively, in comparison to the experimental results. Maximum load and maximum deflection values from both the FEA model and experimental results are detailed in Table Table A.1 and Table A.2.

Table A.1: Comparison between the static results of FEA models and experimental results (maximum deflection and failure loads)

Type of beam	Peak load (kN)		Deflection at the peak (mm)		Ratio of peak load (EXP/FEA)	Ratio of deflection (EXP/FEA)
	EXP	FEA	EXP	FEA		
NC-ST-0	13.56	12.02	0.87	0.57	1.12	1.52
SFC-ST-1	23.61	22.32	1.61	0.50	1.05	3.22
HyFC-ST-1.5	33.46	33.16	1.65	1.46	1.01	1.13

Table A.2: Comparison between the static results of FEA models and experimental results (deflection of the beams at different applied loads)

Type of beam	Applied load (kN)									
	5		10		15		20		Peak	
	EXP	FEA	EXP	FEA	EXP	FEA	EXP	FEA	EXP	FEA
	Deflection (mm)									
NC-ST-0	0.57	0.04	0.76	0.2	-	-	-	-	0.87	0.57
SFC-ST-1	0.71	0.06	0.91	0.1	1.05	0.13	1.32	0.21	1.61	0.50
HyFC-ST-1.5	0.28	0.08	0.44	0.13	0.59	0.18	0.72	0.44	1.65	1.46

As depicted in Figure A.16(a), the experimental results of NC exhibit a non-linear behaviour until the deflection reaches a value of 0.51 mm. This behaviour may account for the deviation observed between the experimental and FEA results. According to the data in Table Table A.1 and Table A.2, the disparities in the early

stage results suggest the possibility that the experimental tests may require pre-loading of the specimens.

Similarly, as illustrated in Figure A.16(b), the experimental results display a non-linear behaviour until the deflection reaches a value of 0.61 mm. This behaviour may help elucidate the observed deviation between the experimental and FEA results. According to the data in Tables Table A.1 and Table A.2 provide a concise overview of the outcomes obtained from both FEA and experimental testing for various concrete types when subjected to static loads. From the findings of the experimental and FEA analyses for HyFC, Figure A.16(c) showcases the most accurate representation for forecasting the visually observed load-deflection curve within the FEA models.

The FEA predictive model underestimated the NC beam's maximum load by 11.36% when contrasted with the experimental findings with a ratio of EXP/FEA equal to 1.12. Likewise, for the SFC and HyFC beam, the predictive model exhibited a slight reduction, specifically 5.46% and less than 1% a ratio of EXP/FEA equal to 1.05 and 1.01, respectively, compared to the experimental results.

However, in the context of maximum deflection, the predictive model underestimated the maximum deflection at the peak load by 34.5%, 69% and 11.5% for NC, SFC and HyFC, respectively, in comparison to the experimental results. Maximum load and maximum deflection values from both the FEA model and experimental results are detailed in Table Table A.1 and Table A.2.

Table A.1 and Table A.2, the discrepancies in the early stage results suggest the possibility that the experimental tests may require pre-loading of the specimens.

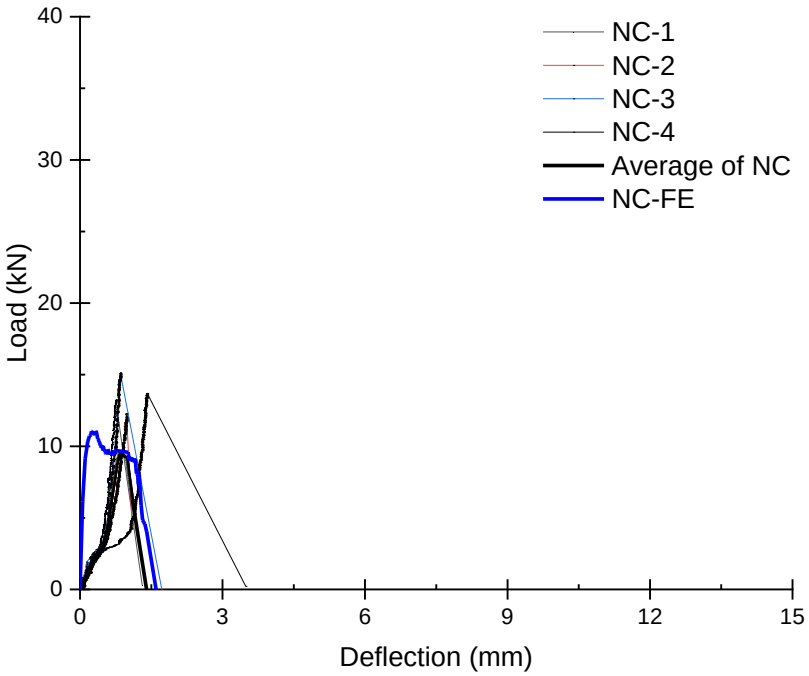
NC-1
NC-2
NC-3
NC-4
Average of NC
NC-FE
Load (kN)
Deflection (mm)
0
10
20
30
40
0
3
6
9
12
15

a) NC

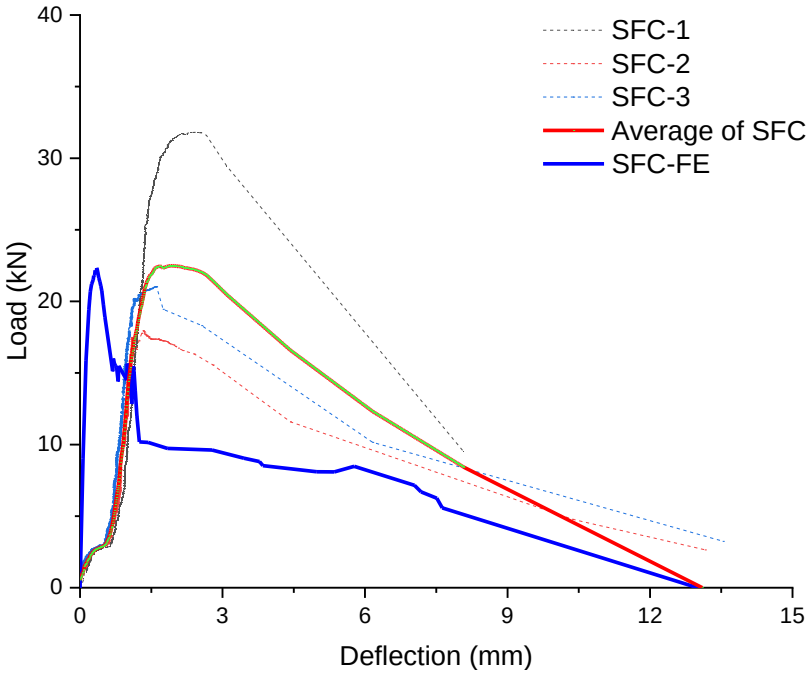
SFC-1
SFC-2
SFC-3
Average of SFC
SFC-FE
Load (kN)
Deflection (mm)
0
10
20
30
40
0
3
6
9
12
15

b) SFC

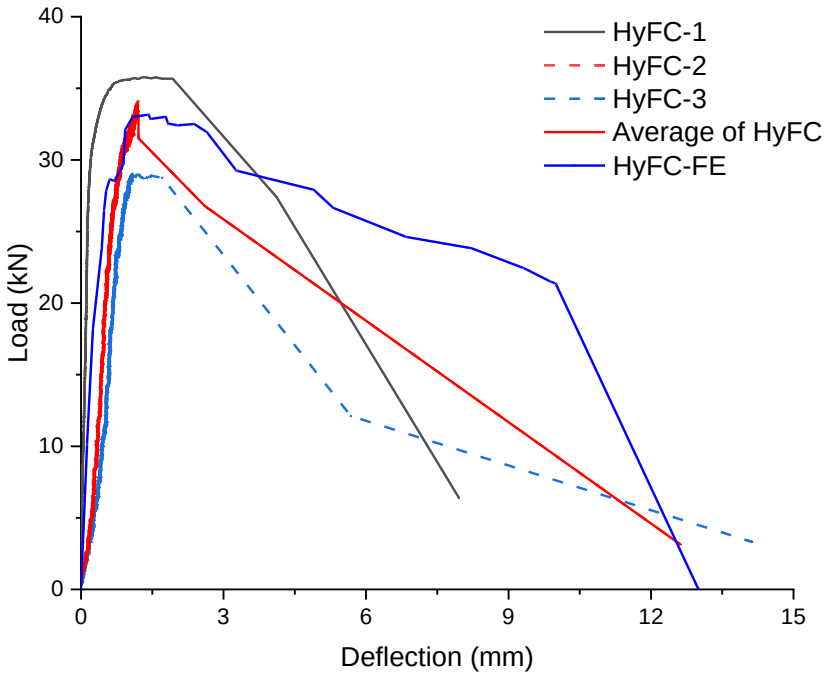

c) HyFRC

Figure A.16: Comparison between experimental results and FEA models: a) NC, b) SFC and c) HyFC beam

Figure A.17 illustrates the region where crack initiation and patterns are anticipated based on stress distribution, as revealed by FEA model results. This figure highlights areas with stress concentration, indicating potential crack development sites. In Figure A.18, it can be observed the crack patterns at the end of the experimental test. In Figure A.17, the proposed FEA model's capability to predict these crack patterns while revealing heightened stress peaks in the same region. These peaks in Figure A.17 suggest potential crack locations and offer insights into the neutral axis position.

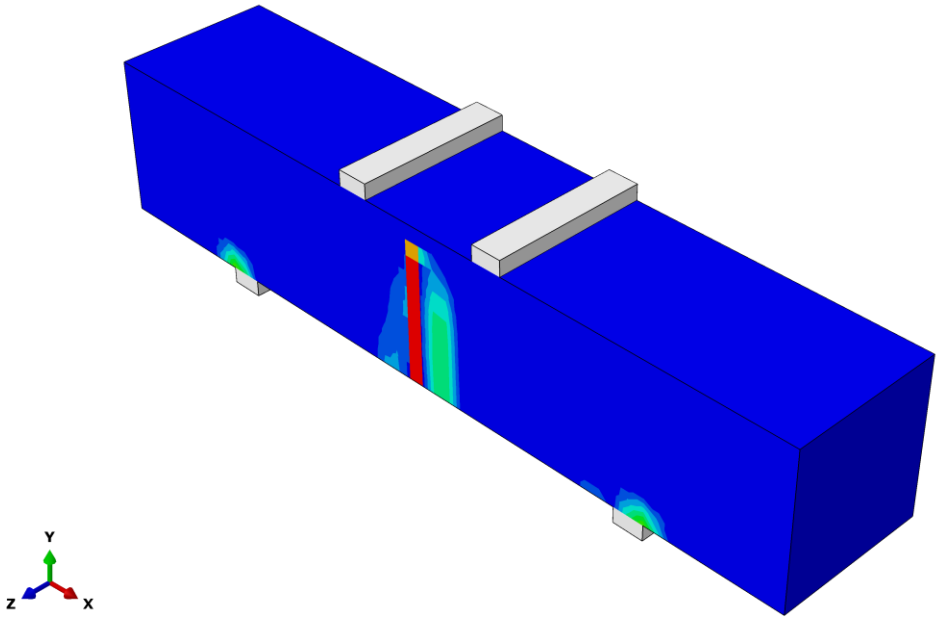

a) Concrete tensile damage -crack pattern- in FEA model

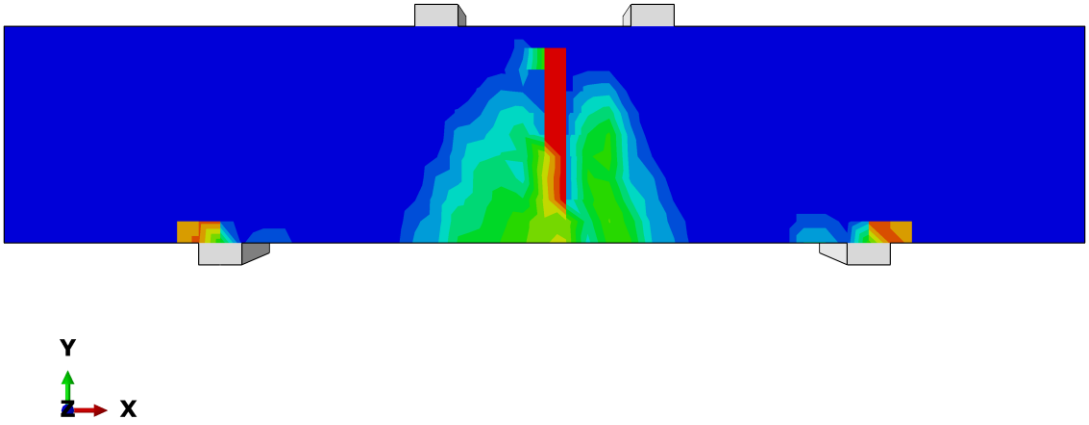

b) Another view of concrete tensile damage -crack pattern- in FEA model

Figure A.17: FEA model results

Figure A.18: The final crack pattern of the experimental results at the failure

By incorporating the XFEM, as demonstrated in Figure A.19 the model provides a more accurate representation of the actual cracks in the specimens and the failure process due to crack propagation. This comparison highlights the enhanced precision achieved by integrating XFEM in crack prediction.

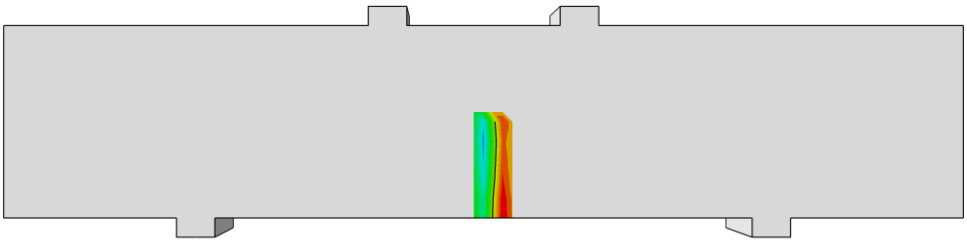

a) Crack PHILSM - this function is used to define/show the location of crack inside a body

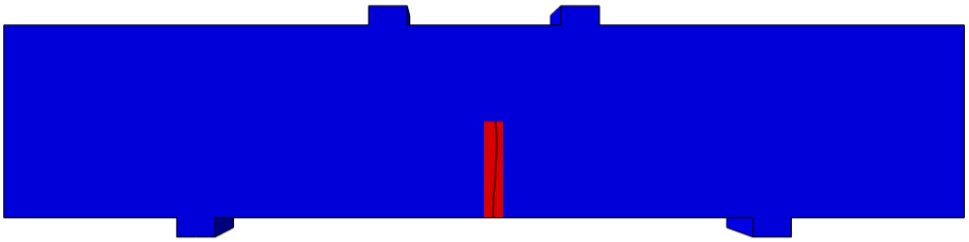

b) Crack STATUSXFEM – is a scalar variable that shows the extent of damage or “cracking” inside an element

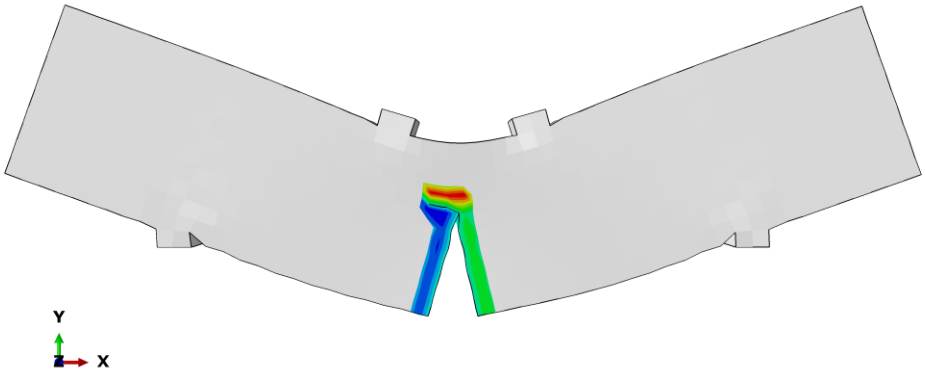

c) Crack pattern with XFEM- in FEA model

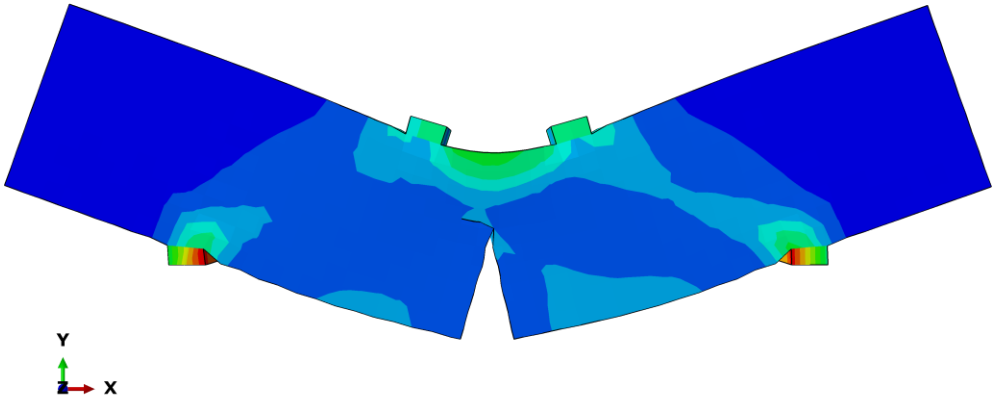

d) Concrete stress -crack pattern with XFEM- in FEA model

Figure A.19: FEA model results with XFEM concept

Low-Cycle Fatigue Analysis Using the Direct Cyclic Approach

This section explores the application of the direct cyclic approach in low-cycle fatigue analysis. The methodology involves subjecting structures to cyclic loading

conditions, with a focus on predicting progressive damage and eventual failure. The approach maintains constant material stiffness and contact conditions throughout the analysis, allowing for efficient computations.

The central concept of the direct cyclic approach is to calculate the "stabilised response" of the structure at discrete points in the loading history. This response encompasses factors such as deformation, stress, and strain. A key feature is the ability to model and predict the evolution of damage within the structure due to cyclic loading, using mathematical models such as continuum damage mechanics and linear elastic fracture mechanics.

The analysis is an iterative process, with each solution used to forecast how material properties will degrade in the subsequent loading increment. This process continues until a point in the loading history is reached where a fatigue life assessment can be made. The primary objective is to estimate the structure's fatigue life, providing essential information for ensuring the safety and durability of various engineering applications.

Low-cycle fatigue analysis in Abaqus/Standard

The direct cyclic analysis feature within Abaqus/Standard offers an efficient computational method for modelling and obtaining stable responses of structures under periodic loading. It is particularly well-suited for conducting low-cycle fatigue calculations on large structures. This capability leverages a combination of Fourier series and time integration techniques to directly capture and stabilise the structural response while considering nonlinear material behaviour.

The direct cyclic low-cycle fatigue procedure is designed to simulate the progressive damage and failure mechanisms, both within bulk materials and at material interfaces. For the former, it can be based on either a continuum damage mechanics approach or the principles of linear elastic fracture mechanics in combination with the extended finite element method. The response is derived by assessing the structural behaviour at discrete points along the loading history, as illustrated in Figure A.20. At each of these points, the solution is used to predict how the material properties will degrade and evolve during the subsequent increment, spanning a number of load cycles. These deteriorated material properties are then applied to compute the solution in the next increment of the

load history. Consequently, the crack or damage growth rate is continually updated throughout the analysis.

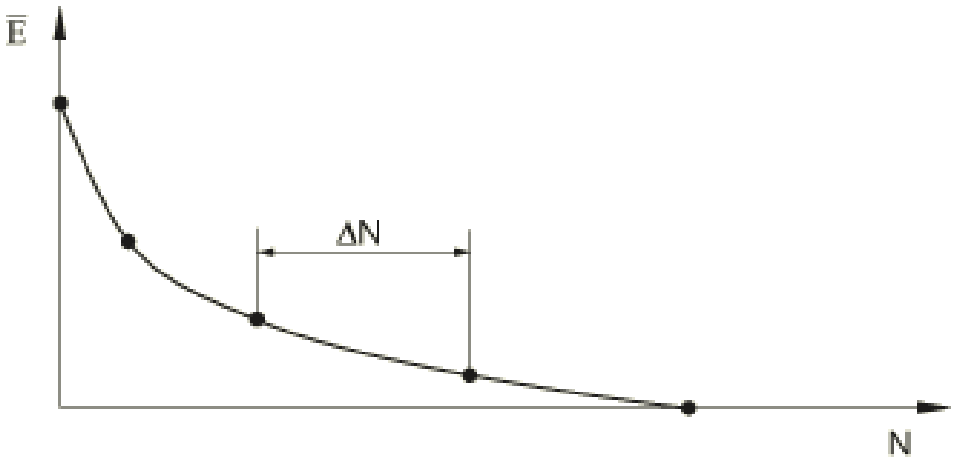

Figure A.20: Elastic stiffness degradation as a function of the cycle number

Damage initiation marks the point at which the response of a material begins to deteriorate. In low-cycle fatigue analysis, the criterion for damage initiation is identified by the accumulation of inelastic hysteresis energy per cycle, denoted as Δ_W. Δ_W, along with material constants, is employed to ascertain the cycle number at which damage initiation occurs, known as N_0. When a stabilized loading cycle, denoted as N, concludes in Abaqus/Standard, it checks whether the damage initiation criterion, N > N_0, is met at any material point. Only when this condition is satisfied does the material stiffness at that particular material point start to degrade.

In the context of modelling progressive damage and failure in bulk materials, there are two distinct approaches. The first approach is rooted in continuum damage mechanics, which is particularly well-suited for ductile materials. Ductile materials exhibit stress reversals and the accumulation of plastic strains under cyclic loading, leading to the initiation and propagation of cracks. This damage initiation and evolution can be described by the stabilized accumulation of inelastic hysteresis strain energy per cycle, as depicted in Figure A.21.

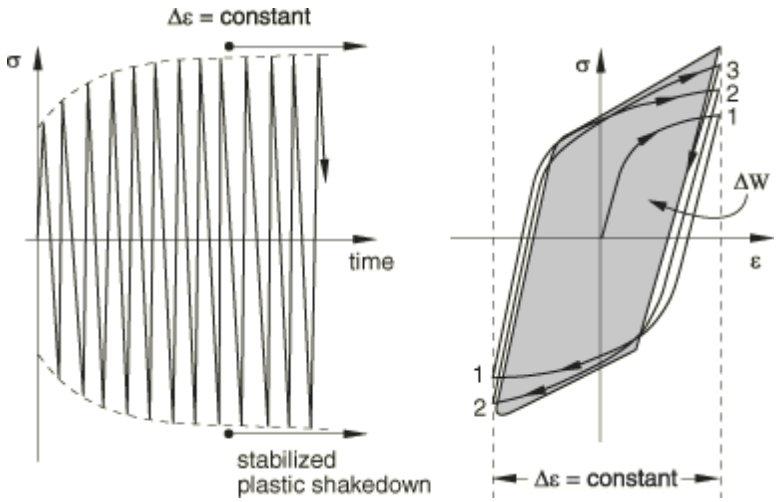

Figure A.21: Plastic shakedown in a direct cyclic analysis

The second approach is based on the principles of linear elastic fracture mechanics combined with the extended finite element method. This approach is more suitable for brittle materials or materials that experience small-scale yielding. In these materials, cyclic loading leads to a degradation of material strength, resulting in fatigue crack growth along an arbitrary path. The onset and growth of the crack can be characterized by the relative fracture energy release rate at the crack tip, following the Paris law (Paris, 1961), as shown in Figure A.22.

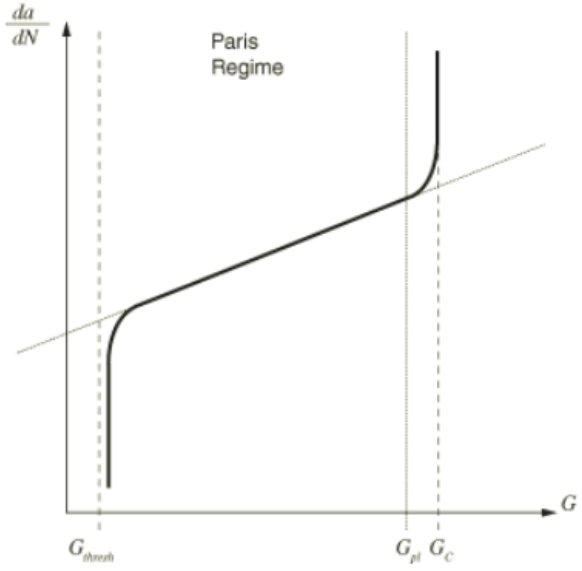

Figure A.22: Fatigue crack growth govern by Paris law

Approaches to Analysing Low-Cycle Fatigue

The conventional method for determining a structure's fatigue limit involves establishing S-N curves, which depict the relationship between applied load and

the number of cycles leading to structural failure for the materials within that structure. This approach is still widely employed as a design tool to estimate the fatigue resistance of engineering structures. However, it tends to be overly cautious and fails to establish a direct link between the number of cycles and the extent of damage or crack length.

An alternative approach focuses on predicting fatigue life by employing a crack/damage evolution law that relies on inelastic strain/energy. This prediction is made once the structure's response stabilises after numerous cycles. Given that it is computationally impractical to simulate the gradual accumulation of damage in a material over a large number of load cycles, numerical studies of fatigue life often involve modelling the structure's response under a small fraction of the actual loading history. This response is then extrapolated over a large number of load cycles using empirical relationships like the Coffin-Manson relationship (as outlined in Coffin, 1954, and Manson, 1953) to estimate the likelihood of crack initiation and propagation. It's important to note that this approach, relying on a constant crack/damage growth rate, may not provide a realistic prediction of how cracks or damage evolve.

The following steps show how to conduct a direct cycle test in Abaqas, as can be seen in Figure A.23.

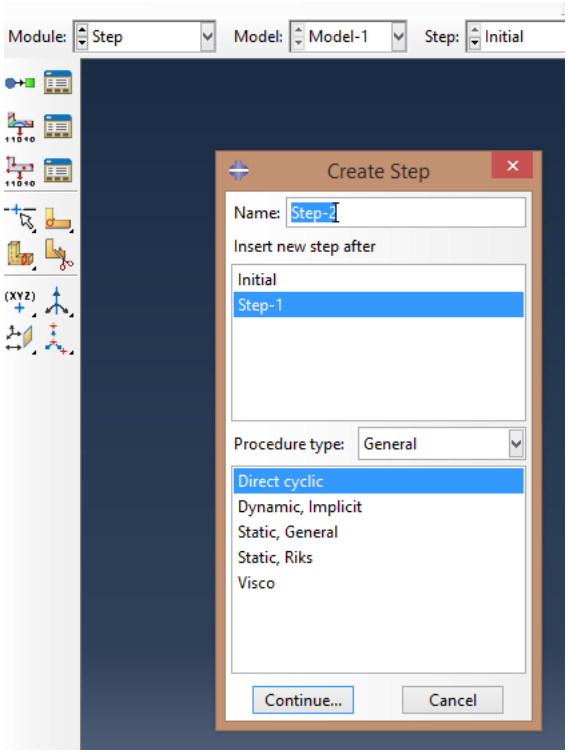

a) Creating a direct cycle step

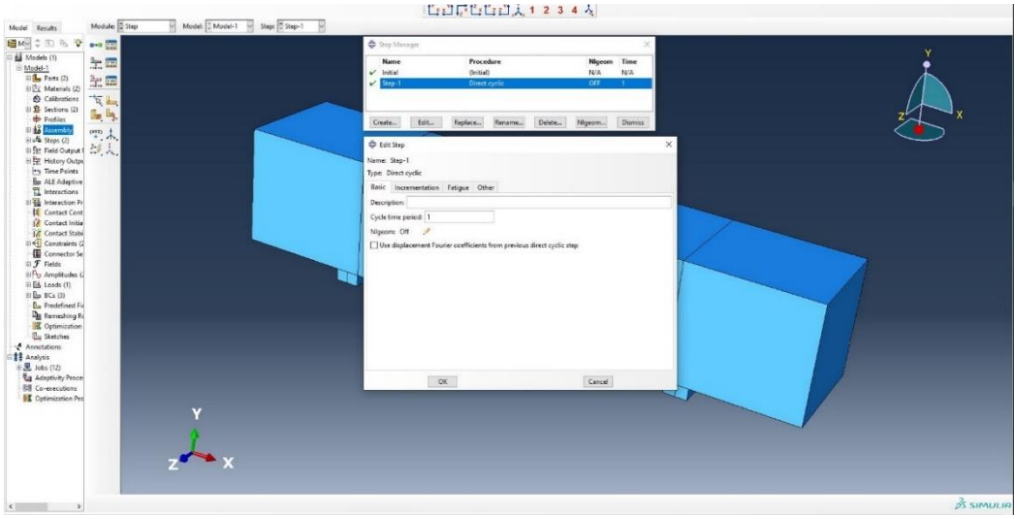

b) Direct cycle step

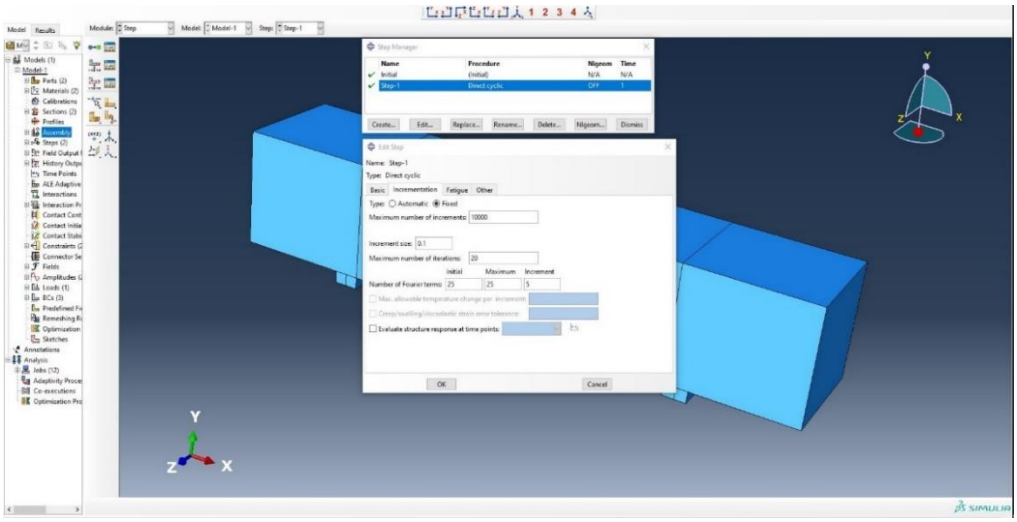

c) Shows the number of increments and iterations

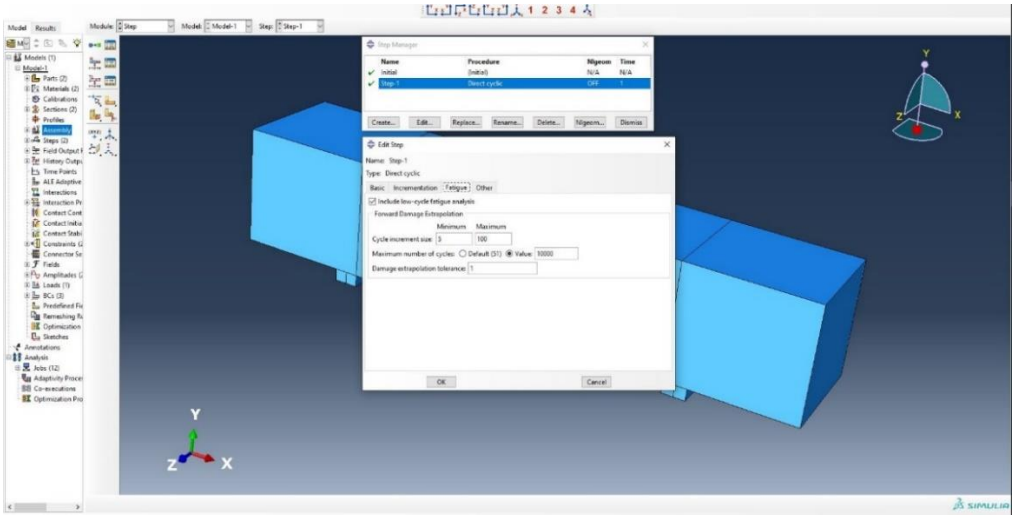

d) Shows the number of cycles for low cycle fatigue analysis

Figure A.23: Process for conducting a direct cycle

A low-cycle fatigue analysis employing the direct cyclic approach comes with certain constraints:

- When the direct cyclic analysis is employed iteratively to achieve a stable solution, it cannot accommodate changes in contact conditions within a single cycle.
- The analysis may not deliver reliable results when there is a compressive load on the crack surface during a loading cycle. This is because the global stiffness is determined only once at the start of each specific loading cycle.
- While geometric nonlinearity can be incorporated in any general step before a direct cyclic step, it's important to note that the cyclic step itself can only consider small displacements and strains, limiting the scope of the analysis in that regard.